School of Medicine
Institute of Infection and Immunity

Ysgol Meddygaeth
Adran Heintiau Imiwnedd

CARDIFF UNIVERSITY
PRIFYSGOL CAERDYDD

Characterisation of CXCL14 Function and Target Cells in Blood and Tissues

Paul Jonathon Collins

Thesis presented for the Degree of Doctor of Philosophy

June 2016

Division of Infection and Immunity
School of Medicine
Cardiff University

THE **PRESIDENT'S**
Research Scholarships

DECLARATION

This work has not been submitted in substance for any other degree or award at this or any other university or place of learning, nor is being submitted concurrently in candidature for any degree or other award.

Signed ………………………………… (candidate)   Date …………………………

STATEMENT 1

This thesis is being submitted in partial fulfillment of the requirements for the degree of …………………………(insert MCh, MD, MPhil, PhD etc, as appropriate)

Signed ………………………………… (candidate)   Date …………………………

STATEMENT 2

This thesis is the result of my own independent work/investigation, except where otherwise stated.
Other sources are acknowledged by explicit references. The views expressed are my own.
Signed ………………………………… (candidate)   Date …………………………

STATEMENT 3

I hereby give consent for my thesis, if accepted, to be available online in the University's Open Access repository and for inter-library loan, and for the title and summary to be made available to outside organisations.
Signed ………………………………… (candidate)   Date …………………………

STATEMENT 4: PREVIOUSLY APPROVED BAR ON ACCESS

I hereby give consent for my thesis, if accepted, to be available online in the University's Open Access repository and for inter-library loans **after expiry of a bar on access previously approved by the Academic Standards & Quality Committee.**

Signed ………………………………… (candidate)   Date …………………………

Acknowledgements

I would like to start by thanking my supervisor Prof. Bernhard Moser for his guidance and mentorship throughout my PhD. His enthusiasm for scientific research knows no bounds, and he has instilled some of that enthusiasm in me (although I might not show it). His belief in my abilities as a researcher has given me a new-found confidence in myself, while his support during the times when I have struggled on a personal level will not be forgotten. I am also extremely grateful to Michelle McCully for getting me up to speed in the lab and in particular showing me how to process skin samples, while I don't know where I would be without her flow cytometry expertise. Michelle has been a tremendous teacher and colleague, and I feel privileged to have worked alongside her. Thank you to Nadia and Alex for your assistance in the receptor cloning experiments, and to the rest of my wonderful lab group including Matthias, Anna Rita, Chris, Andy, Ann, Ariadni, Amy, Teja and Jing Jing, and the old crowd Hung-Chang, Matt, Wajid, Martin, Jo, Ida and Riaz. I couldn't have wished for a better group of people to have shared the past three and a half years with. I must give special mention to Anna Rita Liuzzi, whose support toward the end of my thesis-writing process has been invaluable.

I must thank Prof. Mariagrazia Uguccioni for welcoming me into her lab at the IRB in Bellinzona, Switzerland, so that I could perform the intracellular Ca^{2+} rise assays. Thanks must also go to the members of Prof. Uguccioni's group, Lorenzo, Gianluca, Valentina and Gabriela for their help with performing the experiments, as well as Rocco and Prof. Marcus Thelen for their expertise in analysing and interpreting the data. I must also thank Prof. Mario Mellado and Dr. Laura Martinez-Munoz at the National Centre for Biotechnology in Madrid, Spain for performing the FRET experiments, and Prof. Hugues Lortat-Jacob and Dr. Yoan Monneau at the University of Grenoble, France, for performing the NMR and SPR experiments.

Thanks go to my co-supervisor Prof. David Price for many thought-provoking discussions along the way, as well as to Prof. Phil Taylor and Dr. Chia-Te Liao for their assistance in teaching me the lentiviral transduction method, in addition to their precious insights regarding my macrophage work. I would also like to thank all of my friends at Cardiff University, particularly Diana Costa Bento, Katie Sime and Leah Wallace for the countless coffee and lunch breaks, and for the support and compassion they have shown me when I needed it most.

Publications during this PhD

McCully, M. L., **Collins, P. J.**, Hughes, T. R., Thomas, C. P., Billen, J., O'Donnell, V. B. & Moser, B. (2015). Skin metabolites define a new paradigm in the localization of skin tropic memory T cells. *J Immunol*, **195**, 96-104.

Dai, C., Basilico, P., Cremona, T. P., **Collins, P. J.**, Moser, B., Benarafa, C. & Wolf, M. (2015). CXCL14 displays antimicrobial activity against respiratory tract bacteria and contributes to clearance of *Streptococcus pneumoniae* pulmonary infection. *J Immunol*, **194**, 5980-9.

Manuscript in preparation

Collins, P. J., McCully, M. L., Martinez Munoz, L., Monneau, Y., Lortat-Jacob, H., Mellado, M., Thelen, M., Uguccioni, M., Moser, B. Epithelial chemokine CXCL14 synergises with CXCL12 *via* novel functional interaction with CXCR4.

Abstract

The human chemokine family consists of around 50 peptides that control the migratory patterns and positioning of all leukocytes. One such member of this family is CXCL14. Very highly expressed in many healthy tissues including skin, gut and kidney, loss of CXCL14 expression in chronic inflammatory conditions and certain forms of cancer has led to a proposed role for CXCL14 in immune surveillance at these sites. The function and target cells of CXCL14 are poorly defined however, largely because the identity of its receptor remains unknown.

Here, I have combined the evaluation of chemotactic responses toward CXCL14 with detection of putative CXCL14 receptor(s) on the surface of cells using a synthetic, fluorochrome-conjugated CXCL14, to definitively identify CXCL14 target cells in human. Monocytes were identified as the major target cells in peripheral blood, 28.4 ± 6.1% Monocytes migrating toward 1 µM CXCL14 in *ex vivo* transwell chemotaxis assays compared to 3.01 ± 0.65% toward buffer alone (p=0.0031). Responses to CXCL14 also identified tissue phagocytes extracted from healthy human skin, including an apparently novel population of skin-resident CD14$^+$ cells characterised by lack of CD45 expression. Screening of CXCL14-responsive cells by RNA sequencing for expression of G protein-coupled receptors revealed five major candidates for the CXCL14 receptor, all of which are orphan receptors; GPR35, GPR68, GPR84, GPR141 and GPR183. At present, I am in the process of testing these candidates in functional assays. Finally, I report on a novel ability of CXCL14 to potently synergise with other chemokines, particularly CXCL12. This 'synergy' with CXCL12 likely occurs via a direct interaction between CXCL14 and the receptor for CXCL12, CXCR4, which is broadly expressed on immune cells.

This work identifies mononuclear phagocytes in blood and tissue as the primary targets for CXCL14, providing new and exciting insights into the role played by CXCL14 in immune surveillance of peripheral tissues.

List of Figures

List of Tables

List of Abbreviations

2-ME – 2-Mercaptoethanol

7TM – 7-transmembrane

ACKR – Atypical Chemokine Receptor

AF-CXCL14 – Alexa Fluor 647-conjugated CXCL14

AF-muCCL1 – Alexa Fluor 647-conjugated murine CCL1

ANOVA – Analysis of Variance

APC – Antigen Presenting Cell

AutoF – Auto-Fluorescence

BCR – B cell Receptor

Ca^{2+} – Calcium ion

cAMP – Cyclic AMP

CCL – Chemokine (C-C motif) Ligand

CCR – CC-Chemokine Receptor

CCRL – CC-Chemokine Receptor-Like

CXCL – Chemokine (C-X-C motif) Ligand

CXCR – CXC-Chemokine Receptor

CXCL14-KO – CXCL14-Knockout mouse

CD – Cluster of Differentiation

CI – Chemotactic Index

CMV - Cytomegalovirus

DC – Dendritic cell

DC-SIGN - Dendritic Cell-Specific Intercellular adhesion molecule-3-Grabbing Non-integrin

DETC – Dendritic Epidermal T Cell

DMEM – Dulbecco's Modified Eagle Medium

DTR – Diphtheria Toxin Receptor

EBI2 - Epstein-Barr virus-induced gene 2

ECL – Extracellular Loop

EDTA - Ethylenediaminetetraacetic Acid

EE – Epidermal Equivalent

eGFP – enhanced Green Fluorescent Protein

EP receptor – Prostaglandin E2 receptor

FACS – Fluorescence-Activated Cell Sorting

FCS – Foetal Calf Serum

FITC - Fluorescein Isothiocyanate

FMO – Fluorescence Minus One

FPR – Formyl Peptide Receptor

FRET – Fluorescence Resonance Energy Transfer

FSC – Forward Scatter

GAG – Glycosaminoglycan

GM-CSF – Granulocyte Macrophage-Colony Stimulating Factor

GPCR – G Protein-Coupled receptor

GRK – G protein-coupled Receptor Kinase

GTP – Guanosine Triphosphate

HEK – Human Embryonic Kidney

HEV – High Endothelial Venules

HIV – Human Immunodeficiency Virus

HLA – Human Leukocyte Antigen

HMGB1 - High Mobility Group Box 1 protein

HRH1 – Histamine Receptor H1

HS – Heparan Sulphate

HSCT – Haematopoietic stem cell transplant

ICL – Intracellular Loop

IDEC – Inflammatory Dendritic Epidermal Cell

IFN - Interferon

Ig - Immunoglobulin

IL – Interleukin

ILC – Innate Lymphoid Cell

LC – Langerhans Cell

LPS – Lipopolysaccharide

mAb – Monoclonal Antibody

MACS – Magnetic-Activated Cell Sorting

MAPK – Mitogen-Activated Protein Kinase

M-CSF – Macrophage-Colony Stimulating Factor

MFI – Mean Fluorescence Intensity

MHC – Major Histocompatibility Complex

Mo-DC – Monocyte-derived DC

MPS – Mononuclear Phagocyte System

mRNA – Messenger RNA

MSB – Mixed Salt Buffer

M$_{TR}$ – Tissue-Resident Monocyte

Na-But – Sodium Butyrate

NK – Natural Killer

NKT – Natural Killer T cell

NMR – Nuclear Magnetic Resonance

PBMC – Peripheral Blood Mononuclear Cells

PBS – Phosphate Buffered Saline

PCR – Polymerase Chain Reaction

PGE$_2$ – Prostaglandin E2

pDC – Plasmacytoid DC

PRR – Pattern Recognition Receptor

qPCR – Quantitative real-time PCR

RA – Rheumatoid Arthritis

RISC – RNA-Induced Signalling Complex

RNA-seq – RNA sequencing

RPKM – Reads Per Kilobase of transcript per Million mapped reads

RPMI – Roswell Park Memorial Institute

S1P – Sphingosine 1-Phosphate

s.e.m. – Standard error of the mean

ShRNA – Short hairpin RNA

SiRNA – Short interference RNA

SLO – Secondary Lymphoid Organ

SSC – Side Scatter

TCR – T cell Receptor

$\textbf{T}_{\textbf{CM}}$ – Central Memory T cell

$\textbf{T}_{\textbf{EM}}$ – Effector Memory T cell

$\textbf{T}_{\textbf{RM}}$ – Resident Memory T cell

$\textbf{T}_{\textbf{FH}}$ – T Follicular Helper cell

$\textbf{T}_{\textbf{H}}$ – T Helper cell

Treg – Regulatory T cell

TGF-β – Transforming Growth Factor-Beta

TLR – Toll-like Receptor

TNF – Tumour Necrosis Factor

Chapter 1   Introduction

The human immune system includes cellular and soluble effectors that together, comprise an extremely effective defence against a wide variety of threats to the integrity of the host. Chemokines are a family of small soluble peptides which possess a range of physiological functions, but are defined on the basis of their ability to induce directional migration or chemotaxis in nearby responsive cells. In cooperation with cell-surface adhesion molecules and other molecules with chemotactic activity (e.g. components of the complement cascade), chemokines control the migratory patterns and positioning of all immune cells. Chemokines exert their effects by activating 7-transmembrane (7TM) receptors coupled to intracellular G proteins (G protein-coupled receptors; GPCRs), which are selectively expressed on the target cell surface. In human, approximately 48 chemokines and 18 typical chemokine receptors have been identified to date (Griffith et al., 2014). The specific expression, regulation and receptor binding patterns of each member creates a highly sophisticated functional diversity in the chemokine system. Chemokines play pivotal roles in complex immune processes such as acute and chronic inflammation, the generation of adaptive cellular and humoral immune responses, memory cell differentiation and immune surveillance. Their function extends beyond the immune response however, with chemokines playing vital roles in such disparate processes as behaviour, angiogenesis and reproduction (reviewed in (Hara and Tanegashima, 2012, Kitaya and Yamada, 2011, Rossi and Zlotnik, 2000)). Chemokine function in the context of the human immune system will be discussed in detail later on in this chapter. First, I will discuss the immune cell populations which are present in human blood and peripheral tissues, their functions in health and disease, and the methods used by researchers to study them. My research focuses on monocytes in the blood as well as macrophages and dendritic cells in tissues, collectively known as the mononuclear phagocyte system.

1.1 The Mononuclear Phagocyte System

The term "leukocytes" denotes a diverse group of cell types that mediate the body's immune response. Leukocytes have a common origin in haematopoietic stem cells (HSCs). However, development along distinct differentiation pathways in response to internal and external cues gives rise to leukocyte subsets distinguished by their physical and functional characteristics. The mononuclear phagocyte system (MPS) represents a sub-group of leukocytes originally described as a population of bone

marrow-derived cells that circulate in the blood as monocytes and populate tissues as macrophages in the steady-state and during inflammation (van Furth and Cohn, 1968). Macrophages are resident in every organ throughout the body, with macrophages resident in different tissues displaying remarkable heterogeneity with respect to phenotype, function and turnover (Davies et al., 2013a). Recently, evidence has emerged that many macrophage populations are seeded in tissues during early embryogenesis, independent of the haematopoietic system. Although these embryonic macrophages are maintained throughout life by local proliferation during homeostasis, it appears that they are reconstituted by circulating monocytes following inflammation (Epelman et al., 2014). The discovery of dendritic cells (DCs) as a distinct lineage of mononuclear phagocytes, specialised in antigen presentation to T cells and the initiation of adaptive immune responses (Steinman et al., 1974), revealed additional roles of the MPS in shaping immunity. Whereas the relationship between monocytes, tissue DCs and their progenitors is now beginning to emerge, other areas such as the origin and renewal of tissue macrophages remain less well-defined.

1.1.1 Monocytes

'Monocyte' is the name given to the stage of the MPS which exists in the blood. Functionally characterised by their ability to phagocytose material, produce cytokines and present antigen, early studies identified mononuclear phagocytes on the basis of morphology and glass adherence (van Furth and Cohn, 1968). Human monocytes develop in the bone marrow from dividing monoblasts (bipotent cells that differentiate from HSCs) and are released into the bloodstream as non-diving cells, where they represent approximately 4-10% of circulating leukocytes. With the half-life of human monocytes in circulation being estimated at around 22 hours (van Furth and Cohn, 1968), it is conceivable that as much as 50% of circulating monocytes leave the bloodstream under steady-state conditions each day. Their fate, however, upon entering peripheral tissues, remains a topic for speculation. It is thought that monocytes represent a systemic reservoir of myeloid precursors, giving rise to tissue macrophages and DCs under both steady-state and inflammatory conditions. (Wiktor-Jedrzejczak and Gordon, 1996). However, experimental data demonstrating the differentiation of monocytes *in vivo* remain scarce, and the contribution of monocytes to this complex cellular system is a very active area of research (Auffray et al., 2009, Geissmann et al., 2010, Perdiguero and Geissmann, 2016).

Human monocytes were initially described using histological and cytochemical techniques. Typical morphological features of blood monocytes include an irregular kidney-shaped nucleus and a high cytoplasm-to-nucleus ratio. (Ziegler-Heitbrock, 2000). Monocytes are also the largest of the mononuclear leukocyte subsets, measuring 13-18 μm in diameter. However, they are still very heterogenous in size and shape, making them difficult to distinguish by morphology or by light scatter analysis alone from blood DCs, activated lymphocytes and natural killer (NK) cells. More recently, monocytes have been identified based on specific expression of particular cell-surface markers, with detection by flow cytometry. Expression of markers such as CD14 and CD33, combined with lack of expression of lineage markers that identify T, B, NK cells and DCs, is routinely used to distinguish monocytes from other cell types.

The function of monocytes has largely been inferred from manipulations performed in the laboratory using monocytes isolated from blood. *In vitro*, monocytes display adherence to plastic, are highly phagocytic and, upon stimulation, produce large amounts of reactive oxygen species (ROS) and cytokines such as tumour necrosis factor-alpha (TNFα), interleukin (IL)-1β, IL-6 and IL-10, in addition to other inflammatory mediators (prostaglandins, complement factors, proteolytic enzymes etc.). Expression of a large array of pattern recognition receptors (PRRs), including Toll-like receptors (TLRs), enables monocytes to respond to various microorganisms including bacteria, fungi and viruses, while expression of scavenger receptors also facilitates the recognition of lipids and dying cells (van Furth and Cohn, 1968, Blumenstein et al., 1997). More recently, important roles for monocytes in adaptive immunity have been described. Monocytes affect the polarisation and expansion of lymphocytes, shaping primary and memory T-cell responses in humans and mice (Geissmann et al., 2008). This is despite the observation that monocytes are far less efficient antigen presenting cells (APCs) than DCs (Banchereau and Steinman, 1998). Cytokine-driven culture systems allow the *in vitro* differentiation of monocytes into macrophages and DCs, supporting the proposal that monocytes give rise to these cell types *in vivo* (Sallusto and Lanzavecchia, 1994, Zhou and Tedder, 1996). Such findings must be interpreted with caution, however, as monocytes are primed to respond rapidly to any alterations in their environment. Isolating them, purifying them on gradients and culturing them *in vitro*, therefore, all affect their phenotype and behaviour.

1.1.1.1   Identification of monocyte subsets

The division of blood monocytes into functional subsets was first confirmed around 20 years ago (Ziegler-Heitbrock, 1996), having been alluded to some years previously (Esa et al., 1986, Yasaka et al., 1981). At this time, human monocytes were already being identified by flow cytometry on the basis of expression of CD14, the co-receptor for lipopolysaccharide (LPS), a component of the cell wall of gram-negative bacteria. The introduction of CD16 as an additional monocyte marker, however, led to the observation that a minor proportion of monocytes combined expression of CD16 (a low affinity receptor for the Fc portion of IgG antibodies) with low-level CD14 expression. This $CD14^+CD16^+$ subset was distinguishable from the vast majority of monocytes, which had strong CD14 expression but lacked CD16 ($CD14^{++}CD16^-$). The demonstration that the $CD14^+CD16^+$ subset was expanded in various infectious diseases including sepsis, Tuberculosis and HIV, led to the CD16-expressing subset being referred to as "pro-inflammatory monocytes" (Ziegler-Heitbrock, 1996). *In vitro* observations supported this designation, as it was demonstrated that $CD16^+$ monocytes had higher major histocompatibility complex (MHC) class II expression and, after stimulation by TLR ligands, produced greater quantities of TNFα (Belge et al., 2002). A major breakthrough was made when two morphologically, phenotypically and functionally distinct subsets of monocytes were first described in mouse (Geissmann et al., 2003). The two subsets were defined on the basis of differential expression of chemokine receptors and unique migratory properties. A short-lived "inflammatory subset" demonstrated high CCR2 and low CX3CR1 expression, and was actively recruited to inflamed tissues in the mouse. In contrast, a "resident subset", with a longer half-life in peripheral blood, which did not express CCR2 and had high CX3CR1 expression, was preferentially recruited to non-inflamed tissues (Geissmann et al., 2003). In this study, the researchers showed that chemokine receptor expression also defined the two major monocyte subsets in human. $CD14^{++}CD16^-$ human monocytes expressed CCR2 while lacking CX3CR1 expression, while the $CD14^+CD16^+$ human subset had high expression of CX3CR1 and was negative for CCR2. Human $CD16^+$ monocytes also lacked expression of CCR1, CXCR1 and CXCR2, all of which are receptors for inflammatory chemokines, suggesting that like their murine $CX3CR1^{high}CCR2^-$ counterparts, $CD16^+$ human monocytes are likely excluded from inflamed tissues (Geissmann et al., 2003). This contrasted with the original designation of the $CD16^+$ subset of human monocytes as inflammatory, and led to confusion regarding the functional differences between monocyte subsets, which still remains. Whole-genome expression arrays have since

confirmed that the human and murine monocyte subsets are indeed homologous (Cros et al., 2010). Due to the lack of a clear understanding of their different functions *in vivo*, the major CD14^{++}CD16^{-} monocyte population in humans has since been termed "classical monocytes", with the CD16^{+} subset termed "non-classical monocytes". More recently, monocytes with an intermediate phenotype between the classical and non-classical subsets have been described. These cells have high CD14 and low CD16 expression (CD14^{++}CD16^{+}) and are found at low frequency in blood. However, they possess unique features and have been shown to expand in inflammation (Moniuszko et al., 2009, Skrzeczynska-Moncznik et al., 2008). Division of human blood monocytes into three subsets; classical, intermediate and non-classical, is therefore now widely accepted by the wider research community (Ziegler-Heitbrock et al., 2010). Classical monocytes represent 85-90% of circulating blood monocytes, with the intermediate and non-classical subsets constituting the remaining 10-15%.

1.1.1.2 *Functional differences between monocyte subsets*

Although functional differences between the three monocyte subsets have been described *ex vivo*, there is little data regarding their different functions *in vivo*. Both classical and non-classical monocytes can give rise to DCs during *in vitro* culture (Sanchez-Torres et al., 2001). Subsequently, CD16^{+} monocytes were shown to transmigrate through a layer of resting endothelial cells more efficiently than classical monocytes (Randolph et al., 2002), suggesting that CD16^{+} monocytes may preferentially give rise to tissue DCs during the steady-state. It is unclear, however, how properties ascribed to CD16^{+} monocytes previously are now to be segregated between the intermediate and non-classical subsets. More recently, it was observed that human CD14^{+}CD16^{++} non-classical monocytes "crawled" along the endothelium following intravenous transfer into mice; behaviour that was not observed in CD14^{++}CD16^{-} classical monocytes. Here, the authors proposed that non-classical monocytes patrol blood vessels, perhaps acting as a blood-resident macrophage population that does not exit so readily into peripheral tissues (Cros et al., 2010), consistent with their longer half-life in circulation (Geissmann et al., 2003, Hanna et al., 2015). Comprehensive genotypic and phenotypic analysis of the three human monocyte subsets during healthy conditions has established that the intermediate subset is much more closely related to the non-classical subset than the classical subset (Wong et al., 2011). Indeed, like the non-classical subset, the intermediate subset has been shown to expand during disease (Moniuszko et al., 2009), while

intermediate monocytes best support viral replication during HIV infection (Kim et al., 2010).

The question of whether the monocyte subsets represent distinct cell types, or rather a single lineage at varying stages of differentiation, is an intriguing one. It has been proposed that the intermediate subset represents the direct intermediary link between the classical and non-classical subsets (Ziegler-Heitbrock et al., 2010). During the course of certain infections, there is first an expansion of the intermediate subset, subsequently followed by an increase in the non-classical subset (Weiner et al., 1994, Ziegler-Heitbrock et al., 2010). Furthermore, intermediate monocytes have been shown to express a large number of genes (Wong et al., 2011) and cell-surface markers (Ancuta et al., 2009, Wong et al., 2011) at levels between that of the classical and non-classical subsets. Monocyte repopulation kinetics in patients following haematopoietic stem cell transplantation (HSCT) support this notion, with classical monocytes appearing in the blood first, followed by the intermediate and then the non-classical subsets (Haniffa et al., 2009). Preliminary *in vitro* experiments demonstrated that classical monocytes spontaneously down-regulated several classical subset-associated markers, coupled with the acquisition of some, but not all, of the non-classical associated markers (Wong et al., 2011). However, proof of the lineage relationship between the three subsets is still required.

1.1.1.3 *Monocyte subsets in mouse*

In mice, the subdivision of monocytes into three subsets has also been proposed, although the markers used to identify them are different. Monocyte development and survival in mice is completely dependent on colony-stimulating factor 1 (CSF1; also known as M-CSF). Mice that are deficient in this growth factor or its receptor CSF1R (also known as M-CSFR) exhibit severe monocytopenia (Dai et al., 2002, Wiktor-Jedrzejczak and Gordon, 1996). CSF1R$^+$ monocytes are divided into subsets on the basis of Ly6C and CD43 expression. Classical monocytes show high Ly6C expression and low CD43 (Ly6C++CD43+), intermediate monocytes have high expression of both markers (Ly6C++CD43++), while the non-classical monocytes combine low Ly6C with high CD43 (Ly6C+CD43++) (Ziegler-Heitbrock et al., 2010). CD14 is expressed by mouse monocytes, although the signal is too weak to be used as a mouse monocyte marker. Fate-mapping studies have revealed that in mouse, the abundant subset of Ly6C^{hi} classical monocytes gives rise to Ly6C^{lo} non-classical monocytes during the steady-state (Yona et al., 2013), suggesting that the same may be true in human.

1.1.2 Dendritic cells

1.1.2.1 Myeloid DCs

Peripheral blood DCs are divided into conventional (myeloid) and plasmacytoid subsets. Myeloid DCs account for approximately 50% of circulating DCs in human. They are identified by expression of MHC class II as well as the DC-associated integrin CD11c, while being negative for the monocyte markers CD14 and CD16. Two subsets of myeloid DC have been described, distinguished by differential expression of CD1c and CD141. Both express the common myeloid markers CD13 and CD33, indicating their derivation from the myeloid lineage. CD1c$^+$ DCs outnumber CD141$^+$ DCs in peripheral blood by approximately 10-fold (Ziegler-Heitbrock et al., 2010).

Both subsets of blood myeloid DC have the potential to act as sentinel cells; *in vitro*, they secrete cytokines when activated, effectively stimulate T cells and rapidly mature in response to TLR agonists (Kohrgruber et al., 1999, Piccioli et al., 2007). However, blood DCs do not have typical characteristics of DCs as seen in tissue; they lack dendrites and also lack typical markers of mature DCs, such as CD83. In blood, they most likely do not present antigen to T cells (as they do during *in vitro* co-culture), as the close cell-to-cell contacts that are necessary would not be permitted under flow conditions. Rather, it is assumed that blood DCs are in transit, maturing into fully functional DCs only following entry into tissues. Blood CD11c$^+$ DCs can be induced to undergo macrophage differentiation by culture with M-CSF (Robinson et al., 1999). However, the relationship between blood DCs and tissue phagocytes is not fully understood.

1.1.2.2 Plasmacytoid DCs

Plasmacytoid DCs (pDCs) are present in circulation in roughly equivalent numbers to myeloid DCs, and are potent producers of type I interferon (IFN) in response to viruses (Siegal et al., 1999). Following contact with viruses, it has been shown that pDCs can enter lymph nodes through high endothelial venules (HEVs) to prime T cells (Cella et al., 1999). Human pDCs have low CD11c expression and lack myeloid markers including CD14 and CD33, distinguishing them from conventional DCs and monocytes. CD303 (BDCA-2) expression is specific to pDCs in blood and is used as a marker to identify these cells by flow cytometry. The three DC subsets as well as the three monocytes subsets in human peripheral blood, in addition to the markers commonly used to identify them, are shown in **Figure 1.1.**

Monocytes		Surface markers	Distribution
	"Classical"	CD14++ CD16-	~85%
	"Intermediate"	CD14++ CD16+	~5%
	"Non-classical"	CD14+ CD16++	~10%
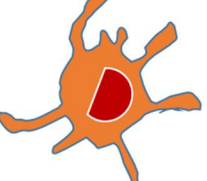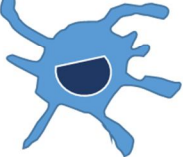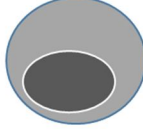
Dendritic cells		Surface markers	Distribution
	cDC1	CD1c+ CD11c+++	45-50%
	cDC2	CD141+ CD11c++ CLEC9A+ XCR1+	5-10%
	pDC	CD11c+ CD123+ BDCA-2+ BDCA-4+	45-50%

Figure 1.1. Monocyte and dendritic cell populations in human peripheral blood during steady-state conditions.

Expression of markers commonly used to identify these populations are indicated. Additionally, frequencies (%) of monocyte subsets within the monocyte pool and dendritic cells within the dendritic cell pool are specified. cDC; conventional DC, pDC; plasmacytoid DC.

1.2 Other Leukocyte Subsets in Peripheral Blood

Peripheral blood mononuclear cells (PBMC) include lymphocytes (which are sub-divided into T, B and NK cells), monocytes and DCs. The frequencies of these populations in human vary across individuals, however lymphocytes typically comprise 65-90% of PBMC; monocytes comprise 10-30% of PBMC, while DCs are rare, only comprising 1-2% of PBMC. Also present in circulation are granulocytes of which the majority are neutrophils, the most abundant leukocyte subset in peripheral blood.

1.2.1 T lymphocytes

The $CD3^+$ compartment of peripheral blood comprises $CD4^+$ and $CD8^+$ αβ T cells, in a roughly 2:1 ratio; $CD4^+$ T cells comprise 25-60% of PBMC, while $CD8^+$ T cells comprise 5-30% of PBMC. Both $CD4^+$ and $CD8^+$ T cells can be further sub-divided into naïve, effector, central memory and effector memory subsets that exist in resting or activated states, all of which express particular markers that can be used in their identification. $CD4^+$ T cells give rise to so-called T helper (T_H) cells, which assist other immune cell subsets in immunological processes, including maturation of B cells into plasma cells and memory B cells, as well as activation of cytotoxic T cell and macrophage killing activity. T_H cells can be further classified into various functional subsets based on the expression profiles of specific cytokines, surface markers and transcription factors. These include regulatory T cells (Tregs), T_H1, T_H2, T_H9 and T_H17 cells, as well as follicular helper T cells (T_{FH}). Different subsets have different roles in the immune response to pathogens, with T_H1 cells being most important against intracellular bacteria and protozoa, while T_H2 cells are most effective against extracellular pathogens including helminths. Comprehensive reviews of the T helper cell functional subsets can be found in (Bluestone et al., 2009, Jiang and Dong, 2013, Nakayamada et al., 2012).

$CD8^+$ T cells, on the other hand, possess the ability to directly kill infected, transformed or otherwise damaged cells, giving them the name cytotoxic T cells. $CD8^+$ T cells recognise short (8-10 amino acids) self- or pathogen-derived peptides presented on the surface of target cells by MHC class I molecules. Upon activation by a professional APC, $CD8^+$ T cells are licensed to kill target cells, which they achieve via the release of cytotoxins (perforin and granzymes) or via cell-surface interactions, such as those mediated by Fas ligand on the T cell and *Fas* on the target cell. Both lead to activation of the intracellular caspase cascade and apoptosis of the cell. Of note, ~2-5% of $CD3^+$

cells in peripheral blood are gamma delta (γδ) T cells, an innate lymphoid population with important roles in immune responses to bacteria, recognition of lipid antigens and antigen presentation to conventional T cells.

1.2.2 B lymphocytes

B cells comprise ~5-20% of PBMC and are easily identified by expression of CD19 or CD20, expression of which is specific to B cells in peripheral blood. CD19 forms part of the B cell receptor complex, the B cell's antigen receptor that upon activation, leads to proliferation and differentiation of the B cell, giving rise to effector cells. Circulating B cells comprise naïve and memory subsets, in addition to antibody-secreting plasmablasts (short-lived, proliferating antibody-secreting cells) and plasma cells (long-lived, non-proliferating antibody-secreting cells). The main function of B cells is the secretion of antibodies, making B cells the major mediators of humoral immunity (in contrast to T cells, which are the major mediators of cellular immunity). Antibodies assist in the removal of extracellular pathogens by several means, including opsonisation, initiation of the complement cascade and activation of the direct killing activities of cytotoxic T cells and NK cells (antibody-dependent cell-mediated cytotoxicity; ADCC). B cells express MHC class II, having important roles in antigen presentation, while they can also regulate the activity of other cell types via the production of a range of cytokines.

1.2.3 Natural killer cells

NK cells comprise ~5-15% of PBMC and represent the third immune cell subset that differentiates from the common lymphoid progenitor, which generates T and B lymphocytes. NK cells are distinguished from the other leukocyte subsets by expression of neural cell adhesion molecule (NCAM), also known as CD56, which facilitates their simple identification by flow cytometry. In contrast to their lymphoid counterparts, NK cells are effectors of the innate immune system as they do not require prior activation to kill target cells. NK cells play a role that is analogous to CD8$^+$ cytotoxic T cells, defending the host from tumours and virally infected cells. They differ from cytotoxic T cells however in that they are capable of killing tumour cells that lack MHC class I. This led to the 'missing self' hypothesis, which predicted the existence of activating and inhibitory receptors on the surface of NK cells (Karre et al., 1986). Subsequent discovery of such classes of receptor revealed the molecular basis for how NK cells decide upon which targets to kill. Activating receptors include CD16, which recognises the Fc portion of IgG antibody and mediates ADCC (Kruse et al.,

2014). Inhibitory receptors include the killer cell immunoglobulin-like receptors (KIRs), which recognise both classical (HLA-A, B, C) and non-classical (HLA-E) MHC class I ligands. Normal cells express MHC class I, with recognition by KIRs inhibiting NK cell killing activity (Moretta and Moretta, 2004). NK cells therefore integrate signals from a sophisticated repertoire of receptors that has evolved to regulate NK cell activity, ensuring that the host is protected against pathogens and the development of tumours, while preventing damaging autoimmune responses.

1.2.4 Granulocytes

Granulocytes (also known as polymorphonuclear cells) are a collection of cell types characterised by the presence of cytoplasmic granules. The neutrophil is the most abundant of the granulocytes, constituting 50-60% of total circulating leukocytes in peripheral blood. As professional phagocytes, neutrophils represent the most rapid responders of the immune system, reaching the site of an infection within 30-60 minutes of its detection. Once they have arrived at the infection site, neutrophils are very short-lived, rapidly phagocytosing pathogens coated with antibodies and complement, as well as damaged cells or cellular debris, before undergoing programmed cell death. Neutrophils also produce neutrophil extracellular traps (NETs), comprising a web of fibres composed of chromatin and serine proteases that trap and kill microbes extracellularly. Furthermore, they produce inflammatory mediators including chemokines that recruit monocytes to the site of infection and stimulate their differentiation into macrophages, thus increasing phagocytosis and enhancing clearance of the infection.

Other granulocytes include eosinophils (~1-5% of circulating leukocytes) which are important in immunity against extracellular pathogens including parasites and helminths. Eosinophils, along with mast cells and basophils, also mediate allergic responses via histamine release. Upon activation, these cells rapidly release preformed mediators including histamine (and heparin, in the case of mast cells), in addition to synthesising lipid mediators of inflammation (prostaglandins and leukotrienes). Also produced are a range of cytokines that activate effector functions of other immune cells. Mast cells circulate in an immature form, while mature (tissue) mast cells are extremely similar in appearance and function to basophils. Basophils are fully mature when in circulation, leading to the initial assumption that mast cells were tissue-resident basophils. However, it has since been shown that the two cells develop from different haematopoietic lineages (Franco et al., 2010). Basophils are

the least abundant type of immune cell in peripheral blood, accounting for ~0.1-0.3% of circulating leukocytes.

1.3 The Skin as an Immunological Organ

As the largest organ in the body, the skin acts as a critical physical barrier, protecting the organs and tissues within from the external environment. The skin is also home to vast numbers of immune cells. These immune cells are diverse in many aspects including origin and function, and maintain an immunological barrier to infection that complements the physical barrier provided by the tissue itself. In this section, I will outline the anatomical make-up of the largest organ in the body, before discussing in detail the immune cells that are present.

1.3.1 Anatomy of the skin

The skin is a highly complex organ which fulfils a variety of functions including, but not limited to, physical sensing, temperature control, barrier function and immunity, as recently reviewed in a special issue of *Science* entitled "Exploring the Skin" (21 November 2014, Vol 346, Issue 6212). Human skin consists of two main compartments, namely the outer epidermis and underlying dermis. The epidermis forms a physical barrier, limiting the entry of microorganisms that make up the substantial microbiome on the skin, as well as other pathogens and particulate matter in the environment. Composed of four stratified layers, the epidermis is made up of specialised epithelial cells called keratinocytes, which constitute more than 90% of total epidermal cells. The outermost layer of the epidermis, the stratum corneum, is composed of dead keratinocytes (known as corneocytes) that perform the main barrier functions. Keratinocytes in the basal layer of the epidermis (known as the stratum basale) are responsible for establishing the upper layer of corneocytes through cell division, their progeny migrating upwards as they differentiate and eventually die. Keratinocytes do not only provide a structural role however, as they provide key support in immune defence through production of cytokines, chemokines and antimicrobial proteins in response to pathogenic stimuli (Nestle et al., 2009). Epidermal keratinocytes express several TLRs (Janeway, 1989), TLR activation on keratinocytes leading to the production of a number of inflammatory chemokines including CXCL8, CCL2 and CXCL10, which control the recruitment of neutrophils, monocytes and inflammatory T cells, respectively. In addition, keratinocytes can be induced to secrete inflammatory mediators such as TNFα and type I IFN (Miller and Modlin, 2007). Specialised cells of the epidermis also include melanocytes, which produce the skin pigment melanin, and Langerhans cells, a specialised type of DC and the major epidermis-resident immune cell.

While the epidermis has a simple histology, the underlying dermis is anatomically more complicated, with a far greater diversity of immune cells. The dermis is composed of a network of resident stromal cells called fibroblasts that produce a collagen-rich extracellular matrix. Separated from the epidermis by a continuous basement membrane, the dermis contains many specialised immune cells, including DCs (of which there are several subsets), CD4$^+$ and CD8$^+$ T cells, innate lymphoid populations such as γδ T cells and NK cells, in addition to macrophages and mast cells. Blood vessels and lymphatic vessels are distributed throughout the dermis, facilitating entry of immune cells from the blood and exit to the lymph node, respectively. Hair follicles serve as a niche for keratinocyte, melanocyte and mast cell progenitors (Kumamoto et al., 2003). The anatomy of human skin and the immune cells which are resident there during normal conditions are shown in **Figure 1.2**.
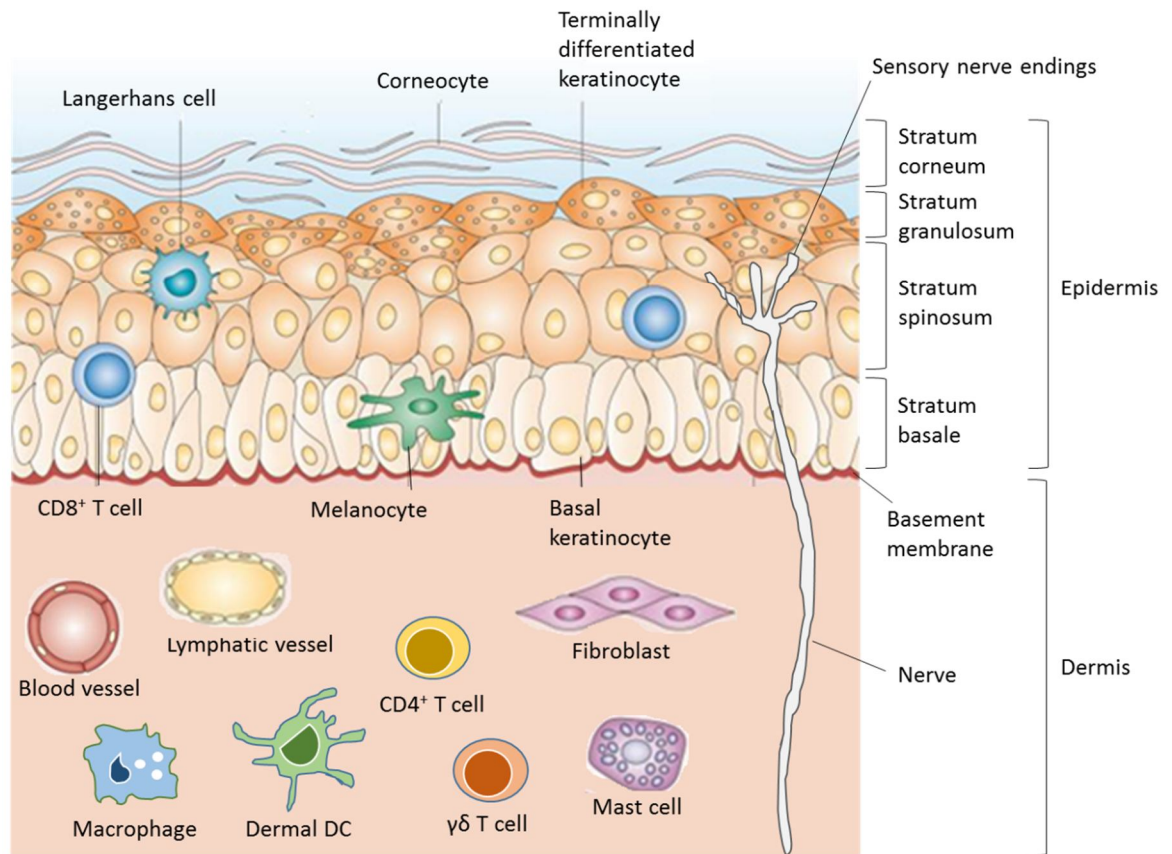
Figure 1.2. Anatomy and resident immune cells of healthy human skin.

The complex structure of the skin reflects the range of functions that it performs, which include maintaining a protective barrier, regulating body temperature, gathering sensory information from the environment and having an active role in the immune system. The epidermis is organised into distinct layers of keratinocytes at different stages of differentiation, namely the stratum basale, stratum spinosum, stratum granulosum and the outermost layer, the stratum corneum, which is responsible for the vital barrier function of the skin. Langerhans cells represent the specialised DCs of the epidermis, while CD8^{+} cytotoxic T cells can be found in the stratum basale and stratum spinosum. The dermis is composed of collagen, elastic tissue and reticular fibres. It contains many specialised immune cells, including dermal DCs, CD4^{+} and CD8^{+} T cells, innate lymphoid cells such as γδ T cells, macrophages and mast cells. Fibroblasts in the dermis also have important immune functions including cytokine production. Blood and lymphatic vessels are present throughout the dermis. The entire surface of the skin receives its nerve supply from the central nervous system, which gathers sensory information regarding touch, pressure, temperature and pain. Figure adapted from (Nestle et al., 2009)

1.3.2 Mononuclear phagocyte system (MPS) of the skin

The MPS in the skin consists of a number of different cell types, each with unique but overlapping functions with respect to the immune response, including phagocytosis, cytokine production and antigen presentation. Data obtained from countless studies performed in both human and mouse have informed us of their origin and function. Here, I will attempt to summarise the existing literature on the MPS in skin, beginning with the specialised epidermal DC population, Langerhans cells.

1.3.2.1 Langerhans cells

Langerhans cells (LCs) represent the specialised DC of the epidermis, where they constitutively reside in the suprabasal layers and are regularly spaced between keratinocytes (Valladeau and Saeland, 2005). Their location makes LCs the first immunological barrier to the external environment. Studies using human skin explants have shown that upon uptake of exogenous antigen, LCs stop sampling the external environment, upregulate and redistribute MHC class II molecules on their cell surface, and upregulate their expression of co-stimulatory molecules such as CD40 as well as the chemokine receptor CCR7 (Larsen et al., 1990). In mouse, up-regulation of CCR7 has been shown to be essential for LC migration via dermal lymphatic vessels to skin draining lymph nodes (Ohl et al., 2004), where they localise in T-cell areas and present antigen to T cells (Randolph et al., 2008). LCs migrate to the draining lymph nodes during the steady state (Hemmi et al., 2001), while their rate of migration has been shown to be increased during inflammation (Stoitzner et al., 2005).

LCs in both human and mouse are identified based on the expression of the haematopoietic marker CD45 and MHC class II. They also express langerin (also known as CD207) on the cell-surface, a type II C-type lectin receptor that binds mannose and related sugars (Valladeau et al., 2000). A unique feature of LCs is the presence of a special type of intracytoplasmic organelle known as the Birbeck granule. Their function remains poorly defined, however it has been shown that their formation is a consequence of antigen capture by langerin, leading to a proposed role in antigen processing and presentation (Valladeau et al., 2000). Other surface markers used to identify LCs include CD1a, a human-specific cell surface molecule expressed at very high levels by LCs and which presents microbial lipid antigens to T cells, and E-cadherin, an adhesion molecule that anchors LCs to neighbouring keratinocytes (Tang et al., 1993).

Most lymphoid-organ and cutaneous DC populations are eliminated following lethal irradiation, being replaced by circulating donor-derived precursor cells following congenic HSCT (Holt et al., 1994, Iijima et al., 2007). LCs in humans (and mice) are partially resistant to radiotherapy however, establishing a unique origin of these cells. Recipient LCs that remain in mice following the radiation regimen are able to repopulate the skin independently of donor circulating precursor cells, with incorporation of bromodeoxyuridine (BrdU) confirming that recipient LCs were proliferating in situ (Merad et al., 2008, Merad et al., 2002). Therefore, in the absence of inflammation, it is hypothesised that epidermal LCs are maintained through self-renewal. It has been shown that murine LCs are seeded in the epidermis from embryonic (yolk sac-derived) precursors prior to birth, independent of haematopoiesis (Merad et al., 2008), and that they have a relatively long half-life during the steady-state, estimated at 53-78 days (Vishwanath et al., 2006). Indeed, following conditional ablation of LCs in langerin-DTR (diphtheria toxin receptor) transgenic mice, their repopulation occurs slowly over several weeks, compared with several days for conventional DCs (Kissenpfennig et al., 2005). While equivalent studies are more difficult to carry out in humans, experimental results suggest that human LCs share similar properties with mouse LCs in terms of their origin and reconstitution kinetics. Human LCs proliferate *in situ* (Czernielewski and Demarchez, 1987, Vaigot et al., 1985), while donor LCs have been shown to persist for years in a recipient of a human limb graft (Kanitakis et al., 2004). Furthermore, recipient LCs have been identified in the epidermis more than one year after transplantation in patients that have received allogeneic HSCT, despite complete engraftment of donor cells in the blood (Collin et al., 2006). These results establish that, similar to their mouse counterparts, human LCs can renew locally and are able to resist radiation-based transplantation regimens.

LCs that are lost during the steady-state or following minor injuries are repopulated locally and independently of circulating precursor cells throughout the lifespan of the mouse. Cell-cycle analysis has shown that ~2-3% of LCs in mouse and human epidermis are proliferating (Merad et al., 2008); this is likely sufficient to maintain LC numbers during the steady-state due to their slow rate of turnover. Renewal of LCs lost during inflammation appears to involve a different mechanism however. Following exposure of murine skin to ultraviolet B radiation, which leads to inflammation and severe LC loss, repopulation of LCs is mediated by circulating monocytes (Ginhoux et al., 2006, Merad et al., 2002). Here, repopulation of epidermal LCs by blood monocytes was dependent on expression of the chemokine receptors CCR2 and CCR6 by monocytes. The infiltrating monocytes proliferated locally and repopulated

the LC pool in 10-15 days (Merad et al., 2002). Of note, in absence of inflammation (i.e. during the steady-state), mice that lack CCR2 or CCR6 have normal numbers of LCs in the epidermis (Cook et al., 2000, Sato et al., 2000). Observations made using human cells *in vitro* support a similar process occurring in human. Monocytes give rise to LCs during *in vitro* culture with granulocyte macrophage colony-stimulating factor (GM-CSF), IL-4 and transforming growth factor-beta 1 (TGF-β1), while differentiation into LCs is accompanied by the sequential expression of CCR2 and CCR6 (Geissmann et al., 1998). Expression of TGF-β1 by keratinocytes, as well as LCs themselves, is required for LCs to develop *in vivo* (Borkowski et al., 1996). Experiments performed by our research group using skin-equivalent models, in which skin is reconstituted *in vitro* from skin stem cells, showed that monocytes can differentiate into LCs in the epithelium. This study also proposed that chemokine (C-X-C motif) ligand 14 (CXCL14) is important in guiding monocytes to the epidermal niches where this differentiation takes place (Schaerli et al., 2005). The role of CXCL14 (and other chemokines) in the development and maintenance of tissue phagocytes is discussed later on.

Of note, an additional epidermal DC subset, distinguishable from LCs by the expression of macrophage mannose receptor (MMR; also known as CD206), is found in the inflamed epidermis of patients with atopic dermatitis (Wollenberg et al., 2002). Referred to as inflammatory dendritic epidermal cells (IDECs), these cells overexpress high-affinity Fc receptor for IgE (FcεR1), facilitating their reactivity to IgE-bound allergens and resulting in the pro-inflammatory allergen-specific response observed in these patients (Bieber, 2007).

1.3.2.2 Dermal DCs

The DC populations found in peripheral tissue may be divided into conventional DCs, plasmacytoid DCs and monocyte-derived DCs. During steady-state conditions, pDCs are absent from the skin, only being found in inflamed skin where they promote wound repair through production of type I interferons (Gregorio et al., 2010), and so they will not be discussed here. In mouse, it has been shown that Ly6C^{hi} monocytes (the equivalent of human CD14^{++}CD16^{-} classical monocytes) continuously extravasate from the blood into tissues including skin and lung during the steady-state, where they perform functions including carriage of antigen to draining lymph nodes and activation of T cells (Jakubzick et al., 2013, Tamoutounour et al., 2013). In these studies however, differentiation of monocytes into DCs was not observed, revising a long-held view that monocytes differentiate into macrophages or DCs by default upon

entering tissues. Moreover, McGovern et al. has recently shown that CD14^{+}, non-autofluorescent cells in human dermis, traditionally referred to as CD14^{+} DCs, align more closely with blood monocytes and dermal macrophages at both a phenotypic and transcriptional level, and are distinct from conventional DCs. The authors also demonstrated that in patients following HSCT, reconstitution of CD14^{+} dermal cells coincided with the recovery of blood monocytes (McGovern et al., 2014, Haniffa et al., 2009). The short half-life of these cells during the steady-state (< 6 days) has led to the suggestion that CD14^{+} cells in the dermis are in fact a short-lived, resident monocyte population, and provides new evidence for the fate of monocytes that leave the blood to enter peripheral tissues on a continuous basis.

Conventional DC populations in human dermis also have a short life-span (in contrast to epidermal LCs), while it seems that they too are dependent on blood-borne precursors for their continual replenishment (McGovern et al., 2014). It has been shown in mouse that conventional DCs are derived from the circulating myeloid DC populations already discussed, sometimes referred to as pre-conventional DCs (Geissmann et al., 2010). Attempts have been made to identify cell surface markers which can be used to distinguish the various DC subsets that reside in human dermis under normal conditions. Human dermis is populated by at least three DC subsets; CD141^{hi} DCs (Haniffa et al., 2012), CD1a^{+} DCs (Angel et al., 2006) and CD14^{+} "DCs" (although recent evidence suggests that they may in fact be a tissue-resident monocyte population – see above) (Haniffa et al., 2009, Nestle et al., 1993). CD1c has also been shown to be a useful marker for identifying myeloid DCs in the dermis (Nestle et al., 1993, Zaba et al., 2007). CD141^{hi} DCs lack CD14 expression, while CD14^{+} DCs co-express CD141 which is further upregulated during spontaneous migration from skin explant culture (Chu et al., 2012). Recently, it has been shown that CD141^{hi} tissue DCs are the counterparts of CD141^{+} blood DCs (Haniffa et al., 2012).

1.3.2.3 Dermal macrophages

Macrophages, the phagocytic cells first described over a century ago by Metchnikoff (Gordon, 2008), are distributed throughout the body being found in almost every tissue. In similar fashion to LCs, the relationship between blood monocytes and tissue macrophages is complicated and represents one of the most rapidly evolving fields of research within immunology. As a single cell type, macrophages exhibit unparalleled heterogeneity, with macrophages in different anatomical locations displaying remarkably different functions Examples include clearance of surfactant by alveolar

macrophages in the lung, synaptic pruning and immune surveillance in the brain by microglia and regulation of the host-microbe balance by intestinal macrophages (Davies et al., 2013a). The suggestion that blood monocytes give rise to tissue macrophages was first made by Van Furth and colleagues, who observed a rapid entry of monocytes from the blood into the peritoneal cavity in a model of sterile inflammation (van Furth and Cohn, 1968). It was later discovered that blood and bone marrow precursors can be differentiated into macrophages by *in vitro* culture with GM-CSF (Stanley et al., 1976, Stanley et al., 1975), while more recent studies have confirmed the precursor-progeny relationship between blood monocytes and tissue macrophages in the context of infection and inflammation (Epelman et al., 2014, Tamoutounour et al., 2013). During the inflammatory response, tissue macrophages can become polarised into one of several specific activation states, depending on the type of inflammation. Two well-established polarised phenotypes are the classically-activated "M1" macrophages and alternatively-activated "M2" macrophages (reviewed by (Mantovani et al., 2005)). The M1 phenotype is linked with T_H1 responses and IFN-γ production by antigen-activated immune cells, leading to a strong pro-inflammatory macrophage phenotype characterised by production of interferons and antimicrobial effectors such as nitric oxide. The M2 phenotype, on the other hand, is induced by the T_H2-associated chemokines IL-4 and IL-13 and is characterised by enhanced endocytic activity, increased MHC class II expression and reduced pro-inflammatory cytokine secretion (Martinez and Gordon, 2014). During the steady-state, the function of macrophages, as well as their relationship with blood monocytes, is less clear.

Human dermal macrophages are large cells with a foamy cytoplasm that express CD14 but not CD1a. A study of the phenotypic profile of dermal DCs and macrophages in normal human skin identified CD163 (a scavenger receptor expressed by most tissue macrophages) and factor XIIIa (a component of the coagulation cascade with a potential function in wound healing) as useful markers for macrophage identification (Zaba et al., 2007). Macrophages are also highly autofluorescent cells, their autofluorescence being most visible in channels excited by the 488 nm laser when phenotyping by flow cytometry (Haniffa et al., 2009). Dermal macrophages are predominantly sessile, i.e. are largely absent among emigrant cells during skin tissue culture, although it has been shown that they are capable of migrating to lymph nodes under certain conditions of inflammation (van Furth et al., 1985). In comparison to dermal DCs, dermal macrophages have a poor capacity for antigen presentation. They express genes that support specific roles in scavenging

cell debris and killing microorganisms, in addition to expressing high levels of the anti-inflammatory chemokine IL-10 (Tamoutounour et al., 2013), suggesting that they may have a more anti-inflammatory, wound healing, M2-like function. Some dermal macrophages, especially those located in close proximity to blood vessels, produce chemokines that play a role in the extravasation of neutrophils into the dermis during infection (Abtin et al., 2014). Therefore, in addition to roles in tissue homeostasis and repair, dermal macrophages might have important roles in the immune response to invading microorganisms.

Human dermal macrophages have a slower rate of turnover and a longer half-life than dermal DCs (Haniffa et al., 2009, McGovern et al., 2014). Early reports postulated that all tissue macrophages were derived from blood monocytes. However, it has since become apparent that the majority of macrophage subsets are seeded in tissues from yolk sac-derived progenitors during embryonic development, prior to the appearance of the haematopoietic system. Furthermore, they maintain themselves during adult life by local proliferation, independently of input from circulating precursors (Schulz et al., 2012, Perdiguero and Geissmann, 2016). However, there is recent evidence to show that macrophages found in the dermis of adult mice consist of a subset that is established prenatally and a subset that develops after birth from Ly6C^{hi} monocytes (Jakubzick et al., 2013, Tamoutounour et al., 2013). It has been postulated that the contribution of monocytes to the dermal macrophage pool may increase throughout life, especially following episodes of inflammation; a feature that has been shown for cardiac macrophages in mouse (Epelman et al., 2014). Therefore, it is likely that the origin of dermal macrophages is complex, consisting of a pool that is established prenatally and a pool established after birth.

1.3.2.4 *Summary of the mononuclear phagocyte system*

Recent findings have challenged the overly simplistic view that there is a population of cells arising from a bone marrow progenitor, which enter the blood as monocytes and subsequently enters tissues, where they differentiate into macrophages and DCs. Certain members of the MPS which are resident in peripheral tissues are of haematopoietic origin and require continuous reconstitution from blood-borne precursors (conventional DCs for example). Other populations however, including macrophages and LCs, are seeded during embryogenesis and maintained in adulthood by local proliferation, independently of the haematopoietic system. Renewal of tissue-resident MPS populations may therefore be achieved by several mechanisms, namely 1) self-renewal of differentiated cells, 2) differentiation of a

tissue-resident precursor or 3) extravasation and differentiation of circulating precursors such as blood monocytes (Merad et al., 2002, Kennedy and Abkowitz, 1998). In reality, these mechanisms are unlikely to be mutually exclusive, and could operate in parallel or sequentially during the life of the organism. Which mechanism(s) predominate at any given time is also likely to depend on environmental influences such as infection and inflammation. The relationship between the haematopoietic progenitor cells, circulating precursors and differentiated cells of the MPS (macrophages and DCs) which are present in normal human skin is shown in **Figure 1.3.**
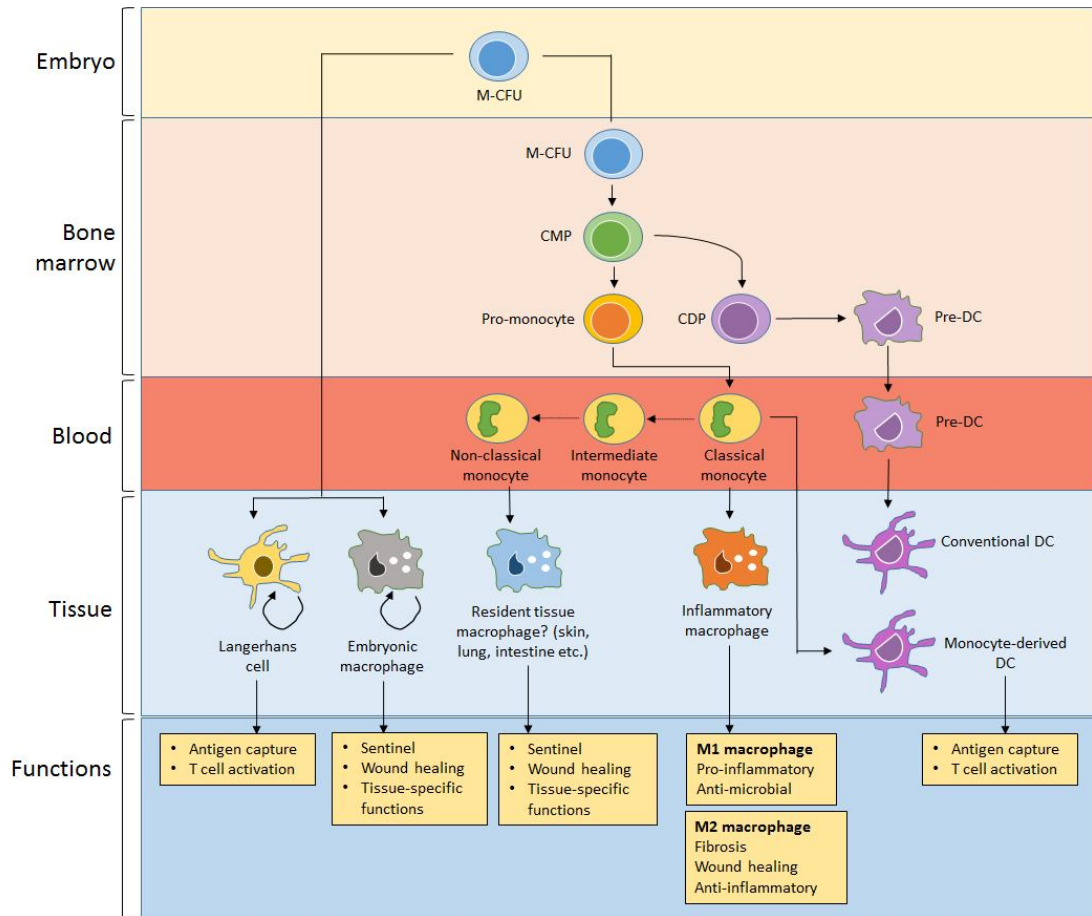
Figure 1.3. The mononuclear phagocyte system.

The cells of the mononuclear phagocyte system are derived from multipotent progenitor cells (myeloid colony-forming units (M-CFU)) in the bone marrow of the mature adult or the yolk sac of the developing embryo. In the bone marrow, monocytes develop from a common myeloid progenitor (CMP), via the pro-monocyte precursor step. Monocyte exit into the bloodstream is dependent on expression of the chemokine receptor CCR2. The CMP also gives rise to the common DC progenitor (CDP), which develops into pre-DCs in the bone marrow before being released into circulation. The major subset of classical monocytes gives rise to the intermediate and non-classical subsets. During the steady-state, there is likely continuous low-level recruitment of classical and non-classical monocytes into tissues, where they replenish the resident macrophage pool, having sentinel and wound-healing functions. Classical monocytes likely also give rise to tissue cells with DC-like functions, including superior antigen-presenting capacity in comparison to macrophages, and which traffic to draining lymph nodes where they activate T cell responses. In contrast, Langerhans cells in the epidermis and a pool of dermal macrophages are maintained during the steady-state through local proliferation. Recent studies indicate that they initially develop from myeloid stem cells in the yolk sac of the developing embryo, and are seeded in tissues before birth. In response to inflammation, classical monocytes differentiate into inflammatory macrophages, which depending on the inflammatory milieu, may polarise into specific phenotypes, broadly defined as M1 and M2. Figure adapted from (Lawrence and Natoli, 2011).

23

1.3.3 Other immune cell types present in healthy human skin

1.3.3.1 T cells

T cells are present in vast quantities in healthy skin, with T cells in human skin outnumbering those found in the blood. $CD4^+$ T cells are found in large numbers in the dermis, with only a small fraction of skin $CD4^+$ T cells being located in the epidermis. In contrast, $CD8^+$ T cells are predominantly localised to the epidermis in human, where they persist for long periods and are commonly referred to as tissue-resident memory T cells (T_{RM}). In contrast to T cells, B cells are rare in healthy skin (Mueller et al., 2014).

1.3.3.2 Innate lymphoid cells

A number of innate lymphoid cell (ILC) populations are found in healthy human skin. γδT cells in the dermis and epidermis contribute to immune responses as well as maintaining barrier integrity. Dendritic epidermal γδT cells (DETC), a subset that exists only in mice, produce molecules including JAML and CD100 in response to infection or wounding that assist in wound closure. In addition, several other innate lymphoid populations have been described in mouse skin, including $NKp46^+$ NK cells and Thy-1^+ IL-13-producing ILC2 cells, and there is evidence to suggest that equivalent populations exist in healthy human skin (Mueller et al., 2014).

1.3.3.3 Mast cells

Mast cells are derived from haematopoietic progenitor cells and undergo differentiation and maturation in peripheral tissues, not being found as mature cells in the blood. The stem cell growth factor receptor (SCFR, also known as c-kit) is typically expressed on mast cells in various tissues, independently of maturation stage or activation status, and serves as a good marker for this cell type (Valent and Bettelheim, 1992). The prototypical function of mast cells is IgE receptor-mediated release of histamine in allergic reactions. Mast cells in the dermis therefore have an important role in the pathology of allergic skin conditions such as atopic dermatitis (Liu et al., 2011b).

1.3.4 Methods employed to study immune cells in human skin

Investigations into the functions of human leukocytes are usually conducted on immune cells isolated from blood. The reason for this is clear; obtaining a peripheral blood sample from a human donor is much less invasive than taking a tissue sample. Furthermore, it is often with considerable difficulty that immune cells are isolated from solid organs such as skin, while immune cell isolation from blood is comparatively easy. Therefore, despite the relative ease with which skin samples can be obtained compared to other organs, we still have only a rudimentary understanding of the origin and function of many of the immune cell subsets which reside there.

Much research on immune cell function in skin has employed imaging techniques such as immunofluorescence and immunohistochemistry, which allow the visualisation of cell-associated markers *in situ*. However, these techniques are limited by the number of colours that can be used simultaneously (generally up to four). Interest is therefore extremely high in using isolation techniques that allow multicolour flow cytometry on immune cells extracted from skin, as this allows much more sophisticated and complex phenotyping to be performed. Several groups, including ours, have devised techniques for the obtaining single cell suspensions from skin samples. Some of these techniques involve initial mechanical disruption of the tissue, followed by the release of cells using an enzyme-based digestion protocol. Others involve allowing skin cells to spontaneously emigrate from skin explants in culture, although in these protocols there is an extended period of time (generally 2-3 days) between tissue sampling and immune cell recovery. Furthermore, certain cell types present in human skin (dermal macrophages for instance) do not spontaneously emigrate from skin explants, instead remaining fixed in the tissue, and can only be recovered by proteolytic digestion (Haniffa et al., 2009).

The recruitment of immune cells to peripheral sites depends on their extravasation from the blood, followed by chemotaxis to their intended destination within the tissue. Chemokines are heavily involved in both of these processes. In cooperation with adhesion molecule interactions, chemokines present on blood microvascular endothelial cells contribute to leukocyte extravasation, whereas chemokine-producing tissue cells define the destination of extravasated leukocytes. Here, I will introduce the human chemokine system and discuss its role in controlling leukocyte migration, with particular attention paid to the homeostatic immune processes occurring in skin during the steady-state. This will bring me on to the focus of my PhD, the human chemokine CXCL14.

1.4 The Chemokine Superfamily

Chemokines are crucial players in instructing all immune cells where to go. From their initial development and maturation in the primary lymphoid organs (bone marrow and thymus) and exit into the bloodstream, to their extravasation into peripheral tissues, to their arrival at distinct locations within the tissue where differentiation to effector cells takes place, chemokines are present at every step along the life cycle of a leukocyte. There is emerging evidence, however, that chemokines do not only regulate cell migration, instead having sophisticated effects on target cells that include adhesion, survival and proliferation (Burns et al., 2006), as well as inhibition of HIV entry (Berger et al., 1999, Oberlin et al., 1996). Furthermore, chemokines have their own functions (independent of interacting with host cells), such as direct antimicrobial activity against many types of pathogenic microorganisms (Wolf and Moser, 2012). This remarkable diversity in the functions of chemokines is an important reason why chemokine biology has become such an active area of research since the discovery of the first chemokine, namely chemokine (C-X-C motif) ligand 8 (CXCL8).

1.4.1 Chemokines

The field of chemokine research began nearly 30 years ago with the discovery of CXCL8 (also known as interleukin-8) by peptide sequencing, which followed the observation that activated monocytes secreted a soluble factor that showed specific chemoattractant activity for neutrophils (Baggiolini et al., 1989). Several agonists which demonstrated chemotactic activity on immune cells were known at the time, including the complement protein C5a, the formylated peptide fMet-Leu-Phe, and the lipid leukotriene B_4. CXCL8 triggered responses in neutrophils similar to those induced by the known chemoattractants, but acted through a novel receptor, leading to the suggestion that CXCL8 represented a novel class of chemotactic proteins. The search for proteins related to CXCL8 began, and the analogs identified were named "chemokines", in abbreviation of "chemotactic cytokines". The three-dimensional structure of CXCL8 has since been elucidated (Clore et al., 1990). It has all the hallmarks of the chemokine family and is shown in **Figure 1.4**.

Chemokines are structurally very similar, highly basic proteins of 70-125 amino acids with molecular masses ranging from 6 to 14 kDa. It is possible to divide the chemokine family into subsets based on the position of two highly conserved, N-terminal cysteine residues. Although sequence identity among chemokines is often quite low, their overall tertiary structure is strikingly similar (Clark-Lewis et al., 1995). Most

chemokines contain four cysteine residues in highly conserved positions which form two disulphide bonds, one between the first and third cysteines and one between the second and fourth cysteines. These disulphide bonds are instrumental in determining the 3-dimensional folding of the peptide, creating a structure which contains three β-sheets with short loops (see Figure 1.4). The two major structural subsets of chemokines are the **C-X-C chemokines** (also known as α-chemokines), where the two N-terminal cysteines are separated by a single amino acid; and the **C-C chemokines** (also known as β-chemokines), where the two N-terminal cysteines are adjacent. There are only three chemokines that fall outside of these two categories. XCL1 (also known as lymphotactin) and XCL2, which possess only two rather than the usual four cysteine residues, corresponding to the second and fourth cysteines of the other classes. The third is CX3CL1 (fractalkine), in which the two N-terminal cysteines are separated by a sequence of three amino acid residues. The human chemokine superfamily is summarised in **Table 1.1**.

Although there are examples of membrane-bound chemokines (CX3CL1 for example (Imai et al., 1997)), most chemokines are secreted. To elicit chemotaxis *in vivo* therefore, they must be immobilised on cell or extracellular matrix surfaces. Being highly basic proteins consisting of many positively charged amino acids, immobilisation of chemokines occurs by low-affinity interaction with negatively charged glycosaminoglycans (GAGs) (Krohn et al., 2013, Lortat-Jacob et al., 2002). Proteoglycans consist of a protein core to which GAG chains are attached, GAGs representing a heterogeneous population of large, unbranched polysaccharides that fall into five main groups; heparin, heparan sulphate, chondroitin sulphate, dermatan sulphate and hyaluronic acid. They are ubiquitously present in the extracellular matrix and on the surface of cells, including leukocytes themselves. Interaction with GAG is thought to facilitate the retention of chemokines on cell surfaces, thereby forming a high local concentration required for cell activation. This interaction occurs via the C-terminal portion of the chemokine, leaving the N-terminal region of the chemokine free to activate the receptor (Handel et al., 2005, Proudfoot, 2006).
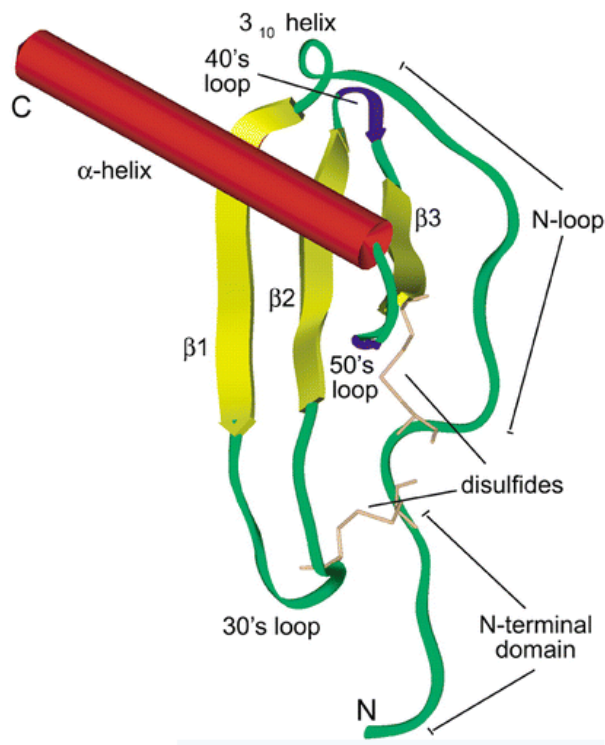
Figure 1.4. Ribbon structure of the prototypical chemokine CXCL8.

An N-terminal region precedes the first cysteine residue. Following the first two cysteines is a loop of approximately ten residues which, in most cases, is succeeded by one strand of a 3_{10} helix. The region of the peptide between the second cysteine and the 3_{10} helix is known as the N-loop. The single-turn 3_{10} helix is succeeded by three anti-parallel β strands, forming a β-pleated sheet. Finally, there is a C-terminal α-helix. Each structural unit is connected by turns known as the 30s, 40s and 50s loops, which reflects the numbering of residues in the mature protein. The 30s and 50s loops contain the latter two of the four cysteine residues. The first two cysteines following the N-terminal sequence limit the flexibility of the N-loop, owing to the disulphide bridges formed with the third and fourth cysteines. Despite this, the flexibility of the N loop is greater than the flexibility of the other regions of the protein (excluding the N and C termini). The flexibility of the N loop is thought to play an important role in chemokine receptor binding and/or activation. Figure adapted from (Fernandez and Lolis, 2002).

1.4.2 Chemokine receptors

Chemokine receptors are 7TM GPCRs, typically 340-370 amino acids in length, which are embedded in the lipid bilayer of the cell membrane. Differentially expressed on all leukocytes, most chemokine receptors signal following ligand binding via coupling of the receptor to G proteins of the G_i subtype. This was first elucidated in experiments which showed that treatment of neutrophils with *Bordetella pertussis* toxin inhibited

stimulation with CXCL8 (Thelen et al., 1988). The conclusion that the CXCL8 receptor is coupled to heterotrimeric G_i proteins, which are sensitive to pertussis toxin treatment, has become the paradigm for the signal transduction of all chemokine receptors known today. In the human genome, a total of 18 'chemotactic' chemokine receptors have been identified to date, namely CCR1-10, CXCR1-6, XCR1 and CX3CR1 (**Table 1.1**). The exception to this paradigm is the atypical chemokine receptors which do not signal, instead appearing to shape chemokine gradients and reduce inflammation by scavenging chemokines in a G protein-independent manner (Nibbs and Graham, 2013). There are five atypical chemokine receptors; DARC (ACKR1), D6 (ACKR2), CXCR7 (ACKR3), CCRL1 (ACKR4) and CCRL2 (ACKR5). The structure of a typical human chemokine receptor (CCR1) is shown in **Figure 1.5**.

Figure 1.5. Structure and amino acid sequence of the human chemokine receptor CCR1.
The typical structure of a chemokine receptor is depicted, showing the seven transmembrane domains (numbered I-VII), three extracellular loops (ECL1-3) and three intracellular loops (ICL1-3). The shaded horizontal band represents the cell membrane. Amino acids are listed with a single letter code. The residues highlighted in red depict peptide motifs which are conserved among all typical chemokine receptors.

Although sequence identity between signalling chemokine receptors varies considerably (ranging from 25-80%), they all share several peptide motifs which are also highly conserved throughout vertebrate evolution. The amino acid sequence DRYLAIV (Asp-Arg-Tyr-Leu-Ala-Ile-Val), or subtle variations of that sequence, is found in the cytoplasmic region of the receptor at the junction of the third transmembrane domain (TM-III) and the second intracellular loop (ICL-2). It has been proposed that the DRYLAIV motif plays a crucial role in coupling the receptor to intracellular signal transduction pathways following chemokine engagement (Nomiyama and Yoshie, 2015), especially since the motif is substantially altered in the atypical chemokine receptors, indicating that this sequence is necessary for G protein-coupling. There are several other motifs and residues that are conserved among chemokine receptors. These include TLPxW, a conserved motif located in the 2nd transmembrane region and NPxxY, a conserved motif located at the boundary between the 7th transmembrane region and the cytoplasmic tail. These conserved amino acid sequences are thought to act as molecular "micro-switches", in that they mediate the transition of the receptor from an inactive to an active state by inducing conformational changes (Nygaard et al., 2009). The conserved motifs important to chemokine receptor function are indicated in **Figure 1.5**. A comprehensive review of the functional roles of conserved chemokine receptor motifs can be found in (Nomiyama and Yoshie, 2015).

Table 1.1. The human chemokine superfamily.

Chemokine				
Common name	Systematic name	Receptor	Leukocyte distribution	Key immune functions
IL-8	CXCL8	CXCR1	Neutrophil > monocyte, NK, mast cell, basophil, CD8$^+$ T cell	Neutrophil trafficking
GCP-2	CXCL6			
NAP-2	CXCL7	CXCR2	Neutrophil > monocyte, NK, mast cell, basophil, CD8$^+$ T cell	Neutrophil egress from bone marrow, neutrophil trafficking
ENA-78	CXCL5			
GROα	CXCL1			
GROβ	CXCL2			
GROγ	CXCL3			
PF4	CXCL4			
IP-10	CXCL10	CXCR3	T_H1, CD8$^+$ T_{CM} and T_{EM}, Treg, T_{FH}, NK, NKT, pDC, B cell	T_H1-type adaptive immunity
MIG	CXCL9			
I-TAC	CXCL11			
SDF-1	CXCL12	CXCR4	Most (if not all) leukocytes	Haematopoiesis, organogenesis, bone marrow homing
BCA-1	CXCL13	CXCR5	B cell, T_{FH}, T_{FR}, CD8$^+$ T_{EM}	B and T cell trafficking to B cell zone of lymph nodes
SR-PSOX	CXCL16	CXCR6	T_H1, T_H17, γδ T, ILC, NKT, NK, plasma cell	Innate lymphoid cell function, adaptive immunity
DMC	CXCL17	Unknown		Macrophage homing to mucosal sites, in particular lung
BRAK	CXCL14	Unknown		Monocyte and macrophage homing to mucosal sites
MCP-1	CCL2	CCR2	Classical monocyte, macrophage, T_H1, iDC, basophil, NK	Monocyte trafficking, T_H1-type adaptive immunity
MCP-4	CCL13			
MCP-3	CCL7	CCR5		
MCP-2	CCL8	CCR1		
MIP-1β	CCL4	CCR3		

Ligand	Chemokine	Receptor	Expressing cells	Function
MIP-1α	CCL3	CCR5	Monocyte, macrophage, T_H1, NK, Treg, CD8$^+$ T cell, DC, neutrophil	T_H1-type adaptive immunity
RANTES	CCL5			
MPIF-1	CCL23			
HCC-1	CCL14	CCR1	Monocyte, macrophage, neutrophil, T_H1, basophil, DC	Innate and adaptive immunity
HCC-2	CCL15			
HCC-4	CCL16			
Eotaxin	CCL11	CCR3	Eosinophil > basophil, mast cell	T_H2-type adaptive immunity, eosinophil distribution and trafficking
Eotaxin-2	CCL24			
Eotaxin-3	CCL26			
TARC	CCL17	CCR4	T_H2, skin- and lung-homing, T, Treg, TH17, CD8+ T, monocyte, B cell, iDC	Homing of T cells to skin and lung, T_H2-type immune responses
MDC	CCL22			
MIP-3α	CCL20	CCR6	T_H17 > iDC, γδ T, NKT, NK, Treg, T_{FH}	iDC trafficking, T_H17 adaptive immune responses
ELC	CCL19	CCR7	Naïve T, T_{CM}, mature DC, B cell	Mature DC, B and T cell trafficking to T cell zone of lymph nodes, egress of DC and T cells from tissue
SLC	CCL21			
I-309	CCL1	CCR8	T_H2, Treg, skin T_{RM}, γδ T	Immune surveillance in skin, T_H2-type adaptive immunity
PARC	CCL18			
TECK	CCL25	CCR9	Gut-homing, T, thymocytes, B cell, DC, pDC	Homing of T cells to gut, GALT development and function
CTACK	CCL27	CCR10	Skin-homing T cell, IgA$^+$ plasma cells	Humoral immunity at mucosal sites including skin
MEC	CCL28			
Lymphotactin	XCL1	XCR1	Cross-presenting CD8$^+$ DC, thymic DC	Antigen cross-presentation by CD8$^+$ T cells
SCM-1β	XCL2			
Fractalkine	CX3CL1	CX3CR1	Non-classical monocyte, macrophage, T_H1, CD8$^+$ T_{EM}, NK, γδ T cell, DC	Patrolling monocytes in innate immunity and T_H1-type adaptive immunity

Table is modified from (Xu et al., 2015) and (Griffith et al., 2014).

Abbreviations: DC, dendritic cell; GALT, gut-associated lymphoid tissue; iDC, immature dendritic cell; ILC, innate lymphoid cell; NK, natural killer; NKT, natural killer T; T_{CM}, central memory T cell; T_{EM}, effector memory T cell; T_{FH}, T follicular helper cell; T_{FR}, follicular regulatory T cell; T_H, T helper; Treg, regulatory T cell; T_{RM}, resident memory T cell. > indicates higher level of receptor expression relative to other cell types.

1.4.3   Interaction between chemokines and their receptors

Interaction between chemokines and their receptors is normally considered in the context of a 1:1 stoichiometric complex. A two-step model was initially proposed for the activation of chemokine receptors (Monteclaro and Charo, 1996), while more recent studies have sought to elucidate the molecular basis for this interaction (Nomiyama and Yoshie, 2015, Rajagopalan and Rajarathnam, 2006, Scholten et al., 2012). In the first step, an interaction occurs between the core globular domain of the chemokine, and the N-terminal extension and second extracellular loop of its receptor. This initial interaction has been shown to define receptor specificity and affinity (Monteclaro and Charo, 1996). A conformational change in the chemokine occurs, presumed to be largely mediated by the flexible N-loop, which brings about the next step. The N-terminal portion of the chemokine prior to the first cysteine interacts with specific residues in the ligand-binding pocket, which is buried in the cavity formed by the extracellular loops (Nygaard et al., 2009). This interaction induces an overall conformational change in the receptor, exemplified by the reorganisation of the transmembrane bundle consisting of seven α-helices (Govaerts et al., 2003). It is now understood that this transmembrane reorganisation is a hallmark of the transition from inactive to active states. Activation of the chemokine receptor is shortly followed by exchange of bound GDP for GTP by the α-subunit of the heterotrimeric G protein. The G proteins disassociate from the receptor and activate several effector molecules downstream, which results in a cascade of diverse signalling events within the cytoplasm of the cell. The signalling cascades which are elicited following chemokine receptor activation are comprehensively reviewed here (Mellado et al., 2001a, Patel et al., 2013), and include activation of the mitogen-activated protein kinase (MAPK) cascade and release of calcium ions (Ca^{2+}) from intracellular stores. It has been demonstrated that induction of such signalling cascades by chemokines leads to activation of transcription factors and altered gene expression in cells. The termination of chemokine receptor signalling in the continued presence of agonist is accomplished by a coordinated series of events, characterised by three distinct processes; desensitisation, sequestration and down-regulation, which are mediated by a family of adapter molecules called beta-arrestins. Within seconds of chemokine receptor activation, phosphorylation of serine and threonine residues within the cytoplasmic loops and C-terminal domain of the receptor by G protein-coupled receptor kinases (GRKs) leads to the recruitment of beta-arrestins. Binding of beta-arrestins blocks coupling between the receptor and heterotrimeric G proteins, leading to termination

of signalling by G protein effectors (desensitisation). Receptor-bound beta-arrestins bind to components of the clathrin endocytic machinery, mediating endocytosis of receptors via clathrin-coated pits within minutes of chemokine binding (sequestration). Once internalised, receptors are trafficked to an acidified endosomal compartment, wherein the ligand is dissociated and the receptor is either recycled to the plasma membrane or targeted for degradation (down-regulation) (Luttrell and Lefkowitz, 2002).

It has been demonstrated that the length and amino acid composition of the N-terminus determines to which receptor(s) a chemokine will bind, whether it will bind with high or low affinity, and whether binding has agonistic or antagonistic effects (Clark-Lewis et al., 1995). For example, CXC chemokines are further classified according to the presence of the tripeptide motif ELR (glutamic acid-leucine-arginine) in the N-terminal region. Chemokines which possess an ELR motif are specific for CXCR1 and/or CXCR2, expressed on cells of myeloid lineage. In contrast, ELR-negative chemokines do not interact with CXCR1/2 and attract a variety of leukocytes via binding to alternative chemokine receptors. Truncation of the N-terminus by enzymatic cleavage of N-terminal residues has been shown to result in either increased or decreased activity of chemokines, or even altered receptor specificity (Mortier et al., 2008). N-terminal modifications, including glycosylation and citrullination, have also been detected on natural chemokines and been shown to modify their activity (Struyf et al., 2003)

The biological consequences of chemokines binding their receptors are multiple and varied, and have been extensively studied both *in vivo* and *in vitro*. As per their definition, an activity of all chemokines is to induce the migration of cells expressing the corresponding receptor toward areas of higher chemokine concentration. Leukocyte activation by chemokines leads not only to chemotaxis, but also to responses that facilitate cell mobility, including the re-structuring of cytoskeletal fibres and adhesion molecule expression. It has also been shown, however, that chemokines may induce responses which are unrelated to leukocyte migration such as cell activation and differentiation (Takahama, 2006), apoptosis (Murooka et al., 2006), angiogenesis (Strieter et al., 1995) or tumour growth and metastasis (O'Hayre et al., 2008, Zlotnik, 2006). Which signalling cascade(s), and ultimately which cellular responses are triggered, depends on the chemokine and the receptor engaged. The requirement for chemokine receptor-mediated signals ranges from the apparently redundant (as in the case of CCR5, which is missing in some individuals), to the

essential (as in the case of CXCR4, which is essential for late embryogenesis and organogenesis) (Murphy et al., 2000).

1.4.4 Chemokines in the control of immune cell migration

Chemokines are critical players in the cell migration required for immune cell development and homeostasis, to that required for the generation of cellular and humoral immune responses, to the pathological recruitment of immune effector cells in disease (Griffith et al., 2014). As different chemokines have different roles in the immune response, chemokines are also divided into functional subsets. The **inflammatory chemokines** are generally absent from healthy tissues, but their expression is rapidly induced in response to proinflammatory stimuli such as cytokines (e.g. TNFα and IL-1β) and microbial products such as LPS. Under pathological conditions, the inflammatory chemokines control the recruitment of immune effector cells to the inflammatory site. Typical inflammatory chemokines include CXCL8 and CXCL1 which, along with complement proteins like C5a, recruit neutrophils in the very early stages of an infection by binding to the receptors CXCR1 and CXCR2, respectively. Inflammatory chemokines are also important in the later stages of the immune response to an infection. For example, CXCL9, CXCL10 and CXCL11 recruit T_H1 cells during the adaptive immune response, via binding to the receptor CXCR3. The inflammatory chemokines typically have a high potency, with concentrations of <10 nM sufficient to stimulate chemotaxis of target cells. There is apparent redundancy within the inflammatory chemokines, with a single chemokine being capable of binding to several receptors and single receptor being recognized by several chemokines. This contrasts with the **homeostatic chemokines**, which control the migratory patterns of immune cells during the steady-state, i.e. in the absence of inflammation. The homeostatic chemokines exhibit much less redundancy, each member usually only binding to a single chemokine receptor.

1.4.4.1 Chemokines in homeostatic immune processes

The development and differentiation of immune cell precursors, which takes place in the bone marrow and the thymus, is under fine control by homeostatic chemokines. The development of haematopoietic precursors from the bone marrow called thymocytes into mature T cells takes place in the thymus, and depends on the interaction of CCL21, CCL25 and CXCL12, produced by the thymic epithelium, with CCR7, CCR9 and CXCR4 expressed on thymocytes (Love and Bhandoola, 2011). In the bone marrow, the steady-state retention and development of haematopoietic stem

cells (HSCs) is heavily dependent on CXCL12 (also known as stromal cell-derived factor 1; SDF-1) produced by bone marrow stromal cells, its interaction with CXCR4 on HSCs promoting their retention within bone marrow niches (Ara et al., 2003). This is exemplified in patients treated with granulocyte colony-stimulating factor (G-CSF), which promotes the destruction of CXCL12 in the bone marrow leading to rapid mobilisation of HSCs into peripheral blood (Petit et al., 2002) – a common method of obtaining HSCs for transplant. CXCL12-CXCR4 interactions have also been shown to be necessary for the normal development of multiple immune cell lineages in the bone marrow, including B cells, monocytes, neutrophils, NK cells and pDCs (Mercier et al., 2012). Similarly, CCR2 expression on monocytes is necessary for their mobilisation from the bone marrow into circulation, as well as their recruitment to sites of inflammation (Boring et al., 1997, Tsou et al., 2007)

Secondary lymphoid organs (SLOs) include the lymph nodes and spleen, as well as Peyer's patches in the gut. The homeostatic production of chemokines plays an essential role in the development of SLOs during early life, in addition to maintaining the architecture of mature SLOs and recruiting immune cells to these sites (Griffith et al., 2014). Networks of follicular dendritic cells in the B cell follicles produce CXCL13, promoting the homeostatic localisation of B cells in the lymph node via CXCR5 (Legler et al., 1998). At the same time, follicular reticular cells (FRCs) within the T cell area produce CCL19, CCL21 and CXCL12, which promote the entry and localisation of naïve T cells via CCR7 and CXCR4. Most naïve lymphocytes enter lymph nodes via HEVs, which present CCL21 and CCL19 on the luminal endothelium. CXCL12, produced by FRCs and transcytosed across the HEV for presentation on the luminal endothelium, also participates in this process. Once they have entered the lymph node, T cells follow CCL19 and CCL21 gradients into the T cell area (Masopust and Schenkel, 2013). Here, naïve T cells scan DCs for antigen using their T cell receptor (TCR), the DCs also being recruited to the T cell area of the lymph node via CCL19 and CCL21 gradients following up-regulation of CCR7 in response to antigen capture. Prolonged signalling of CCL19 via CCR7 on naïve T cells eventually leads to down-regulation of the receptor and loss of CCR7-mediated retention signals. At this time, T cells that have not encountered their cognate antigen exit the lymph node via sphingosine-1-phopshate (S1P) gradients, after which CCR7 is upregulated and the cycle begins again (Cyster, 2005). Even in the absence of an immune response therefore, naïve lymphocytes actively migrate, circulating from the blood to the SLOs and back into the blood.

Immune processes which occur in the steady-state and are under the control of homeostatic chemokines also occur in peripheral tissues. 'Immune surveillance' is the process by which immune cells patrol the body's tissues, recognising and destroying invading microorganisms to prevent infection, as well as guarding against cancer by eliminating transformed cells. Effective immune surveillance depends on the localisation of immune cells throughout all of the body's tissues, not only in lymphoid organs, and chemokines are thought to play an important role in this process. Much of the research conducted on the cells governing immune homeostasis in peripheral tissues (including skin) concerns resident T cell populations. Work by our group has identified the chemokine receptor CCR8 as a marker for skin-resident T cells. CCR8 was shown to be expressed on the majority of T cells in healthy human skin, while CCR8$^+$ T cells are rare in blood and completely absent from the gut (another epithelial tissue and common site of pathogen entry) (McCully et al., 2012, Schaerli et al., 2004). These data suggest that healthy skin is the physiological target site of CCR8$^+$ T cells. Adding further weight to this notion is the fact that the sole ligand of CCR8, chemokine (C-C motif) ligand 1 (CCL1), is constitutively expressed at strategic locations in healthy human skin, including dermal microvessels and in close proximity to LCs in the epidermis (Schaerli et al., 2004). It has since been demonstrated that CCR8 expression on skin T cells specifically identifies those cells with a 'long-lived memory' phenotype (McCully et al., 2012). Murine models of skin infection with herpes simplex virus (HSV) have identified a skin-resident population of CD8$^+$ tissue-resident T cells with a memory phenotype (T$_{RM}$). These cells are long-lived, patrol the tissue in a sentinel-like fashion and provided local protection to re-infection with HSV (Gebhardt et al., 2009). The existence of CCR8$^+$ T$_{RM}$ cells in healthy human skin has led to the suggestion that they too have sentinel function, engaging in immune surveillance. Whether or not they confer long-term immune protection, however, remains to be elucidated. It has been discovered that skin-specific factors produced by keratinocytes during the steady-state, including prostaglandin E2 (PGE$_2$) and the active vitamin D metabolite 1α,25-dihydroxyvitamin D3 (1,25(OH)$_2$D3), induce CCR8 expression on activated human naïve T cells during *in vitro* culture (McCully et al., 2015, McCully et al., 2012). These findings provide the strongest evidence yet that expression of CCR8 identifies T cells with a specific function to home to healthy human skin. CCR4, CCR6 and CCR10 have all been implicated in the homing of effector T cells to the skin during inflammatory conditions, however it is unlikely that these receptors regulate homeostatic migration. CCR10$^+$ cells are not detected in healthy skin, while the CCR4 ligands CCL17 and CCL22, and the sole CCR6 ligand CCL20 are barely detectable in normal skin but increase substantially with the

inflammation associated with atopic dermatitis, psoriasis and cutaneous lymphomas (McCully and Moser, 2011). Furthermore, CCR4$^+$ T cells have been identified in inflammatory conditions affecting the liver and lung (Oo et al., 2010, Vijayanand et al., 2010), indicating that CCR4 aids the non-selective migration of effector cells to many inflamed sites. Of note, another chemokine receptor with a well-defined selective tissue-homing function during homeostasis is CCR9 which, in conjunction with the α4β7 integrin, is involved in T cell-homing to the gut in response to constitutive expression of CCL25 by intestinal epithelial cells (Iwata et al., 2004).

Apart from CCL1, the only other homeostatic chemokines that are detectable in healthy human skin are CXCL12 and CXCL14 (McCully and Moser, 2011, Meuter and Moser, 2008, Pablos et al., 1999). Unlike CCL1, however, CXCL14 is also present in many other peripheral tissues during the steady-state. Its widespread expression in the periphery but absence from primary and secondary lymphoid tissues makes CXCL14 unique among the homeostatic chemokines. CXCL14 is highly selective for blood monocytes, while failing to exhibit chemotactic activity on lymphocytes (Kurth et al., 2001). It is therefore intriguing to think that CXCL14 may play an important role in maintaining resident populations of myeloid 'immune surveillance' cells in healthy peripheral tissues. In skin, these may include such populations as dermal macrophages and DCs, or epidermal LCs. Confusion persists with regard to the target cells of CXCL14 however, owing to the fact that the receptor for CXCL14 has not yet been discovered. Here, I will summarise what is known about CXCL14, including its spatial and temporal patterns of expression, its activity on immune cells and work involving the CXCL14-knockout mouse. I will follow this by outlining the aims of this project and the important research questions with regard to CXCL14 function that I have sought to answer during my PhD.

1.4.5 Chemokine (C-X-C motif) ligand 14

1.4.5.1 Structural properties

CXCL14, also known as breast and kidney-expressed chemokine (BRAK), B cell- and monocyte-activating chemokine (BMAC) and macrophage inflammatory protein 2-gamma (MIP-2g), was one of the last chemokines to be discovered (Frederick et al., 2000, Hromas et al., 1999, Sleeman et al., 2000). Initially expressed as a 99-amino acid pro-peptide, cleavage of a 22-amino acid sequence from the NH$_2$-terminal end yields a full-length protein consisting of 77 amino acids (**Figure 1.6**). Unlike some members of the α-chemokine sub-family, CXCL14 does not possess an ELR motif in

its N-terminal region. In fact, CXCL14 has an unusually short N-terminal amino acid sequence, there being just two amino acid residues (Ser-Lys) prior to the first cysteine. In most chemokines, the N-terminal region consists of five or more amino acids, and these residues have been shown to be important in receptor interaction (Clark-Lewis et al., 1994). Another unique characteristic of CXCL14 is that its peptide sequence includes an insertion of five amino acids ([41]VSRYR[45]), not seen in any other CXC chemokines (**Figure 1.7**). Despite these peculiarities in its structure, the amino acid sequence of CXCL14 is highly conserved among vertebrate species as diverse as mammals, birds and fish. Indeed, human and mouse CXCL14 differ by only two conservative amino acid substitutions (Ile_{36} -> Val_{36} and Val_{41} -> Met_{41}) (Wolf and Moser, 2012). CXCL12 is the only other human chemokine which is as highly conserved throughout evolution (DeVries et al., 2006). In fact, both CXCL12 and CXCL14 are regarded as evolutionary ancient chemokines due to their highly conserved sequence throughout different vertebrate classes (**Figure 1.6**). Interestingly, there is recent evidence to show that CXCL14 and CXCL12 modulate one-another's activity, suggesting that the two chemokines may have evolved together (Salogni et al., 2009, Tanegashima et al., 2013a, Tanegashima et al., 2013b).

Figure 1.6. Structure, peptide sequence and evolutionary conservation of CXCL14 and CXCL12.
(a) Mature human CXCL14 is a 77 amino acid peptide with all the hallmark structural features of a chemokine, including three anti-parallel β-strands and a C-terminal α-helix. Its high isoelectric point (pI = 9.90) is also consistent with its function as an antimicrobial peptide. **(b)** Human CXCL12 is a 68 amino acid peptide that has a similar structure to CXCL14. Both chemokines exhibit a remarkable degree of sequence similarity throughout evolution. Sequence alignments were performed using Clustal Omega multiple sequence alignment tool. Amino acids conserved between all species are shown by an asterisk. Figure adapted from (Wolf and Moser, 2012) and (Lu et al., 2016).

```
                                                                ⇩        ⇩                      ⇩
CXCL14    ---------SKCKCSRKGPK-IRYSDVKKLEMKPKYPHCEEKMVIITTKSVSRYRGQEHCLHPKLQ
CXCL12    ---KPVSLSYRCPCRFFESH-VARANVKHLKILN-TPNCA-LQIVARLK----NNNRQVCIDPKLK
CXCL13    -VLEVYYTSLRCRCVQESSVFIPRRFIDRIQILPRGNGCPRKEIIVWKK-----NKSIVCVDPQAE
CXCL8     AVLPRSAKELRCQCIKTYSKPFHPKFIKELRVIESGPHCANTEIIVKLS-----DGRELCLDPKEN
CXCL10    ---VPLSRTVRCTCISISNQPVNPRSLEKLEIIPASQFCPRVEIIATMK----KKGEKRCLNPESK
CXCL9     ---TPVVRKGRCSCISTNQGTIHLQSLKDLKQFAPSPSCEKIEIIATLK-----NGVQTCLNPDSA
CXCL1     ---ASVATELRCQCLQTLQG-IHPKNIQSVNVKSPGPHCAQTEVIATLK-----NGRKACLNPASP
CXCL2     ---APLATELRCQCLQTLQG-IHLKNIQSVKVKSPGPHCAQTEVIATLK-----NGQKACLNPASP

CXCL14    STKRFIKWYNAWNEKRRVYEE------------------------
CXCL12    WIQEYLEKALNKRFKM-----------------------------
CXCL13    WIQRMMEVLRKRSSSTLPVPVFKRKIP------------------
CXCL8     WVQRVVEKFLKRAENS-----------------------------
CXCL10    AIKNLLKAVSKERSKRSP---------------------------
CXCL9     DVKELIKKWEKQVSQKKKQKNGKKHQKKKVLKVRKSQRSRQKKTT
CXCL1     IVKKIIEKMLNSDKSN-----------------------------
CXCL2     MVKKIIEKMLKNGKSN-----------------------------
```

Figure 1.7. Sequence alignment of CXCL14 and selected other CXC chemokines.
Alignment of human CXCL14 with other CXC chemokines reveals unique features of CXCL14. Evident is the short N-terminal region of CXCL14, there being only two amino acids prior to the first cysteine. The five-residue sequence unique to CXCL14 (VSRYR) is also highlighted in blue. The four cysteine residues that are characteristic of all CC and CXC chemokines are highlighted in red. Other residues shared between CXCL14 and most or all of the other chemokines are indicated by an arrow. Sequence alignments were performed using Clustal Omega multiple sequence alignment tool.

1.4.5.2 Expression in human tissues

Published studies regarding the functions of CXCL14 in physiological and pathological situations are few in number, and in many cases contradictory. Initial studies revealed that CXCL14 transcripts were abundant in many human tissues during the steady-state, notably in skin, but also in intestine, kidney, pancreas, heart, brain, placenta, liver, skeletal muscle and breast (Cao et al., 2000, Frederick et al., 2000, Hromas et al., 1999, Kurth et al., 2001). Expression in healthy peripheral tissues, but absence from secondary lymphoid organs (Meuter and Moser, 2008), suggested that CXCL14 has a unique role among chemokines in the control of immune cell trafficking during homeostasis. In skin, CXCL14 protein is present at remarkably high levels throughout the epidermis, where it is associated with basal keratinocytes as well as more differentiated keratinocytes in a suprabasal location (Frederick et al., 2000, Schaerli et al., 2005). Epidermal expression of CXCL14 appears much more prominent than any other chemokine with constitutive expression at this site, including CCL1, which targets skin-homing immune surveillance T cells

and CXCL12, which has broad target cell selectivity (Schaerli et al., 2005). In the dermis, CXCL14 expression is much more scattered and was demonstrated to localise with blood vessels in the superficial dermal plexus. Furthermore, it was shown that macrophages, mast cells and possibly fibroblasts are CXCL14-producing cells in human dermis under normal conditions (Meuter and Moser, 2008, Schaerli et al., 2005).

1.4.5.3 *Chemoattractant activity and target cells*

Studies performed by our group have shown that CXCL14 is a low potency chemoattractant for human blood monocytes and the human monocytic cell line THP-1 (Kurth et al., 2001, Schaerli et al., 2005, Sleeman et al., 2000). Using an *in vitro* model of human epidermis, where epidermal equivalents (EEs) were generated from epidermal stem cells derived from outer root sheaths of healthy human hair follicles, it was shown that CXCL14 produced by EEs recruited CD14$^+$ monocytes to the suprabasal layer. Here, they underwent differentiation into Langerhans-like cells, acquiring DC-like morphology, while expression of CD1a and langerin was detected on some cells (Schaerli et al., 2005). Monocytes have been shown to be the precursors for differentiation into LCs in inflammatory settings in mouse, and this *in vitro* data suggest that the same may be true in human skin. Others have provided evidence for a role for CXCL14 in the chemotaxis of immature DCs (Salogni et al., 2009, Shellenberger et al., 2004), neutrophils (Cao et al., 2000) and activated NK cells (Starnes et al., 2006). Furthermore, CXCL14 involvement in trophoblast and NK cell recruitment to the uterus during pregnancy has been proposed (Kuang et al., 2009b, Mokhtar et al., 2010). The *in vivo* relevance, however, of many of these findings is yet to be established. The target cells and physiological functions of CXCL14 reported in the literature are summarised in **Table 1.2**.

Up to this point, work conducted using the CXCL14 knockout (CXCL14-KO) mouse has failed to enhance our understanding of its physiological functions. Differences in the expression pattern of CXCL14 exist between human and mouse; CXCL14 is expressed in the lungs of mice, while being absent from human lungs (Meuter and Moser, 2008). Our group has reported previously a severe breeding defect in these mice (Meuter et al., 2007), which may arise from abnormal trophoblast migration to the uterus (Kuang et al., 2009a). In viable CXCL14-KO mice no immune phenotype was detected, with macrophage and DC populations in healthy epithelial tissues, recruitment of immune cells to inflamed peritoneum and skin wound healing following mechanical injury all appearing to be unimpaired (Meuter et al., 2007). This may be

explained by functional redundancy, as is commonly seen in the chemokine system i.e. other chemokine(s) being able to compensate for the absence of CXCL14. However, its unique features, including extremely high expression in a range of healthy non-lymphoid tissues and selectivity for myeloid cells (monocytes in particular), point toward a non-redundant function for CXCL14 in immune regulation that remains to be elucidated.

1.4.5.4 Antimicrobial activity

The ability to kill microorganisms, including common pathogens, has been described for the majority of chemokines. *In vitro* experiments using CXCL14 have revealed that CXCL14 has broad-spectrum antimicrobial activity for gram-positive and gram-negative bacteria, including skin commensals as well as frequent pathogens, while CXCL14 also killed the yeast *Candida albicans* (Maerki et al., 2009). CXCL14 was also shown to be important in the clearance of *Streptococcus pneumoniae* pulmonary infection in mice (Dai et al., 2015). This, together with CXCL14 expression in the epidermis as well as the taste buds of the tongue (Hevezi et al., 2009) strongly support a role for CXCL14 in antimicrobial immunity *in vivo*. CXCL14 shares several structural features with non-chemokine anti-microbial peptides, such as a high density of positive charges at physiological pH, a core structure consisting of three anti-parallel β-strands reminiscent of β-defensin, and a C-terminal α-helix that is typical of LL-37 (Wolf and Moser, 2012).

1.4.5.5 CXCL14 in disease

Expression of CXCL14 by epidermal keratinocytes is suppressed at the sites of skin inflammation characteristic of atopic dermatitis and psoriasis (Kurth et al., 2001, Maerki et al., 2009). Furthermore, treatment of freshly isolated keratinocytes and dermal adherent cells (including fibroblasts) with the pro-inflammatory cytokines TNFα and IL-1β dramatically reduced their expression of CXCL14, in complete contrast to inflammatory chemokines such as CCL20 which displayed vastly increased expression (Schaerli et al., 2005). These findings further support an important role for CXCL14 in the control of immune cell function in peripheral tissues during the steady-state. Although numerous reports have implicated CXCL14 in cancer, its expression is increased in some forms of cancer and decreased in others, leading to confusion on whether CXCL14 displays anti-tumour or tumour-promoting properties (Augsten et al., 2009, Frederick et al., 2000, Ozawa et al., 2006, Shurin et al., 2005, Wente et al., 2008).

Table 1.2. CXCL14 target cells and reported functions of CXCL14 in human immunity

Target cells for CXCL14	Functional effects of CXCL14 activity	Source of CXCL14	Reference
B cells, macrophages, CESS (human B cell line), A20 (murine B cell line), THP-1 (human monocytic leukaemia cell line)	Chemoattraction of CESS and THP-1 cells	Synthesised murine CXCL14	Sleeman et al. 2000
Human neutrophils and monocyte-derived DC	Strong neutrophil chemoattractant, weaker chemoattractant for human mono-DC	Human CXCL14 in supernatant from transfected 293T cells	Cao et al. 2000
Freshly isolated human monocytes (weak), monocytes treated with PGE_2 or forskolin (strong)	Monocyte chemoattractant. CXCL14 signals via Bordetella pertussis toxin-sensitive receptor in PGE_2-treated monocytes	Synthesised human CXCL14	Kurth et al. 2001
Human endothelial cells, monocyte-derived iDCs	Potent inhibitor of chemotaxis for human endothelial cells	Recombinant human CXCL14	Shellenberger et al. 2004
Human monocyte-derived iDCs	Stimulates iDC migration and maturation. Induces NF-Kb activation in these cells	Recombinant human CXCL14	Shurin et al. 2005
$CD14^+$ DC precursors derived from $CD34^+$ HPCs and blood $CD14^+$ monocytes	Stimulation of $CD14^+$ monocyte migration, possible contribution to the differentiation of $CD14^+$ precursors into Langerhans-like cells in epidermal tissue under steady state conditions	Recombinant human CXCL14 and CXCL14 from supernatant of primary keratinocyte culture	Schaerli et al. 2005
Activated human NK cells, monocyte-derived iDCs	Stimulation of activated human NK cells and iDCs, no effect on proliferation or cytotoxic activity of NK cells	Recombinant human CXCL14 and synthesised human CXCL14	Starnes et al. 2006
Human and murine iDCs	Mediator for activin A-induced migration of iDCs	Recombinant human CXCL14	Salogni et al. 2009
Human trophoblasts	Inhibition of human trophoblast invasion and migration	Recombinant human CXCL14	Kuang et al. 2009
Human uterine NK cells	Stimulation of uterine NK cell migration during the secretory phase of the menstrual cycle	Recombinant human CXCL14	Mokhtar et al. 2010
Human THP-1 cells and iDCs	Chemoattractant for THP-1 cells and iDCs	Recombinant human CXCL14	Tanegashima et al. 2010
PGE_2-treated THP-1 cells	Chemoattractant for THP-1 cells	Recombinant human CXCL14	Dai et al. 2015

Abbreviations: DC, dendritic cell; iDC, immature dendritic cell; mono-DC, monocyte-derived DC; NK, natural killer; HPC, haematopoietic precursor cell; PGE_2, prostaglandin E2.

1.4.5.6 *Identity of the CXCL14 receptor(s)*

Discrepancies in the CXCL14 target cells reported by different research groups may be explained by the different sources of CXCL14 used, or the varying sources of cells (e.g. primary DCs from blood/tissue vs. DCs derived from monocytes cultured *in vitro*). In any case, the target cells of any chemokine are defined by expression of its cognate receptor. At this time, the identity of the receptor to which CXCL14 binds in order to induce chemotaxis of target cells is unknown. It has been shown recently that CXCL14 is able to bind the CXCL12 receptor CXCR4 (Tanegashima et al., 2013a, Tanegashima et al., 2013b), which is consistent with its proposed role in modulating CXCL12 activity at CXCR4 (Salogni et al., 2009, Tanegashima et al., 2013a). Curiously, CXCR4 is expressed ubiquitously, suggesting that all types of leukocytes are potential target cells for CXCL14 binding and, possible, function. This contrasts with the limited numbers of immune cells that were shown to respond to CXCL14. In addition, it has since been demonstrated that CXCL14 does not trigger activation of intracellular signalling events upon binding to CXCR4 (Otte et al., 2014), suggesting that binding to CXCR4 is not sufficient to initiate CXCL14-mediated chemotactic responses. Therefore, the receptor used by CXCL14 to elicit chemotaxis of target cells including monocytes remains elusive, thus preventing the definitive identification of CXCL14 targets.

1.5 Hypotheses

Monocytes are the primary target cells of the human chemokine CXCL14, which induces chemotaxis of monocytes via an as yet unidentified GPCR. The ability to respond to CXCL14 will identify monocyte-derived cells in healthy human skin, a peripheral site in which CXCL14 is very highly expressed during the steady-state.

1.6 Research Aims

- To define the target cells of CXCL14 in human peripheral blood, by their ability to migrate in response to CXCL14 in addition to their expression of putative CXCL14 receptor(s)
- By the same approach, determine which immune cell populations resident in healthy human skin are targets for CXCL14

- To confirm the identity of the receptor by which CXCL14 induces chemotaxis of target cells
- To investigate the function of CXCL14 with respect to other homeostatic chemokines, most notably CXCL12

Chapter 2   Materials and Methods

2.1   Chemokines

2.1.1   Chemokines used in functional assays

Human CXC chemokines used in this study were CXCL8, CXCL10, CXCL12, CXCL13 and CXCL14. Human CC chemokines used were CCL2, CCL5, CCL19 and CCL21. All had been chemically synthesised previously according to established protocols (Clark-Lewis et al., 1991). The mouse chemokine murine CCL1 was chemically synthesised by Almac (Craigavon, UK).

2.1.2   Fluorochrome-labelled chemokines

A custom-made, synthetic version of human CXCL14 conjugated to the fluorochrome Alexa Fluor® 647 (AF-CXCL14) was synthesised by Almac. Briefly, an additional Lysine residue was added to the C-terminus of the mature human CXCL14 peptide, to which the Alexa Fluor® 647 compound was covalently attached. A custom-made AF647-labeled murine CCL1 (AF-muCCL1) synthesised by Almac was also used.

2.2   Cell Culture Media and Buffers

2.1.1   Media

Complete RPMI Medium

The cell culture medium used throughout, unless otherwise stated, was RPMI-1640 medium (Life Technologies; Paisley, Scotland) supplemented with 10% heat-inactivated foetal calf serum (FCS), 50 mg/ml penicillin/streptomycin, 2 mM L-glutamine, 1 mM sodium pyruvate and 1% non-essential amino acids (NEAA; all from Life Technologies).

Complete DMEM Medium

Where indicated, Dulbecco's Modified Eagle Medium (DMEM; Life Technologies) used to culture cells was supplemented with 10% FCS and 50 ng/ml penicillin/streptomycin.

2.2.1 Buffers

FACS Buffer

Fluorescence-activated cell sorting (FACS) buffer comprised of sterile phosphate-buffered saline (PBS) supplemented with 2% FCS and 0.02% sodium azide, passed through a 0.22 µm filter prior to use.

MACS Buffer

Magnetic-activated cell sorting (MACS) buffer comprised of sterile PBS supplemented with 2% FCS and 5 mM EDTA, passed through a 0.22 µm filter prior to use.

Chemotaxis Buffer

Plain RPMI-1640 was supplemented with 1% human serum albumin (CSL Behring, Bern) and 20 mM HEPES (Life Technologies).

2.3 Blood Cell Isolation

2.3.1 Isolation of peripheral blood mononuclear cells

All research involving work with human blood and tissue samples was approved by the local Research Ethics Commission and informed consent was obtained from each participating subject. PBMC were prepared from the heparinised blood of healthy human volunteers using Lymphoprep density gradient separation media (Axis-Shield; Dundee, Scotland). Blood was layered on 15 ml Lymphoprep to a total maximum volume of 40 ml, prior to centrifugation at 1680 rpm at 18 °C for 20 minutes with no brake. The PBMC layer, which is present following centrifugation at the interface between the Lymphoprep and the plasma, was aspirated manually using a pasteurette and transferred to a fresh tube. PBMC were washed three times in PBS to remove platelets, and then resuspended in MACS buffer. Cell counts were performed using a haemocytometer, with trypan blue (Sigma-Aldrich; Gillingham, UK) staining used to assess cell viability. Total PBMC were used in some experiments, while in others one or more leukocyte subsets were enriched from PBMC using MACS technology (see below).

2.3.2 Enrichment of monocytes from PBMC

Total monocytes were isolated from PBMC using either anti-CD14 microbeads (positive selection) or using the Monocyte Isolation Kit II (negative selection; both from Miltenyi Biotec; Bisley, UK), according to the manufacturer's instructions. In negative selection, incubation with a cocktail of biotin-conjugated monoclonal antibodies (mAbs) directed against CD3, CD7, CD16, CD19, CD56, CD123 and glycophorin A, is followed by incubation with anti-biotin microbeads. Cells are washed in MACS buffer before magnetically-labelled non-monocytes are depleted over an LS column placed in the magnetic field of a MidiMACS separator. Cells were passed through a second LS column during negative selection (only a single column was used in positive selection). In early 2014, Miltenyi Biotec released the 'pan-monocyte isolation kit', which contains an improved cocktail that does not deplete CD16$^+$ cells, allowing for the simultaneous enrichment of classical (CD14^{++}CD16$^-$), intermediate (CD14^{++}CD16$^+$) and non-classical (CD14$^+$CD16^{++}) monocytes. This kit was used for the negative selection of peripheral blood monocytes from then on. In all cases, monocyte purity ranged from 94 to 99%.

2.3.3 Enrichment of myeloid DCs from PBMC

Blood myeloid DCs comprise two subsets; CD1c$^+$ DCs and CD141$^+$ DCs. Total myeloid DCs were isolated from PBMC using the myeloid DC isolation kit (Miltenyi Biotec), according to the manufacturer's instructions. Non-myeloid DCs were labelled with a cocktail of biotin-conjugated mAbs before subsequent magnetic depletion with anti-biotin microbeads over a single LD column. The resulting myeloid DC purity was 60-70%, representing a significant enrichment from the 1-2% myeloid DC that make up total PBMC.

2.3.4 Enrichment of T cells from PBMC

Total CD3$^+$ T cells were isolated from PBMC using the Pan-T cell Isolation Kit (Miltenyi Biotec), according to the manufacturer's instructions. Briefly, T cells were isolated by negative selection using a cocktail of biotin-conjugated mAbs against CD14, CD15, CD16, CD19, CD34, CD36, CD56, CD123 and CD235a (Glycophorin A). Non-T cells were subsequently magnetically depleted using anti-biotin microbeads over two consecutive LS columns. Resulting T cell purity ranged from 96 to 99%.

2.3.5 Enrichment of neutrophils

Following separation of peripheral blood by centrifugation over a Lymphoprep gradient as previously described, the granulocyte layer at the interface of the Lymphoprep and the red blood cell pellet was recovered. Red blood cells which had been transferred along with the granulocytes were lysed using red cell lysis buffer (eBioscience; Hatfield, UK) for 15 min at RT. Neutrophils were subsequently purified by negative selection using the EasySep™ Human Neutrophil Enrichment Kit (StemCell Technologies, Cambridge, UK). Briefly, non-neutrophils were depleted using a cocktail of bi-specific tetrameric antibody complexes directed against CD2, CD3, CD9, CD19, CD36, CD56, glycophorin A, and dextran-coated magnetic particles. Labelled cells were then depleted using an EasySep™ magnet. Resulting neutrophil purity ranged from 95-97%.

2.4 Cell Culture

2.4.1 Stimulations

PBMC, purified monocytes or THP-1 cells were stimulated for 1-2 days with Prostaglandin E2 (PGE_2; Sigma-Aldrich). PGE_2 was used at a concentration of 1 µM, unless otherwise stated. Selective EP receptor agonists used included 19R(OH)PGE_1, Butaprost and Cay10598, while selective EP receptor antagonists used included SC19220, AH6809 and ONO-AE3-208 (all from Cayman Chemical; Ann Arbor, Michicgan, USA). Agonists and antagonists were used at 10 µM concentration. Sodium butyrate (Sigma-Aldrich) was used at a concentration of 1 mM. Cells were cultured in 12-, 24- or 48-well plates (Nunc, Thermo Fisher Scientific) in a humidified incubator maintained at 37 °C and a mixture of 95% air, 5% CO_2.

2.1.2 Generation of monocyte-Derived DCs

Monocytes purified from PBMC by negative selection were seeded at 5 x 10^5 cells/ml in 6-well plates, and cultured for 6 days in medium supplemented with 100 ng/ml GM-CSF and 50 ng/ml IL-4 (both from Miltenyi Biotec). Medium and cytokines were replenished on days 2 and 4. On day 6, immature DCs were harvested and either used for phenotyping/functional assays or placed back into culture for 24 hours in cRPMI supplemented with 100 ng/ml LPS (Sigma-Aldrich) and 20 ng/ml TNFα, (Miltenyi Biotec), to induce maturation.

2.1.3 T cell expansions

T cell blasts expressing CXCR3, CCR5 and CCR2 were generated according to the protocol described in (Qin et al., 1998). Briefly, CD3$^+$ T cells were resuspended at 2 x 10^6/ml in cRPMI in 24-well plates. Human T Activator CD3/CD28 Dynabeads® (Invitrogen) were added at a bead/cell ratio of 1:4, while medium was supplemented with 100 U/ml IL-2 (Proleukin, Chiron). After 5-6 days, beads were removed using a magnet and T cell blasts were re-plated in fresh cRPMI containing 100 U/ml IL-2 and expanded up to day 21, with media and IL-2 replenished every 3-4 days.

2.4.2 Culture of immortalised cell-lines

THP-1

THP-1, a human acute myeloid leukaemia cell-line, was purchased from the American Type Culture Collection (ATCC; LGC Standards, Teddington, UK). THP-1 cells were cultured in cRPMI supplemented with 50 µM 2-mercaptoethanol (2-ME; Sigma-Aldrich) and were maintained at a cell density of between 2 x 10^5 and 8 x 10^5 cells/ml.

300-19

The murine pre-B cell line 300.19 has been routinely used by our group and others for stable transfection with chemokine receptors (Loetscher et al., 1996, Petkovic et al., 2004). Parental (non-transfected) and stable 300.19 transfectants were cultured in cRPMI supplemented with 50 µM 2-ME. Cultures were not allowed to exceed a cell density of 2 x 10^6 cells/ml. 300.19 cell lines stably transfected with the human chemokine receptors CCR2, CCR5, CCR7, CXCR3, CXCR4, CXCR5 and CCRL2, and the mouse chemokine receptor muCCR8, were used in functional assays.

293T

Human embryonic kidney (HEK) 293T cells were cultured in DMEM in a T75 flask. When cells reached 90-100% confluence, they were passaged by detaching the cells using 0.05% trypsin-EDTA (Life Technologies) for 5 min at 37 °C. 293T cells were used between passage 2 and 4 for production of lentiviral particles (see below).

All cell-lines were routinely tested by PCR for the presence of mycoplasma contamination, and any cultures found to be contaminated were thrown out and replaced.

2.5   Recovery of Immune Cells from Human Split Skin

Human split skin samples (approx. 10 cm^2, 0.4 mm thick) were obtained using a dermatome from the breast region of healthy patients undergoing cosmetic surgery. The skin was cut into 1 cm^2 fragments and partially digested in in 30 ml cRPMI (without serum) containing dispase II (2.5 mg/ml), collagenase D (1 mg/ml) and DNase I (20 U/ml; all from Roche diagnostics, Burgess Hill, UK) in a sterile Erlenmeyer flask (Corning; Sigma-Aldrich) for 18-20 minutes at 37 °C in a shaking water bath. Digestion was stopped by transferring the skin to a petri dish containing cold PBS, and the epidermis was carefully separated from the dermis using forceps. In some experiments, the epidermis and the dermis were cultured separately for 48-72 hours at 37 °C in 6-well plates, in cRPMI supplemented with 10% human AB serum (Sigma-Aldrich). Immune cells which spontaneously migrated out of the tissue during this period were harvested by collecting the supernatant. In other experiments, the dermis was subjected to overnight digestion in medium containing 10% human AB serum and 1 mg/ml collagenase D, which caused total disruption of the tissue. In both cases, single-cell suspensions were obtained by passing the supernatant through a 40-µm cell strainer. Remaining tissue fragments were subjected to mechanical disruption using a syringe plunger and thorough washing with PBS in order to collect as many cells as possible. Cells were washed twice in PBS, counted and resuspended in MACS buffer prior to use in phenotyping and/or functional assays.

2.6   Phenotyping and Functional Assays

2.6.1   Transwell chemotaxis assay

Corning® HTS transwell 96 well permeable supports with 5 µm pores, or HTS transwell 24 well permeable supports with 8 µm pores (Sigma-Aldrich) were used in chemotaxis assays. Chemokine was resuspended in chemotaxis buffer to the desired concentration and placed in the lower chamber. A well containing chemotaxis buffer with no chemokine (blank) was used as a control for random cell migration. Cells were resuspended in chemotaxis buffer and placed in the upper chamber; ~100,000 cells were used per test (**Figure 2.1**). The transwell plate was incubated at 37 °C for between 0.5 and 5 hours, depending on the cell type being tested. See **Table 2.1** for a summary of the specific assay conditions used for each cell type. Upon termination of the assay, the volume in the lower chamber containing migrated cells was collected.

If required, staining for phenotypic markers was performed as described below, and migration was assessed by flow cytometry. AccuCheck counting beads (Life Technologies) were used to enable absolute cell counts, and each test was run in duplicate. Cell migration is expressed either as a percentage of the total input cells or as the chemotactic index, which is defined as the number of cells migrated in response to chemokine divided by the number of cells which migrated in response blank.
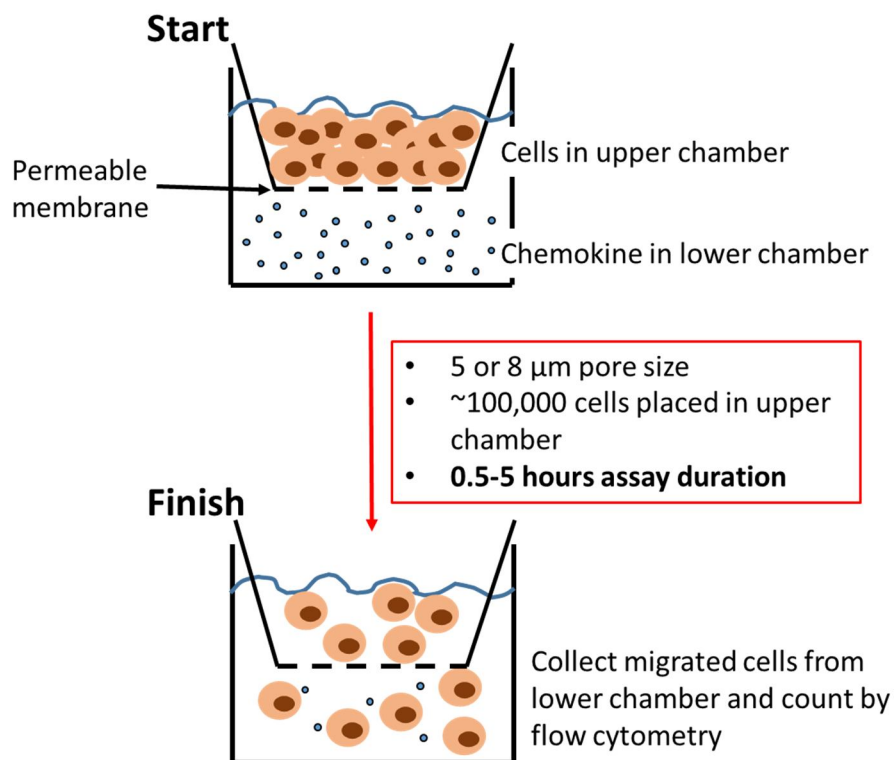
Figure 2.1. Transwell system used in chemotaxis assays.

(**Top**) Chemokine (resuspended in chemotaxis buffer) is placed in the lower chamber. The insert is then lowered into the well, while cells are placed in the upper chamber. The cells and the chemokine are separated by a permeable membrane containing pores of 5 or 8 µm in diameter. The transwell plate is then incubated at 37 °C for between at 0.5 and 5 hours. (**Bottom**) Upon termination of the assay, the insert is lifted out of the well and cells which have migrated are collected from the lower chamber, stained for phenotypic analysis and counted by flow cytometry.

Table 2.1. Parameters of the transwell chemotaxis assay used for different cell types.

Cell	Pore size (μm)	24- or 96-well	Assay duration (hours)
Primary cells			
PBMC	5	96	2-4
Monocytes	5	96	2-4
T cells	5	96	2-4
Neutrophils	5	96	0.5-1
Blood myeloid DCs	5	96	2-4
Monocyte-derived DCs	5 or 8	24 or 96*	4
Skin cells	5 or 8	24 or 96*	4
Cell lines			
THP-1	5 or 8	24 or 96*	3-5
300.19 transfectants	5	96	3-5

* The 8-μm pore polycarbonate inserts are only available in 24-well format.

2.6.2 Cell staining and flow cytometry

All fluorochrome-conjugated mAbs used in flow cytometry experiments, including the clone and supplier, are shown in **Table 2.2**. To begin, cells were washed in PBS by centrifugation at 400 x g for 6 min. This was followed by staining with Live/Dead Fixable Aqua Dead Cell Stain Kit (Life Technologies), used at 1:100 dilution, for 12 min at room temperature. This allowed for the exclusion of dead cells from the analysis. All subsequent steps were performed in FACS buffer. A wash step was followed by blocking of endogenous Fc receptors using human normal immunoglobulin (KIOVIG; Baxter, Staines-upon-Thames, UK) at 1:1000 dilution for 15 min at 4 °C. Cells were then incubated with mAbs directed against cell-surface antigens for 30 min at 4 °C. Appropriate isotype controls were used in all cases. A wash step was followed by resuspension of cells in 150 μl FACS buffer for acquisition.

Sample acquisition was performed using the FACS Canto II or Fortessa instruments (BD, Oxford, UK). Live cells were gated based on their light scatter properties, the exclusion of aggregates on forward scatter area/height plots, while dead cells were discarded on the basis of Live/Dead staining. Data analysis was performed using FlowJo software version 10.0.4 (TreeStar Inc).

Table 2.2. Fluorochrome-conjugated monoclonal antibodies used for flow cytometry.

Antigen	Conjugate	Dilution	Clone	Supplier
Cell-surface marker				
CD1a	FITC	1 in 60	HI149	BioLegend
CD1c (BDCA-1)	BV421	1 in 20	L161	BioLegend
CD3	BV421	1 in 30	UCHT1	BioLegend
CD4	APC	1 in 30	RPA-T4	BD
CD11b	PE	1 in 30	ICRF44	eBioscience
CD11c	PE	1 in 30	S-HCL-3	BD
CD14	PE-Cy7	1 in 40	61D3	eBioscience
CD14	BV421	1 in 40	M5E2	BioLegend
CD15	APC	1 in 10	HI98	BD
CD16	FITC	1 in 30	3G8	BD
CD19	PE-Cy5	1 in 20	HIB19	BioLegend
CD19	APC	1 in 30	SJ25C1	eBioscience
CD33	PE	1 in 30	WM53	BD
CD33	BV421	1 in 40	WM53	BD
CD45	PerCP/Cy5.5	1 in 30	HI30	BioLegend
CD56	PE	1 in 10	B159	BD
CD86 (B7-2)	PE	1 in 10	2331	BD
CD141 (BDCA-3)	APC	1 in 20	M80	BioLegend
CD163	PE	1 in 20	GHI/61	BioLegend
CD207 (Langerin)	PE	1 in 40	10E2	BioLegend
CD209 (DC-SIGN)	FITC	1 in 30	DCN46	BD
CD303 (BDCA-2)	BV421	1 in 20	201A	BioLegend
HLA-DR	APC-H7	1 in 40	L243	BD
Chemokine receptor				
CCR2	APC	1 in 30	K036C2	BioLegend
CCR5	PE	1 in 20	2D7	BD
CCR7	PE-Cy7	1 in 25	G043H7	BioLegend
CXCR1	PE	1 in 40	5A12	BD
CXCR3	FITC	1 in 10	49801.111	R&D
CXCR4	PE	1 in 10	12G5	eBioscience
CXCR4	BV421	1 in 20	12G5	BioLegend
CXCR5	PE	1 in 20	51505.111	R&D
CCRL2	PE	1 in 20	K097F7	BioLegend

All monoclonal antibodies listed are mouse anti-human. Abbreviations: DC-SIGN; Dendritic Cell-Specific Intercellular adhesion molecule-3-Grabbing Non-integrin, FITC; fluorescein isothiocyanate, PE; phycoerythrin, BV; brilliant violet; APC, allophycocyanin; Cy, cyanine; PerCP, peridinin chlorophyll.

2.6.3 Labelling with Alexa Fluor® 647-conjugated CXCL14

Alexa Fluor® 647-CXCL14 (AF-CXCL14) was used to label the putative CXCL14 receptor on the surface of cells. Binding of AF-CXCL14 was performed in FACS buffer for 30 min at 4 °C in a step prior to antibody staining. Binding of AF-muCCL1 to cells was used as a control for non-specific binding. Use of AF-muCCL1 to detect murine CCR8 expression by primary mouse T cells has recently been published by our group (McCully et al., 2015).

2.6.4 Intracellular Ca^{2+} rise

The murine pre-B cell line 300.19 stable transfected with CXCR4 (300.19-CXCR4$^+$) was used in experiments measuring intracellular Ca^{2+} rise. 2 x 10^5 cells were prepared in 200 µl mixed salt buffer (MSB; 136 mM NaCl, 4.8 mM KCl, 20 mM HEPES, 1 mM $CaCl_2$ and 10 mM glucose). Cells were loaded with 1 µM Fura-2-acetoxymethyl ester (Fura-2AM; ThermoFisher), a ratiometric fluorescent dye which binds to free intracellular calcium, on poly-D-lysine-coated slides (MatTek, Ashland, Massachusetts, USA) for 20 min at 37 °C. Loaded cells were washed with MSB and imaging was recorded with a 40x oil-immersion objective on an inverted microscope (Axiovert 200; Carl Zeiss) with excitation at 340 nm and 380 nm using the Polychrom V illumination system from TILL photonics GmbH. An image was recorded each second. The first chemokine injection was made after 50 seconds of recording, while in instances where a second chemokine injection was made, this was done at 100 seconds. Recording was stopped after 300 seconds. Analysis was performed using ImageJ software, with the 340/380 ratio providing a relative measure of cytoplasmic-free Ca^{2+} concentration. Fluorescence values were exported to Microsoft Excel for the generation of graphs.

2.6.5 Chemokine receptor internalisation

Cells were incubated for 1 hour at 37 °C in cRPMI supplemented with the indicated chemokine and concentration. Expression of its cognate receptor on the cell surface was determined by flow cytometry.

2.7 Techniques used to Study Protein-Protein Interactions

2.7.1 Nuclear magnetic resonance spectroscopy and surface plasmon resonance

Nuclear magnetic resonance (NMR) and surface plasmon resonance (SPR) experiments were carried out in order to study the physical interaction between two chemokines (NMR and SPR) or between chemokine and GAGs (SPR). Reagents (chemokines) were provided by myself, however the experiments were performed by Hugues Lortat-Jacob and Yoan Monneau at the University of Grenoble (Grenoble, France).

NMR experiments were performed at 298K on a Bruker 850-MHz spectrometer with 1.7 mm CryoProbe. SOFAST-HMQC spectra were recorded on 30 µl of either 75 µM free 15N-labelled CXCL12 or a 1:1 mixture of 15N-labelled CXCL12 and unlabelled CXCL14 (each at a concentration of 75 µM). The CXCL12 residues whose NMR signal changed position in the presence of CXCL14 were identified by visual comparison of the spectra from CXCL12 alone and CXCL12 + CXCL14.

SPR experiments were performed on a Biacore instrument (GE Healthcare). Reducing end biotinylated heparan sulphate and C-terminal biotinylated CXCL12 or CXCL14 were prepared as described (Sadir et al., 2004, Sarrazin et al., 2005). Heparan sulphate (20 µg/ml), CXCL12 or CXCL14 (both at 5 µg/ml) were injected over a streptavidin-activated sensorchip and captured to a level of 80, 1600 and 2900 resonance units (RU), respectively. For binding assays, the protein of interest (soluble CXCL12 or CXCL14) in HBS-P running buffer (10mM HEPES, 0.15 M NaCl, 0.005% P20, pH 7.4) were injected at 50 µl/min over both a negative control (streptavidin only) and a functionalized surface for 5 min at 25°C. The surfaces were regenerated with a 3 min pulse of 2 M NaCl (HS) or a 1 min pulse of 10 mM HCl (CXCL12 or CXCL14).

2.7.2 Förster resonance energy transfer

Förster (or fluorescence) resonance energy transfer (FRET) experiments were carried out in order to study the formation of CXCR4 and CCR2 homodimers on transiently transfected HEK293T cells. All FRET experiments were performed by Mario Mellado and Laura Martinez-Munoz at the National Centre for Biotechnology in Madrid, Spain. HEK293T cells were transiently cotransfected with CXCR4-CFP (cyan fluorescent protein, donor fluorophore) and CXCR4-YFP (yellow fluorescent protein, acceptor

fluorophore) at different ratios, and FRET saturation curves were extrapolated from the data using a non-linear regression equation applied to a single binding site model in GraphPad Prism version 5.0 (GraphPad Software, Inc., CA, USA), as previously described (Martinez Munoz et al., 2009).

To determine the effect of ligand treatments on CXCR4 homodimer formation, HEK293T cells were transiently cotransfected with CXCR4-CFP/CXCR4-YFP (donor/acceptor) at a fixed ratio that gives maximum FRET efficiency (established from the FRET saturation curve). Cotransfected cells were then stimulated for 30 minutes at 37ºC with CXCL12 (1 nM or 100 nM), CXCL14 (300 nM) or CXCL12 + CXCL14 (1 nM + 300 nM, respectively). An increase in FRET efficiency is indicative of CXCR4 homodimer formation.

To determine the effect of ligand treatments on the CCR2 homodimer formation, HEK293T cells were transiently cotransfected with CCR2-CFP/CCR2-YFP at a fixed ratio that gives maximum FRET efficiency. Cotransfected cells were then stimulated for 30 minutes at 37ºC with CCL2 (0.1 nM or 100 nM), CXCL14 (300 nM) or CCL2 + CXCL14 (0.1 nM + 300 nM, respectively). An increase in FRET efficiency is indicative of CCR2 homodimer formation.

2.8 Quantitative Real-time PCR

2.8.1 RNA isolation

Cells for RNA extraction were resuspended in Buffer RLT Plus (Qiagen) for cell lysis, to which 2-ME was added immediately prior to use (10 µl 2-ME per 1 ml Buffer RLT Plus). Cells in lysis buffer were stored at -80 °C prior and thawed prior to RNA extraction. Total RNA was extracted from cells using the RNeasy Plus Mini Kit (Qiagen), which incorporates a step for removal of genomic DNA. The recovered RNA was resuspended in 35 µl deionised water and examined using a NanoDrop ND1000 (Thermo Scientific) for RNA concentration and purity (ratios of OD at wavelengths of 230, 260, and 280 nm). RNA was either used the same day for cDNA generation, or was stored at -80 °C prior to use.

2.8.2 Generation of cDNA

cDNA was synthesised from 1 µg RNA by reverse transcription (RT) using the High Capacity RNA-to-cDNA kit (Applied Biosystems), according to the manufacturer's instructions. cDNA was used immediately in quantitative real-time PCR (qPCR) experiments, or placed at -20 °C for long-term storage.

2.8.3 qPCR

The amount of target gene transcript was determined using pre-designed TaqMan Gene Expression Assays and reagents (all from Thermo Fisher), according to the manufacturer's instructions. Briefly, each 20 µl reaction contained cDNA (2 µl), TaqMan Gene Expression Assay (1 µl), TaqMan Universal MasterMix II, no UNG (10 µl) and RNase-free water (7 µl). A no template control (where no cDNA is added) served as a control for extraneous nucleic acid contamination, while a no reverse transcriptase control (where the cDNA generation step is carried out in the absence of reverse transcriptase) served as a control for carryover of genomic DNA. Reactions were performed using a ViiA7 real-time PCR system (Applied Biosystems). All tests were performed in triplicate. TaqMan Gene Expression Assays with the following Thermo Fisher assay identification numbers were used:

ACTB (Beta-actin) – Hs99999903_m1

CCR2 – Hs00704702_s1

2.8.4 Analysis

Relative quantification of target gene mRNA levels was performed using the comparative $2^{-\Delta\Delta Ct}$ method, as described (Livak and Schmittgen, 2001, Schmittgen et al., 2000). Briefly, relative quantification relates the PCR signal of the target transcript in a treatment group to that of another sample, such as an untreated control. Target expression levels are normalised to that of an internal control gene. Steps were taken to ensure the reliability of the data obtained from real-time qPCR experiments; the internal control gene selected was β-actin, as treatment of the cells was found to have little effect on the expression level of β-actin. Also, PCR performed on a range of cDNA dilutions revealed that the PCR efficiencies of both target and internal control genes were between 90 and 100%. Data was analysed using the ExpressionSuite Software (Life Technologies). mRNA abundance was normalised to the amount of β-actin expressed by cells, and is presented as relative expression in arbitrary units.

2.9 RNA Sequencing

2.9.1 Sample preparation

Primary cells

CD14^{++}CD16$^-$ classical monocytes, CD14$^+$CD16^{++} non-classical monocytes and B cells were FACS sorted from three healthy donors. Briefly, PBMC were isolated from 40 ml peripheral blood by Lymphoprep centrifugation. 10 million PBMC were set aside, while monocytes were isolated from the remaining PBMC (approx. 50 million) by negative selection using the pan-monocyte isolation kit (Miltenyi Biotec). Monocytes were stained with anti-human CD14-PE-Cy7 and anti-human CD16-FITC to enable sorting of the classical and non-classical subsets.

The leftover PBMC were stained with anti-human CD14-PE-Cy7, anti-human CD16-FITC, anti-human CD3-BV421 (for exclusion of monocytes, NK cells and T cells, respectively) and anti-human CD19-APC to enable FACS sorting of CD19$^+$ B cells.

Dead cells were excluded during the sort by Live/Dead stain. FACS sorting was performed using a BD FACSAria II, and cells were sorted into cRPMI + 20% FCS. Cells were kept cold at all times. Cells recovered from the sort were spun down, resuspended in Buffer RLT Plus and stored at -80°C prior to shipping.

THP-1

THP-1 cells were cultured for 24 hours under four conditions; 1 µM PGE$_2$, 1 mM sodium butyrate, PGE$_2$ and sodium butyrate (Na-but) combined, or medium alone. Migration of PGE$_2$- and PGE$_2$+Na-but-treated THP-1 cells toward CXCL14 was assessed by transwell chemotaxis assay. The assay was run for 3 hours, and migrated cells were collected from two wells per condition.

24 hour bulk-treated cells, and cells that had migrated toward CXCL14, were collected, spun down and resuspended in Buffer RLT Plus and stored at -80 °C for storage prior to shipping.

All samples were shipped to the Vaccine and Gene Therapy Institute, Port Saint Lucie, Florida for next-generation RNA sequencing. Samples were shipped on dry ice to prevent thawing in transit.

2.9.2 Sequencing

RNA was isolated from samples for sequencing in accordance with the protocol above (2.8.1 RNA Isolation). Next-generation sequencing (NGS) of mRNA was performed on the Illumina Genome Analyser II sequencing machine, providing a read coverage of approximately 40 million mapped reads per sample (bi-directional, with 20 million mapped reads in each direction). Sequencing files arrived as FASTQ files, two files per sample (forward and reverse reads). The human genome assembly (GRCh37) and the companion gene coordinates file (Homo_sapiens.GRCh37.75.gtf.gz) were downloaded from Ensembl.org and indexed using bowtie2. Reads were mapped to the genome using Tophat2, using the gene coordinates reference to steer mapping towards known transcripts. Resulting BAM files (mapped reads) were processed using Cufflinks to produce normalised expression counts per gene (reads mapped per kilobase length of transcript per million mapped reads; RPKM). Samples were compared using Cuffdiff to calculate the fold-change in expression of each gene, which was log-transformed.

2.10 Cloning of Small Hairpin RNA

2.10.1 Design of shRNA inserts

Small hairpin RNA (shRNA) sequences targeted against the chemokine receptor CCR2 were designed for expression in the pLenti-SU6EW Lentiviral vector, kindly provided by Professor Philip Taylor (Cardiff University). A simplified vector map is shown in **Figure 2.2**. This vector contains the mouse U6 promoter, which requires an initial 'G' nucleotide for the shRNA insert to be expressed. ShRNAs were designed based on sequences published online by Sigma-Aldrich in their MISSION™ shRNA library. Sequences beginning with a natural 'G' nucleotide were favoured, however where none were available an artificial 'G' nucleotide was added at the start of the sequence. Forward and reverse shRNA primers were synthesised by Sigma-Aldrich and reconstituted in DNase/RNase-free water to a final concentration of 100 µM.
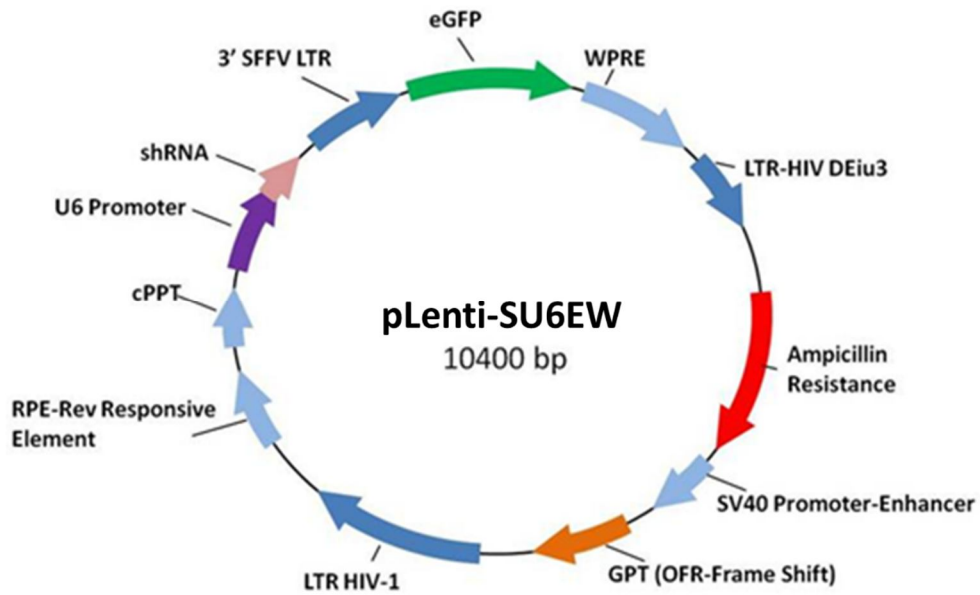
Figure 2.2. pLSU6EW lentiviral transfer vector used for expression of shRNA in THP-1 cells.

Shown is a simplified map of the pLSU6EW plasmid, into which shRNA sequences targeted against the chemokine receptor CCR2 was cloned downstream of a mouse U6 promoter. The plasmid co-expresses enhanced green fluorescence protein (eGFP) and also contains an ampicillin resistance gene to aid with selection of positive colonies.

2.10.2 Cloning of shRNA into pLenti-SU6EW

ShRNA was cloned into the pLSU6EW vector using the In-Fusion HD cloning kit (Clontech; Takara Bio Europe SAS, Saint-Germain-en-Laye, France), according to the manufacturer's instructions. First, the vector was linearised downstream of the U6 promoter using *Pme1*, a restriction endonuclease that blunt cuts the sequence GTTT_^AAAC, for 60 min at 37 °C. The enzyme was inactivated for 15 min at 65 °C, followed by purification of the linearised vector using a NucleoSpin column (Macherey-Nagel, Germany). A reaction without enzyme was run in parallel, and digested as well as undigested vector were run on a 1% agarose gel to confirm linearization. Next, the shRNA insert was prepared. Forward and reverse shRNA primers were mixed 1:1 (25 µl each, 50 µl total volume) and heated at 98 °C for 10 min to stimulate annealing of the primers, before cooling to room temperature. The cloning reaction was performed by combining 200 ng *Pme1*-digested pLSU6EW vector with 2 µl shRNA insert (giving a vector:insert ratio of approximately 1:5) and 2 µl 5X In-Fusion HD enzyme premix containing T4 DNA ligase (Clontech), adjusted to

a final volume of 10 μl using deionised water. The cloning reaction was incubated at 50 °C for 15 min, before cooling on ice.

2.10.3 Transformation of *E. coli* and selection of positive clones

The product of the cloning reaction was used for transformation of TOP10 Chemically Competent *E. coli* (Invitrogen) by heat shock. Briefly, 1 μl product was added to 20 μl TOP10 *E. coli* cells and incubated on ice for 30 min. The plasmid/competent cell mixture was then placed on a heat block at 42 °C for 30 seconds (heat shock), followed immediately by a one-minute recovery on ice. After the recovery, 250 μl S.O.C. medium (Invitrogen) was added, followed by incubation for 60 min at 37 °C on a shaking platform, set at a speed of 220 rpm. The bacterial culture was then spread out and grown on a LB agar plate supplemented with 100 μg/ml ampicillin for the selection of transformed cells at 37 °C overnight.

The next day, colonies were selected on the basis of being a good size, round and separated from other colonies, with 12-20 colonies selected per plate for colony PCR. RT-PCR of the colonies was performed using the following forward and reverse primers (Forward: 5'-GGTACAGTGCAGGGGAAAGA-3' and Reverse: 5'-CAAACCTACAGGTGGGGTCT-3'). PCR reactions were performed for 30 cycles using the following parameters:

1. 98 °C for 30 min
2. 98 °C for 10 sec
3. 60 °C for 30 sec   — Repeat steps 2-4 for 30 cycles
4. 72 °C for 60 sec
5. 72 °C for 10 min
6. 4 °C for infinity

The final PCR product was separated from the PCR reaction on a 1.5% agarose gel to confirm successful cloning of the shRNA insert into the vector. The PCR product without insert (where the vector has simply re-ligated, without incorporating the shRNA insert) is approx. 550 bp in size, and could easily be distinguished from PCR products where the shRNA insert is included (approx. 600 bp in size).

2.10.4 Purification of plasmid DNA by mini-prep and sequencing

Up to five positive colonies were sampled using a pipette tip and transferred to 10 ml LB broth supplemented with 100 μg/ml ampicillin. Bacteria were placed in a 37 °C

incubator on a shaking platform (180 rpm) and left overnight. The next day, 1 ml of the bacterial culture was aspirated and stored at 4 °C, while up to 5 ml was used for purification of plasmid DNA, performed using the QIAprep Spin Miniprep Kit (Qiagen), as per the manufacturer's instructions. Plasmid DNA was eluted into 30 µl deionised H_2O, and purified plasmids were examined using a NanoDrop ND1000 for their DNA concentration and quality. The resulting vectors were sequenced in both directions to confirm identity, with the same forward and reverse primers used for sequencing as were used in the colony PCR (primer sequences are shown above). Up to 200 ng plasmid was mixed with 2 pM forward or reverse primer and sent to Eurofins (Wolverhampton, UK) for sequencing. The resulting sequences were analysed using CLC Genomics Workbench 5 (CLC Bio).

After the sequence of the vector had been confirmed, 1 ml of the E. coli stock left over from the mini-prep was added to 200 ml LB broth supplemented with 100 µg/ml ampicillin, and placed in a 37 °C incubator on a shaking platform (180 rpm) and left overnight. The next day, plasmid DNA was purified using the QIAfilter Plasmid Maxi Kit (Qiagen), according to the manufacturer's instructions. Plasmid DNA was eluted into 100 µl deionised H_2O, while DNA concentration and quality were confirmed using a NanoDrop ND1000. The plasmid was stored at -80°C until use in the production of lentiviral particles

2.11 Production of Lentivirus and Transduction of THP-1 cells

2.11.1 Packaging of lentiviral particles

For production of lentivirus, HEK293T packaging cells were seeded at 2-2.5 x 10^6 cells in a T75 flask on the afternoon of the day prior to commencing virus production. The next morning, confluency was checked under the microscope (ideal confluency = 50-70%). The spent medium was aspirated from the flask and cells were gently washed in pre-warmed PBS. PBS was then aspirated and replaced with 12 ml fresh, pre-warmed complete DMEM. Cells were placed back at 37 °C while the lentiviral components were prepared.

A second generation lentivirus system, consisting of three plasmids, was used in the production of lentivirus, while Effectene transfection reagent (Qiagen) was used to transfect 293T cells. Briefly, 1 µg lentiviral plasmid (pLSU6EW containing shRNA insert) was combined with 0.75 µg pCMVdelta8.91 (plasmid containing the HIV

structural genes gag, pol and rev) and 0.5 µg pMD2g (plasmid containing the Vesicular Stomatitis Virus envelope protein VSV-G, used to pseudotype the virus so that it can infect any mammalian cell). pCMVdelta8.91 and pMD2g were kindly provided by Professor Philip Taylor (Cardiff University). After mixing the three plasmids together, the volume was made up to 300 µl with Buffer EC. 18 µl Enhancer was added, followed by vortexing for 1 second and incubation at room temperature for 5 min. 60 µl Effectene was then added, followed by vortexing for 10 seconds and incubation at room temperature for 10 min. The prepared lentiviral mix was added to 2.6 ml pre-warmed DMEM, before being transferred dropwise to the 293T cells. Cells were subsequently cultured for 48-60 hours at 37 °C.

Media containing lentiviral particles was collected post-transfection and centrifuged at 500 x g for 10 min to pellet cell debris from the 293T cells. Clear supernatant containing the lentiviral particles was mixed with Lenti-X concentrator (Clontech) at a 3:1 ratio (15 ml supernatant + 5 ml Lenti-X concentrator), inverted several times to mix, and then placed at 4 °C overnight. The following day, the supernatant was centrifuged at 1500 x g for 45 min at 4 °C to pellet the lentiviral particles. Following removal of the supernatant, the virus pellet was resuspended in 1 ml serum-free AimV medium (Invitrogen) and stored at -80 °C.

2.11.2 Transduction of THP-1 cells

2×10^5 THP-1 cells in 300 µl cRPMI were seeded per well in a 24-well plate, and 100 µl lentivirus was added (final volume = 400 µl). The following day, 600 µl cRPMI was added to make the volume up to 1 ml. After two more days, THP-1 cells were photographed using the EVOS FL Cell Imaging System (Life Technologies) to document eGFP expression. The cells were then harvested and washed twice in medium by centrifugation at 400 x g for 5 min, before being placed back into culture. The proportion of eGFP$^+$ cells (transduction efficiency) was accurately determined by flow cytometry. eGFP$^+$ cells were FACS sorted using a BD FACSAria prior to functional assays.

2.12 Stable Expression of Orphan GPCRs in 300.19 cells

2.12.1 Cloning of GPCRs

mRNA was obtained from monocytes isolated from PBMC using CD14 microbeads, and generation of cDNA was performed as previously described. Custom primers were designed for the amplification and cloning of four orphan GPCR cDNAs by PCR. Forward and reverse primers are shown below:

GPR68 – Forward: ATAGGATCCGCCCAAAGATGGGGAACATC

Reverse: TATCTCGAGTTAGGCCAACCTGCCCGTG

GPR84 – Forward: ATAGGATCCGCCTCTATCATGTGGAACAGCTC

Reverse: TATCTCGAGTTAATGGAGCCTATGGAAACTCCG

GPR141 – Forward: ATAGGATCCGCCTCGATGCCTGGCCACAATACCTCCA

Reverse: TATCTCGAGTTAACGGCACAAAACACAATTCCATAAGCC

GPR183 – Forward: ATAGGATCCGGACCACCACCAATGGATATAC

Reverse: TATCTCGAGTCACTTTCCATTTGAAGACTTGG

Following amplification, the PCR product was purified using the NucleoSpin Gel and PCR Clean-up kit (Macherey-Nagel). cDNA was cloned into the pBlueScript II (pBS) vector by linearization of the vector using the restriction endonucleaseas BamHI and XhoI, followed by ligation with T4 DNA ligase and 2x Rapid Ligation Buffer (both Promega; Southampton, UK), as per the manufacturer's instructions. The resulting vectors were used to transform Stellar™ Competent Cells (Clontech), followed by selection of positive clones based on resistance to ampicillin and subsequent mini-prep of plasmid DNA, as previously described. The resulting vectors were sequenced in both directions to confirm identity. The only receptor for which we obtained a cDNA clone from a different source was GPR35, which was purchased from Bloomsburg University cDNA Resource Centre (Bloomsburg, PA, USA) and is distributed in Invitrogen's pcDNA3.1+ vector.

After the identity had been confirmed, the cDNA clone was excised from pBS using *BamHI* and *XhoI* restriction endonucleases and ligated into the lentiviral transfer vector pSIEW (kindly provided by Prof. Philip Taylor, Cardiff University) using T4 DNA ligase and 2x Rapid Ligation Buffer.

2.12.2 Packaging of lentiviral particles

Production of lentivirus incorporating the GPCR clone was performed using HEK293T packaging cells, as previously described.

2.12.3 Transduction of 300.19 cells

1×10^5 300.19 cells in 300 µl cRPMI were seeded per well in a 24-well plate, and 100 µl lentivirus was added (final volume = 400 µl). The following morning (day 1), 600 µl cRPMI was added to make the volume up to 1 ml. On the afternoon of the same day, 1 ml cRPMI was added to make the volume up to 2 ml. On day 2, the volume was made up to 10 ml with cRPMI, and cells were transferred to a T25 flask. On day 3, 300.19 cells were photographed using the EVOS FL Cell Imaging System (Life Technologies) to document eGFP expression. The cells were then harvested and washed twice in medium by centrifugation at 400 x g for 5 min, before being placed back into culture. The proportion of eGFP+ cells (transduction efficiency) was accurately determined by flow cytometry. eGFP+ cells were FACS sorted using a BD FACSAria prior to functional assays.

2.13   Statistical Analysis

All statistical analysis was performed with the use of GraphPad Prism version 6 (GraphPad Software, Inc.). Column statistics were carried out in the first instance to assess distribution of data sets and identify whether datasets were parametric or non-parametric. For comparison of two sample means, either Student's t test (parametric), Mann-Whitney U test (unpaired, non-parametric), or Wilcoxon signed-rank test (paired, non-parametric) were used. For comparison of the means of three or more groups, either the one-way analysis of variance (ANOVA) followed by Bonferroni post-hoc test (parametric data sets), or the Kruskal-Wallis test followed by Dunn's post-hoc test (unpaired, non-parametric data sets) were used. In instances where groups were split on two independent variables, the two-way ANOVA was used. Data are displayed as mean ± standard error of the mean (s.e.m.). In each case, the statistical test used to determine significance is indicated, and $p < 0.05$ was considered significant.

Chapter 3 CXCL14 Target Cells in Blood and Skin

3.1 Introduction

CXCL14 is a fascinating member of the chemokine family. Its high level of expression in healthy peripheral tissues, especially those of mucosal origin, but total absence from secondary lymphoid tissues makes it unique among the constitutively expressed, so-called 'homeostatic' chemokines. Failure to promote chemotaxis of naïve or activated T cells (Cao et al., 2000, Sleeman et al., 2000) distinguishes CXCL14 from other non-ELR CXC chemokines. However, attempts to accurately describe CXCL14 target cells have been hindered by not knowing the identity of its cognate receptor, leading to conflicting experimental observations from different groups. Cells which have been reported to display chemotaxis toward CXCL14 include CESS (a human B cell line), human neutrophils, human and murine immature dendritic cells, human monocytes (especially following activation with PGE_2), activated human NK cells from blood and human uterine NK cells (Cao et al., 2013, Cao et al., 2000, Hara and Tanegashima, 2012, Kurth et al., 2001, Shellenberger et al., 2004, Sleeman et al., 2000, Starnes et al., 2006). Inconsistencies in the data obtained from these studies may be explained by use of CXCL14 from different sources. Sources include synthesised protein, CXCL14 isolated from conditioned media from transfected mammalian cells, as well as commercially available recombinant CXCL14 from various suppliers.

In this study, immune cells were isolated from the peripheral blood and skin of healthy human subjects, and their ability to respond to CXCL14 was assessed using two methods: (1) Leukocyte migratory responses toward CXCL14 were measured by transwell chemotaxis assay, and (2) binding of a custom-made, synthetic CXCL14 with an Alexa Fluor 647 fluorochrome covalently attached to its C-terminus (AF-CXCL14) was assessed by flow cytometry. Fluorochrome-labelled chemokines have been used by ourselves and other to study the distribution of chemokine receptors on immune cells (McCully et al., 2015, Strong et al., 2006). It was therefore our intention to apply AF-CXCL14 in investigating the distribution of the putative CXCL14 receptor on immune cells isolated from human blood and skin.

3.2 Aim

- To identify the leukocyte subsets in human blood and peripheral tissues (focus on skin) which represent the major targets for CXCL14

3.3 CXCL14 Target Cells in Peripheral Blood

3.3.1 Gating strategy for identification of immune cell subsets in PBMC by flow cytometry

Single cell suspensions of PBMC were stained with fluorochrome-conjugated monoclonal antibodies (mAbs) directed against CD3, CD14, CD16, CD19 and CD56. Following exclusion of dead cells and cell aggregates, this staining panel enabled the identification of T, B, NK and NKT cells, as well as monocytes. A representative gating strategy is shown (**Figure 3.1**). Gating on the three monocyte subsets defined by differential expression of CD14 and CD16 was performed following exclusion of CD56$^+$ NK cells, as NK cells also express CD16. DC populations in peripheral blood were analysed in other experiments (see Figure 3.7 and Figure 3.8) due to their low frequency in PBMC.
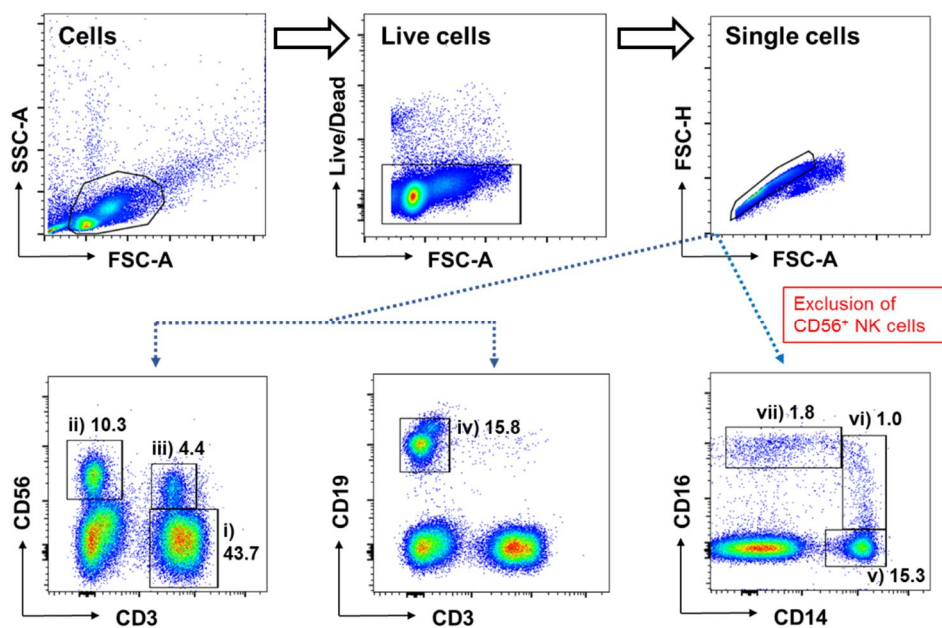
Figure 3.1. Gating strategy for identification of the major subsets in human PBMC by flow cytometry.

PBMC were isolated from the blood of healthy volunteers by density centrifugation. Live single cells were gated on by excluding debris (top left panel), dead cells (top centre panel) and cell aggregates (top right panel). Cells were stained with fluorochrome-conjugated mAbs directed against lineage markers, enabling the identification of i) T cells (CD3+), ii) NK cells (CD56+), iii) NKT cells (CD3+CD56+) and iv) B cells (CD19+). After using Boolean gating to exclude CD56+ NK cells (which express CD16), the three monocyte subsets, defined by CD14 and CD16 expression, are shown; v) classical (CD14++CD16-), vi) intermediate (CD14++CD16+) and vii) non-classical (CD14+CD16++) monocytes. Numbers indicate the percentage of each cell type in PBMC and is representative of >8 donors.

3.3.2 Monocytes display chemotactic responses toward CXCL14, while T, B and NK cells do not

Chemotactic responses of PBMC to CXCL14 were assessed using the transwell chemotaxis assay. Input cells, as well as migrated cells recovered from the lower chamber, were stained with the same antibody panel as shown in Figure 3.1. Representative FACS plots show the accumulation of CD14$^+$ monocytes in the migrated cell fraction with increasing concentration of CXCL14. Collective data from five independent experiments using different donors shows the chemotactic response of monocytes, T cells, B cells and NK cells in response to CXCL14 (**Figure 3.2**). Migration is presented as the percentage of input cells of each cell type that migrated to the lower chamber in response to the indicated concentrations. A dose-dependent migration of monocytes toward CXCL14 was observed, the response ranging from 3.01 ± 0.65% toward buffer alone (blank), to 28.4 ± 6.1% toward 1 µM CXCL14 (p=0.0031). T and B cells did not migrate toward CXCL14. NK cells displayed a small increase in migration from blank (2.91 ± 0.4%) to 100 nM CXCL14 (4.2 ± 0.32%), although this did not reach significance (p=0.064).
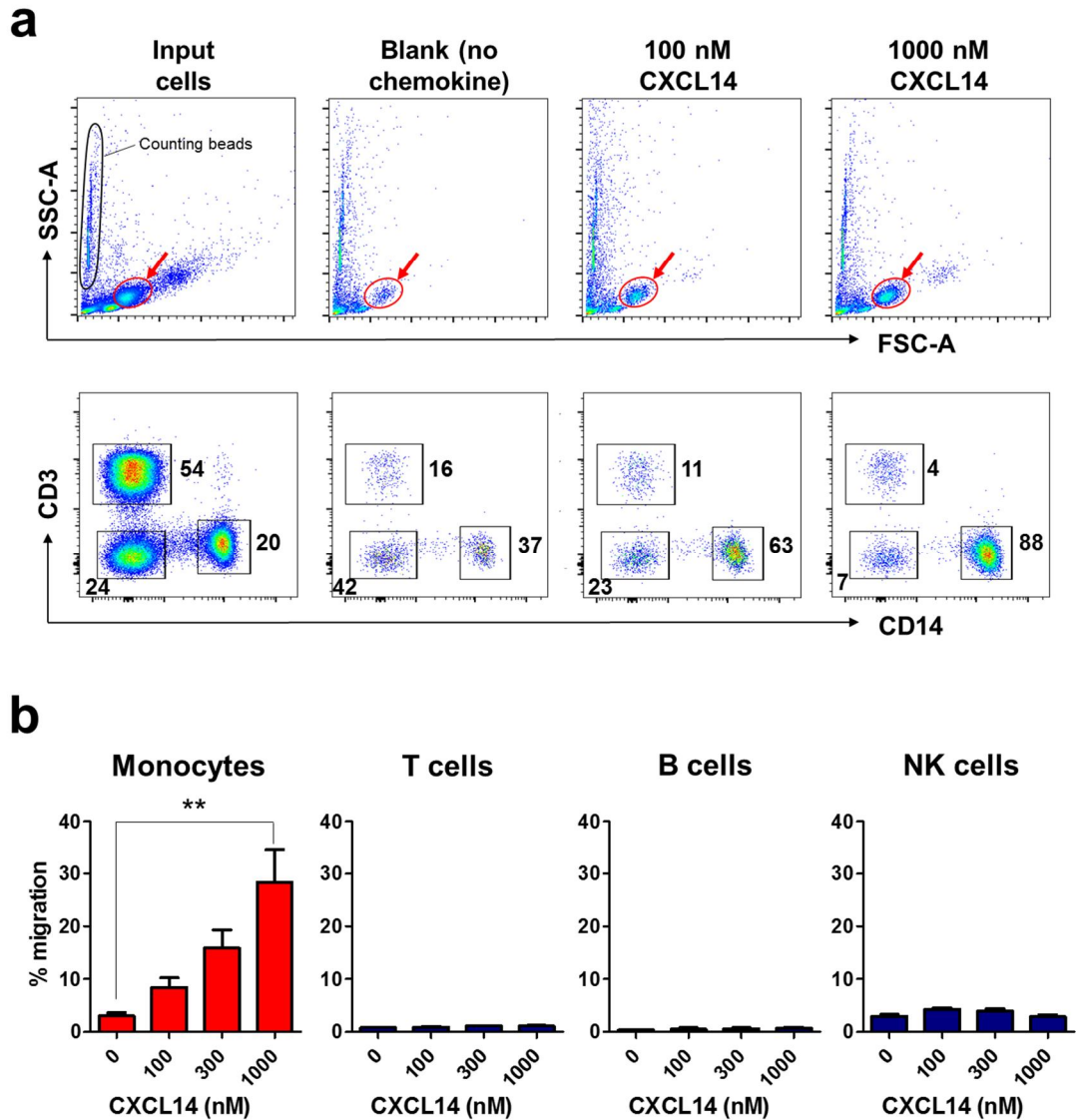
Figure 3.2. Monocytes migrate in response to CXCL14, while T, B and NK cells do not.
Migratory responses of PBMC toward CXCL14 were tested by transwell chemotaxis assay.
(a) FACS plots from a representative experiment demonstrate the increase in the proportion
of CD14+ monocytes, relative to other cell types, among the cells that migrated in response
to increasing concentrations of CXCL14. Forward scatter vs side scatter is plotted in the upper
panels, monocytes being indicated by a red circle and arrow. AccuCheck counting beads,
added to samples to enable enumerate migrated cells, are also shown. In the lower panels,
numbers indicate the frequency of monocytes (CD14+; x-axis) and T cells (CD3+; y-axis)
amongst total migrated cells. **(b)** Migration of monocytes, T, B and NK cells toward CXCL14.
Data are presented as the percentage of input cells of each cell subset recovered from the
lower chamber, and are mean + s.e.m. of 5 independent experiments using PBMC from
different donors; **P = 0.0031, Kruskall-Wallis ANOVA.

3.3.3 Alexa Fluor 647-conjugated CXCL14 can be used to label cells expressing putative CXCL14 receptors

PBMC were incubated with AF-CXCL14 in a step prior to staining with the antibody panel described in Figure 3.1. Binding of AF-CXCL14 was performed at 4 °C; at this temperature; there should be minimal internalisation of the receptor. Detection by flow cytometry therefore depends on the interaction between chemokine and receptor being relatively stable and able to withstand several wash steps before acquisition. FACS plots from a representative experiment show binding of a range of concentrations (0-100 nM) of AF-CXCL14 to monocytes, T, B and NK cells. Numbers indicate the percentage of AF-CXCL14+ cells (**Figure 3.3**). As expected, and in agreement with the migration data, monocytes were positive for expression of CXCL14 receptor(s), the majority of monocytes staining positively at 50 and 100 nM AF-CXCL14. In contrast, the majority of T, B and NK cells were negative for receptor expression. 50 nM AF-CXCL14 was selected as the optimal concentration for labelling as it allowed for the greatest differentiation between cells which do respond to CXCL14 (monocytes) and cells which do not (T, B and NK cells). It should be noted that at this concentration, a small minority of T and NK cells do exhibit binding of AF-CXCL14; this staining may be non-specific, or it may identify minor subsets of each cell type that respond toward CXCL14. Indeed, γδ-T cells constitute around 2-5% of peripheral blood T cells, which is consistent with the proportion of CD3+ cells which labelled with 50 nM AF-CXCL14 in Figure 3.3. In addition, it has been reported that NK cells isolated from peripheral blood, upon activation *in vitro* with IL-2, undergo modest migration in response to CXCL14 (Starnes et al., 2006). However, further investigation is required to determine if there exists distinct subsets or activation states within these broadly defined lymphocyte populations that represent targets for CXCL14.
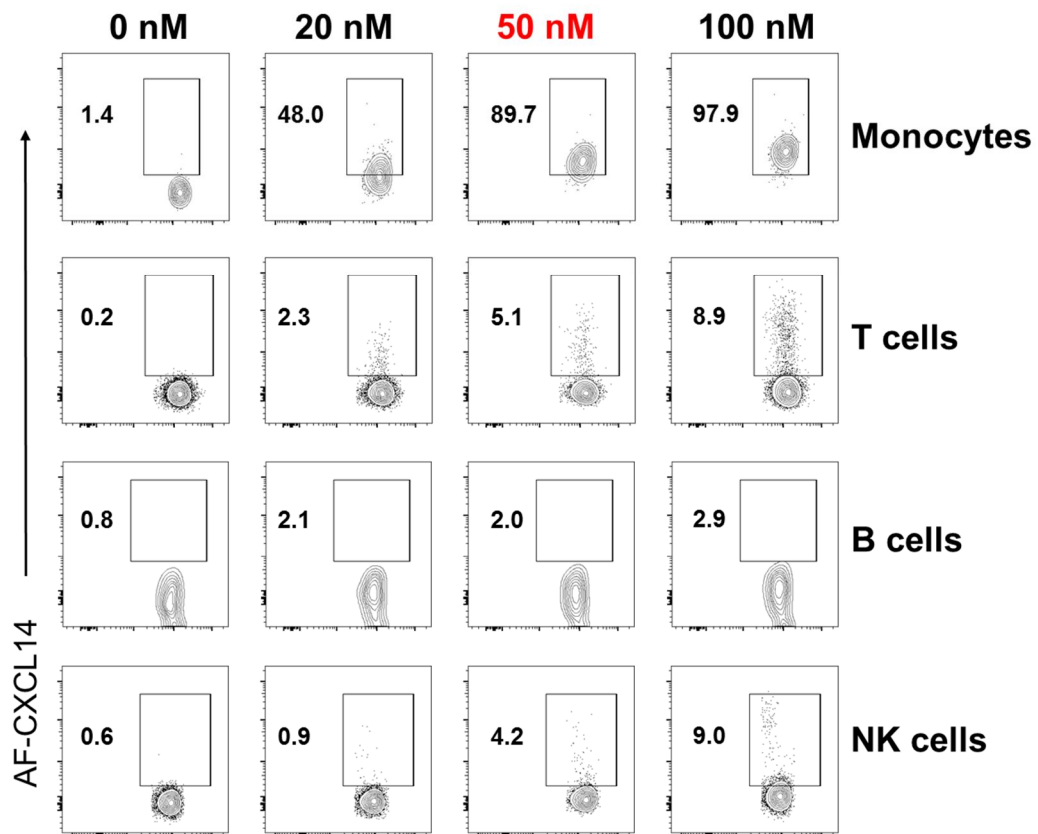
Figure 3.3. Alexa Fluor 647-CXCL14 can be used to label cells expressing CXCL14 receptor(s).

PBMC were incubated with 0-100 nM AF-CXCL14 for 30 minutes at 4 °C, followed by staining with mAbs to distinguish the different cell types. Shown are representative FACS plots of AF-CXCL14 binding (x-axis) to CD14+ monocytes (top row), CD3+ T cells (second row), CD19+ B cells (third row) and CD56+ NK cells (bottom row). Numbers indicate the percentage of AF-CXCL14+ cells. Plots are representative of >5 independent experiments. 50 nM AF-CXCL14 was selected as the optimal concentration for labelling and this concentration was used in all future experiments.

3.3.4 Classical and intermediate monocytes are the major targets of CXCL14, while non-classical monocytes are not targets

In order to look more closely at the monocyte subsets defined by differential CD14 and CD16 expression, monocytes were purified from PBMC by negative selection. Dot plots show depletion of T, B, NK and NKT cells, and concurrent enrichment of monocytes (**Figure 3.4a**). Of the three subsets, classical monocytes displayed the greatest migratory response toward CXCL14, 16.2 ± 3.45% classical monocytes (CD14^{++}CD16$^-$) migrating toward 1 µM CXCL14 (compared to 0.7 ± 0.15% toward buffer alone; p=0.0045) correlating to a chemotactic index (CI) of >20. Intermediate monocytes (CD14^{++}CD16$^+$) displayed a more modest response toward CXCL14, 8.58 ± 2.28% intermediate monocytes migrating toward 1 µM CXCL14 (compared to 0.45 ± 0.15% toward buffer alone; p=0.0054). In contrast, non-classical monocytes (CD14$^+$CD16^{++}) did not display migration toward CXCL14. Although background migration was higher for this subset (3.1 ± 0.46% non-classical monocytes migrated toward buffer only), no specific migration toward CXCL14 was observed (2.78 ± 0.42% non-classical monocytes migrated toward 1 µM CXCL14) (**Figure 3.4b**). In concurrence with the migration data, binding of AF-CXCL14 revealed that the majority of classical monocytes express CXCL14 receptor(s), 72.0 ± 6.28% staining positively for receptor expression. Intermediate monocytes also demonstrated binding of AF-CXCL14 (50.7 ± 6.65% intermediate monocytes were AF-CXCL14$^+$), while only a small fraction of non-classical monocytes displayed binding (6.3 ± 5.05% non-classical monocytes were AF-CXCL14$^+$) (**Figure 3.4c and d**).
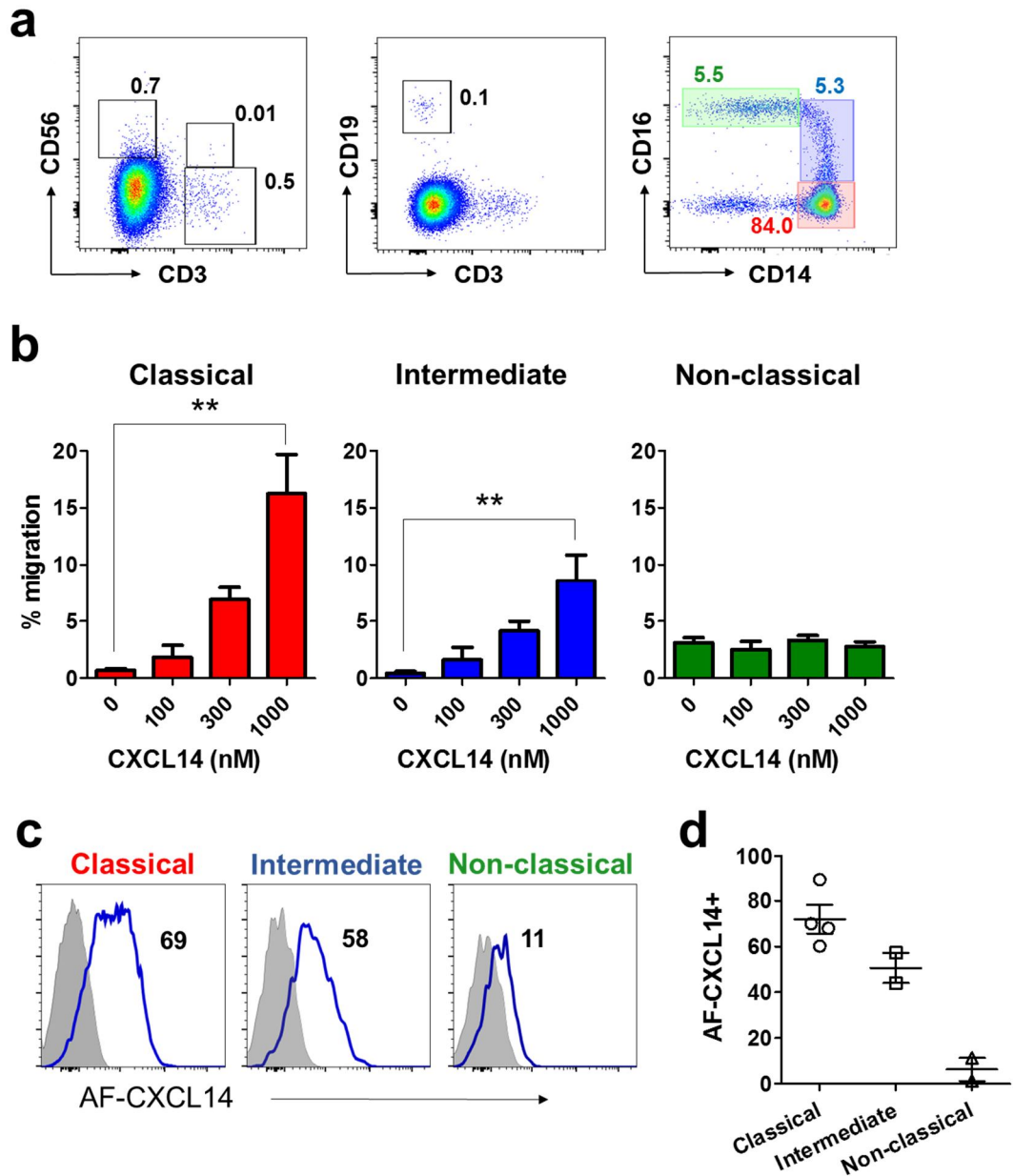
Figure 3.4. Classical and Intermediate monocytes are the major targets of CXCL14, while non-classical monocytes are not targets.

Monocytes were purified from PBMC by negative selection. **(a)** Enrichment of monocytes following depletion of T, B, NK and NKT cells. Classical (CD14++ CD16-; red gate), intermediate (CD14++ CD16+; blue gate) and non-classical (CD14+ CD16++; green gate) monocytes are shown. **(b)** Migration of classical, intermediate and non-classical monocytes in response to CXCL14. Data are mean + s.e.m. of 5 donors from 3 independent experiments. **P<0.01, Kruskall-Wallis ANOVA. **(c)** Representative FACS plots show binding of 50 nM AF-CXCL14 to the three monocyte subsets (blue histograms). Grey filled histograms represent unlabelled cells. Numbers indicate the percentage of AF-CXCL14+ cells. **(d)** Graph shows cumulative data of AF-CXCL14 binding to monocyte subsets. Data shown is mean ± s.e.m. from 2-4 donors.

The absence of appreciable AF-CXCL14 binding to lymphoid cell populations was confirmed in several experiments using PBMC. Representative FACS plots (**Figure 3.5a**) in addition to cumulative data (**Figure 3.5b**) demonstrate that T cells (4.0 ± 0.73% AF-CXCL14$^+$), B cells (2.4 ± 0.34% AF-CXCL14$^+$) and NK cells (3.6 ± 0.35% AF-CXCL14$^+$) display extremely weak binding, confirming that each of the lymphocyte subsets likely do not represent targets for CXCL14.
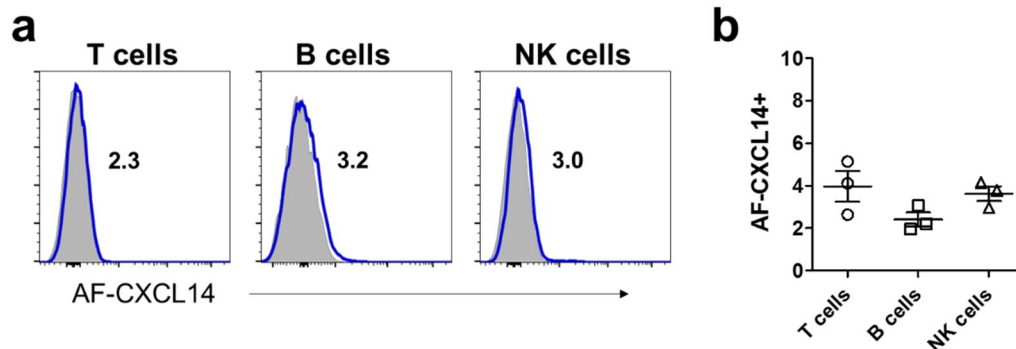
Figure 3.5. Lymphoid populations do not express CXCL14 receptor(s).
PBMC were labelled with 50 nM AF-CXCL14 for 30 min at 4 °C. **(a)** Representative FACS plots show binding of AF-CXCL14 (blue histograms) to T, B and NK cells. Grey filled histograms represent unlabelled cells. **(b)** Cumulative data of AF-CXCL14 binding to T, B and NK cells. Data shown is mean ± s.e.m. and is from 3 independent experiments.

3.3.5 Neutrophils migrate toward a high concentration of CXCL14, but do not bind AF-CXCL14

Neutrophils were isolated by negative selection from the granulocyte/red blood cell fraction following Ficoll separation of peripheral blood and phenotyping was performed by flow cytometry. Following gating on live, single cells (**Figure 3.6a**), staining with fluorochrome-conjugated antibodies directed against the typical neutrophil markers CD15, CD16 and CXCR1 confirmed their identity (**Figure 3.6b**). Migration of neutrophils in response to the CXCR1-ligand CXCL8 and CXCL14 was assessed by transwell chemotaxis assay. In contrast to PBMC, which require a duration of 3-4 hours for substantial migration to be observed, neutrophil migration was extremely rapid. Indeed, migrated neutrophils could be seen in the lower chamber after as little as 15 minutes, and the assay was terminated after 1 hour. This likely reflects the fact that *in vivo*, neutrophils are the first cells to arrive at the site of

inflammation. Peak migration in response to CXCL8 was observed at 10 nM (78.5 ± 16.0% neutrophils migrated toward 10 nM CXCL8). The relatively low concentration of CXCL8 required for induction of optimal migratory responses in neutrophils is consistent with the role of CXCL8 as an inflammatory chemokine. In contrast, much higher concentrations of CXCL14 were required to stimulate neutrophil migration. Neutrophils displayed a weak response toward 300 nM CXCL14 (4.8 ± 3.6% cells migrated), while a much stronger response was observed toward 1000 nM CXCL14 (48.2 ± 19.3% cells migrated; **Figure 3.6c**). Binding of AF-CXCL14 to neutrophils was also performed, however virtually no binding was observed (**Figure 3.6d**). The discrepancy between migration toward CXCL14 and binding of AF-CXCL14 may be explained by a low density of the putative CXCL14 receptor on the cell surface, necessitating a high concentration of CXCL14 to stimulate neutrophil migration, while prohibiting sufficient amounts of AF-CXCL14 to bind for it to be detected by flow cytometry. An alternative explanation for the lack of binding observed may be that neutrophils possess a receptor for CXCL14 that is distinct from the one expressed by monocytes, which binds CXCL14 with lower affinity.
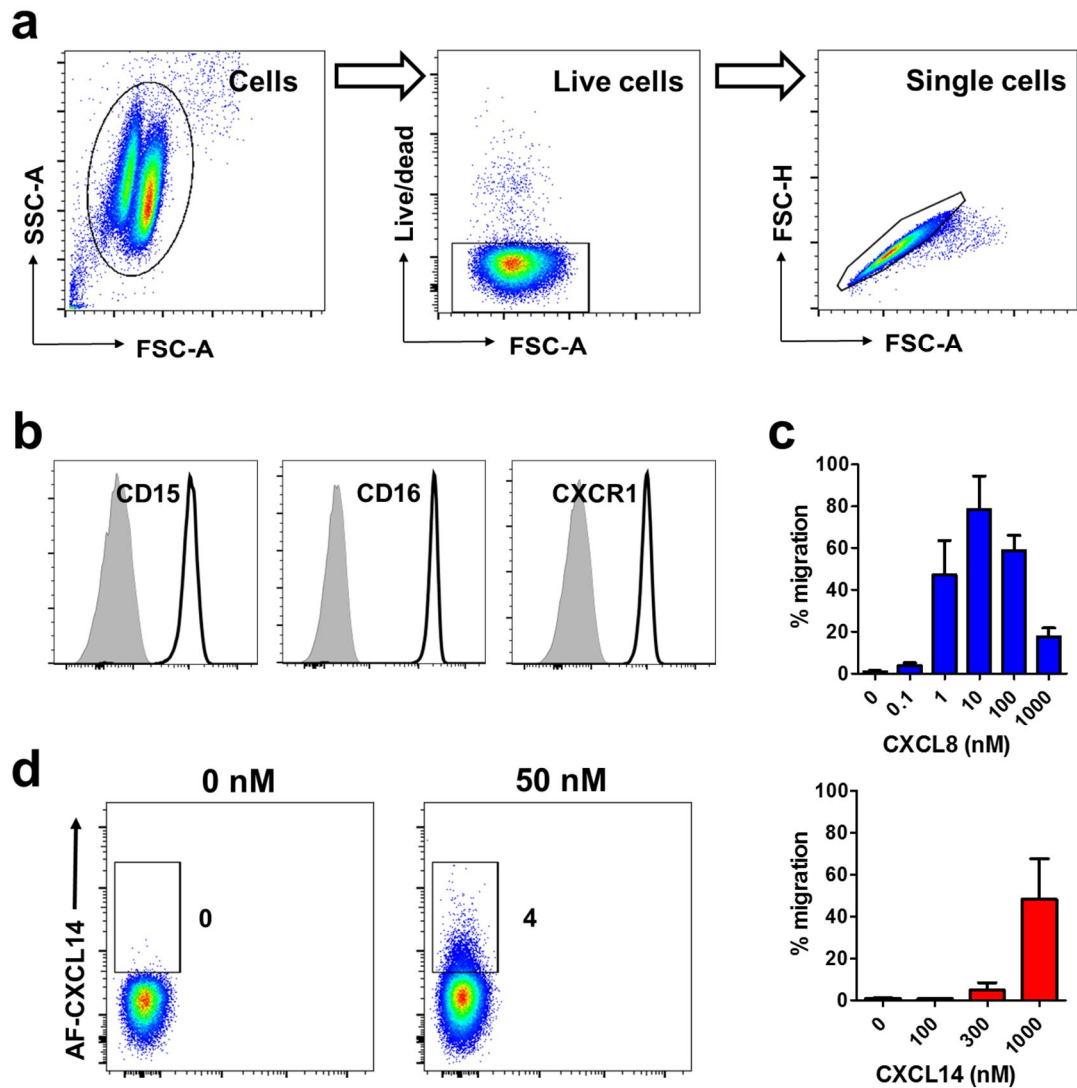
Figure 3.6. Neutrophils undergo migration in response to CXCL14.

Neutrophils were purified by negative selection as described in Materials and Methods and subjected to flow cytometric analysis. **(a)** Gating strategy to identify live, single cells and **(b)** FACS plots showing expression of neutrophil-associated markers CD15, CD16 and CXCR1 (black histograms). Grey filled histograms indicate stained with isotype-matched control antibodies. **(c)** Migration of neutrophils in response to CXCL8 (blue) and CXCL14 (red) was assessed by transwell chemotaxis assay. Data shown is mean + s.e.m. of two independent experiments. **(d)** Binding of 50 nM AF-CXCL14 to neutrophils (right). Cells incubated with buffer alone (i.e. no AF-CXCL14) are shown (left) to display how AF-CXCL14+ gate was positioned. Plots shown are representative of two experiments. The percentage of cells which are AF-CXCL14+ is indicated.

3.3.6 Plasmacytoid DCs are Not Targets for CXCL14

Human blood DCs can be subdivided into three distinct populations. There are two subsets of myeloid DC, which are positive for the common myeloid marker CD33 and are distinguished on the basis of differential expression of CD1c and CD141. The third population is the plasmacytoid DCs (pDC), with CD303 (BDCA-1) shown to be a unique marker for identification of these cells (Ziegler-Heitbrock et al., 2010). All three DC populations also express MHC class II. PBMC were stained for HLA-DR and CD303 expression, which identified a small population of pDC, accounting for 0.2-0.5% of total PBMC (**Figure 3.7a**). Binding studies with AF-CXCL14 revealed that the large majority of pDC were negative for expression of CXCL14 receptor(s) (**Figure 3.7b**). In migration assays using PBMC, pDC did not undergo chemotaxis at all in response to CXCL14. In fact, no pDC were found in the lower chamber upon termination of the assay. This Indicates that either pDCs do not respond to CXCL14, or that they were unable to move through the pores. A suitable positive control for migration of pDC could not be found. Despite expression of high levels of CXCR3, pDC do not respond efficiently to CXCR3 ligands (Vanbervliet et al., 2003). Migration toward CXCL12 has been shown by others (Vanbervliet et al., 2003), but my attempts to replicate this were unsuccessful (data not shown). However, the fact that pDC are smaller in size than monocytes and neutrophils would suggest that they should be capable of passing through the pores in the transwell insert.
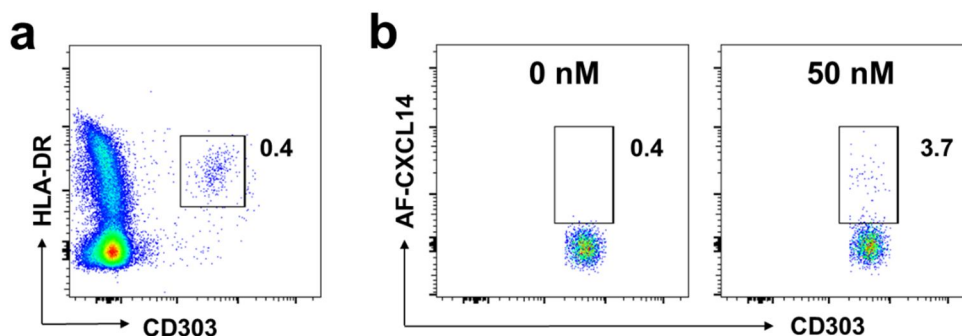
Figure 3.7. Plasmacytoid DCs are not targets for CXCL14.
PBMC were stained for markers which identify plasmacytoid DC (pDC). **(a)** After gating on live, single cells, plotting HLA-DR vs CD303 enabled identification of pDC. Shown is a plot from a representative experiment, where the number indicates the percentage of pDC in total PBMC for this particular donor. Staining was performed on PBMC from three donors in total. **(b)** Binding of AF-CXCL14 to pDC. Numbers indicate percentage of AF-CXCL14+ cells, and are representative of two independent experiments using different donors.

3.3.7 Myeloid DC are not targets for CXCL14

PBMC were stained for cell-surface markers which facilitate identification of the two populations of myeloid DC. After gating on live, single cells, gating on CD33$^+$ cells was followed by exclusion of monocytes based on CD14 and CD16 expression. Plotting CD1c vs CD141 revealed the two subsets of myeloid DC (**Figure 3.8a**). CD1c$^+$ DC account for approximately 0.3-0.5% of PBMC, while CD141$^+$ DC are a very minor population, accounting for only 0.01-0.05% of PBMC.

To enable a proper analysis of these populations, myeloid DC were enriched from PBMC by negative selection using MACS technology. Although the selection did not yield a pure population of myeloid DC, >99% of non-DCs were removed (in one experiment starting with 40 million PBMC, 0.2 million cells were recovered post-enrichment) Removal of contaminating non-DCs revealed a second population of CD141$^+$ DCs, which had intermediate CD141 expression while being completely negative for CD1c, which contrasts with the CD141^{high} cells which have low expression of CD1c (**Figure 3.8b**). The published literature on blood DC populations describes a single population of CD141$^+$ DCs only (Boltjes and van Wijk, 2014, Ziegler-Heitbrock et al., 2010). Therefore, I am unsure of the relevance of this observation at this time.

Migratory responses of myeloid DC toward CXCL14 and CCL21 were assessed by transwell chemotaxis assay. CD1c$^+$ DC did not display migration in response to CXCL14, however they did display a 4-fold increase in migration toward CCL21 (11.78% cells migrated toward 100 nM CCL21, compared to 2.84% toward buffer alone; **Figure 3.8c**). The majority of CD1c$^+$ DC failed to bind AF-CXCL14 (**Figure 3.8d**), confirming that these cells are not targets for CXCL14. Frustratingly, very low numbers of CD141$^+$ DC were recovered post-enrichment (as they are >10-fold lower in abundance in PBMC compared to CD1c$^+$ DC, the number recovered from 40 million PBMC was in the region of 5,000). This prohibited the proper examination of CD141$^+$ DCs for responses toward CXCL14, and it is my intention to re-examine this population in future experiments.
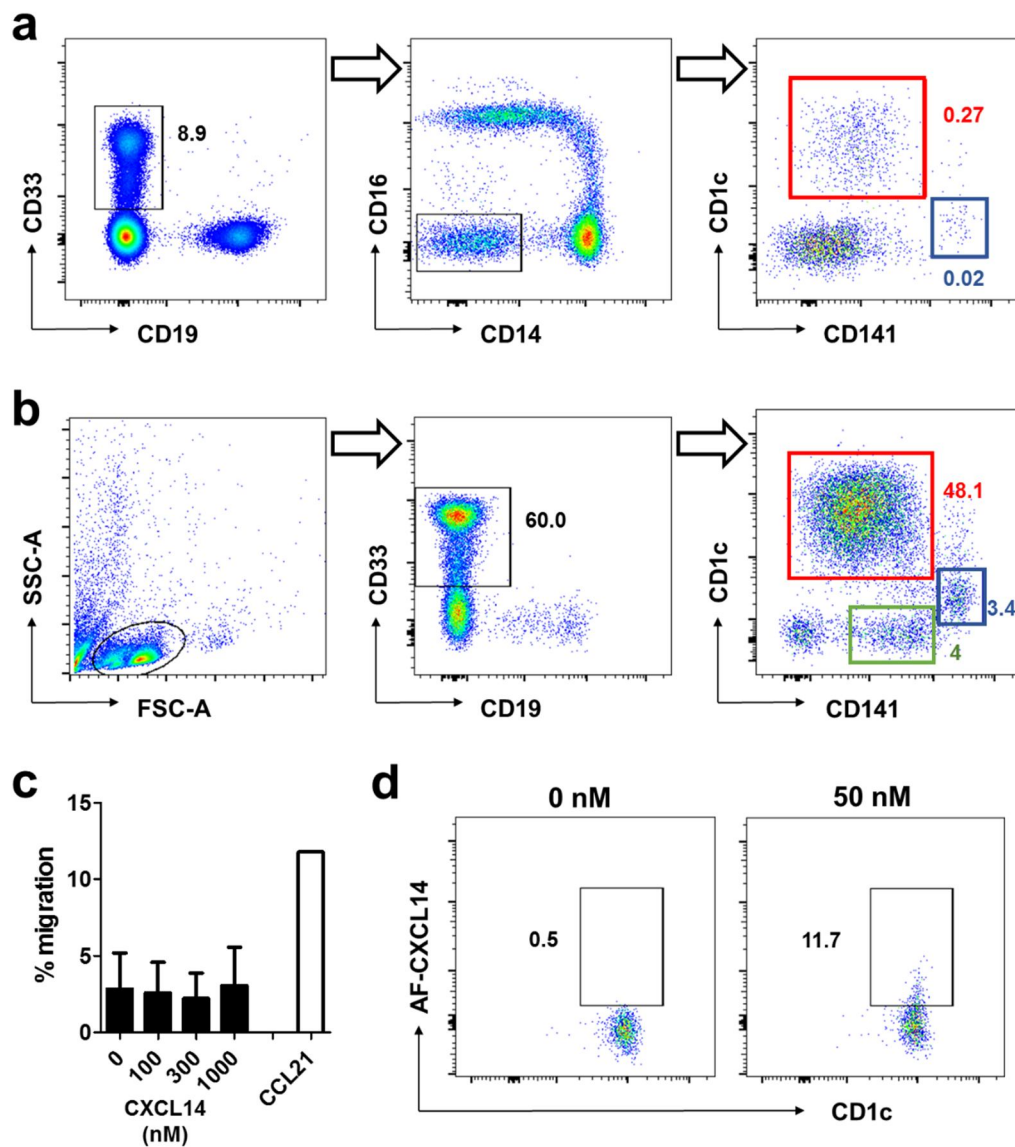
Figure 3.8. Myeloid DC are not targets for CXCL14.

Cells were stained for markers which identify the two subsets of myeloid DC. **(a)** Total PBMC. After gating on live, single cells, gating on CD33+ cells (left) was followed by exclusion of monocytes based on CD14 and CD16 expression (centre). Plotting CD1c vs CD141 identifies the two populations of myeloid DC (right); CD1c+ DC (red gate) and a small population of CD141+ DC (blue gate). Numbers indicates the percentage of each population in total PBMC, representative of two donors. **(b)** Myeloid DC enriched by negative selection. FSC vs SSC plot shows that monocytes, which have a higher FSC/SSC profile than lymphocytes and DCs, were not present in the enriched fraction (left). Gating on cells expressing the common myeloid marker CD33 was performed (centre), followed by gating on myeloid DC subsets (right). Removal of non-DCs revealed a second CD141+ DC population, characterised by intermediate CD141 expression and an absence of CD1c expression (green gate). Numbers indicate the percentage of each population in the total enriched cells. **(c)** Migration of CD1c+ DCs toward CXCL14 and 100 nM CCL21. Data shown is mean + s.e.m. of two independent experiments. **(d)** Binding of 0 and 50 nM AF-CXCL14 to CD1c+ myeloid DCs. Numbers indicate percentage AF-CXCL14+ cells and are representative of two donors.

3.3.8 *In vitro* monocyte-derived DCs do not respond to CXCL14

Monocytes were purified from PBMC by negative selection and cultured in the presence of GM-CSF and IL-4 to generate monocyte-derived DCs (mo-DC) (Sallusto and Lanzavecchia, 1994). After 6 days, monocytes had lost expression of CD14 and gained expression of the DC and macrophage C-type lectin receptor DC-SIGN (CD209; **Figure 3.9a**). Immature mo-DC were matured with a combination of LPS and TNFα for 24 hours, displaying a marked change in morphology characterised by clustering of cells and elongation/increase in size. Mo-DC also up-regulated expression of MHC class II and the co-stimulatory molecule CD86 (B7-2; **Figure 3.9b**). Both immature and mature mo-DC were tested for migration toward CXCL14 and expression of CXCL14 receptor(s). While immature mo-DC did appear to display weak but uniform binding of AF-CXCL14, no migration toward CXCL14 was observed. Apparent labelling with AF-CXCL14 may be explained by non-specific uptake of the reagent due to immature DCs having high endocytic activity. Mature mo-DC, which are less endocytically active, did not label with AF-CXCL14 and also did not migrate toward CXCL14. Finally, mo-DC acquired strong responsiveness to CCL21 following maturation, consistent with up-regulation of CCR7 which facilitates their traffic to the lymphoid organs *in vivo* (**Figure 3.9c**).
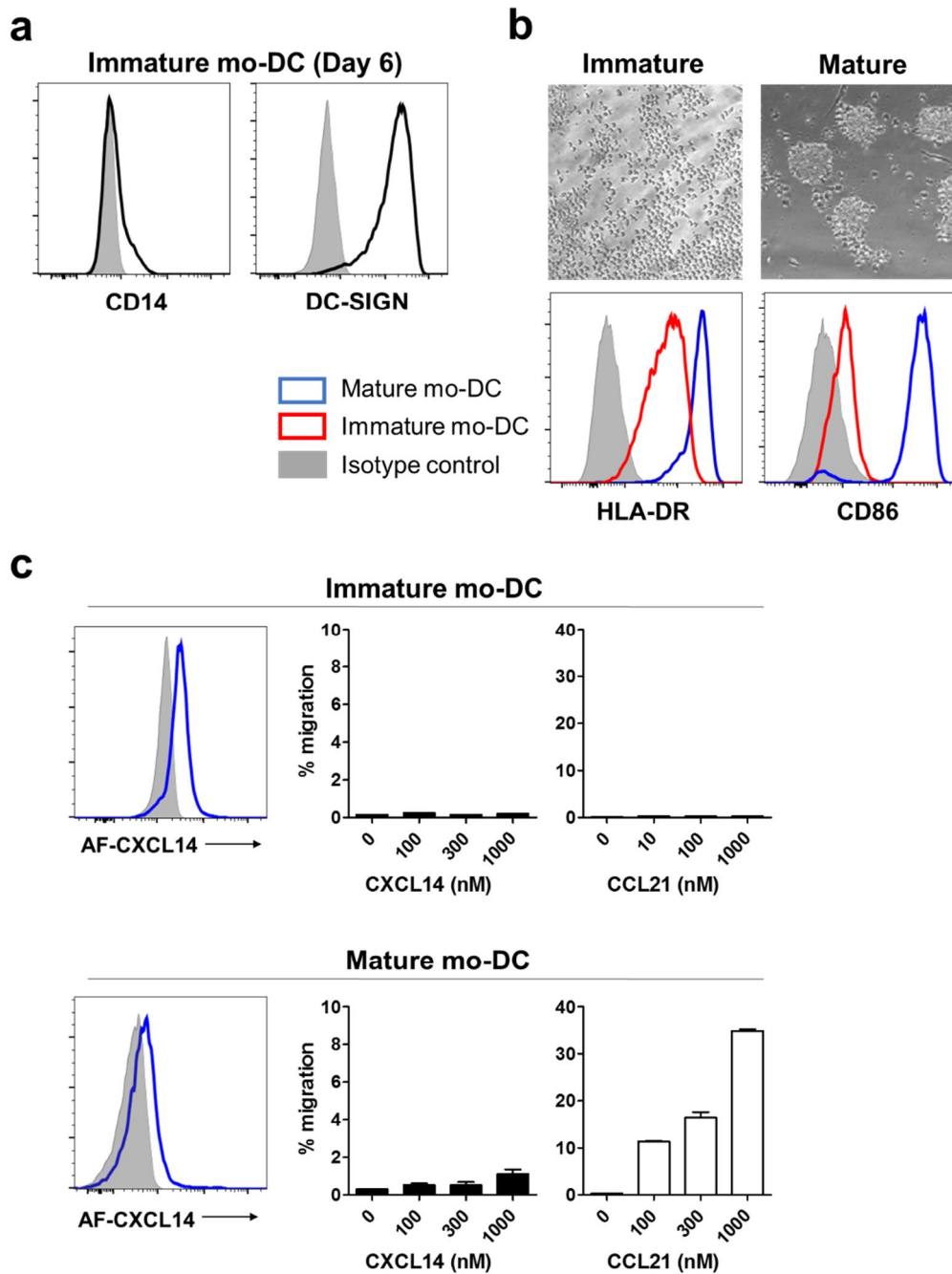
Figure 3.9. *In vitro* monocyte-derived DCs do not respond to CXCL14.

Blood monocytes were cultured for 6 days in the presence of GM-CSF and IL-4 to generate immature monocyte-derived DCs (mo-DC), followed by maturation for 24 hours in the presence of LPS and TNFα. **(a)** By day 6, immature mo-DC have lost CD14 expression and up-regulated expression of DC-SIGN (CD209). **(b)** Comparison of the morphology of immature and mature mo-DC as well as surface expression of MHC class II and the costimulatory molecule CD86, two proteins involved in antigen presentation and activation of T cells. In (a) and (b), grey filled histograms indicate staining with isotype-matched control antibodies. **(c)** Binding of AF-CXCL14 and migration toward CXCL14 or CCL21 of immature (top) and mature (bottom) mo-DC. Grey filled histogram indicates unstained cells. Migration is mean + s.e.m. of two independent experiments, while microscope images and staining plots are representative of 2-3 independent experiments.

3.4 Responses to CXCL14 can be modelled in the Human Monocytic Leukaemia Cell-line THP-1

3.4.1 Responsiveness to CXCL14 is maintained in cultured monocytes by prostaglandin E2

It was demonstrated in previous work by our group that addition of PGE_2 to 1-2 day monocyte cultures induced acquisition of responsiveness to CXCL14 (Kurth et al., 2001). In clear contrast to my own findings, the study by Kurth et al. showed that monocytes freshly isolated from peripheral blood responded only very weakly to CXCL14. Despite my observation that freshly isolated monocytes exhibit a robust and reproducible migratory response toward CXCL14, I decided to see if the PGE_2 effect on monocytes was still valid. Freshly isolated PBMC were placed into culture in medium alone, or in medium supplemented with 1 µM PGE_2. Migration toward CXCL14 was assessed the following day using the transwell chemotaxis assay. Interestingly, it was observed that monocytes cultured in medium alone up-regulated CD16 expression, so that the majority of cells were positive for both CD14 and CD16. In contrast, up-regulation of CD16 expression was not observed in monocytes cultured with PGE_2, the relative proportions of the three monocyte subsets defined by CD14 and CD16 expression resembling that seen in freshly isolated PBMC (shown in Figure 3.1). A further observation was that the minor population of $CD14^+CD16^{++}$ non-classical monocytes was largely absent from the cells recovered after 24 hours in culture, either alone or with PGE_2 (**Figure 3.10a**). Of note, >50% of monocytes were dead following overnight culture in medium alone, while this figure was reduced to 10-30% by addition of PGE_2 (data not shown).

Migration of PBMC toward CXCL14 following 1-day culture is shown (**Figure 3.10b**). Here, migration toward chemokine is displayed in the form of the chemotactic index, i.e. the fold-increase in migration compared to buffer alone (blank). This was done to normalise the data, as each of the different cell subsets gave varying levels of background migration (from 1-2% for monocytes to ~10% for T and NK cells). PGE_2-treated monocytes exhibited a nearly 11-fold increase in migration to 1000 nM CXCL14 (15.62 ± 0.01% migration to 1000 nM CXCL14, compared to 1.44 ± 0.23% migration toward buffer alone; p<0.001). Unstimulated monocytes, as well as T cells, B cells and NK cells (either unstimulated or PGE_2-stimulated) did not display any migration toward CXCL14 (**Figure 3.10b**).
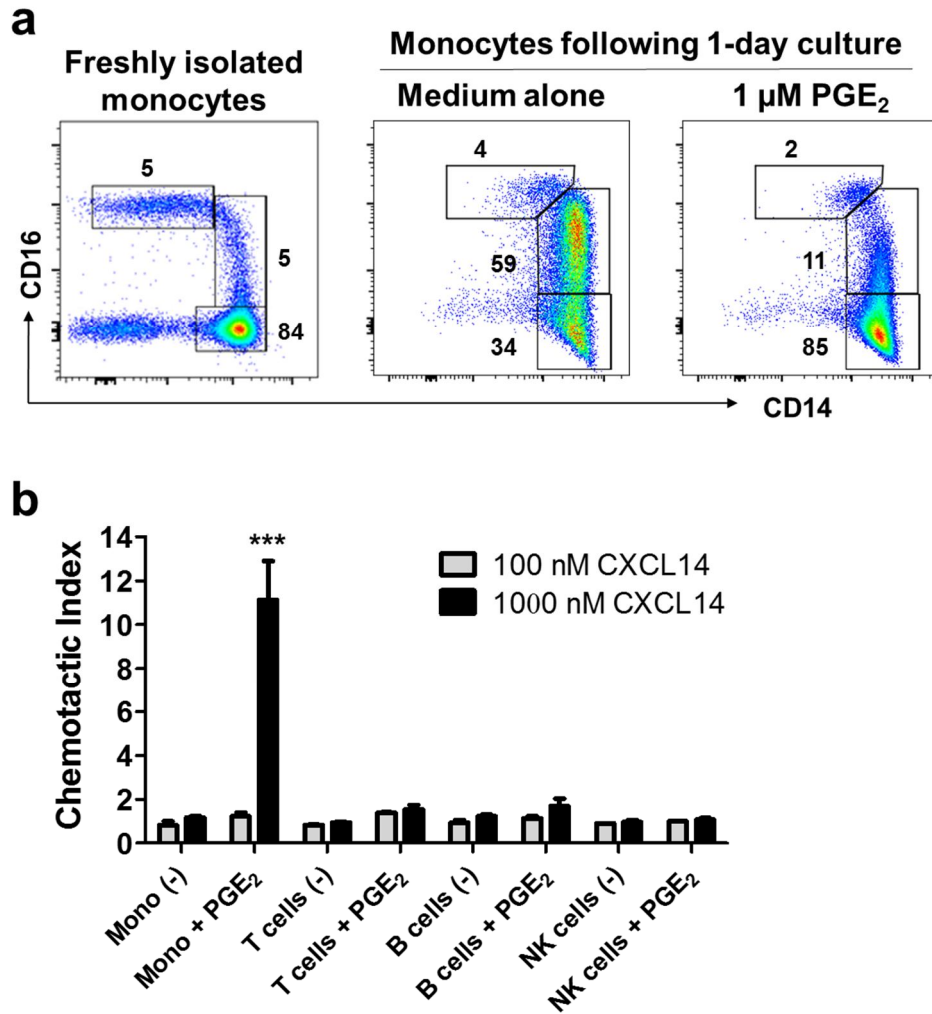
Figure 3.10. Overnight culture with prostaglandin E2 maintains monocyte responsiveness to CXCL14.

PBMC were cultured for 20-24 hours in medium alone, or in medium supplemented with 1 μM PGE$_2$. **(a)** Representative FACS plots showing the monocyte subsets defined by CD14 and CD16 expression in freshly isolated monocytes (left) and in monocytes following overnight culture (right). Numbers indicate the frequency (percentage) of each of the three populations. **(b)** Migration of overnight-cultured PBMC to CXCL14, where migration is expressed as the fold-increase in migrated cells compared to the blank (chemotactic index). Data shown is mean + s.e.m. of two independent experiments. ***$P<0.001$ compared to all other groups using two-way ANOVA. (-) indicates no treatment i.e. cells cultured in medium alone.

3.4.2 Induction of CXCL14-responsiveness in monocytes by PGE$_2$ can be replicated in THP-1 cells

In order to study the monocyte response to CXCL14 more closely, I attempted to reproduce my findings from primary human monocytes in a monocytic cell-line. A modest chemotactic response toward CXCL14 has previously been reported in the human monocytic leukaemia cell-line THP-1 (Hara and Tanegashima, 2012, Tanegashima et al., 2010b). THP-1 cell-responsiveness toward CXCL14 was tested by transwell chemotaxis assay. THP-1 cells were cultured in the absence (medium alone) or presence of 1 μM PGE$_2$. After 24-48 hours in culture, migration toward CXCL14, as well as the monocyte chemoattractant CCL2, was performed. Culture with PGE$_2$ elicited a strong response to micromolar concentrations of CXCL14, while THP-1 cells cultured in medium alone failed to migrate (33.6 ± 5.2% of PGE$_2$-treated cells, compared to 1.42 ± 0.33% of untreated cells migrated toward 3 μM CXCL14; $p<0.001$) (**Figure 3.11a**). PGE$_2$-treated THP-1 cells did not migrate to sub-micromolar concentrations of CXCL14 (not shown). Of note, the chemotactic response of THP-1 cells to CCL2 was unaffected by stimulation with PGE$_2$ (**Figure 3.11b**).
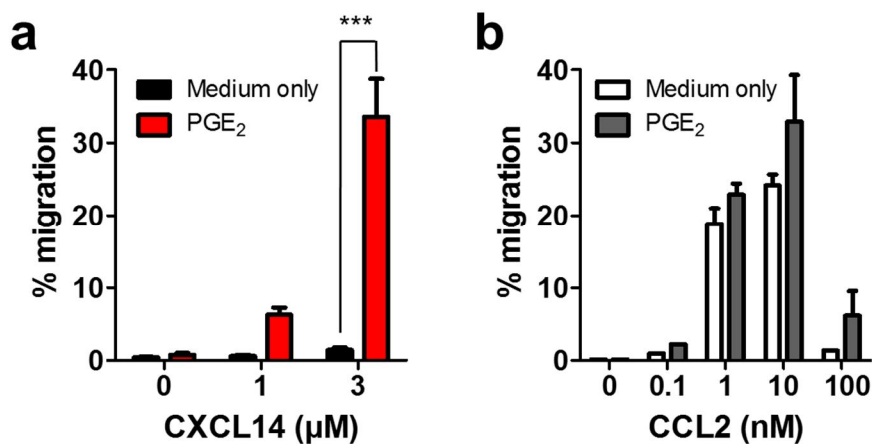
Figure 3.11. The monocytic leukaemia cell-line THP-1 can also be induced to migrate to CXCL14 by treatment with PGE$_2$.
Migration of THP-1 cells in response to **(a)** CXCL14 or **(b)** CCL2 following 1-2 day culture in medium alone, or in medium supplemented with 1 μM PGE$_2$. Data shown are mean + s.e.m. (a) is an average of 10 independent experiments; ***$P<0.001$ using a two-way ANOVA. (b) is an average of two independent experiments.

PGE$_2$ exerts its effects on cells via four receptors, designated EP1 to EP4. In order to determine at which receptor(s) PGE$_2$ was inducing responsiveness toward CXCL14, THP-1 cells were treated with a number of selective EP receptor agonists and antagonists. THP-1 cells stimulated with 1 µM PGE$_2$ migrated well in response to 3 µM CXCL14, as expected (37.9% of input cells migrated). The combined EP1 and EP3 agonist 19R(OH)PGE$_2$ did not induce a migratory response to CXCL14 above that of unstimulated THP-1 cells (1.3% migrated), while the EP2 agonist Butaprost induced a weak response to CXCL14 (8.49% migrated). In contrast, the EP4 agonist Cay10598 induced the strongest response to CXCL14, similar to that induced by PGE$_2$ itself (35.2% migrated; **Figure 3.12a**).

Next, THP-1 cells were stimulated overnight with 1 µM PGE$_2$ in the presence of various selective EP receptor antagonists. Again, THP-1 cells stimulated with PGE$_2$ alone migrated well in response to 3 µM CXCL14 (35.6% of input cells migrated). Addition of the selective EP1 antagonist SC19220, as well as the EP1-3 antagonist AH6809, had only a modest inhibitory effect on migration to CXCL14 (32.1% and 26.6% of cells migrated toward 3 µM CXCL14, respectively). In contrast, the selective EP4 antagonist ONO-AE3-208 completely abolished induction of CXCL14 responsiveness by PGE$_2$, migration returning to the level of unstimulated THP-1 cells (1.4% of cells migrated toward 3 µM CXCL14; **Figure 3.12b**). These data clearly show that it is primarily the EP4 receptor which is responsible for the induction of CXCL14 responsiveness by PGE$_2$ in THP-1 cells. EP2 and EP4 have been shown to induce elevation of cyclic AMP (cAMP) levels in cells following activation, in contrast to EP3 which prevents conversion of ATP to cAMP through inhibition of adenylate cyclase activity (Sugimoto and Narumiya, 2007). Involvement of EP4 (and possibly EP2 also) in the induction of CXCL14 responses in THP-1 cells by PGE$_2$ was confirmed by showing that induction can also be achieved by treatment with forskolin, a naturally occurring compound which raises levels of cAMP in cells through direct activation of adenylate cyclase (data not shown).
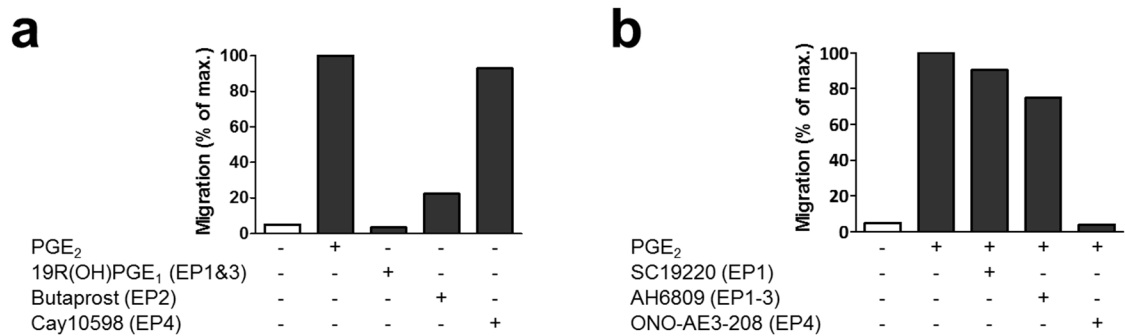
Figure 3.12. PGE$_2$ induces CXCL14-responsiveness in THP-1 cells primarily via the EP$_4$ receptor.

(a) THP-1 cells were cultured for 24 hours in the presence of 1 µM PGE$_2$ or the selective EP receptor agonists 19R(OH)PGE$_2$, Butaprost or CAY10598 (10 µM of each). Migration in response to 3 µM CXCL14 was assessed by transwell chemotaxis assay. Migration is normalised to PGE$_2$ (given as 100%). **(b)** THP-1 cells were cultured for 24 hours in the presence of 1 µM PGE$_2$ alone or in combination with 10 µM of the selective EP receptor antagonists SC19220, AH6809 and ONO-AE3-208. Migration in response to 3 µM CXCL14 was assessed by transwell chemotaxis assay. Migration is normalised to PGE$_2$ alone (given as 100%). For both (a) and (b), data shown is from a single experiment which is representative of two independent experiments.

3.4.3 The β-sheets region of CXCL14 has chemotactic activity, while the N-terminal and C-terminal regions do not

Synthetic peptides of discrete regions of CXCL14 were synthesised as described in (Dai et al., 2015), and are shown in **Table 3.1**. The peptides were tested to determine which portion(s) of the molecule are responsible for the different roles of CXCL14, namely its chemotactic and antimicrobial activities. Interestingly, we found that there is a division of labour within the CXCL14 molecule. The central part of the molecule representing the β-sheet was able to induce chemotaxis of PGE$_2$-treated THP-1 cells (7.79 ± 2.03% cells migrated toward 10 µM peptide 14-54, compared to 0.38 ± 0.16% toward buffer only). The strength of the migratory response was approximately 4-fold lower compared to that elicited by native CXCL14 (Figure 3.11a), indicating that other components of the peptide are required for induction of a full response. The N-terminal and C-terminal peptides, however, failed to induce chemotaxis by themselves (**Figure 3.13**). Interestingly, antimicrobial activity against gram-negative bacteria was largely associated with the N-terminal peptide 1-13, although the central β-sheet also had some killing activity (Dai et al., 2015). While other CXC chemokines have five or more

residues in their NH$_2$-terminal region which have been shown to be essential for interaction with their cognate receptors (Clark-Lewis et al., 1994, Rajagopalan and Rajarathnam, 2006), CXCL14 has a short NH$_2$-terminus, consisting of only two amino acids. It may be therefore that the N-terminal region of CXCL14 is not important for interaction with its receptor, a notion that would appear to be supported by the lack of chemotactic activity possessed by the N-terminal peptides. In addition, a unique characteristic of CXCL14 is that it has an insertion of five amino acids ([41]VSRYR[45]) which is not seen in other CXC chemokines (underlined in Table 3.1). This insertion is within the β-sheet region of the peptide, possibly representing a novel determinant governing its chemotactic activity.

Table 3.1. Synthetic peptides, representing discrete regions of CXCL14, tested for chemotactic activity on PGE$_2$-treated THP-1 cells.

Peptide[a]	Molecular weight (Da)	Amino acid sequence
N-terminal 1-17	1955.33	SKCKCSRKGPKIRYSDV
N-terminal 1-13	1492.20	SKCKCSRKGPKIR
N-terminal 1-11	1221.50	SKCKCSRKGPK
N-terminal 1-10	1093.33	SKCKCSRKGP
N-terminal 1-9	996.21	SKCKCSRKG
N-terminal 1-8	939.16	SKCKCSRK
β-sheets 14-54	4917.50	YSDVKKLEMKPKYPHCEEKMVIITTKS<u>VSRYR</u>GQEHCLHPK
C-terminal 55-77	3048.00	LQSTKRFIKWYNAWNEKRRVYEE

[a]Numbering represents the position of the amino acid residues in the full-length CXCL14 protein
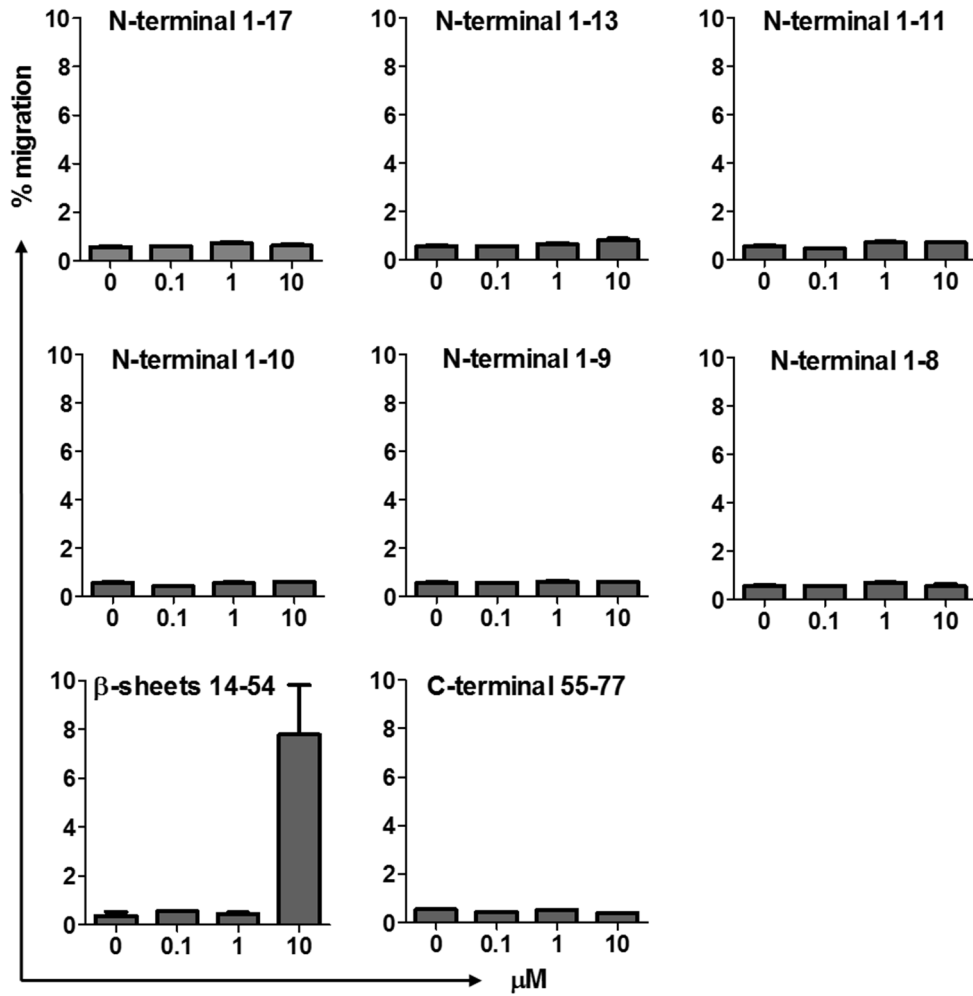
Figure 3.13. The β-sheets region of CXCL14 has chemotactic activity, while the N-terminal and C-terminal regions do not.

THP-1 cells were treated for 24 hours with 1 µM PGE$_2$, followed by testing migratory responses toward each of the synthetic CXCL14 peptides listed in Table 3.1. Peptide concentrations ranging from 0.1-10 µM were tested for chemotactic activity. Data shown is mean + s.e.m. of two independent experiments.

3.4.4 AF-CXCL14, the reagent used to identify cells expressing CXCL14 receptor(s), is functionally active

I confirmed that AF-CXCL14, used to identify CD14^{hi} monocytes as CXCL14 target cells in peripheral blood (see Figures 3.3-3.5) was functionally active by its ability to induce chemotaxis of PGE_2-treated THP-1 cells. Cells gave a very robust migration in response to 3 µM AF-CXCL14, although no migration was observed in response to 1 µM (**Figure 3.14**). These results may suggest that attachment of the AF647 fluorochrome at its C-terminus has rendered AF-CXCL14 slightly less active than the native chemokine. However, the fact that it is active in the range (1-3 µM) that native CXCL14 is active on PGE_2-treated THP-1 cells indicates that the reagent is suitable for use in binding studies. Of note, in future binding studies using immune cells isolated from human skin (see next section), binding of murine CCL1 conjugated to AF647 (AF-muCCL1) was used as a control for non-specific binding of AF-CXCL14. Chemotactic activity of AF-muCCL1 on 300.19 cells stably transfected with its cognate receptor murine CCR8 (muCCR8) was confirmed by myself in our lab (**Figure 3.14**), while use of this reagent to label muCCR8 expressed on the surface of primary murine T cells has recently been published by our group (McCully et al., 2015).
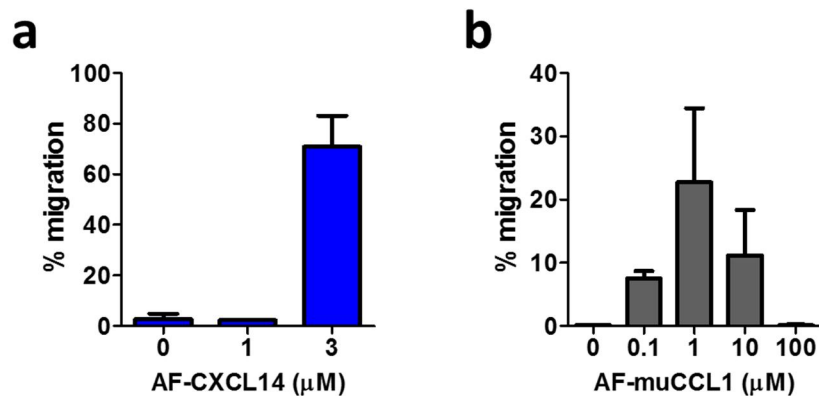
Figure 3.14. AF-CXCL14 and AF-muCCL1 have chemotactic activity.
(a) THP-1 cells were treated overnight with PGE_2, and migration toward AF-CXCL14 was assessed the following day by transwell chemotaxis assay. **(b)** 300.19 cells stably transfected with murine CCR8 were assessed for migration toward AF-muCCL1 by transwell chemotaxis assay. Data are mean + s.e.m. of two independent experiments.

3.5 CXCL14 Target Cells in Human Skin

3.5.1 Gating strategy to identify immune cell populations isolated from epidermis by flow cytometry

Human split skin samples were partially enzymatically digested to enable separation of the dermis from the epidermis. Epidermal sheets devoid of dermal tissue were left intact and placed into culture for 2-3 days, during which time the resident immune cells emigrated out of the tissue into the medium. Emigrant cells were collected and single cell suspensions were stained with fluorochrome-conjugated mAbs against CD45, CD3, CD1a, CD14, CD207 (langerin) and HLA-DR. A representative experiment is shown. The forward scatter vs. side scatter gate shows a disparate population, consisting of cells of all shapes, sizes and granularities. Following exclusion of cell aggregates and dead cells (the majority of emigrant cells recovered from the epidermis were found to be dead), gating on CD45 vs side scatter reveals three distinct populations (**Figure 3.15a**). There is a minor population of $CD45^+$ SSC^{lo} cells (~2% of total live cells), the majority of which are $CD3^+$ T cells (**Figure 3.15b**). The remaining $CD45^+$ cells are here referred to as "high" side scatter, accounting for ~22% of all live cells ($CD45^+$ SSC^{hi}). The majority of these cells are Langerhans cells, a specialised population of DCs that reside in the epidermis, as evidenced by their expression of CD1a, HLA-DR and langerin (**Figure 3.15c**). The $CD45^{neg}$ population, which typically does not include cells of haematopoietic origin as CD45 is considered a marker expressed on all immune cells, are discussed later on in this chapter (see Figure 3.20 and Figure 3.21).
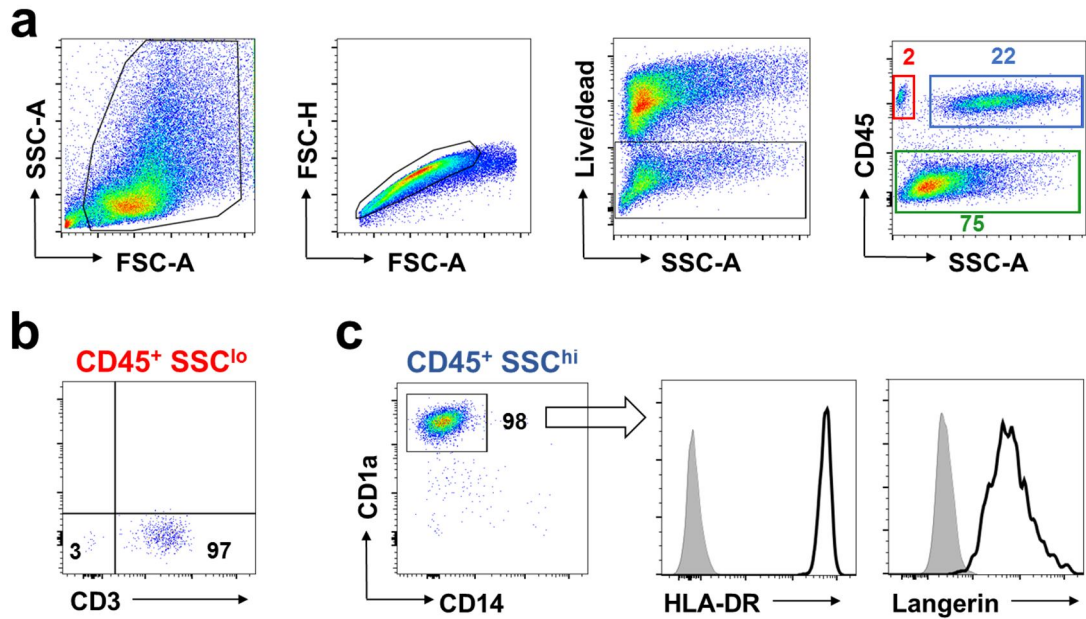
Figure 3.15. Gating strategy to identify immune cell populations isolated from human epidermis by flow cytometry.

Epidermal sheets were cultured for 48-72 hours, after which time emigrant cells were collected and stained with fluorochrome-conjugated mAbs and analysed by flow cytometry. Shown are plots from a single experiment that is representative of three independent experiments using skin from different donors. **(a)** Following exclusion of debris (far left), cell aggregates (centre left) and dead cells (centre right), plotting CD45 vs side scatter (far right) reveals three discrete populations; a CD45+, low side-scatter (SSC) population (2% of total live cells; red gate), a CD45+, high side-scatter population (22% of total live cells; blue gate) and a CD45-neg population (75% of total live cells; green gate). **(b)** The CD45+ SSC-lo population is largely comprised of CD3+ T cells. **(c)** Analysis of the CD45+ SSC-hi epidermal population. Gating on CD1a vs CD14 reveals that 98% of cells have high expression of CD1a, while lacking CD14 (left). Subsequent analysis of these cells reveals that they express high levels of MHC class II as well as staining uniformly positive for langerin (black histograms), confirming that they are Langerhans cells. Grey filled histograms indicate staining with isotype-matched control antibodies.

3.5.2 Gating strategy to identify immune cell populations isolated from dermis by flow cytometry

Like the epidermis, dermal tissue was also cultured for 2-3 days to allow immune cells to emigrate out of the tissue. Following collection of dermal emigrant cells, single-cell suspensions were stained with fluorochrome-conjugated mAbs against the same

markers as for the epidermis, except langerin was replaced with CD1c (Langerin is a specific marker for Langerhans cells, and these cells are only present in the epidermis). A representative experiment is shown. In similar fashion to the epidermis, exclusion of cell aggregates and dead cells followed by plotting CD45 vs side scatter reveals three distinct populations. Unlike the epidermis however, the most abundant population is that characterised by CD45 expression and low side scatter (CD45$^+$ SSC^{lo}; 46% of all live cells). The CD45$^+$ cells with high side scatter (CD45$^+$ SSC^{hi}) accounts for 39% of all live cells. Only a minority of emigrant cells recovered were negative for CD45 expression, accounting for 13% of all live cells recovered from the dermis (**Figure 3.16a**).

Similarly to the epidermis, the majority (91%) of CD45$^+$ SSC^{lo} cells are CD3$^+$ T cells. The remaining 9% likely comprise of other lymphoid populations such as NK cells (**Figure 3.16b**). Found within the CD45$^+$ SSC^{hi} population are the dermal DCs, of which there are two major subsets; CD1a$^+$ DC and CD14$^+$ DC (Haniffa et al., 2015). Tissue CD14^{neg}CD141^{hi} DC, distinct from CD14$^+$ and CD1c$^+$ DCs, have been recently described, but these cells are rare in healthy skin and are not discussed here. The CD1a$^+$ DCs are more abundant than the CD14$^+$ DCs, by approximately 2-fold (**Figure 3.16c**). The two DC populations can also be distinguished by their level of expression of other cell-surface markers including HLA-DR and CD1c, with the CD1a$^+$ DC having higher expression of both. The two types of dermal DC also separate into distinct populations on the CD45 vs SSC plot, with CD1a$^+$ DC having a higher side scatter profile and lower CD45 expression than the CD14$^+$ DC (**Figure 3.16d**).
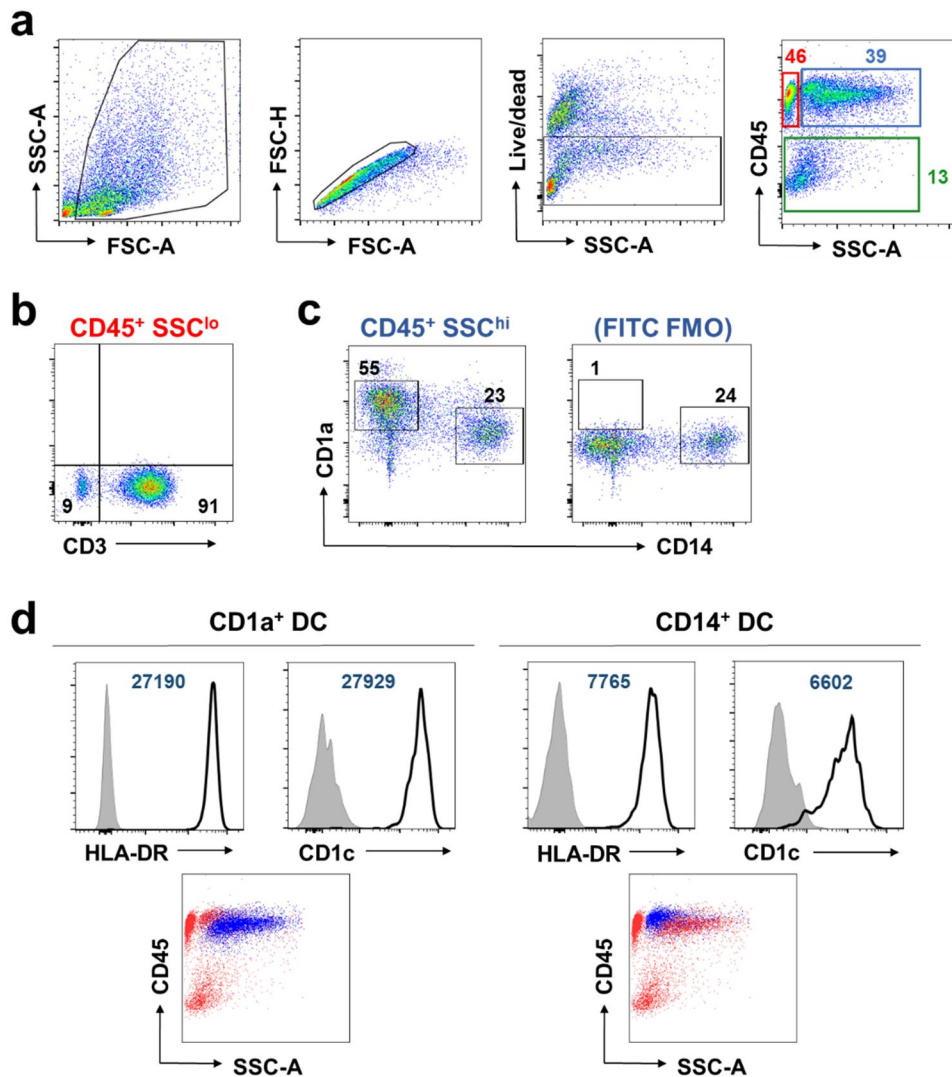
Figure 3.16. Gating strategy to identify immune cell populations isolated from human dermis by flow cytometry.

Dermal tissue was cultured for 48-72 hours, after which time emigrant cells were collected and stained with fluorochrome-conjugated mAbs and analysed by flow cytometry. Shown are plots from a single experiment, representative of three independent experiments. **(a)** Following exclusion of debris (far left), cell aggregates (centre left) and dead cells (centre right), plotting CD45 vs side scatter (far right) reveals three discrete populations; a CD45+ SSC-lo population (46% of live cells; red gate), a CD45+ SSC-hi population (39% of live cells; blue gate) and a CD45-neg population (13% of live cells; green gate). **(b)** The CD45+ SSC-lo population comprises mostly of CD3+ T cells. **(c)** Contained within the CD45+ SSC-hi population are the two subsets of dermal DC; CD1a+ DC and CD14+ DC. CD1a vs CD14 is plotted for cells stained with all antibodies (left), while also shown is the same plot for the fluorescence-minus-one (FMO) control, where cells were stained with all antibodies except for anti-CD1a-FITC (right). **(d)** Comparison of CD1a+ DC (left) and CD14+ DC (right) for expression of HLA-DR and CD1c (black histograms). Grey filled histograms indicate staining with isotype-matched control antibodies. Numbers are MFI (geometric mean). In the lower plots, the position of each of the DC subsets on the CD45 vs SSC plot is shown (cell type indicated is shown in blue).

3.5.3 Epidermal Langerhans cells are not targets for CXCL14

The bulk population of emigrant cells recovered from the epidermis were tested for expression of CXCL14 receptor(s) by binding of AF-CXCL14, while functional responses to CXCL14 were tested by transwell chemotaxis assay. LCs displayed only a very weak binding of AF-CXCL14, with a slight increase in fluorescence in comparison to AF-muCCL1 control (**Figure 3.17a**). In four donors tested, 11.15 ± 2.21% LCs stained positively with AF-CXCL14 (**Figure 3.17b**). However, the fact that there is an overall shift in the populations along the axis, rather than a distinct population of 'positive' cells, leads me to believe that this perceived staining is due to non-specific binding/uptake. This is supported by the observation that LCs did not undergo chemotaxis in response to CXCL14 (0.24 ± 0.08% LCs migrated in response to 1 µM CXCL14, compared to 0.14 ± 0.02% in response to buffer alone; p=0.43) (**Figure 3.17c**). It can therefore be concluded that LCs are probably not targets for CXCL14.
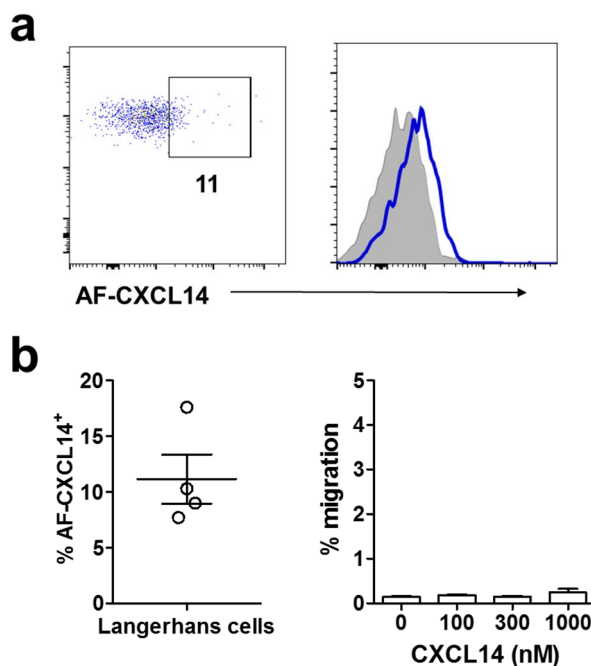
Figure 3.17. Langerhans cells are not targets for CXCL14.
(a) Binding of AF-CXCL14 to epidermal emigrant cells was analysed by flow cytometry. Representative dot plot and histogram to show binding of 50 nM AF-CXCL14 to Langerhans cells (LCs). Number indicates the percentage of positive cells. Grey filled histogram indicates binding of AF-muCCL1. **(b)** Cumulative data from four donors shows the percentage of LCs which are AF-CXCL14+. Data shown is mean ± s.e.m. **(c)** Migration of LCs toward CXCL14. Data is mean + s.e.m. of four independent experiments using different donors.

3.5.4 Lymphocytes isolated from both epidermis and dermis are not targets for CXCL14

Bulk epidermal and dermal emigrant cells were tested for expression of CXCL14 receptor(s) by binding of AF-CXCL14, while functional responses to CXCL14 were tested by transwell chemotaxis assay. As demonstrated in Figure 3.15 (epidermis) and Figure 3.16 (dermis), the majority of cells found in the $CD45^+$ SSC^{lo} gate were $CD3^+$ T cells. Only a small minority of T cells displayed labelling with AF-CXCL14 (4.29 ± 0.32% dermal T cells and 3.80 ± 0.13% epidermal T cells were $AF-CXCL14^+$) (**Figure 3.18a**). Neither dermal nor epidermal T cells displayed specific migration toward CXCL14, although migration of both was observed in response to CXCL12. The analysis and interpretation of dermal T cell migratory responses was slightly complicated by the fact that they displayed high background migration, 15.5 ± 1.7% of dermal T cells migrating toward buffer alone. However, CXCL14 (100-1000 nM) failed to stimulate migration above background, while 38.2 ± 10.4% of dermal T cells migrated in response to 100 nM CXCL12 (chemotactic index = 2.46). Epidermal T cells exhibited lower background migration, 5.4 ± 1.6% of cells migrating toward buffer alone. Again, no specific migration toward CXCL14 was observed, while 24.1 ± 17.4% migrated toward 100 nM CXCL12 (chemotactic index = 4.46; **Figure 3.18b**). These data indicate that skin lymphocytes, like lymphocytes in blood, are not targets for CXCL14.
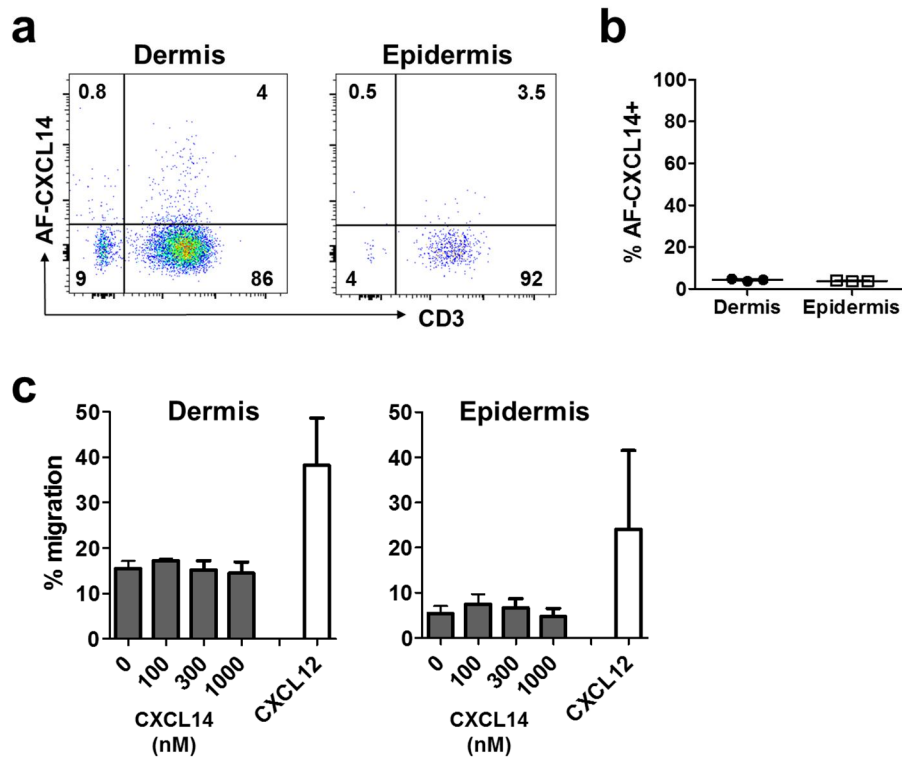
Figure 3.18. Skin lymphocytes are not targets for CXCL14.

Lymphocytes from dermis and epidermis were assessed for binding of AF-CXCL14 and chemotactic responses toward CXCL14. **(a)** Representative dot plots show binding of 50 nM AF-CXCL14 to the CD45+SSC-lo population present in emigrant cells recovered from the dermis (left) and epidermis (right), the majority of which are CD3+ T cells. **(b)** Cumulative data from three independent experiments shows the percentage of dermal and epidermal T cells which were AF-CXCL14+. Data is displayed as mean ± s.e.m. **(c)** Migration of dermal and epidermal T cells toward 100-1000 nM CXCL14 and 100 nM CXCL12 is shown. Data shown is mean + s.e.m. of four independent experiments.

3.5.5 CD14$^+$ DCs express CXCL14 receptor(s), while CD1a$^+$ DCs do not

Both dermal DC subsets are of myeloid origin, as demonstrated in patients who are deficient in blood monocytes and myeloid DCs due to IRF8 and GATA2 mutation. These patients lack dermal DC subsets and have reduced numbers of macrophages, however their epidermal LC pool is completely intact (Bigley et al., 2011, Hambleton et al., 2011). This implies that dermal DCs are directly dependent on either circulating monocytes and/or DCs, or a shared HSC-derived precursor. The specific contributions, however, of circulating monocytes and DCs to skin DC subsets remain unclear. Although it has recently been demonstrated that the CD14$^+$ DC subset which

resides in human dermis is in fact more transcriptionally aligned to monocytes and macrophages than DCs (McGovern et al., 2014), I will continue to refer to them as CD14$^+$ DCs here, as per the existing convention.

Skin DCs were assessed for binding of AF-CXCL14. Only a minor proportion of CD1a$^+$ DCs (13.5 ± 1.8%) stained positively for expression of CXCL14 receptors. In contrast, CD14$^+$ DCs displayed strong binding of the labelled chemokine (91.7 ± 1.2% CD14$^+$ DCs were AF-CXCL14$^+$). Representative data for AF-CXCL14 binding is displayed in the form of dot plots (and accompanying histograms) in **Figure 3.19a**, and cumulative data from three donors is displayed graphically in **Figure 3.19b**. Migratory responses toward CXCL14 were assessed by transwell chemotaxis assay. CD1a$^+$ DCs displayed minimal migration toward CXCL14 (2.03 ± 0.31% CD1a$^+$ DCs migrated toward 1000 nM CXCL14, compared to 0.90 ± 0.67% toward buffer alone; chemotactic index = 2.26), while migrating slightly more toward CXCL12 (4.88 ± 3.94% cells migrated toward 100 nM CXCL12). Despite their presumed expression of CXCL14 receptor(s), CD14$^+$ DCs did not migrate in response to CXCL14 **Figure 3.19c**. Non-specific migration of CD14$^+$ DCs was extremely low (0.04 ± 0.02% CD14$^+$ DCs migrated toward buffer alone); indeed, in one experiment no CD14$^+$ DCs were recovered from the lower chamber. I hypothesised that the setup of the transwell assay was not optimal to observe migration of this particular cell subset, and so I made several attempts to address this issue. Migration assays were performed using filters with larger pores (8 μm instead of the usual 5 μm), while pre-coating of the transwell filters with collagen type-IV was also tested in the theory that this may aid cell attachment, and hence migration. However, no migration of CD14$^+$ DCs was observed (data not shown).
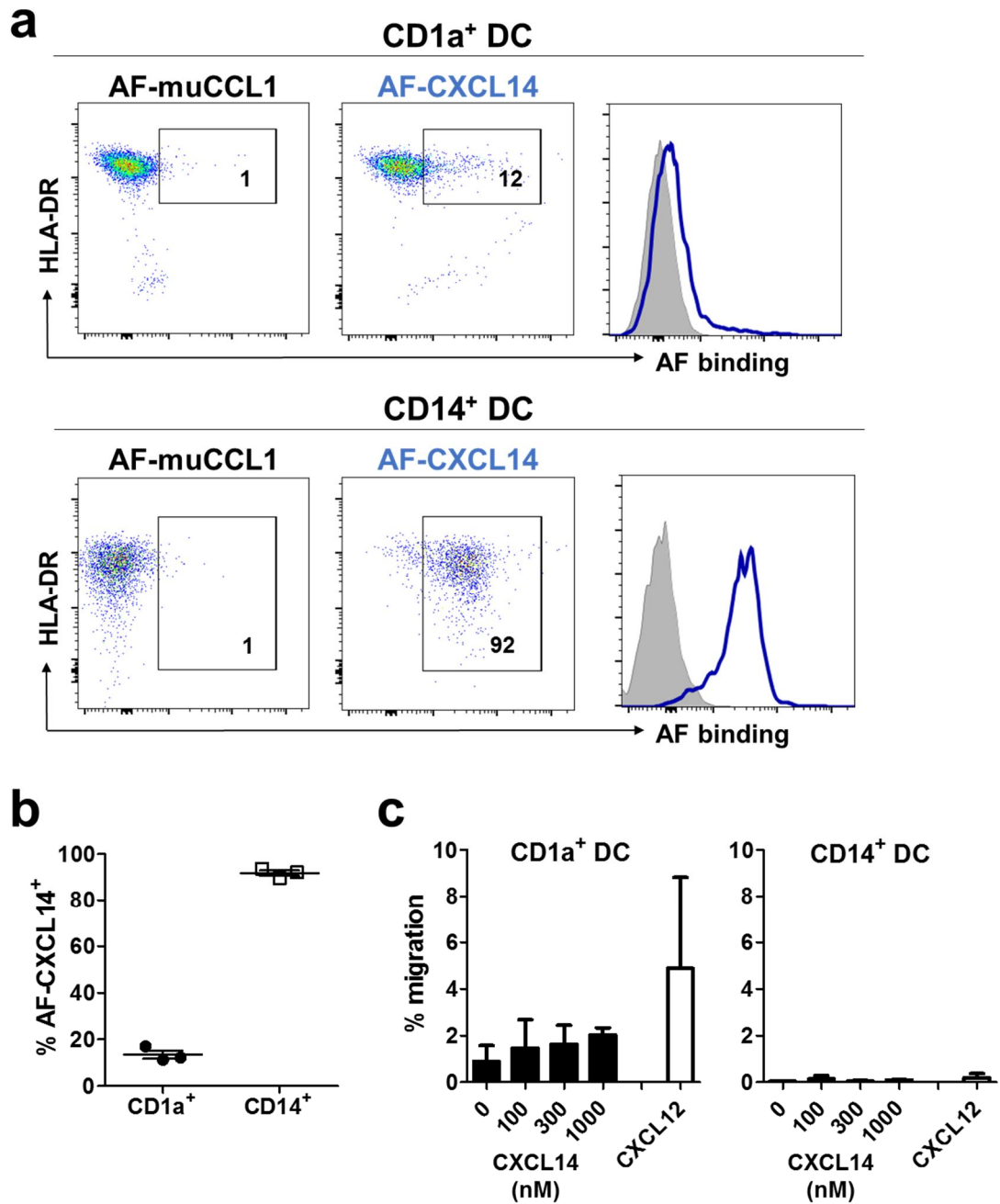
Figure 3.19. CD14+ DCs are targets for CXCL14.

Dermal DCs were assessed for binding of AF-CXCL14. **(a)** Representative dot plots and histogram to show binding of AF-CXCL14 (and AF-muCCL1 as control) to CD1a+ DCs (top) and CD14+ DCs (bottom). Numbers indicate the percentage of AF-CXCL14+ cells. Grey filled histogram indicates binding of AF-muCCL1. **(b)** Cumulative data shows the % of AF-CXCL14+ cells found within the two subsets of dermal DC. Data shown is mean ± s.e.m. of three independent experiments using different donors. **(c)** Migration of the dermal DC subsets toward CXCL14 (100-1000 nM) and CXCL12 (100 nM) is shown. Data shown is mean + s.e.m. of three donors.

3.5.6 Within the CD45^{neg} population of the epidermal emigrant cells, there is a subset which are targets for CXCL14

When studying immune cells extracted from tissue, many researchers exclude from their analysis all cells that are negative for expression of CD45, on account of this 'pan-immune cell' marker being considered to be present on all cells of haematopoietic origin. However, upon examination of the CD45^{neg} population isolated from human skin samples, I made a startling discovery. Approximately 75% of the live emigrant cells recovered from the epidermis were negative for CD45 expression (see Figure 3.15a). Upon further analysis of this population, we found that a subset of the CD45^{neg} cells expressed both CD14 and CD1a, cell-surface proteins with roles in pathogen-sensing (CD14) and antigen presentation (CD1a) normally associated with immune cells of the myeloid lineage (**Figure 3.20a**). Remarkably, these CD45^{neg}CD1a$^+$CD14$^+$ displayed strong binding of AF-CXCL14, with representative staining plots shown in **Figure 3.20b**. This contrasted with the remaining CD45^{neg} cells, which lack CD1a and CD14 expression and displayed only very weak binding. Data from four donors is combined in **Figure 3.20c**, where 85.2 ± 3.6% epidermal CD45^{neg}CD1a$^+$CD14$^+$ cells stained positive for AF-CXCL14, while only 10.6 ± 5.0% CD45$^-$CD1a$^-$CD14$^-$ cells were positive (p=0.0003). This staining data was reflected exquisitely in transwell chemotaxis assays, with CD45^{neg}CD1a$^+$CD14$^+$ cells demonstrating a dose-dependent increase in migration toward CXCL14 (16.4 ± 3.3% CD45^{neg}CD1a$^+$CD14$^+$ cells migrated toward 1000 nM CXCL14, compared to 2.2 ± 0.9% toward buffer alone; chemotactic index = 7.6, p=0.02). In contrast, the remaining CD45^{neg} cells failed to migrate toward CXCL14 (1.6 ± 0.33% CD45^{neg}CD1a^{neg} cells migrating toward 1000 nM CXCL14, compared to 2.1 ± 0.6% toward buffer alone; chemotactic index = 0.77, p=0.88). The CD45^{neg}CD1a$^+$CD14$^+$ cells did not migrate in response to CXCL12 (**Figure 3.20d**), an intriguing finding because CXCR4 is expressed on virtually all cells of haematopoietic origin. Lack of CXCR4 expression, combined with being CD45-negative, may indicate that these cells are unusual in their origin/function.
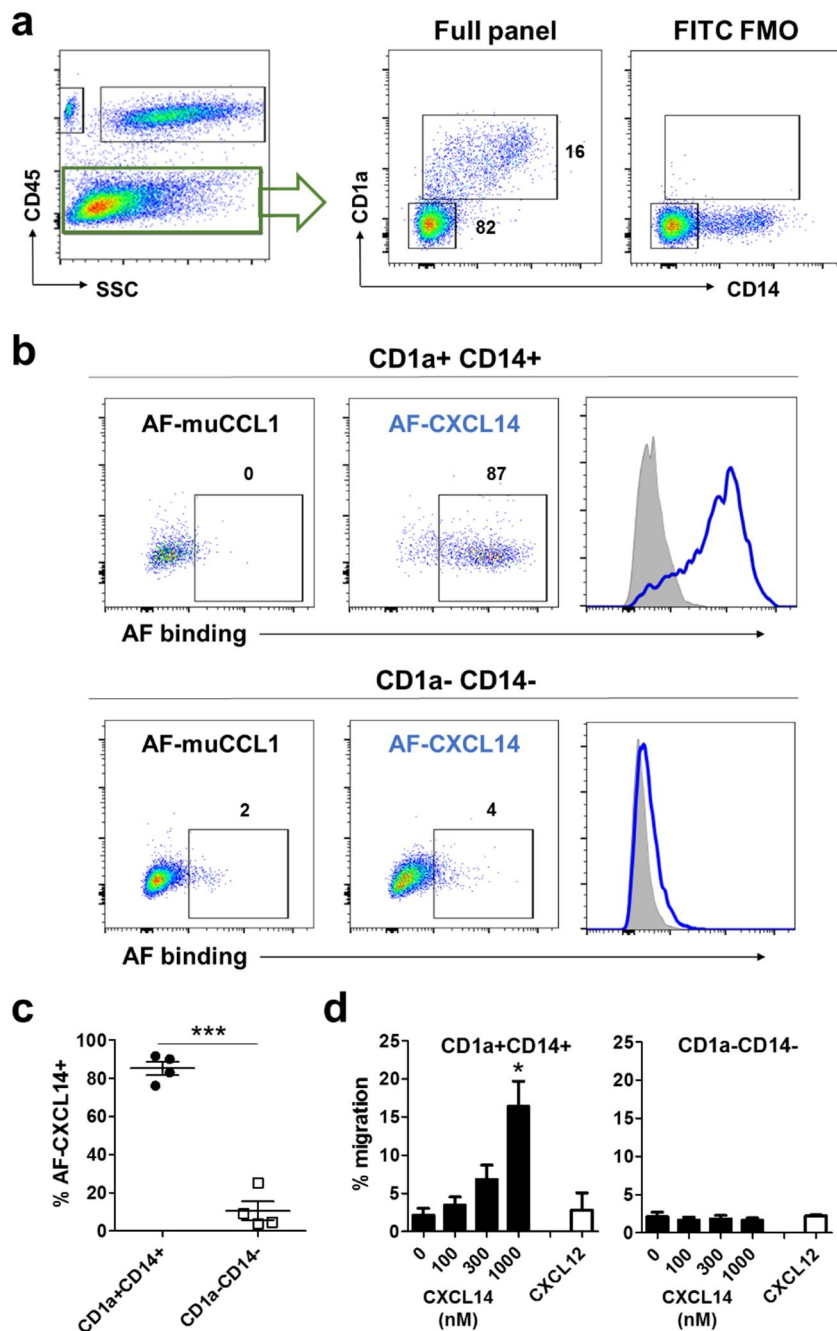
Figure 3.20. Contained within the CD45-neg epidermal fraction is a population of cells which are targets for CXCL14.

(a) Representative dot plots show expression of CD1a and CD14 by the CD45-neg fraction of the epidermal emigrant cells. Cells stained with all antibodies except for anti-CD1a-FITC are shown for comparison (FITC FMO; right). **(b)** Representative dot plots and histogram show binding of AF-muCCL1 and AF-CXCL14 to CD1a+CD14+ cells (top row), and CD1a^{neg}CD14^{neg} cells (bottom row). Numbers indicate the % of AF-CXCL14+ cells. Grey filled histogram indicates binding of AF-muCCL1. **(c)** Cumulative data shows the % of AF-CXCL14+ cells found within the epidermal CD45^{neg} population. Data shown is mean ± s.e.m. of four donors, ***$P<0.001$ using a paired t-test. **(d)** Migration of CD1a+CD14+ cells (left) and the remaining CD45^{neg} fraction (right) toward 100-1000 nM CXCL14 and 100 nM CXCL12. Data is mean + s.e.m. of four donors, *$P<0.05$ compared to 0 nM using a Kruskall-Wallis ANOVA.

3.5.7 CD45^{neg}CD1a^{+}CD14^{+} cells are also found in the dermis

In contrast to the epidermis, only a minority of dermal emigrant cells were negative for CD45 expression (Approximately 13% of live cells were CD45^{neg}; Figure 3.16a). However, as for the epidermis, I identified a minor subset within the CD45^{neg} fraction which was positive for both CD14 and CD1a expression (**Figure 3.21a**). Despite there being small numbers of cells, I was able to show that they bound AF-CXCL14, in contrast to the remaining CD45^{neg}, most of which were negative for expression of CXCL14 receptor(s) (**Figure 3.21b**). Combined data from three donors is shown in (**Figure 3.21c**), where 80.6 ± 9.5 dermal CD1a^{+}CD14^{+} cells stained positive for AF-CXCL14, while 25.9 ± 5.9% dermal CD1a^{neg}CD14^{neg} cells were AF-CXCL14^{+}. This indicates that the CD1a^{+}CD14^{+} cells expressed CXCL14 receptor(s), which again was confirmed by migration to CXCL14. Despite high non-specific background migration (14.3 ± 8.5% migration toward buffer alone), CD1a^{+}CD14^{+} cells migrated strongly toward 1000 nM CXCL14 (66.9 ± 19.8% migration; chemotactic index = 4.7). However, this did not reach significance (p=0.21, Kruskall-Wallis ANOVA), which can probably be explained by the low number of experimental repeats (n=3). In contrast, CD1a^{neg}CD14^{neg} cells failed to migrate toward CXCL14 (23.6 ± 7.5% cells migrated toward 1000 nM CXCL14, compared to 24.8 ± 8.1% toward buffer alone; chemotactic index = 1.05) (**Figure 3.21d**).
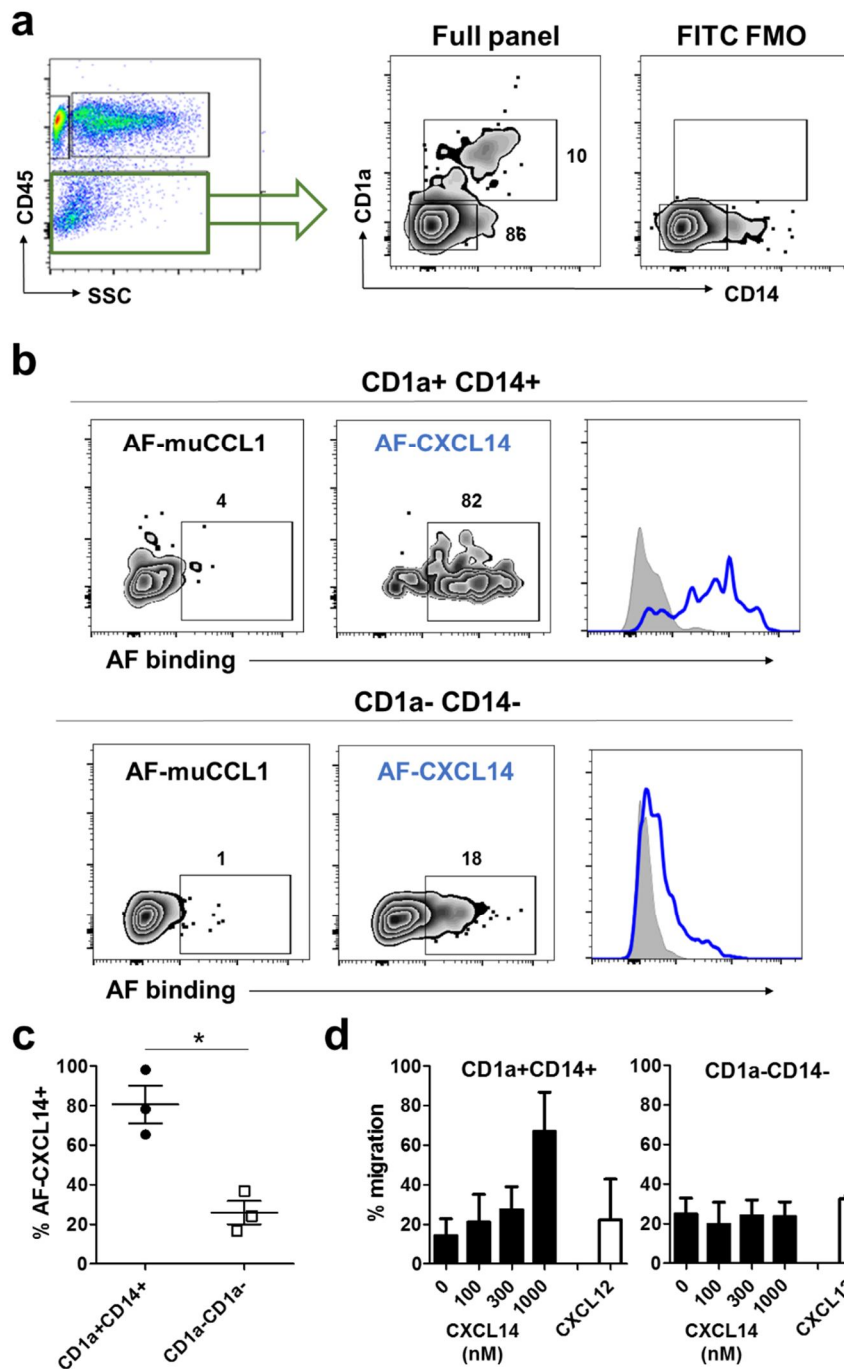
Figure 3.21. Contained within the CD45^{neg} dermal fraction is a population of cells which are targets for CXCL14.

(a) Representative dot plots show expression of CD1a and CD14 by the CD45-neg fraction of the dermal emigrant cells. Cells stained with all antibodies except for anti-CD1a-FITC are shown for comparison (FITC FMO; right). **(b)** Representative dot plots and histograms show binding of AF-muCCL1 and AF-CXCL14 to CD1a+CD14+ cells (top), and CD1a^{neg}CD14^{neg} cells (bottom). Numbers indicate the % of AF-CXCL14+ cells. Grey filled histogram indicates binding of AF-muCCL1. **(c)** Cumulative data shows the % of AF-CXCL14+ cells found within the epidermal CD45^{neg} population, and is mean ± s.e.m. of three donors *$P<0.05$ using a paired T test. **(d)** Migration of CD1a+CD14+ cells (left) and the remaining CD45^{neg} fraction (right) toward 100-1000 nM CXCL14 and 100 nM CXCL12. Data is mean + s.e.m. of three donors.

3.5.8 Dermal macrophages are extracted by overnight proteolytic digestion of the dermis

Following separation of the dermis and epidermis, dermal tissue was digested overnight in medium containing collagenase D. Upon inspection the following day, the tissue had completely dissociated. Here, cells recovered from the dermis by total overnight digestion are referred to as extracted cells, in contrast to cells which are allowed to spontaneously migrate out of the tissue over 2-3 days and have been referred to thus far as emigrant cells. Extracted single cell-suspensions were stained with fluorochrome-conjugated mAbs against CD45, HLA-DR, CD1c, CD14 and CD163. The FITC channel was left empty to aid in the identification of macrophages, as they have higher autofluorescence than the other immune cell subsets, and autofluorescence is most readily detectable in channels excited by the 488-nm laser (Haniffa et al., 2009). Following successive exclusion of debris, cell aggregates and dead cells, the live single cell population was successively refined by gating on CD45$^+$ cells, which includes DCs, macrophages, lymphocytes and mast cells, and then on HLA-DR$^+$ cells, which excludes mast cells and lymphocytes. This resulted in two major fractions separable by autofluorescence (AutoF): AutoF^{lo} and AutoF^{high} (**Figure 3.22a**). The AutoF^{high} macrophages account for between one-third and one-half of the CD45$^+$HLA-DR$^+$ fraction. The same gating strategy performed on dermal emigrant cells was performed, showing a total absence of AutoF^{high} cells from the CD45$^+$HLA-DR$^+$ fraction, confirming that macrophages can only be recovered from the dermis by overnight digestion and do not emigrate out of the tissue (**Figure 3.22b**). Phenotyping of the AutoF^{high} fraction confirmed their expression of CD163 and CD14 (although the latter is expressed at lower levels than on CD14$^+$ DC) and absence of CD1c (**Figure 3.22c**). Binding studies were performed using AF-CXCL14 and interestingly, we observed a subset of macrophages, accounting for approximately 25% of the total population, which were AF-CXCL14$^+$. These were clearly distinct from the remaining 75% of AutoF^{high} cells, which did not bind AF-CXCL14 (**Figure 3.22d**).
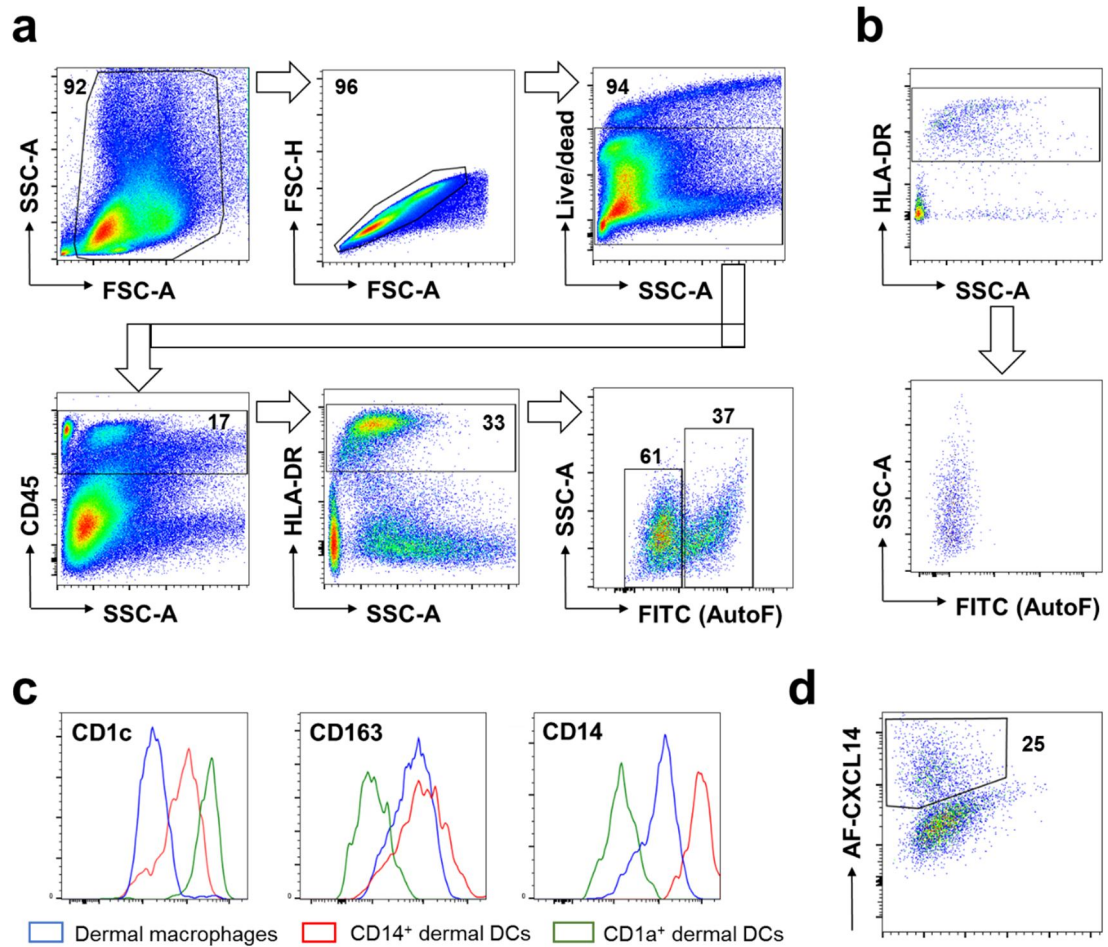
Figure 3.22. Macrophages are extracted from the dermis by overnight digestion, and a proportion of them express CXCL14 receptor(s).

Dermis was subjected to overnight collagenase digestion, and recovered cells were stained with fluorochrome-conjugated monoclonal antibodies and analysed by flow cytometry. **(a)** Gating strategy used to identify resident macrophages. Successive gating on cells, singlets and live cells (top panels) was followed by progressive refinement of the total live cell population by gating on CD45+ cells, then HLA-DR+ cells. Autofluorescence (AutoF), recorded in the FITC channel (488-nm laser), was plotted vs SSC on the CD45+HLA-DR+ cells, enabling identification of AutoF[high] macrophages. Plots are representative of two independent experiments. **(b)** The same gating strategy, performed on dermal emigrant cells, reveals that no AutoF[high] macrophages are present in the emigrant cells. **(c)** Surface phenotype of resident CD45+HLA-DR+ dermal cells. Macrophages were gated on as described in (a), while dermal DCs populations were gated on as described in Figure 3.16; macrophages (blue), CD14+ DCs (red) and CD1a+ DCs (green). **(d)** Binding of AF-CXCL14 to dermal macrophages, detected by flow cytometry. Number indicates % of cells which are AF-CXCL14+, and is representative of two donors.

In an unexpected finding, overnight digestion of the dermis yielded much greater numbers of CD45^{neg}CD1a$^+$CD14$^+$ cells than were recovered when cells were allowed to spontaneously emigrate from this tissue. Amazingly, in one donor, there were equivalent numbers of CD45^{neg}CD1a$^+$CD14$^+$ cells as total CD45$^+$ cells. 16% of live, single cells recovered were CD45^{neg}CD1a$^+$CD14$^+$ (**Figure 3.23a**), compared to 17% of live single cells which were CD45$^+$ (see Figure 3.22a). It would therefore appear that large numbers of these cells are residing in the dermal tissue and that, like macrophages, most are fixed in the dermis and can only be recovered by total digestion. Expression of CXCL14 receptor(s) on extracted CD45^{neg}CD1a$^+$CD14$^+$ cells was confirmed by binding of AF-CXCL14 (**Figure 3.23b**), while phenotyping confirmed expression of CD14 (**Figure 3.23c**). Interestingly these cells do not express CD163, which is present on dermal macrophages and CD14$^+$ DC. They also lack expression of CD1c which is highly expressed on CD1a$^+$ DC (Figure 3.22c and (Haniffa et al., 2009)). The unique phenotype of these cells, coupled with their apparent abundance relative to the well characterised immune cell populations that are present in human skin, provides strong support for a thorough investigation of this novel cell population.
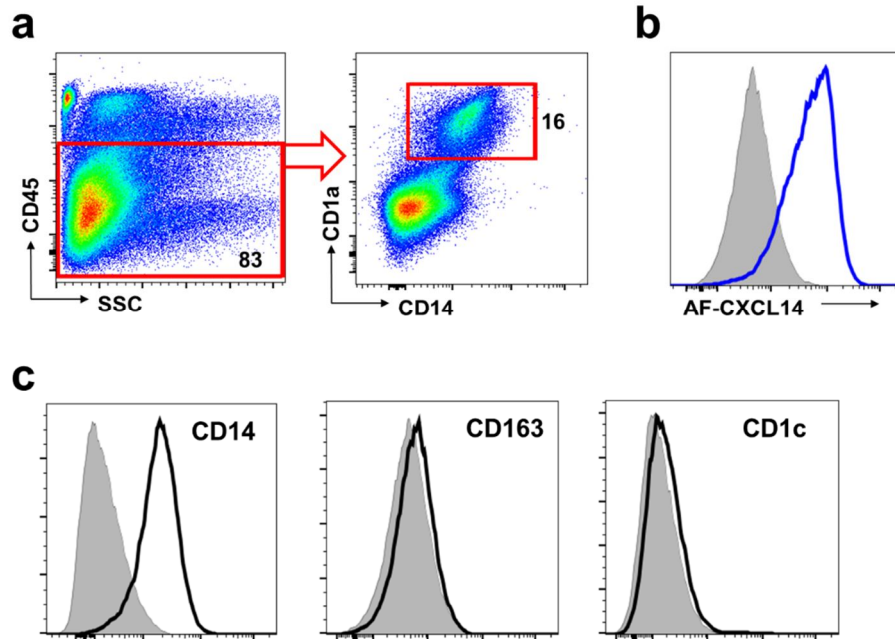
Figure 3.23. Large numbers of CD45^negCD1a^+CD14^+ cells are recovered following overnight proteolytic digestion of the dermis.

Dermis was subjected to overnight collagenase digestion and phenotyping was performed on extracted cells by flow cytometry. **(a)** Dot plots show gating on CD45-neg cells (left) followed by plotting CD1a vs CD14 expression (right). Numbers indicate the percentage of total live single cells. **(b)** Binding of AF-CXCL14 to CD45^negCD1a+CD14+ cells is indicated by the blue histogram. Grey filled histogram indicates binding of AF-muCCL1. **(c)** Expression of CD14, CD163 and CD1c on CD45^negCD1a^+CD14^+ cells. Grey filled histogram indicates staining with isotype-matched control antibodies. Data are from a single donor.

3.6 Discussion

The importance of chemokines in the control of immune cell traffic (as well as function) is underscored by various studies demonstrating a correlation between defects in the chemokine system and disease (Griffith et al., 2014, McDermott et al., 2015). While the role played by chemokines in recruiting immune effector cells to inflammatory sites is well described (Griffith et al., 2014), their role in maintaining immune homeostasis during the steady-state is much less understood. CXCL14 is considered a homeostatic chemokine, owing to its high level of expression in a wide range of healthy tissues including skin, lung and kidney, as well as gastrointestinal and reproductive tracts. Its absence from secondary lymphoid organs, however, sets CXCL14 apart from the other homeostatic chemokines CXCL12, CCL19, CCL21 and CXCL13 (Meuter and Moser, 2008). In this part of the project, I have performed a thorough interrogation of immune cell subsets isolated from human blood and skin for their ability to respond to CXCL14. I report that CXCL14 selectively induces migration of CD14+ blood monocytes (and neutrophils, see below), while other leukocyte subsets present in peripheral blood, including T cells, B cells, NK cells and DCs, do not migrate. Furthermore, migration toward CXCL14 and/or expression of CXCL14 receptor(s) identified CD14+ populations in healthy human skin, assigning a novel role to CXCL14 in the maintenance of myeloid populations in peripheral tissues during the steady-state. These findings have profound implications for the maintenance of mucosal immunity in humans, while revealing more about the true function of this poorly defined chemokine.

Since its discovery at the end of the 20th century (Frederick et al., 2000, Hromas et al., 1999, Kurth et al., 2001), a whole host of functions have been described for CXCL14, from induction of chemotaxis in a range of human leukocyte subsets including B cells, monocytes, neutrophils, DC precursors and activated NK cells (Cao et al., 2000, Kurth et al., 2001, Shellenberger et al., 2004, Sleeman et al., 2000, Starnes et al., 2006) to broad-spectrum antimicrobial activity (Dai et al., 2015, Maerki et al., 2009). However, several contradictions can be found within this body of literature. For instance, there are reports describing a role for CXCL14 in the recruitment of human DCs and DC precursors *in vitro* (Schaerli et al., 2005, Shellenberger et al., 2004). However, no defect in the distribution or function of DCs could be found upon thorough examination of the CXCL14-KO mouse (Meuter et al., 2007). While this may be explained by functional redundancy in the chemokine system, clarification of the immune cell subsets targeted by CXCL14 is long overdue.

Attempts to identify the targets of CXCL14 have been hampered by the fact that the identity of the receptor to which CXCL14 binds is not known. We therefore acquired a custom-made, synthetic CXCL14 with an Alexa Fluor 647 fluorochrome attached to its C-terminus (AF-CXCL14). Having a reagent which could be used to 'label' cells expressing CXCL14 receptor(s) proved an invaluable tool for investigating the distribution of the CXCL14 receptor on leukocyte subsets.

Migration toward CXCL14 and expression of CXCL14 receptor(s) identified monocytes as the major targets of CXCL14 among blood leukocytes, while also distinguishing between the three monocyte subsets which are defined by differential expression of CD14 and CD16. Classical (CD14^{++}CD16$^-$) monocytes displayed the strongest response, migration being observed toward as low as 100 nM CXCL14 and increasing up to 1 μM of the chemokine. Intermediate (CD14^{++}CD16$^+$) monocytes displayed a weaker response to CXCL14, while non-classical (CD14$^+$CD16^{++}) monocytes showed no response at all. The three monocytes subsets exhibit unique genotypic and phenotypic profiles (Ingersoll et al., 2010, Wong et al., 2011), however the functional differences between them is yet to be elucidated. Due to the 'inflammatory' chemokine receptors CXCR1, CXCR2 and CCR2 being selectively expressed on classical monocytes, it has been proposed that classical monocytes have a function which resembles that traditionally assigned to monocytes, exiting circulation to enter inflamed tissues where they differentiate into macrophages or DCs (Geissmann et al., 2003, van Furth and Cohn, 1968). By contrast, it has been proposed that non-classical monocytes are excluded from sites of inflammation and that they may even remain in the bloodstream, operating as a blood-resident macrophage population (Cros et al., 2010, Geissmann et al., 2003). Classical monocytes are by far the most abundant subset, and the short half-life of monocytes in blood (~22 hours) suggests that they are continuously leaving the blood in large numbers. Their ability to respond to CXCL14 may therefore provide new insights into the fate of classical monocytes. By entering tissues in response to CXCL14, classical monocytes may replenish tissue-resident phagocyte populations during the steady-state. The ability to respond to CXCL14 was found to identify several populations isolated from healthy human skin including dermal CD14$^+$ DCs, as well as a novel population of cells which do not express CD45. The full implications of these findings are discussed below, as well as in the General Discussion. To complete the discussion regarding blood monocytes; there is intense debate regarding the developmental relationship of the three monocyte subsets. However, re-population kinetics in patients following HSCT suggest that classical monocytes likely give rise

to the intermediate, followed by non-classical subsets (McGovern et al., 2014). The data presented here are compatible with this notion. Classical monocytes lose the ability to respond to CXCL14 as they move along the developmental pathway toward non-classical monocytes. This, in turn, correlates with the requirement of classical monocytes to respond effectively to signals (including CXCL14) to enter tissues. In contrast, non-classical monocytes are unresponsive to the same signals, instead remaining in the bloodstream.

The other leukocyte subset in peripheral blood which migrated toward CXCL14 in chemotaxis assays was neutrophils. However, binding of AF-CXCL14 to neutrophils was not observed. Neutrophils were unresponsive to 100 nM CXCL14 (unlike monocytes, which showed some migration toward 100 nM CXCL14), neutrophil responses beginning at 300 nM and increasing up to 1 µM. This may indicate that neutrophils express CXCL14 receptor(s) at lower levels than monocytes, perhaps below the threshold that is detectable using fluorescently-labelled CXCL14. One potential way of confirming expression of CXCL14 receptor(s) by neutrophils would be to test binding of radiolabelled CXCL14, which is a more sensitive approach to detecting chemokine receptor expression, and has been used previously to detect CXCL14 receptor expression on THP-1 cells (Tanegashima et al., 2010b). However, we have yet to perform this experiment. Chemotactic activity for neutrophils has been described previously (Cao et al., 2000), highlighting the importance of further investigation to determine whether or not neutrophils are targets for CXCL14. It must be noted that eosinophils and basophils, also present in peripheral blood, were not tested for CXCL14 responses. The predominant role of these cell types is in the mediation of allergic responses, with inflammatory chemokines (especially the CCR3 ligands) being involved in the recruitment and local activation of these cells in chronic allergic conditions including asthma (Uguccioni et al., 1997, Ying et al., 1999). Due to there being no publications reporting the involvement of CXCL14 in allergic conditions, it was not considered pertinent to include these cell types in my analysis.

With the exception of neutrophils, binding of AF-CXCL14 to immune cells from blood and skin correlated extremely well with migratory responses, giving us confidence that the reagent was binding to its intended target. The observation that AF-CXCL14 had chemotactic activity for PGE_2-treated THP-1 cells also convinced us of its suitability for use. Others have established the specificity of binding of labelled chemokines by demonstrating that unlabelled ligand efficiently competes with labelled chemokine for binding to the receptor (Strong et al., 2006). In binding experiments performed with

monocytes however, addition of excess (10X) unlabelled CXCL14 resulted in a considerable increase in binding of AF-CXCL14 (data not shown). The reason for this puzzling finding is not clear at this point. A possible explanation is that high chemokine concentrations drive the formation of CXCL14 oligomers which have a greater affinity for the CXCL14 receptor, leading to an increase in binding (see Introduction to Chapter 5 for a review of chemokine oligomer formation).

CXCL14 expression is found in many peripheral tissues, however its pattern of expression and the cells by which it is produced has been most extensively studied in the skin, where epidermal keratinocytes as well as macrophages and mast cells in the dermis produce CXCL14 during the steady-state (Maerki et al., 2009, Meuter and Moser, 2008, Schaerli et al., 2005). Using an *in vitro* tissue model, human epidermal equivalents were shown to be capable of inducing the differentiation of CD14$^+$ monocytes into Langerhans-like cells. CXCL14 was assigned an important role in this process, guiding CD14$^+$ cells to distinct epidermal niches, where their differentiation into LCs took place (Schaerli et al., 2005). Further to this, it has been shown that human blood monocytes can be differentiated into Langerhans-like cells *in vitro* by culture with GM-CSF, IL-4 and TGFβ1 (Geissmann et al., 1998). While there is strong evidence that monocytes give rise to LCs in mouse during inflammation (Ginhoux et al., 2006), a direct relationship between blood monocytes and tissue DCs during the steady-state is yet to be demonstrated. The ultimate fate of a large proportion of monocytes, therefore, remains something of a mystery. In light of the observation that monocytes were the primary targets of CXCL14 in blood, I postulated that ability to respond to CXCL14 and/or expression of CXCL14 receptor(s) may identify tissue cells which have differentiated from monocyte precursors under non-inflammatory conditions. In this regard, I performed a thorough analysis of cells isolated from healthy human skin for responsiveness to CXCL14. LCs isolated from the epidermis did not express CXCL14 receptor(s) and did not exhibit migration toward CXCL14, indicating that CXCL14 does not play an important role in the differentiation of LCs during the steady-state. This has been indicated by studies in mouse which have shown that during the steady-state, epidermal LC populations are maintained through local proliferation and self-renewal, independently of circulating precursors including monocytes (Merad et al., 2002). This situation changes upon injury to the epidermis however. Following exposure of mouse skin to ultraviolet B radiation, which leads to skin inflammation and loss of LCs, circulating monocytes were shown to replenish epidermal LCs. Furthermore, recruitment of monocytes to the skin was dependent on their expression of CCR2, as well as production of the CCR2 ligands CCL2 and CCL7

by inflamed skin (Ginhoux et al., 2006, Merad et al., 2002). Interestingly, CCR2 exhibits a remarkably similar pattern of expression on circulating monocytes as does the putative CXCL14 receptor, with CCR2 being most highly expressed on classical $CD14^{++}CD16^-$ monocytes, while expression is absent from the non-classical $CD14^+CD16^{++}$ subset. In contrast, in the steady-state, mice that lack CCR2 have normal numbers of LCs in the skin (Sato et al., 2000). In agreement with a CXCL14-independent mechanism of LC generation, our group has shown previously that mice which lack CXCL14 possess normal numbers of fully functional LCs (Meuter et al., 2007).

Cells isolated from the dermis included the two resident populations of dermal myeloid DCs. Human dermal DCs were initially described more than 20 years ago as a DC population distinct from epidermal LCs which spontaneously emigrates from skin explants cultured *ex vivo* (Lenz et al., 1993, Nestle et al., 1993). Phenotypic analysis of dermal emigrant cells confirmed that there were in fact two dermal DC subsets, distinguished by differential expression of CD14 and CD1a (a comprehensive review of human dermal DCs can be found in (Haniffa et al., 2015)). I was able to identify the two dermal DC populations in my own analyses. Consistent with the published literature, $CD1a^+$ DC outnumbered $CD14^+$ DC by approximately 2:1 (Nestle et al., 1993), while $CD1a^+$ DC exhibited higher expression of HLA-DR and CD1c (Haniffa et al., 2009, Haniffa et al., 2015). How the dermal DC populations are maintained during the steady-state, and whether the two subsets are derived from the same or distinct precursors, is not clear. It was therefore interesting to find that expression of CXCL14 receptor(s) distinguished so clearly between the two subsets, with AF-CXCL14 binding to $CD14^+$ DCs but not to $CD1a^+$ DCs. A shared ability to respond to CXCL14 may indicate that $CD14^+$ monocytes in the blood populate and replenish the $CD14^+$ dermal DC population in the skin. Indeed, it was recently proposed that dermal $CD14^+$ 'DCs' be re-classified as a tissue-resident population of monocyte-derived macrophages (McGovern et al., 2014). In this study, dermal $CD14^+$ cells were shown to be phenotypically and transcriptionally related to blood $CD14^+$ monocytes and dermal macrophages, while being distinct from $CD1a^+$ DCs and $CD16^+$ blood monocytes. Furthermore, the decline and reconstitution kinetics of $CD14^+$ blood monocytes and dermal $CD14^+$ cells in patients following HSCT supported their precursor-progeny relationship (McGovern et al., 2014). These findings, combined with the short half-life of dermal $CD14^+$ cells (maximum 6 days) (McGovern et al., 2014) might finally explain the fate of at least a proportion of blood monocytes which exit the bloodstream in large numbers on a daily basis.

In contrast to dermal DCs, macrophages do not migrate spontaneously from skin explants cultured *ex vivo*, instead remaining fixed in the tissue. Macrophages also express CD14 and have an overlapping antigen expression profile with CD14$^+$ dermal DCs, which can make them difficult to distinguish (Zaba et al., 2007). I therefore employed a strategy to isolate and phenotype dermal macrophages described by Haniffa and colleagues (Haniffa et al., 2009). The strategy involved overnight collagenase digestion of the dermal tissue, after which time the tissue was completely dissociated. The higher side scatter properties of macrophages makes them highly autofluorescent cells, with autofluorescence being most easily detected in the FITC channel. Dermal DCs and macrophages both fall into the CD45$^+$MHC class II$^+$ fraction of dermal cells. Therefore, following successive gating on CD45 and HLA-DR, macrophages were identified on the basis of their autofluorescence. Expression of CD14, in addition to the tissue macrophage marker CD163 (Haniffa et al., 2009), confirmed their identity. Interestingly, approximately 25% of dermal macrophages expressed CXCL14 receptor(s), as demonstrated by binding of AF-CXCL14. The precursor-progeny relationship between blood monocytes and tissue macrophages first proposed nearly 50 years ago (van Furth and Cohn, 1968) has recently been confirmed in mouse models of inflammation (Epelman et al., 2014, Tamoutounour et al., 2013). Despite this, there is increasing evidence that many tissue macrophage populations are embryonic-derived, being seeded in tissues prior to birth and maintaining themselves through adult life by local proliferation, independently of input from circulating precursors (Perdiguero and Geissmann, 2016). Recent findings from mouse however show that dermal macrophages consist of a subset that is established prenatally, and a subset that develops after birth from Ly6C^{hi} monocytes (Jakubzick et al., 2013, Tamoutounour et al., 2013). It could be postulated that my findings indicate that the same is true in human, with binding of AF-CXCL14 identifying dermal macrophages which are derived from CD14^{hi} blood monocytes. This hypothesis should be investigated by transcriptional profiling of the two dermal macrophage subsets (AF-CXCL14^{pos} and AF-CXCL14^{neg}) to see if the former is more closely related to blood monocytes.

Finally, I have described for the first time a population of cells extracted from human skin that co-express the myeloid DC markers CD14 and CD1a, but which are negative for the pan-leukocyte marker CD45. The distinction between CD45$^+$ and CD45^{neg} cells by flow cytometry was very clear, therefore I am confident in stating that these cells are a true CD45^{neg} population. These cells demonstrated binding of AF-CXCL14 as well as robust migratory responses, identifying this novel population as CXCL14

target cells. CD45^{neg}CD1a$^+$CD14$^+$ cells were present among emigrant cells recovered from both the dermis and epidermis. Proteolytic digestion of the dermis yielded far greater numbers, suggesting that they represent a significant compartment in healthy human skin. There are numerous published accounts of research undertaken in human and mouse that describe selection of CD45$^+$ leukocytes for further analysis, while CD45-negative cells are discarded (Haniffa et al., 2009, Malosse and Henri, 2016, McGovern et al., 2014). It is highly likely, therefore, that these cells have been overlooked in the past. CD45 is a member of the protein tyrosine phosphatase family, a family of signalling molecules that regulate a variety of cellular processes including cell growth, division and differentiation. At least 8 isoforms of CD45 have been described, all of which are generated by alternative splicing of a single gene to produce 8 different mRNAs. Each of the CD45 isoforms has a unique extracellular domain, and the isoforms are differentially expressed on all cells of haematopoietic origin. The role of CD45 in T cell activation has been most extensively studied, where it is essential for the activation of T cells via the TCR. The intracellular portion of CD45 has intrinsic tyrosine phosphatase activity and associates with several components of the TCR signalling cascade, including Lck and Zap-70, to support signal transduction (Altin and Sloan, 1997). The role of CD45 in mononuclear phagocytes is not very well understood, although it has been shown that macrophages from CD45-knockout mice are unable to maintain integrin-mediated adhesion and are deficient in cytokine signalling, suggesting a role for CD45 in the activation of intracellular signalling cascades in these cells (Roach et al., 1997, Zhu et al., 2008). We have no data yet regarding the function of this novel population of CD45^{neg}CD1a$^+$CD14$^+$ cells found in human skin. The fluorochrome-conjugated anti-CD45 mAb used to characterise them by flow cytometry recognises all of the known CD45 isoforms. RNA-seq of CD45^{neg}CD1a$^+$CD14$^+$ cells will reveal if they are truly CD45-neg, or if they express a novel isoform of CD45 that has not been described. The approaches that should be taken to further characterise these cells and confirm their origin/identity are detailed in the General Discussion.

Chapter 4   Attempts to Identify the CXCL14 Receptor

4.1 Introduction

4.1.1 The GPCR superfamily

The human genome is thought to consist of approximately 21,000 protein-coding genes (Pennisi, 2012), with the GPCR superfamily representing the largest class of membrane proteins in human. Approximately 800 different human genes (or ~4% of the entire protein-coding genome) are known, or have been predicted based on sequence homology, to code for GPCRs. The receptors themselves display incredible diversity in size, function and the nature of the ligands by which they are bound. However, they all share some common architectural features. All GPCRs are embedded in the plasma membrane of the cell by seven sequences of 25 to 35 consecutive amino acid residues that show a high degree of hydrophobicity (transmembrane domains; TM1-TM7). The transmembrane domains are linked by three extracellular loops (ECL1-ECL3) and three intracellular loops (ICL1-ICL3). Finally, there is an extracellular N-terminus and an intracellular C-terminus (Figure 1.5). More than half of the ~800 GPCRs identified in human have sensory functions, mediating perception of our external environment in the form of olfaction, light perception, taste and pheromone signalling (Mombaerts, 2004). The remaining ~360 non-sensory GPCRs mediate signalling by endogenous ligands, ranging from small molecules such as nucleotides, lipids and small peptides, to complex proteins. GPCRs bound by endogenous ligands mediate diverse physiological processes as nervous transmission, mood regulation and feeding behaviour, to the immune response and the growth and metastasis of certain types of tumours. Several classification systems have been used to organise the GPCR superfamily, with some systems grouping the receptors by how their ligand binds, and others grouping them based on structural and/or functional features. Recently, the GRAFS system has been used to group the mammalian GPCRs into five main families (Glutamate, Rhodopsin, Adhesion, Frizzled and Secretin = GRAFS), based on sequence homology and functionality (Fredriksson et al., 2003b). The largest of these families is the Class A of Rhodopsin-like receptors, with about 284 members which recognise endogenous ligands (in addition to >400 sensory receptors). All of the class A receptors share sequence homology with rhodopsin, the light-sensitive receptor of rod photoreceptor cells and the first GPCR to have its crystal structure determined (Palczewski et al., 2000). The remaining GPCRs are divided into the Secretin family (class B, and which

has 15 members), Glutamate family (class C, 22 members), Adhesion family (class D, 33 members) and Frizzled family (class E, 11 members). Finally, there are six GPCRs (five non-sensory GPCRs and one olfactory receptor) which have ambiguous structural similarities to several different GPCR families, and as such cannot be readily assigned to any of the five main families. A breakdown of the five human GPCR families are shown in **Table 4.1**. The fact that GPCRs which are bound by endogenous ligands are the targets for the majority of drugs in clinical use (Overington et al., 2006), highlights the importance of enhancing our understanding of GPCRs to the treatment of human disease.

Table 4.1. Families of the human GPCR superfamily.

Family	Class A (rhodopsin)	Class B (secretin)	Class C (glutamate)	Class D (adhesion)	Class E (frizzled)	Other
Receptors with known endogenous ligands	197	15	12	1	11	0
Orphans	87 (54)[a]	-	7 (1)[a]	32 (6)[a]	0	5 (1)[a]
Sensory (olfaction)	390	-	-	-	-	1
Sensory (vision)	10	-	-	-	-	-
Sensory (taste)	30	-	3	-	-	-
Sensory (pheromone)	5	-	-	-	-	-
Total	719	15	22	33	11	6

[a]Numbers in brackets refer to orphan receptors for which an endogenous ligand has been proposed in at least one publication, but has yet to be confirmed.

4.1.2 Chemokine receptors

The rhodopsin family of GPCRs can be sub-divided into four main groups, which have been designated α, β, γ, δ (Fredriksson et al., 2003b). Upon analysis of the phylogenetic relationship between all of the human GPCRs (minus olfactory receptors), all 18 signalling and 5 non-signalling chemokine receptors are seen to cluster on a single branch of the γ-subgroup of rhodopsin-like receptors, confirming their relatedness to one-another in evolutionary, and not only functional terms (**Figure 4.1**). The genes encoding the chemokine receptors also appear in clusters on several chromosomes. For example, *CCR1-5, CCR8, CCR9, CCR11 (CCRL1), CCRL2, CX3CR1, CCBP2 (ACKR2)* and *XCR1* are all positioned on chromosome 3p2. This can likely be explained by local gene duplication from a common ancestor giving rise

to the other members, which also explains their relatedness to each other in evolutionary terms. The human CC and CXC chemokines themselves show a similar chromosomal arrangement, forming two major clusters on chromosome 17 and chromosome 4, respectively (Zlotnik et al., 2006). Of note, the gene which encodes human CXCL14 is located separately from the CXC cluster, on chromosome 5, perhaps indicating that the receptor for CXCL14 does not cluster with the other chemokine receptors either.

Other receptors which mediate chemotaxis in response to non-chemokine chemoattractants, such as the formyl peptide receptors (FPR1, FPRL1 and FPRL2) and the complement protein C5a receptors (C5R1 and C5R2), also cluster in close proximity to the chemokine receptors. This indicates that receptors which mediate the specific function of chemotaxis are all closely related. The branch of the γ-subgroup of the rhodopsin family of GPCRs that includes the chemokine receptors also includes several orphan receptors. These are receptors for which there is no confirmed ligand, and they have the prefix 'GPR' in their name. The GPCR superfamily contains more than 100 orphan receptors, the majority of which are found within the family of rhodopsin-like receptors (**Figure 4.1**).
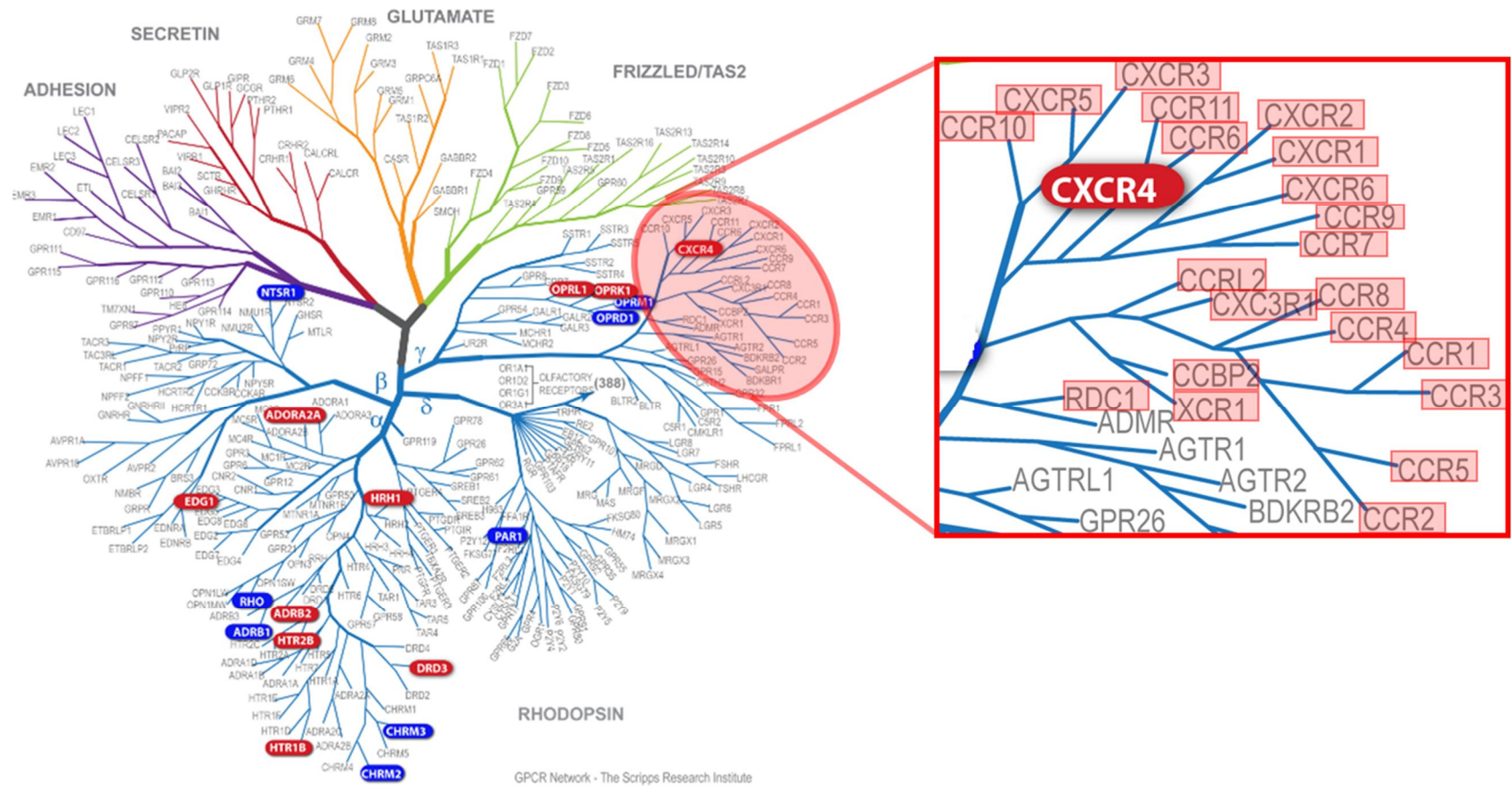
Figure 4.1. The human GPCR family tree.

Phylogenetic or evolutionary tree of the human GPCR superfamily, showing their organisation into five families based on shared sequence homology, namely rhodopsin (blue), secretin (red), glutamate (orange), adhesion (purple) and frizzled (green). The family of rhodopsin-like receptors can be subdivided into four main groups, namely α, β, γ and δ, as shown. The chemokine receptors (shaded in red) all cluster together on a single branch of the γ-subgroup of rhodopsin-like receptors, indicating their evolutionary relatedness and high degree of sequence homology. The receptors highlighted in red and blue are those for which the structure has been solved e.g. CXCR4. This figure is adapted from The GPCR Network, a collaboration between a number of researchers working on GPCRs, and is freely available to download from http://gpcr.usc.edu/index.html.

4.1.3 The CXCL14 receptor

CXCL14 exhibits unique structural and functional features among the chemokine family. A very short N-terminus of just two amino acids prior to the first cysteine residue suggests that CXCL14 may induce receptor activation by a different mechanism compared to other chemokines, many of which have been shown to depend on their N-terminal sequence for their activity (Clark-Lewis et al., 1995). Sensitivity to pertussis toxin treatment confirms that the CXCL14 receptor, like all other signalling chemokine receptors, couples to an intracellular G protein of the Gαi class (Kurth et al., 2001).

CXCL14 is considered a homeostatic chemokine, constitutively produced by tissue cells in the absence of infection. The other homeostatic chemokines, including CXCL12, CXCL13, CCL19 and CCL21, all induce chemotaxis of target cells via a single chemokine receptor, namely CXCR4 (CXCL12), CXCR5 (CXCL13) and CCR7 (CCL19 and CCL21). The selectivity of CXCL14 for monocytes (albeit neutrophils exhibit a weak response) is unique among the homeostatic chemokines and suggests that CXCL14 acts via an as yet unidentified receptor. However, it must be assumed that the receptor for CXCL14 will possess certain structural features shared by all chemokine receptors, such as key amino acid motifs which have been shown to be important in coupling to intracellular G proteins and activation of signalling events following chemokine binding (Nomiyama and Yoshie, 2015).

4.1.4 Hypothesis

The receptor for CXCL14 is a GPCR, distinct from the known chemokine receptors, which is expressed in cells that exhibit functional responses to CXCL14, namely $CD14^{++}CD16^-$ classical monocytes and PGE_2-treated THP-1 cells.

4.2 Aims

- Using an RNA sequencing approach, to identify candidates for the CXCL14 receptor based on differential expression in cells which are targets for CXCL14

(human CD14^{hi} monocytes, PGE$_2$-treated THP-1 cells) and cells which are not (human CD16^{hi} monocytes, lymphocytes, untreated THP-1 cells).

- Following identification of suitable candidates, to perform sequence and phylogenetic analysis in order to discern their relatedness to known chemokine receptors, as well as a comprehensive literature search of reported functions and known ligands.

- To screen the final list of candidates by two methods: stable expression of the receptor in an appropriate cell-line, and short hairpin RNA (shRNA)-mediated knockdown in THP-1 cells.

4.3 RNA Sequencing of THP-1 cells

4.3.1 Induction of CXCL14 responsiveness in THP-1 cells with PGE$_2$ is enhanced by sodium butyrate

I have already shown that the human myeloid leukaemia cell line THP-1 can be induced to migrate in response to CXCL14 by treatment with PGE$_2$ (**Figure 3.11**). Due to the difficulties inherent in working with primary immune cells (time-consuming isolation procedures, variability between donors), THP-1 cells were initially used as a model for studying the CXCL14 receptor. Sodium butyrate, the sodium salt of butyric acid, is a compound which causes histone hyperacetylation through the inhibition of histone deacetylase (HDAC) activity. This activity can enhance gene expression, which in turn increases protein expression. Inhibition of HDAC activity is estimated to affect the expression of only 2% of mammalian genes (Candido et al., 1978, Davie, 2003). However, it has been shown previously that sodium butyrate treatment enhances the surface expression of some chemokine receptors (Meiser et al., 2008, Sabroe et al., 2000). It was observed that addition of sodium butyrate to THP-1 cultures alongside PGE$_2$ led to significantly enhanced migration of THP-1 cells toward CXCL14 (**Figure 4.2a**). Treatment with sodium butyrate failed to induce a migratory response toward CXCL14 in THP-1 cells by itself (**Figure 4.2b**).
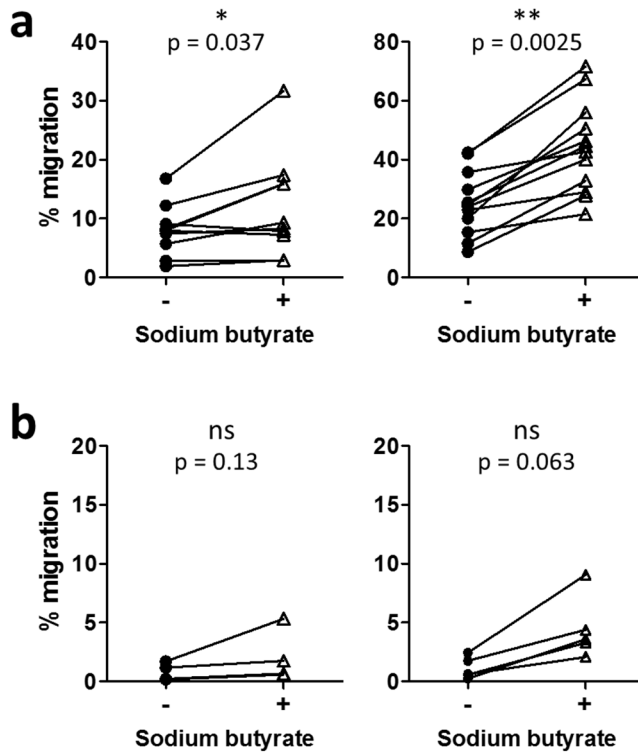
Figure 4.2. Sodium butyrate enhances the effect of PGE$_2$ in THP-1 cells.

THP-1 cells were cultured for 24 hours with (**a**) 1 µM PGE$_2$ or (**b**) medium only in the presence (+) or absence (-) of 1 mM sodium butyrate. Migration toward 1 µM (left) and 3 µM (right) CXCL14 was then assessed by transwell chemotaxis assay. Results are shown in matched experiments, where the Wilcoxon matched pairs test was used to determine significance. P values are indicated. *P<0.05, **P<0.01, ns = not significant.

4.3.2 THP-1 sample collection

Due to their ease of handling and manipulation compared to primary cells, in addition to the robustness and reproducibility of the response to CXCL14 following stimulation, THP-1 cells were considered a reliable model for investigating the identity of the CXCL14 receptor. THP-1 cells treated with six different conditions were collected from a single experiment and subjected to transcriptome analysis by RNA sequencing (see Materials and Methods). The six conditions were chosen based on the following hypotheses:

a. Expression of the CXCL14 receptor will be low or absent in untreated THP-1, because these cells do not respond to CXCL14

b. Treatment with PGE_2 likely increases cell-surface CXCL14 receptor expression, as demonstrated by induction of migration to CXCL14. It therefore follows that expression of the gene encoding the CXCL14 receptor will also be up-regulated with PGE_2 treatment

c. Addition of sodium butyrate along with PGE_2 will strengthen any PGE_2-related response

d. Migration toward CXCL14 will select for only those cells which have acquired responsiveness toward the chemokine (as opposed to bulk-treated cells where likely some cells acquire responsiveness while others do not). Therefore, expression of the receptor will be even greater in the migrated (as opposed to bulk-treated) population

Table 4.2. Six treatment conditions of THP-1 cells submitted for RNA sequencing.

Sample	Treatment duration	Treatment		Selected by migration to CXCL14?	Number of cells collected (x10^5)
		PGE_2	Sodium butyrate		
1	24 hr	-	-	No	5
2	24 hr	-	+	No	5
3	24 hr	+	-	No	5
4	24 hr	+	-	Yes	1
5	24 hr	+	+	No	5
6	24 hr	+	+	Yes	1

Untreated and sodium butyrate (Na-But)-treated THP-1 cells displayed very minimal migratory responses toward CXCL14, 0.62% and 2.07% of cells migrating toward 3 µM CXCL14, respectively. In contrast, PGE$_2$- and PGE$_2$ + Na-But-treated THP-1 cells displayed considerable migration, 25.5% and 44.5% of cells migrating toward 3 µM CXCL14, respectively. Background migration (i.e. migration in response to medium alone, without chemokine) was very low in all cases (<1%). For the RNA sequencing, 5 x 10^5 bulk treated cells were collected for each of the four conditions. For collection of PGE$_2$-treated and PGE$_2$+Na-But-treated cells that migrated in response to CXCL14, transwell chemotaxis assays were performed in triplicate. One of the wells was used to quantify the migration (**Figure 4.3**), while migrated cells from the other two wells were pooled (10^5 migrated cells were collected for each of the two conditions).
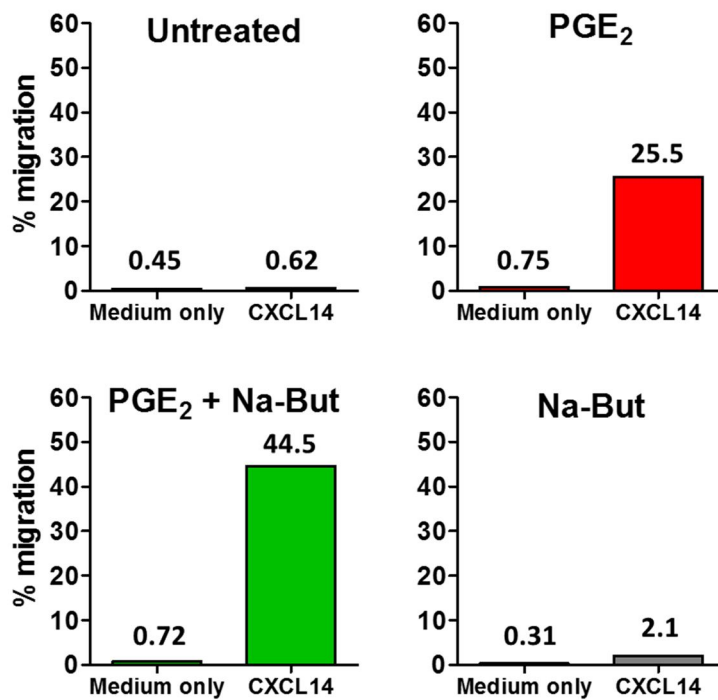
Figure 4.3. Result of the transwell chemotaxis assays performed in experiment where THP-1 cells were collected for RNA sequencing.

THP-1 cells were cultured for 24 hours in medium only (untreated) or medium supplemented with PGE$_2$, sodium butyrate (Na-But) or PGE$_2$ + Na-But. Migration toward buffer only (no chemokine) or 3 µM CXCL14 was assessed by transwell chemotaxis assay. Numbers shown above the bars indicate the % of total input cells which migrated in response to the chemokine.

4.3.3 Data analysis

Initial analysis revealed that on average, across the six treatment groups, approximately 15,000 genes were expressed in THP-1 cells (i.e. had an expression level above zero). So as to select only those genes which encode for GPCRs in my analysis, the entire list of expressed genes was cross-referenced with the comprehensive list of GPCRs published and regularly updated by the Committee on Receptor Nomenclature and Drug Classification, part of the International Union of Basic and Clinical Pharmacology (NC-IUPHAR). The up-to-date list of all known GPCRs, including orphan receptors, is available to view and download at http://www.guidetopharmacology.org/GRAC/ReceptorFamiliesForward?type=GPCR. Of the ~360 non-olfactory GPCRs, 282 were expressed in one or more samples. Those which did not fit the expected expression profile of the CXCL14 receptor laid out in my experimental hypotheses (see hypotheses a–d above) were eliminated first. Genes which had high expression (>10 RPKM) in untreated THP-1 cells were eliminated (**21 genes**), followed by genes in which expression was completely absent or very low (<0.5 RPKM) in cells treated with PGE$_2$ (**140 genes**). Genes which failed to exhibit any increase in expression with PGE$_2$ compared to untreated were excluded (**52 genes**). Note that here, even genes which showed only a very modest increase with PGE$_2$ treatment (less than 2-fold) were included in my analysis. Finally, genes where an up-regulation with PGE$_2$ + sodium butyrate could be attributed to an effect of the sodium butyrate (as an identical change in expression was observed in the sodium butyrate only-treated group) were also excluded (**17 genes**). See **Figure 4.4** for a flow-chart showing the process of excluding genes from our analysis.

Remaining were a total of 52 genes, which were categorised into the five GPCR families shown in **Figure 4.1**. 37 of the 52 belong to the class A of rhodopsin-like receptors, which includes all of the known chemokine receptors. Of these 37, nine code for orphan receptors. Of the 28 non-orphan class A receptors, associated gene ontology (GO) terms were used to select receptors with known or suspected function in chemotaxis, while also aiding in the elimination the receptors with well-characterised functions which are distinct from chemotaxis. For example, genes *PTGER1* and *TSHR* encode the PGE$_2$ receptor EP1 and the thyroid stimulating hormone (TSH) receptor, respectively. These genes have known function in lipid signalling (*PTGER1*) and regulation of thyroxine production in response to TSH (*TSHR*), and as such do not have chemotactic function and could be excluded (16 genes were excluded on the basis that their function and ligand(s) are well-described

and unrelated to chemotaxis, and these are listed in **Table 4.3**). 12 non-orphan receptors were identified to have chemotactic function based on associated gene ontologies, leading to a final exhaustive list of 21 class A GPCR-encoding genes with expression profiles that matched that expected of the putative CXCL14 receptor, of which 9 encoded for orphan receptors (**Figure 4.5**).

Table 4.3. Class A GPCRs with non-chemotactic functions excluded from list of genes identified by RNA sequencing of THP-1 cells.

Gene symbol	Receptor name	Endogenous ligand(s)	Function
LPAR6	Lysophosphatidic acid receptor 6	Lysophospatidic acid	Implicated in myeloid cell maturation.
ADORA2B	Adenosine A2B receptor	Adenosine, netrin-1 (mouse)	Induces cAMP accumulation upon binding adenosine. Expressed in mouse brain where it mediates netrin-1-dependent outgrowth of dorsal spinal cord axons.
ADORA3	Adeonsine A3 receptor	Adenosine	Expressed in cardiac ventricular cells, where it mediates the protective effect of adenosine release during cardiac ischaemia.
MLNR	Motilin receptor	Motilin, a hormone synthesised by cells of the small intestine	Expressed in enteric neurons of the duodenum and colon, where it regulates gastrointestinal tract contraction.
SUCNR1	Succinate receptor 1	Succinate, an intermediate of the citric acid cycle	Mediates the hypertensive effect of succinate and is expressed in the retina of rodents, where it is a potent angiogenic factor, mediating vessel outgrowth during retinal development.
F2RL3	Protease-activated receptor 4 (PAR4)	Thrombin	Important for activation of human platelets by thrombin.
S1PR2	Sphingosine-1-phosphate receptor 2	Sphingosine 1-phosphate	Inhibition of cell migration.
ADRA2B	Alpha-2B-adrenergic receptor	Adrenaline and noradrenaline	Regulates neurotransmitter release from sympathetic nerves and from adrenergic nerves in the central nervous system.
ADRA2C	Alpha-2C-adrenergic receptor	Adrenaline and noradrenaline	Regulates neurotransmitter release from sympathetic nerves and from adrenergic nerves in the central nervous system.
PTGER1	Prostaglandin E receptor type 1 (EP1)	Prostaglandin E2 (PGE$_2$)	Mediates some of the non-immune related physiological effects of PGE$_2$ in mice, including stress behaviour, sensitivity to pain and regulation of blood pressure.
GPBAR1	G protein-coupled bile acid receptor 1	Bile acids and steroid hormones	Mediates increased energy expenditure in brown adipose tissue in response to bile acids, which helps to prevent obesity.
GRPR	Gastrin-releasing peptide receptor	Gastrin-releasing peptide	Activation of GRPR in human airways is associated with the proliferative response of bronchial cells and with long-term tobacco use.
SSTR2	Somatostatin receptor 2	Somatostatin	Mediates the biological effects of somatostatin, a peptide hormone that regulates the endocrine system.
TSHR	Thyroid-stimulating hormone receptor	Thyroid-stimulating hormone	Mediates the activity of the pituitary hormone TSH that stimulates the thyroid gland to produce thyroxine, a hormone which affects many biological processes including metabolism, body temperature and heart rate.
CHRM3	Muscarinic acetylcholine receptor 3	Acetylcholine	Mediates neurotransmission in the ocular iris pupillary sphincter and the detrusor muscle in humans.
CHRM4	Muscarinic acetylcholine receptor 3	Acetylcholine	Inhibits acetylcholine release in the striatum.
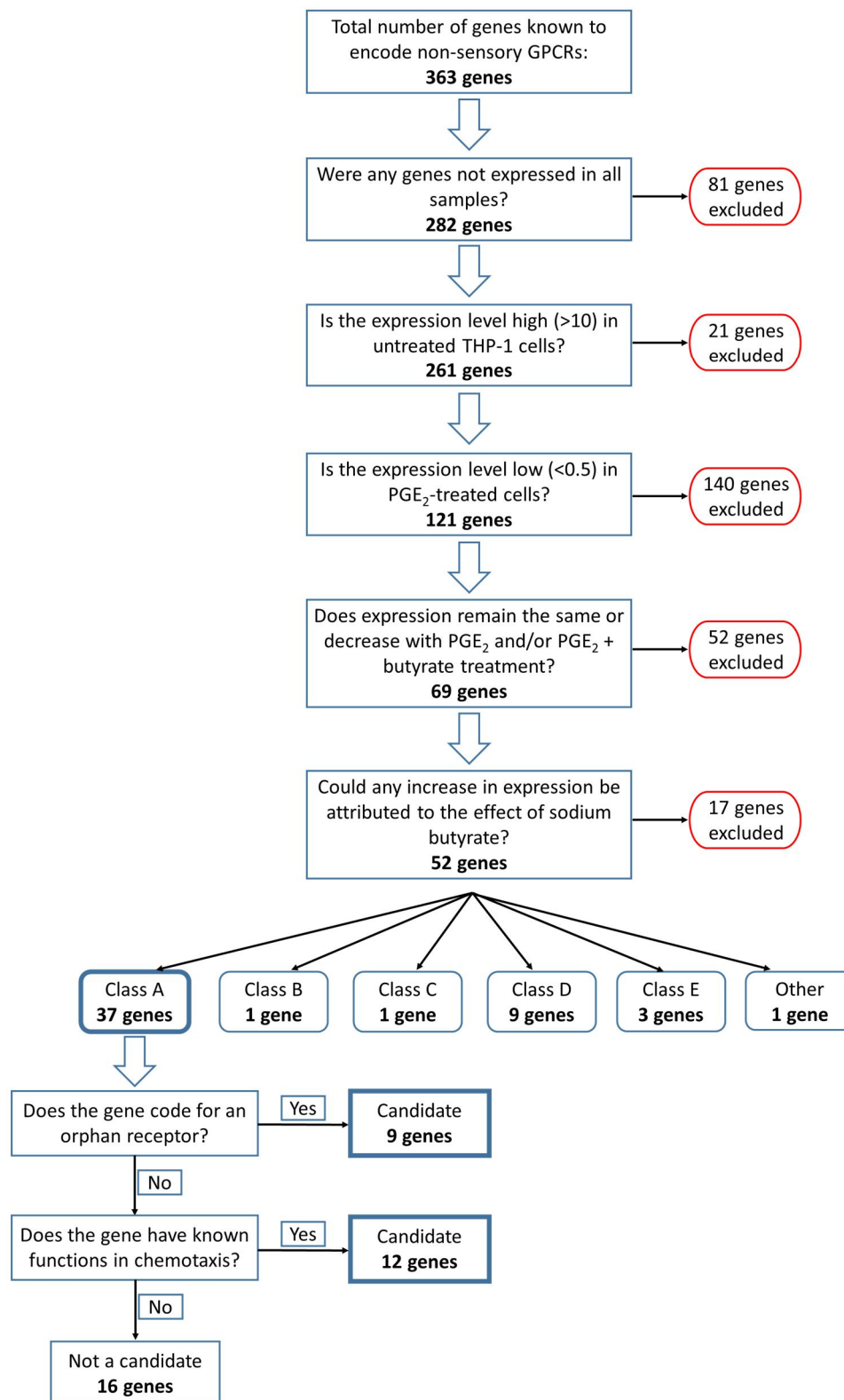
Figure 4.4. Flow chart showing the strategy for identifying gene candidates for the CXCL14 receptor based on RNA sequencing of THP-1 cells.

Candidates were selected from the ~360 non-sensory GPCR-encoding genes. Genes which are unlikely to encode the CXCL14 receptor were successively eliminated on the basis of their expression profiles, which class of GPCR they belonged to, and whether or not they have a function which is well-characterised and distinct from chemotaxis.

Gene	Range (average)
GPR176	0.29 – 2.04 (0.95)
GPR68	0.71 – 128.02 (34.08)
GPR3	0.87 – 2.70 (1.56)
GPR141	1.94 – 7.14 (6.20)
GPR65	1.37 – 9.09 (3.21)
GPR84	1.48 – 13.90 (7.03)
GPR146	2.16 – 14.40 (5.77)
GPR35	4.70 – 149.76 (52.51)
GPR183	6.63 – 80.55 (31.44)
PTAFR	1.37 – 6.45 (3.57)
LTB4R2	2.68 – 5.57 (3.91)
HRH1	1.65 – 12.17 (7.47)
FPR2	2.35 – 102.78 (40.49)
FPR1	0.38 – 69.24 (30.16)
CMKLR1	0.21 – 3.15 (1.46)
CCRL2	2.11 – 5.81 (3.96)
C5AR2	0.55 – 11.85 (4.92)
C5AR1	0.93 – 26.89 (10.96)
C3AR1	0.55 – 17.71 (8.94)
OPRL1	2.38 – 4.39 (3.08)
LPAR1	3.33 – 9.84 (8.18)

Log(2) fold-change in expression

Figure 4.5. List of gene candidates for the CXCL14 receptor identified from RNA-seq of THP-1 cells.

Shown is the log(2) fold-change in expression of the class A GPCRs that were included in my analyses, based on the selection strategy laid out above. To simplify, data shown is mean + s.e.m. and is an average of the fold-change in expression in the four treatment groups (PGE_2 bulk, PGE_2 migrated, PGE_2 + butyrate bulk, PGE_2 + butyrate migrated) relative to untreated THP-1. The numbers to the right show the range in expression in arbitrary units, i.e. expression in untreated THP-1 is on the left, while the highest recorded expression across all of the treatment groups is on the right. The number in brackets represents the average level of expression across all groups (excluding untreated and butyrate alone). Abbreviations: PTAFR; Platelet-activating factor receptor, LTB4R2; Leukotriene B4 Receptor 2, HRH1; Histamine Receptor H1, FPR; Formyl Peptide Receptor; CMKLR1; Chemokine-Like Receptor 1, CCRL2; C-C chemokine Receptor-Like 2, C5AR; Complement component 5a Receptor, C3AR; Complement component 3a Receptor, OPRL1; Opioid Receptor Like-1, LPAR1; Lysophosphatidic Acid Receptor 1.

The candidates for the CXCL14 receptor include an atypical chemokine receptor (CCRL2), as well as a number of chemotactic receptors whose ligands are diverse and include fatty acids (CMKLR1), components of the complement cascade (C3AR1, C5AR1 and C5AR2) and N-formylated peptides (FPR1 and FPR2). Furthermore, there are a number of orphan GPCRs of unknown function and ligand specificity. However, despite the fact that sequencing of THP-1 cells has considerably focused our efforts to identify the CXCL14 receptor from the total number of non-sensory GPCRs (which number around 360; **Figure 4.1**) to just 21 candidates, to thoroughly investigate 21 candidates in turn would still represent a very considerable undertaking in terms of time and resources. Therefore, I decided to perform a second RNA-seq study, this time in primary human cells, in the expectation that it would allow me to exclude some of the existing candidates and refine my search even further.

4.4 RNA Sequencing of Primary Cells

4.4.1 Primary cell sample collection

I have previously shown that, among the leukocyte subsets present in peripheral blood in human, $CD14^{++}CD16^{-}$ classical monocytes are the major responders to CXCL14, demonstrating a dose-dependent migratory response toward the chemokine in addition to expression of CXCL14 receptor(s). On the other hand, $CD14^{+}CD16^{++}$ non-classical monocytes, in addition to lymphocyte populations, do not migrate toward CXCL14 and do not express CXCL14 receptor(s) (Figure 3.2 and Figure 3.4). Primary immune cell populations were FACS sorted for RNA sequencing from peripheral blood taken from three healthy human donors. One 'positive responder' cell ($CD14^{+}$ classical monocytes) and two 'negative responder' cells ($CD16^{+}$ non-classical monocytes and B cells) were selected as the populations to be interrogated.

FACS sorting of the three populations from three healthy human donors was performed simultaneously, as described in the Materials and Methods. Migratory responses of classical monocytes and non-classical monocytes toward CXCL14 were assessed in parallel to the sorting of populations for RNA sequencing by FACS, with the results of the chemotaxis assay shown in **Figure 4.6**. Although the responses differed, as can be expected due to donor-to-donor variation, all three donors exhibited migration of their classical monocytes toward CXCL14, while the non-classical monocytes showed no response.

Table 4.4. Primary immune cell populations sorted from the peripheral blood of three healthy human donors for RNA sequencing.

Donor	Sample	Cell type	Number of cells (x 10^5)
1	1-a	Classical monocytes	2.4
	1-b	Non-classical monocytes	0.8
	1-c	B cells	1
2	2-a	Classical monocytes	1.6
	2-b	Non-classical monocytes	0.3
	2-c	B cells	1.5
3	3-a	Classical monocytes	1.8
	3-b	Non-classical monocytes	1
	3-c	B cells	1.2
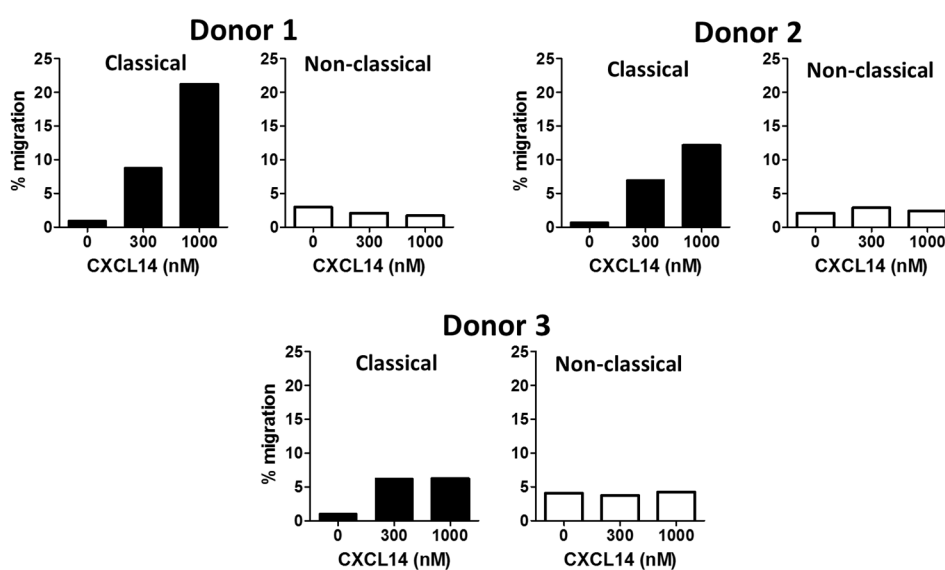
Figure 4.6. Migration of classical and non-classical monocytes toward CXCL14 from the three donors used in sorting populations for RNA sequencing.

Transwell chemotaxis assays were performed using the same monocytes purified by negative selection as used for FACS sorting of populations for RNA sequencing. Migration is expressed as percentage of input and each condition was run in duplicate.

4.4.2 Data analysis

4.4.2.1 *Expression of monocyte- and B cell-associated markers confirms reliability of sequencing data*

Recent studies into human monocytes have reported that each of the three monocyte subsets possesses a unique cell-surface marker and gene expression profile (Ingersoll et al., 2010, Wong et al., 2011). B cells represent an entirely different lineage of immune cell compared to monocytes, and express several cell-surface proteins which are unique to B cells, including components of the B cell receptor (BCR) complex and immunoglobulins. The reliability of the sequencing data obtained from the primary human immune cells could therefore be verified by expression of genes which are specific to each particular cell type. Expression of selected cell type-specific genes is shown in **Table 4.5**. As expected, expression of CD14 and CD16 (the latter is composed of two Fc receptors; CD16a and CD16b) segregate with the classical and non-classical monocytes, respectively. Differential expression of chemokine receptors defined the three cell types, with the inflammatory chemokine receptors CCR2, CCR5 and CCR1 being most highly expressed on the classical monocytes, and the CX3CR1 receptor being specific to non-classical monocytes, as expected. B cells displayed expression of CCR7 (required for their recirculation via the peripheral lymphoid organs) and although the expression level of CXCR5 was comparatively low in B cells (RPKM of 1.3, compared to 389.3 for CCR7), CXCR5 expression was completely absent from both monocyte subsets. Finally, expression of genes which code for BCR (CD19-22) members and immunoglobulins was specific to B cells, with expression being very high (RPKM in the hundreds if not thousands) in B cells and very low or absent in both monocyte subsets. The data shown in **Table 4.5** therefore provides reassurance that my selection of candidate GPCRs for the CXCL14 receptor is based on reliable data, since the expression profiles of B cell- and monocyte-associated markers are as expected.

Table 4.5. Expression of cell-specific markers by sorted classical monocytes, non-classical monocytes and B cells.

Cell type	Gene	Absolute expression values		
		Classical monocytes	Non-classical monocytes	B cells
Classical monocytes	CD14	8.0	0.1	1.0
	CD11b (ITGAM)*	6.9	0.4	1.1
	CCR2	45.6	0.2	5.2
	CCR5	6.5	0.4	0.2
	CCR1	59.4	4.0	0.1
Non-classical monocytes	CD16a (FCGR3A)*	32.3	1414.1	0.4
	CD16b (FCGR3B)*	1.9	197.9	0.0
	CX3CR1	2.4	190.4	0.2
B cells	CD19	0.0	0.0	12.6
	CD20 (MS4A1)*	2.7	0.8	3494.1
	CD21 (CR2)*	0.0	0.0	19.3
	CD22	1.0	0.3	217.4
	IGHM	0.6	0.4	1511.0
	IGHA1	0.1	0.0	249.4
	IGHA2	0.0	0.0	53.2
	IGHD	0.2	0.1	212.3
	CCR7	0.3	0.3	389.3
	CXCR5	0.0	0.0	1.3

Expression is given as reads per kilobase of transcript per million mapped reads (RPKM). *gene name is shown in brackets next to the common name. Chemokine receptors are highlighted in red. Abbreviations; IGHM, immunoglobulin heavy constant mu; IGHA, immunoglobulin heavy constant alpha; IGHD, immunoglobulin heavy constant delta.

4.4.2.2 Expression of GPCRs

It was decided that the best strategy for analysing the primary cell RNA-seq data set would be to treat it independently of the THP-1 data, and produce a separate list of the differentially expressed GPCRs which fit the expected expression profile of the CXCL14 receptor. Then, I will compare the two lists and see which receptors are present in both, prior to generating the final list of candidates. For the analysis of the primary cell RNA-seq, it was important to define the hypotheses for the expected expression profile of the gene encoding the CXCL14 receptor, which were as follows:

a. Expression of the CXCL14 receptor will be highest in classical monocytes

b. The CXCL14 receptor will be expressed in classical monocytes from each of the three donors

c. Expression of the CXCL14 receptor will be low or absent in non-classical monocytes and B cells

Like in the THP-1 study, the entire list of expressed genes was cross-referenced with the exhaustive list of non-sensory GPCRs published by the Committee on Receptor Nomenclature and Drug Classification, part of the International Union of Basic and Clinical Pharmacology (NC-IUPHAR). Of the ~360 non-sensory GPCRs, 212 were expressed in one or more of the three cell types. Genes which had a higher expression in B cells or non-classical monocytes compared to classical monocytes were excluded from analysis first (**140 genes**). Genes which were highest in classical monocytes, but whose expression in classical monocytes was still extremely low (<0.5) were subsequently eliminated (**36 genes**). Next, genes which were highest in classical monocytes, but still had relatively high expression (>15) in one or both of the other subsets, were eliminated (**6 genes**).

Left at this point were 30 genes. I decided to look at their expression values in each of the three donors, and exclude any genes in which expression was completely absent in classical monocytes from one or more donors. For example, *GPR61*, a class A gene encoding an orphan receptor, had average expression values of 0.91, 0 and 0.05 in classical monocytes, non-classical monocytes and B cells, respectively. However, a closer look at the expression across the three donors reveals that *GPR61* was only expressed in classical monocytes from donor 2 (expression value 2.71), and that expression was completely absent in classical monocytes from donors 1 and 3. This "pairwise" analysis led to the elimination of 8 more genes, leaving a total of 22 genes. The remaining 22 genes were divided into the different classes of GPCR, and comprised 20 genes encoding class A receptors, one gene encoding a class B receptor (*CALCRL*) and one gene encoding a receptor of the frizzled class (*FZD5*). The 20 genes encoding class A receptors are shown in **Figure 4.7**. Of these, 7 are orphan receptors. Of the other 13, the chemokine receptors CCR2, CCR5 and CCR1 are present, as are the chemotactic receptors formyl peptide receptor 3 (FPR3) and histamine receptor H1 (HRH1), the latter being present in the list of candidate receptors generated from the THP-1 study (**Figure 4.5**). Also present in both lists is the atypical chemokine receptor CCRL2.
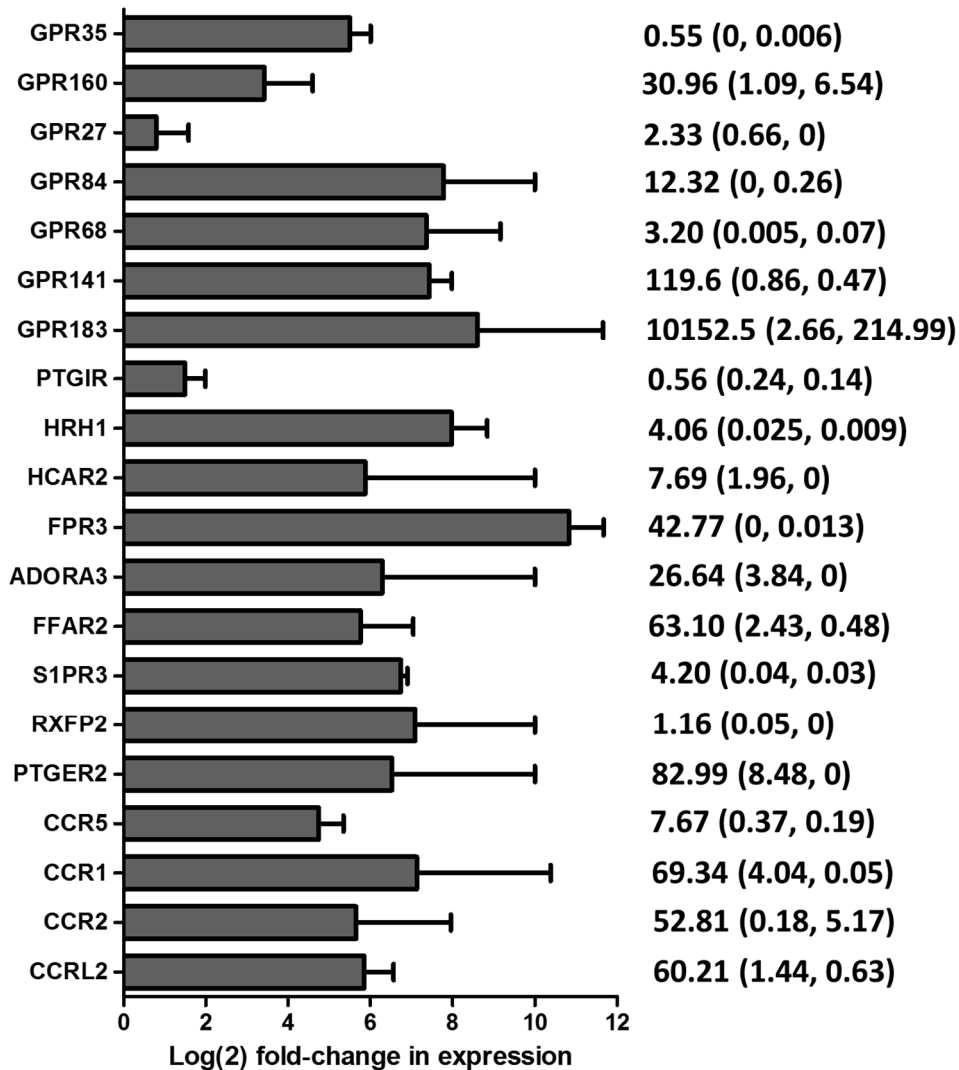
Figure 4.7. List of candidate GPCRs identified from RNA-seq of primary human monocytes and B cells.

Shown is the log(2) fold-change in expression of the class A GPCRs selected based on their expression profile in classical monocytes, non-classical monocytes and B cells from three human donors. Data shown is mean + s.e.m. and is the fold-increase in expression in the positive responder (classical monocytes) compared to the negative responders (non-classical monocytes and B cells). The numbers to the right show the expression level in classical monocytes, while the values in brackets show the expression level in non-classical monocytes and B cells, respectively. Expression is given as RPKM (Reads Per Kilobase of transcript per Million mapped reads). Abbreviations: CCRL2; C-C chemokine Receptor-Like 2, CCR; C-C chemokine receptor, PTGER2; Prostaglandin E Receptor, subtype 2, RXFP2; Relaxin/insulin-Like Family Peptide receptor 2, S1PR3; Sphingosine-1-Phosphate Receptor 3, FFAR2; Free Fatty Acid Receptor 2, ADORA3; Adenosine A3 Receptor, FPR3; Formyl Peptide Receptor 3, HCAR2; Hydroxycarboxylic Acid Receptor 2, HRH1; Histamine Receptor H1, PTGIR; Prostaglandin I2 (prostacyclin) Receptor.

4.5 Final List of Candidates for the CXCL14 Receptor

Upon combining the RNA-seq data from the THP-1 study and the primary cells, the class A GPCRs with expression profiles in both data sets which matched that predicted for the putative CXCL14 receptor are as follows:

CCRL2 – C-C chemokine receptor-like 2 (ACKR5); an atypical chemokine receptor which binds a number of CC and CXC chemokines but does not couple to G protein-mediated signalling pathways

HRH1 – histamine receptor H1; a receptor that mediates the biological activities of the biogenic amine histamine, an inflammatory mediator released by basophils and mast cells that mediates vasodilation and pruritus

GPR183 – orphan receptor

GPR35 – orphan receptor

GPR84 – orphan receptor

GPR141 – orphan receptor

GPR68 – orphan receptor

These seven receptors were subjected to a range of investigations into their suitability as candidates for the CXCL14 receptor, beginning with a comprehensive review of the existing published literature.

4.5.1 Investigation of non-orphan receptors

4.5.1.1 Histamine receptor H1

The seven candidates include five orphan receptors and two receptors of known function/ligand specificity. The gene *HRH1* encodes one of four histamine receptors (HRH1-4). HRH1 and HRH2 are expressed on T-helper cells, with HRH1 being predominantly expressed on T_H1 cells and HRH2 being expressed on T_H2 cells (Jutel et al., 2001). Indeed, stimulation of naïve T cells with the T_H1 cytokine IL-12 results in up-regulation of HRH1 expression, while stimulation with the T_H2 cytokine IL-4 results in its suppression. T_H1 cells respond to histamine stimulation by mobilisation of

intracellular calcium stores that can be blocked by a HRH1 antagonist. Furthermore, mice lacking HRH1 have lower percentages of IFNγ-producing cells compared to wild type mice (Jutel et al., 2001). It has also been observed that HRH1-deficient mice have reduced airway inflammation in a model of asthma, and this was attributed to defective T-cell trafficking to the lung, the authors identifying histamine as a chemotactic factor for T cells. Indeed, blockade of HRH1, but not of HRH2, ablated the migratory response *in vitro* (Bryce et al., 2006).

Although HRH1 has been demonstrated to possess chemotactic activity, the fact that its expression on cells of the immune system appears to be restricted to T cells means that it is likely not the CXCL14 receptor. I have demonstrated that T cells isolated from both human blood and skin do not respond to CXCL14 or express CXCL14 receptor(s). Therefore, HRH1 is not being considered a candidate for the CXCL14 receptor.

4.5.1.2 C-C Chemokine receptor-like 2

CCRL2 (also known as ACKR5) is thought to be an atypical chemokine receptor, involved in modulating responses to other chemokines. This was first alluded to by Hartmann et al., who demonstrated that CCL5 was able to induce expression of CCRL2 on B-cell lines, and that the MAP kinases were phosphorylated upon CCL5 stimulation of CCRL2-transfected cells, suggesting a direct effect of CCL5 through CCRL2. MAP kinase phosphorylation was insensitive to pertussis toxin treatment, suggesting that CCRL2 does not couple to Gαi proteins. Furthermore, no calcium mobilisation or migratory responses upon CCL5 stimulation were detected in B-cell lines or CCLR2-transfected cells (Hartmann et al., 2008). Later, the homeostatic chemokine CCL19 was identified as a CCRL2 ligand, CCL19 binding to CCRL2 with an affinity comparable to binding of CCR7. Binding of CCL19 to CCRL2 did not result in calcium mobilisation or migration, however confocal microscopy revealed that CCRL2 was internalised following binding of CCL19 (Leick et al., 2010). The chemotactic protein chemerin has also been identified as a protein that binds, but is not internalised by, CCRL2 (Zabel et al., 2008). Therefore, although it has been shown to mediate certain signalling events following chemokine binding, it is thought that CCRL2 is a non-classical chemokine receptor that is involved in modulating the activities of other chemokines and chemoattractant molecules.

Our lab possessed 300.19 cells stably transfected with CCRL2 (CCRL2-expressing lines were generated several years ago by previous members of the lab). Two

separate lines were used in chemotaxis assays for testing responses toward CXCL14. Surface expression of CCRL2 was confirmed by flow cytometry (**Figure 4.8a**). Both lines failed to display any migration in response to CXCL14 (**Figure 4.8b**). As CCRL2 is not thought to mediate chemotaxis in response to any chemokine, it was not possible to include a positive control for migration.
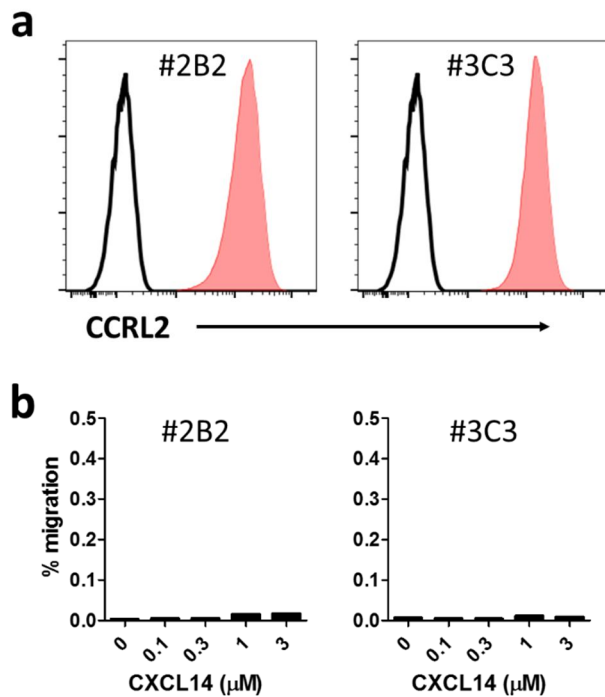
Figure 4.8. The 300.19 cell-line stably expressing CCRL2 does not migrate in response to CXCL14.

Two CCRL2-expressing 300.19 cell lines, designated '2B2' and '3C3', were tested for migratory response toward CXCL14. (**a**) Surface expression of CCRL2 was confirmed by flow cytometry. Black empty histogram indicates staining of untransfected cells. (**b**) Migration toward up to 3 μM CXCL14 was assessed using the transwell chemotaxis assay. Migration is displayed as % of input cells and is from a single experiment, where each condition was run in duplicate.

Following exclusion of HRH1 and CCRL2, this left five orphan GPCRs remaining as the primary candidates for the CXCL14 receptor; GPR35, GPR68, GPR84, GPR141 and GPR183. To confirm the identity of the receptor, the candidates were to be screened by two methods, as outlined in the aims. Before these experiments were commenced however, sequence similarity and phylogenetic relationships of the five candidates in relation to the existing chemokine receptors was investigated.

4.5.2 Investigation of the five orphan receptors

4.5.2.1 Sequence analysis

Chemokine receptors are distinguished from other GPCRs by several features of their amino acid sequence, most notably the presence of a number of conserved amino acid motifs at discrete locations. The DRYLAIV motif, located at the junction of the third transmembrane domain and the second intracellular loop, is thought to play a crucial role in coupling the receptor to the $G\alpha i$ proteins that mediate activation of signal transduction pathways associated with chemotaxis following chemokine engagement (Nomiyama and Yoshie, 2015). The observation that the DRYLAIV motif is substantially altered in the atypical chemokine receptors, so-called because they are unable to initiate classical signalling pathways after ligand binding (Nibbs and Graham, 2013), reinforces this notion. Other motifs conserved among chemokine receptors include the TLPxW motif and the NPxxY motif, located in the 2nd transmembrane region and at the boundary between the 7th transmembrane region and cytoplasmic tail, respectively. These conserved sequences are thought to act as molecular micro-switches, mediating transition of the receptor from an inactive to an active conformation following ligand binding (Nygaard et al., 2009).

Sequence analysis of the five candidates reveals interesting features with regard to their amino acid sequences. None of them have a canonical DRYLAIV motif, each of the five candidates possessing a different amino acid in at least three positions. Indeed, only GPR68 and GPR35 have an intact DRY motif, these three residues (Asp-Arg-Tyr) thought to be of greatest importance for coupling to intracellular $G\alpha i$ proteins. Four of the five candidates also show changes in each of the other two motifs, the exception being GPR84 which has an intact NPxxY motif (**Table 4.6**). However, the chemokine receptor CXCR6 has a DRFIVVV motif, and yet still mediates chemotaxis of certain subsets of T cells in response to CXCL16. CXCL16 has unusual features, being considerably larger than most other chemokines (254 amino acids), containing a mucin-like stalk which enables it to be expressed as a cell surface-bound molecule

as well as a soluble chemokine (Matloubian et al., 2000, Wilbanks et al., 2001). The unusual features of CXCL14 in comparison to other chemokines (e.g. very short N-terminal sequence prior to the first cysteine residue) may therefore indicate that the CXCL14 receptor too has features that distinguish it from the typical chemokine receptors.

Chemokine receptors are typically 340-370 amino acids in length, with GPR68 (365 amino acids), GPR35 (309 amino acids) and GPR183 (361 amino acids) fitting this profile. GPR84 is a little longer at 396 amino acids, while GPR141 is a little shorter (299 amino acids). Finally, many of the chemokine receptor-encoding genes cluster on chromosome 3 of the human genome, therefore the cytogenetic location of the candidates may give some clue as to whether it likely codes for an as yet undiscovered receptor. All of the genes encoding the five candidates are found on different chromosomes, with none being present on chromosome 3 (**Table 4.6**). However, other chemokine receptor genes are found at unique locations throughout the genome, including *CXCR3* (Xq13.1), *CXCR4* (2q22.1) and *CXCR5* (11q23.3).

Table 4.6. Properties of the five candidates for the CXCL14 receptor.

Receptor	Conserved motifs			Number of amino acids	Cytogenetic location
	DRYLAIV	TLPxW	NPxxY		
GPR68	DRYLAVA	SLPxW	DPxxY	365	**14**q32.11
GPR84	GRYLLIA	LLQxF	NPxxY	396	**12**q13.13
GPR35	DRYVAVR	TLPxV	DAxxY	309	**2**q37.3
GPR141	TRYLIFF	TVPxR	DLxxF	299	**7**p14.1
GPR183	DRFIAVV	ALPxR	DPxxY	361	**13**q32.3

Overall sequence similarity between the chemokine receptors is highly variable, chemokine receptors typically displaying anything between 25 and 80% amino acid identity. A dendogram showing the degree of protein sequence similarity between all known human chemokine receptors and the five candidates under investigation is shown in **Figure 4.9**. The shorter the distance to the point of divergence of two receptors, the more similar their sequences are. What is clear is that none of the five orphan receptors exhibit a great degree of sequence similarity to any of the known chemokine receptors, or to one-another. What is worth noting however, is that those which do have similar sequences (such as CXCR1 and CXCR2) are bound by the same ligands (CXCL6, CXCL7 and CXCL8). Those receptors which only have a single

142

ligand (e.g. CXCR4 and CXCR5) do not show much similarity to the other receptors. Upon considering the sequence analysis of the five CXCL14 receptor candidates, it is clear that they all represent distinct receptors with unique features. However, owing to its high level of expression in many healthy tissues and selectivity for monocytes, CXCL14 is a unique chemokine. Hence, it is not alarming that the candidates for its receptor under investigation are themselves unique from the chemokine receptors already described.
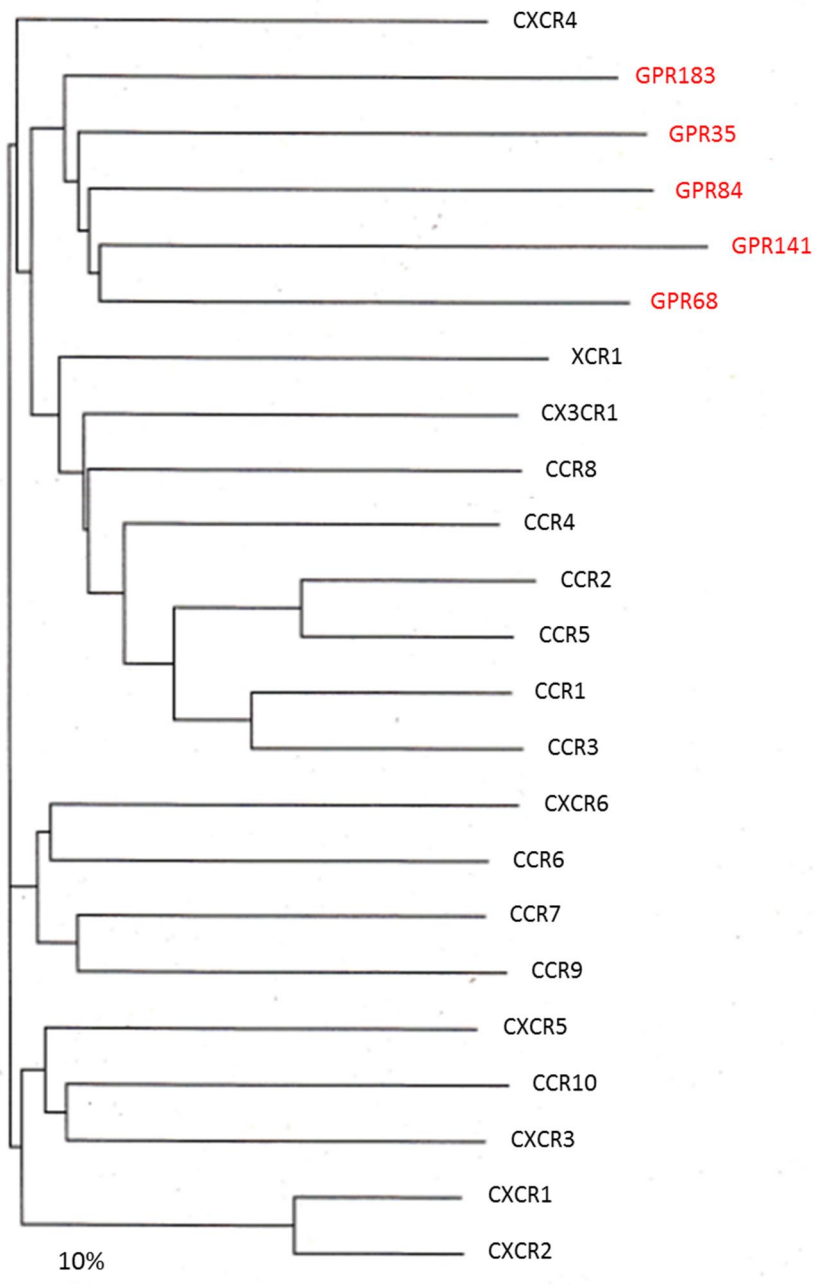
Figure 4.9. Sequence similarity of the CXCL14 receptor candidates to the known human chemokine receptors.

Dendrogram showing the degree of protein sequence similarity among all known human chemokine receptors and my five candidates. Protein sequences were obtained from the National Centre for Biotechnology Information protein database. The phylogenetic tree was constructed using the ClustalW program provided by the European Bioinformatics Institute and analysed using TreeView. The scale bar reflects the horizontal distance at which sequences diverge by 10% (90% identity). Amino acid identity between a pair of chemokine receptors is given by $1 - x$, where x is the sum of the 2 horizontal distances to the right of the pair's vertical branch point. For example, the horizontal distances before the vertical branch point of CXCR1 and CXCR2 are 12.9 and 11.8%, respectively. Therefore, the amino acid identity between these chemokine receptors is $100 - (12.9 + 11.8)\%$ or 75.3%.

4.5.2.2 Literature search

GPR68

GPR68 is a gene which encodes a member of the GPCR family known as ovarian cancer G protein-coupled receptor 1 (OGR1), due to its initial isolation from an ovarian cell line cDNA library (Xu and Casey, 1996). An approximately 3-kb transcript has been detected in a variety of tissues including brain, spleen, lung, placenta and peripheral blood leukocytes. Later it was reported that OGR1 mediates the activation of downstream signalling cascades including intracellular calcium release and inositol phosphate formation in response to protons (Ludwig et al., 2003). It has therefore been proposed that OGR1 is a proton-sensing receptor involved in pH homeostasis. However, others have reported that OGR1 is a receptor for sphingosylphosphorylcholine, a bioactive lipid (Mogi et al., 2005, Xu et al., 2000). Therefore, the precise nature of its function and ligand specificity remains controversial.

GPR84

A cDNA encoding GPR84 was identified using an expressed sequence tag (EST) database search method (Wittenberger et al., 2001). The deduced 396-amino acid protein is 85% identical to its mouse ortholog indicating. Northern blot analysis has revealed wide-ranging expression of a 1.5-bk transcript in brain, heart, muscle, colon, thymus, spleen, kidney, liver, intestine, placenta, lung and peripheral blood leukocytes (Wittenberger et al., 2001). As of yet, there is no data on the function of this receptor, nor have any ligands been predicted. Its high sequence similarity to the mouse ortholog is consistent with that of CXCL14, making GPR84 a promising candidate.

GPR141

By searching human genome databases for sequences similar to rhodopsin-like GPCRs, Fredriksson et al. identified a number of new GPCR-encoding genes, including GPR141 (Fredriksson et al., 2003a). The deduced 299-amino acid protein has a TRY motif instead of DRY at the junction between the third transmembrane region and the second intracellular loop, while there is no classic NPxxY motif in TM7. Human GPR141 shares 67% amino acid identity with mouse GPR141, while an ortholog has also been reported in zebrafish, suggesting that GPR141 is relatively

well conserved throughout evolution. As of yet, there is no data on the likely ligand(s) or physiological function of this receptor.

GPR35

The *GPR35* gene was discovered by searching for genes related to *GPR1* by PCR of genomic DNA with degenerate primers based on the conserved transmembrane regions (O'Dowd et al., 1998). The gene encodes a predicted 309-amino acid protein. Expression of GPR35 transcripts was detected in all foetal and adult human tissues examined, with expression highest in adult lung, small intestine, colon and stomach (Horikawa et al., 2000). In 2015, Albert Zlotnik's group published work demonstrating that the human chemokine CXCL17 induced chemotactic responses in PGE_2-treated THP-1 cells by signalling through a novel chemokine receptor. Treatment of THP-1 cells with PGE_2 resulted in increased expression of GPR35, confirmed by RT-PCR. Transfection of human or mouse cells with GPR35 resulted in responsiveness to CXCL17 in the form of calcium mobilisation, however they were unable to show that GPR35 mediated chemotactic responses toward CXCL17 (Maravillas-Montero et al., 2015). When CXCL17 was first described, it was shown to induce robust chemotactic responses in CD14^{+} human blood monocytes, while CD16^{+} cells (a mix of CD16^{+} monocytes, granulocytes and NK cells) and CD3^{+} T cells were unresponsive (Pisabarro et al., 2006). It remains to be confirmed if GPR35 truly represents the receptor by which CXCL17 induces chemotaxis of target cells.

I tested migratory responses of human PBMC and PGE_2-treated THP-1 cells toward CXCL17 by transwell chemotaxis assay, as these were reported previously by Pisabarro et al. and Maravillas-Montero et al., respectively. However, no migration toward CXCL17 was observed (**Figure 4.10**).
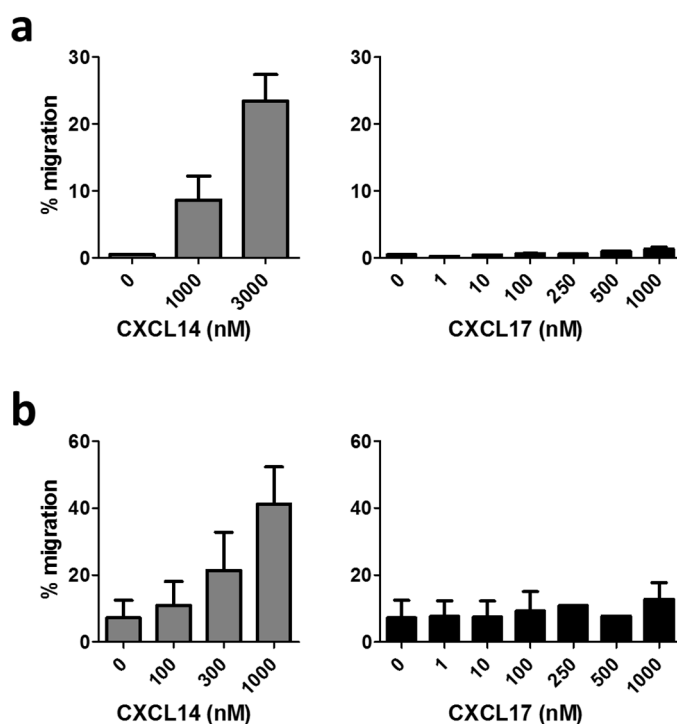
Figure 4.10. CXCL17 did not induce migration of PGE$_2$-treated THP-1 cells or primary human monocytes.

Migratory responses of (**a**) PGE$_2$-treated THP-1 cells or (**b**) primary human monocytes toward CXCL14 (grey bars) and CXCL17 (black bars) were assessed by the transwell chemotaxis assay. Migration is presented as the percentage of input cells and are mean + s.e.m. of two independent experiments.

GPR183

GPR183, also known as Epstein-Barr virus-induced gene 2 (EBI2), was first identified as an orphan GPCR which is highly expressed in spleen and upregulated upon Epstein-Barr virus (EBV) infection (Birkenbach et al., 1993). It was subsequently shown that EBI2 is constitutively expressed in naïve B cells, its level increasing after activation, where it has a role in B-cell migration within lymphoid follicles and their position in the early stages of a humoral response (Gatto et al., 2009, Pereira et al., 2009). 7α,25-dihydroxycholesterol (7α,25-OHC) was identified as an endogenous ligand for EBI2, 7α,25-OHC triggering pertussis toxin-sensitive EBI2 activation as well as B-cell migration *in vitro* (Hannedouche et al., 2011, Liu et al., 2011a). It has recently been shown that EBI2 forms heterodimers with CXCR5, and by doing so regulates CXCL13-mediated B-cell responses (Barroso et al., 2012), thereby further

demonstrating the role of EBI2 in B-cell positioning in lymphoid follicles. In my RNAseq data from primary cells, GPR183 (EBI2) displayed a high level of expression in B cells (average of 215 across the three donors). However, its expression in classical monocytes was nearly 50-fold higher compared to B cells (average of 10,150 across the three donors), while expression was almost absent in non-classical monocytes. Therefore, it was decided to include GPR183 in my investigations.

At this point, the five orphan receptors were to be screened using two techniques:

- Knockdown of gene expression (and hence protein expression) by RNA interference in THP-1 cells
- Expression of the receptor by stable retroviral transduction of the murine pre-B cell line 300.19

Knockdown and/or stable expression of the receptor would then be followed by assessment of migratory responses toward CXCL14 by transwell chemotaxis assay. For the knockdown experiments, I would be looking for either a partial or complete abolishment of the migratory response toward CXCL14 (following overnight pre-treatment of THP-1 cells with PGE_2). In contrast, in the stable expression experiments, I would be looking for transduced cells to display a migratory response to CXCL14, with non-transduced cells as a control giving no response.

4.6 Methods Used to Screen CXCL14 Receptor Candidates

4.6.1 Method 1: Expression in the murine pre-B cell-line 300.19

The five candidate receptors were cloned into the lentiviral vector pSIEW which co-expresses enhanced green fluorescent protein (eGFP), incorporated into lentiviral particles and expressed in the 300.19 cell line, as described in Materials and Methods. Suitable reagents were not available for detecting expression of the orphan receptors on the cell surface. Therefore, in order to be confident that following lentiviral transduction the gene was being transcribed and that the resulting protein was being folded correctly and trafficked to the cell surface, a positive control was required.

4.6.1.1 Method validation – expression of murine CCR8 in 300.19 cells

The murine pre-B cell line 300.19 has been routinely used by our group for stable expression of exogenous chemokine receptors. To confirm that 300.19 cells were amenable to lentiviral transduction in our hands, and that the receptor was being expressed, 300.19 cells were transduced with lentiviral particles containing the murine CCR8 (muCCR8) gene. Expression of muCCR8 on the surface of transduced 300.19 cells (identified by expression of eGFP) was subsequently confirmed by two methods; binding of Alexa Fluor 647-labelled muCCL1 (AF-muCCL1) and chemotactic responses toward muCCL1 (**Figure 4.11**).
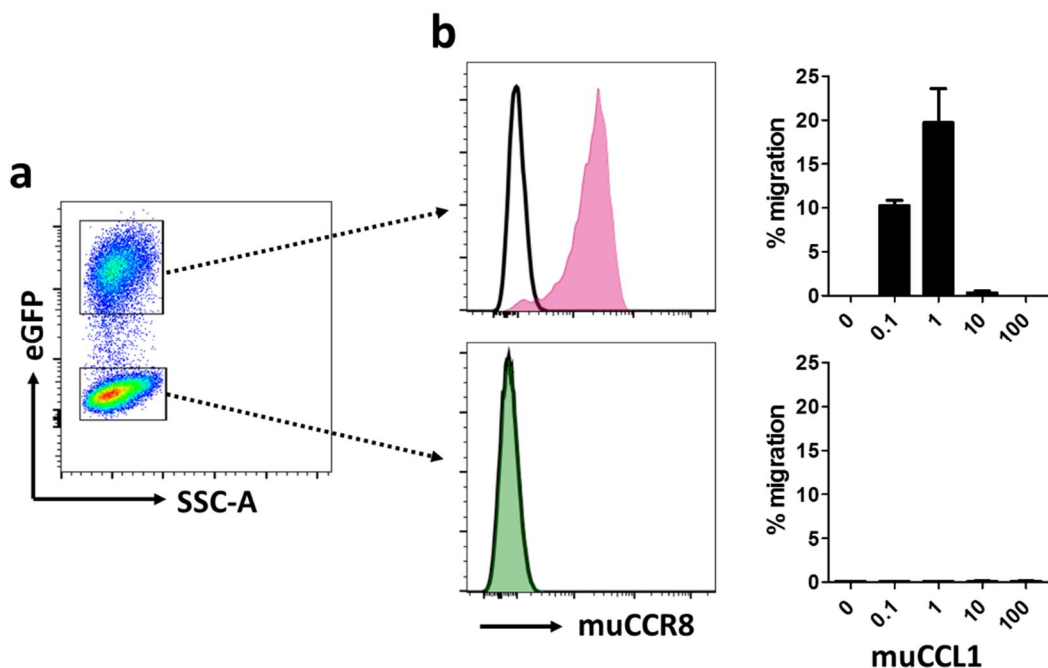
Figure 4.11. Following transduction with lentiviral particles containing muCCR8, 300.19 cells express the receptor on the cell surface and migrate toward muCCL1.
300.19 cells were transduced with lentiviral particles which co-express muCCR8 and eGFP. (**a**) Following the transduction with lentiviral particles, 300.19 cells in which the viral DNA had successfully integrated into the host cell genome were identified by expression of eGFP (In the plot shown, 27% of cells are eGFP[+]). Transduction of 300.19 cells with lentiviral particles expressing muCCR8 was performed on three separate occasions, with similar results. (**b**) Binding of AF-muCCL1 (detected by flow cytometry; black line indicates binding to non-transduced cells) and migratory responses toward muCCL1 (assessed by transwell chemotaxis assay) of transduced (eGFP+, top) and non-transduced (eGFP-, bottom) cells. Migration is displayed as percentage of input and is mean + s.e.m. of two independent experiments.

4.6.1.2 Expression of orphan GPCRs

I had demonstrated that stable expression of a GPCR in 300.19 cells by lentiviral transduction can be achieved, and that the receptor is expressed on the cell surface and is fully functional. Therefore, 300.19 cells were subsequently transduced with lentiviral particles incorporating each of the five orphan receptors under investigation. Transduced cells were FACS sorted on the basis of expression of eGFP and, following recovery in culture for 2-3 days, subjected to assessment of responses toward CXCL14. As shown in **Figure 4.12**, none of the five receptors mediated chemotactic responses toward 1-1000 nM CXCL14, while transduced cells also did not bind AF-CXCL14. Unfortunately, therefore, this technique has not revealed the identity of the CXCL14 receptor.
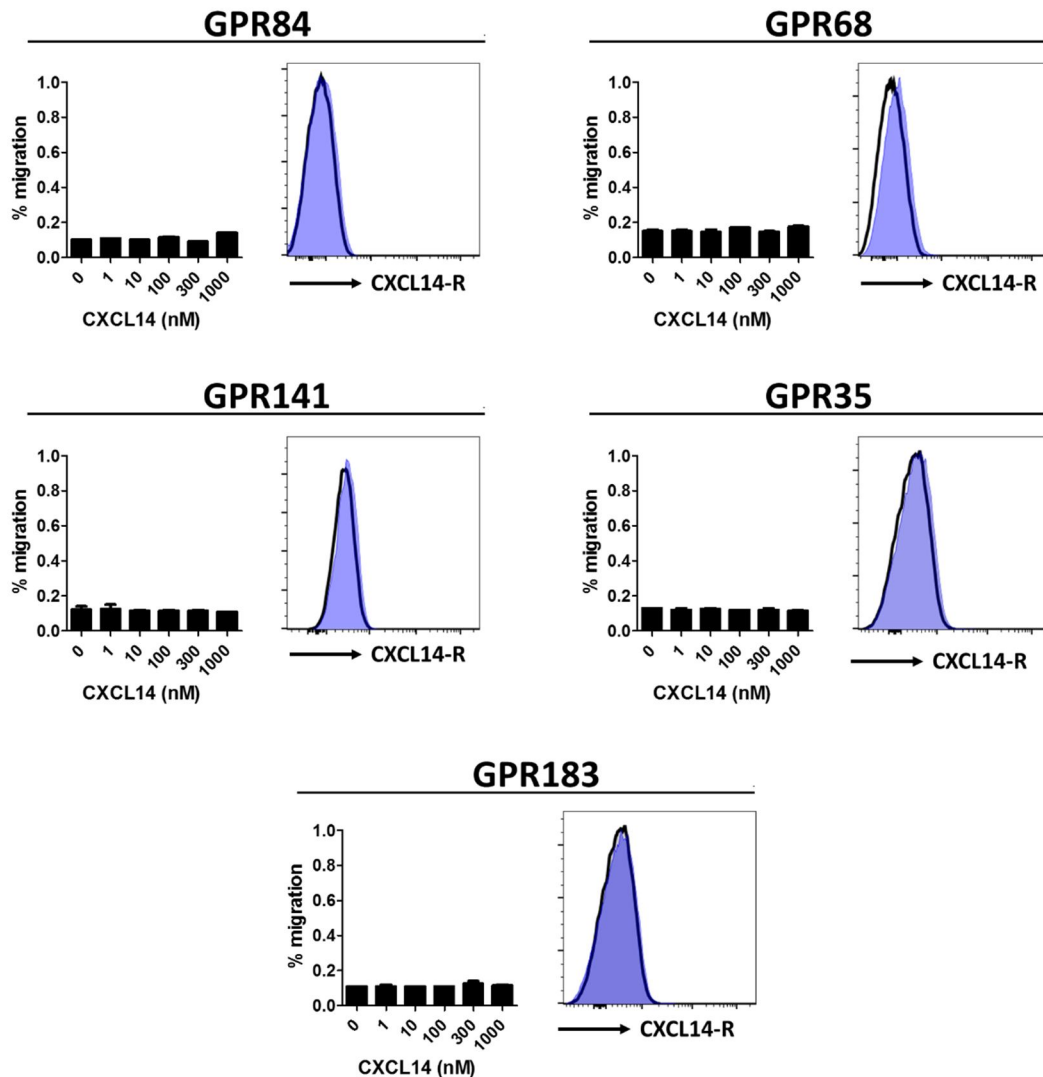
Figure 4.12. None of the five orphan receptors mediate chemotaxis toward CXCL14 or binding of AF-CXCL14.

The murine pre-B cell line 300.19 was stably transduced with one of five orphan GPCRs in turn, and chemotactic responses toward CXCL14 were assessed by transwell migration assay (bar charts). In addition, binding of AF-CXCL14 was assessed by flow cytometry (blue histograms). Black line indicates binding of AF-CXCL14 to non-transduced cells. Migration is displayed as percentage of input cells and is mean + s.e.m. of two independent experiments.

4.6.2 Method 2: ShRNA-mediated gene-silencing

RNA interference (RNAi) is defined as a mechanism of post-transcriptional gene silencing produced by small RNAs, which take the form of endogenous microRNA (miRNA) and exogenous small interference RNA (siRNA) or short hairpin RNA (shRNA). Delivery of shRNA to cells has been shown to be an effective strategy for

long-term gene silencing (Brummelkamp et al., 2002, Yu et al., 2002). ShRNA is transcribed in the nucleus from an expression vector bearing a short double-stranded DNA sequence with a hairpin loop. The shRNA transcript then enters the cytoplasm of the cell, where it is processed by the endoribonuclease Dicer, and single-stranded mature shRNA is loaded into the RNA-induced silencing complex (RISC). The mature shRNA guides RISC to the complementary region of target mRNA, upon which the target mRNA is degraded (**Figure 4.13**). The properties of the promoter are important for efficient shRNA expression. In our screening procedures, an RNA polymerase III vector based on the mouse U6 promoter was used, as has been used previously by others (Yu et al., 2002).
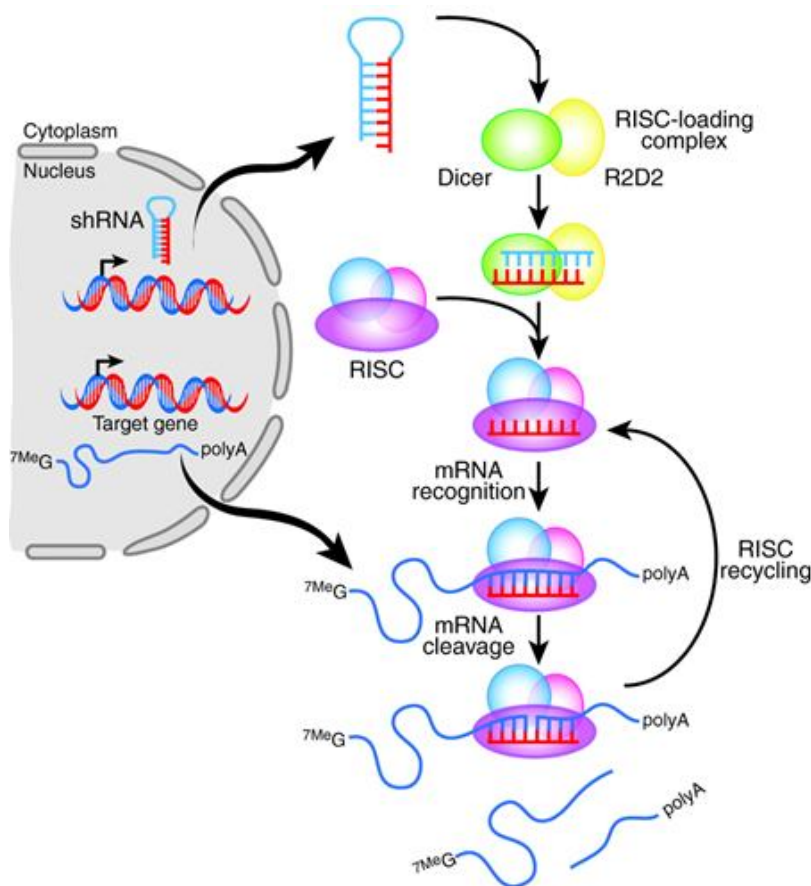
Figure 4.13. Small hairpin RNA-mediated gene silencing.

The shRNA is expressed in the nucleus of the cell from a DNA-based vector. The shRNA transcript is then processed in the cytoplasm by the RNase III family member Dicer in concert with the double-stranded RNA-binding protein R2D2 into a siRNA duplex. The resulting 19-21-nucleotide single-stranded mature shRNA is incorporated into the multi-subunit RNA-induced silencing complex (RISC), and guides RISC to the complementary site in the target mRNA, which engages the endonucleocytic activity of RISC, resulting in mRNA cleavage. The shRNA-loaded RISC is recycled for several rounds of mRNA cleavage. Figure adapted from (Dominska and Dykxhoorn, 2010).

4.6.2.1 Method validation – silencing of CCR2 in THP-1 cells

To confirm the validity of using shRNA-mediated gene silencing to screen CXCL14 receptor candidates in THP-1 cells, I tested the technique by attempting to knock down expression of the known chemokine receptor CCR2. This receptor was chosen because it is expressed at high levels on the surface of THP-1 cells and mediates a robust migratory response to the ligand CCL2 (**Figure 4.14a**). Firstly, I needed to confirm that the THP-1 response to CCL2 was unaffected by treatment with PGE_2, since for the candidate screening, the cells would need to be treated with PGE_2 to induce responsiveness to CXCL14. Treatment with PGE_2 did not affect surface expression of CCR2, while the migratory response to CCL2 was also unaffected (**Figure 4.14b**). Secondly, it was necessary to demonstrate that THP-1 cells were amenable to transduction with the lentiviral vector that would be used to deliver the shRNA to the cells. THP-1 cells were transduced with lentiviral particles without shRNAs, and as before, transduction efficiency was assessed by expression of eGFP. Increased transduction efficiency was observed with increasing quantity of virus, while the proportion of $eGFP^+$ cells remained stable for as long as two weeks, indicating that transduction did not affect the survival or proliferation rate of the cells. Furthermore, induction of responsiveness to CXCL14 with PGE_2 treatment remained intact in transduced cells (**Figure 4.15**).
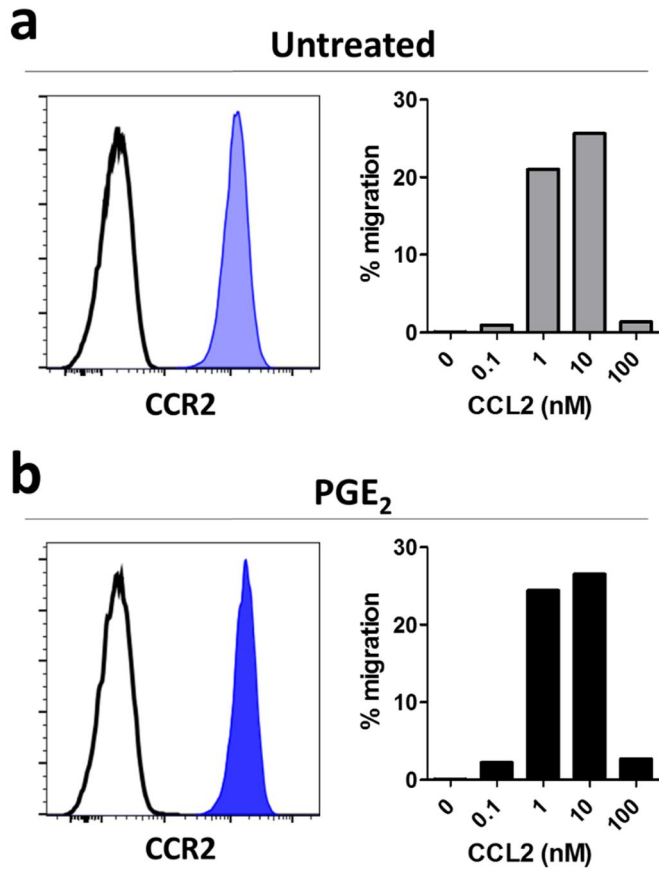
Figure 4.14. Surface expression of CCR2 and the chemotactic response to CCL2 in THP-1 cells is unaffected by PGE$_2$ treatment.

THP-1 cells were cultured for 24 hours in **(a)** medium alone, or **(b)** medium supplemented with 1 µM PGE$_2$. Surface expression of CCR2 was determined by flow cytometry (left, blue filled histogram. Black empty histogram indicates staining with isotype-matched control antibody). Transwell chemotaxis assay was used to test migratory responses toward 0.1-100 nM CCL2 (right). Data representative of two independent experiments is shown.
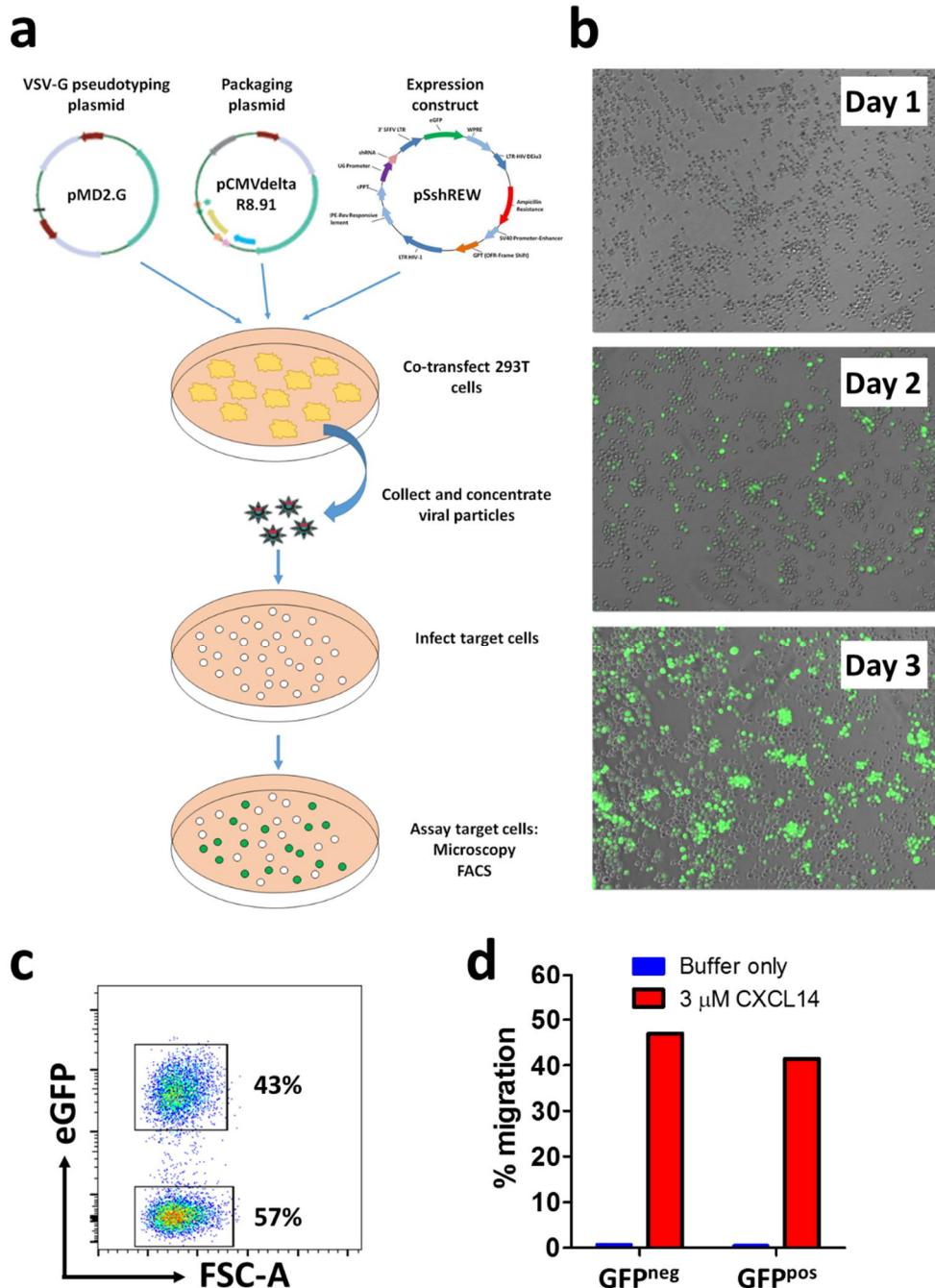
Figure 4.15. THP-1 cells are amenable to lentiviral transduction, and transduction does not affect induction of responsiveness toward CXCL14 with PGE$_2$.

(**a**) Schematic displaying the process of making lentiviral particles incorporating the shRNA insert, prior to infection of THP-1 cells and assessment of transduction efficiency (**b**) Successful transduction of THP-1 cells was assessed by eGFP expression, detected by fluorescence microscopy. (**c**) After the cells were washed to remove any remaining virus and placed back into culture, the transduction efficiency (% of eGFP+ cells) was confirmed by flow cytometry on day 6 post-transduction. (**d**) Migratory responses of the mixed population of eGFP+ (transduced) and eGFP^{neg} (non-transduced) THP-1 cells toward 3 μM CXCL14 were tested using the transwell chemotaxis assay. Data shown are from a single experiment.

Three shRNAs, targeted against nucleotides 801-821, 392-412 and 600-620 of human CCR2, were selected from sequences published online by Sigma-Aldrich in their MISSION™ shRNA library. ShRNAs were delivered to THP-1 cells using the lentiviral system described. In addition, a fourth shRNA with no complementarity to any known human mRNA (non-silencing shRNA) was used as control. Following transduction, eGFP+ cells were sorted by FACS prior to assessment of CCR2 knock down. The three shRNAs designed to knock down human CCR2 expression are shown in **Table 4.7**, and they gave very different results. Two of the three shRNAs targeted against CCR2 (#1 and #3) failed to yield any knock down, as mRNA and surface protein expression were shown to be unaffected. Furthermore, migration toward CCL2 remained intact. In contrast, shRNA #2 yielded efficient knockdown of CCR2 expression, calculated as ~80-85% knock down at both the mRNA and protein level. CCR2 mRNA was found to be reduced by 81.35 ± 3.45% by qPCR (**Table 4.7**). Similarly, MFI of CCR2 expression for shRNA #2 was 1,946, compared to an average of 12,880 across the other three groups (non-silencing shRNA, CCR2 shRNA #1 and CCR2 shRNA #3). This equates to 84.9% knock down at the protein level. Interestingly, this degree of CCR2 knock down was sufficient to completely abolish the migratory response of THP-1 cells toward CCL2 (**Figure 4.16**).

Table 4.7. Three shRNAs designed against human CCR2.

shRNA	Sequence	Target nucleotides of CCR2 mRNA	Ct value* (% knockdown)
1	GCTTCTGGACTCCCTATAATAT<u>CTCGAG</u>ATATTATAGGGAGTCCAGAAG	801-821	23.49 (0%)
2	GGCTGTATCACATCGGTTATT<u>CTCGAG</u>AATAACCGATGTGATACAGCC	392-412	26.10 (81.35%)
3	GTTATGTCTGTGGCCCTTATTT<u>CTCGAG</u>AAATAAGGGCCACAGACATAA	600-620	23.27 (0%)

Red; 'G' nucleotide added at the start of the sequence. Blue; Sequence that is targeted to CCR2 mRNA. Underlined; shRNA hairpin sequence. *mRNA knockdown was assessed by qPCR and relative mRNA levels were calculated using the ΔΔCt method, normalised to expression of a housekeeping control (beta-actin).
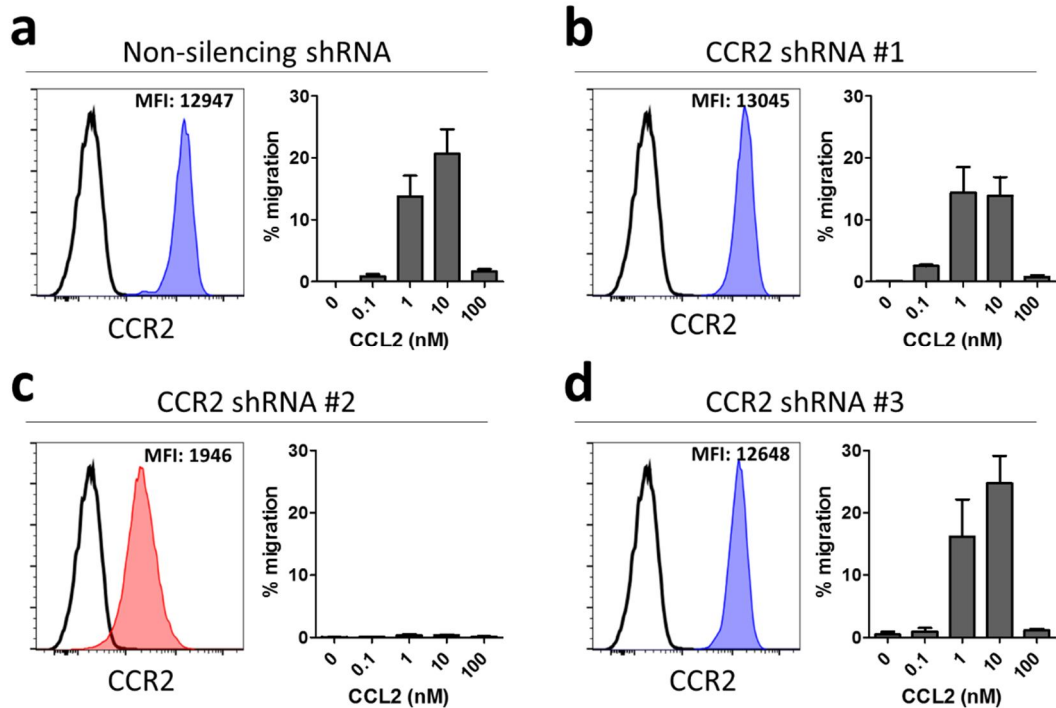
Figure 4.16. ShRNA-mediated knockdown of CCR2 completely abolishes the migratory response of THP-1 cells toward CCL2.

THP-1 cells were transduced with (**a**) non-silencing shRNA or (**b-d**) three shRNA directed against human CCR2. Surface expression of CCR2 was detected by flow cytometry (filled histograms; black empty histogram indicates staining with isotype-matched control antibody). Mean fluorescence intensity (MFI) values given are the geometric mean of CCR2 expression and are representative of two independent experiments. Migratory responses toward CCL2 (bar charts) were assessed by transwell chemotaxis assay. Data shown is mean + s.e.m. of two independent experiments.

The reason for the failure of two of the three shRNAs to give knockdown of CCR2 is not known for sure but may be explained by the addition of an artificial "G" nucleotide at the start of the sequence, as this is the first base required by the U6 promoter for the shRNA to be expressed. In contrast, shRNA #2, which did give knockdown, had a 'natural' G nucleotide at the start of its sequence. It was therefore decided that in future experiments, where possible, shRNAs would be designed with a natural G nucleotide at the start of the sequence.

Three shRNAs each were designed against two of the candidate orphan receptors (GPR68 and GPR84) and delivered to THP-1 cells by the lentivirus method described. However, stable knockdown was not achieved with any of them (assessed by qPCR; data not shown) for reasons that are not understood. Screening of candidates by shRNA was therefore postponed at this point, although work is ongoing to try and improve the robustness of this technique.

4.7 Discussion

The aim of this part of the project was to establish the identity of the receptor by which CXCL14 induces chemotactic responses in target cells, namely monocytes. A monocytic cell line (THP-1) and primary immune cells from peripheral blood (classical and non-classical monocytes, and B cells) were interrogated for their expression of GPCRs by RNA sequencing. This led to the generation of a list of 'candidates' for the CXCL14 receptor, formulated based on its predicted expression profile. Some of the candidates were ruled out based on their function already being well-characterised. The final candidate list consisted of five orphan receptors, which were subjected to thorough analysis of their amino acid sequence and phylogenetic relationship to known chemokine receptors, as well as assessment of their ability to mediate chemotactic responses toward CXCL14 by being stably expressed in the murine pre-B cell line 300.19.

It has been published previously by our group that PGE_2 induces responsiveness to CXCL14 in THP-1 cells (and primary monocytes), in the form of migration and calcium mobilisation (Kurth et al., 2001). I was able to replicate the PGE_2 effect in THP-1 cells and show that it is mediated primarily by the EP4 receptor (Figure 3.12). This is not surprising, as others have published that PGE_2-mediated effects on immune cells (Kabashima et al., 2003, Stock et al., 2011), and in particular modulation of chemokine receptor expression on monocytes (Panzer and Uguccioni, 2004), is mediated by the EP4 receptor. The physiological effects of PGE_2 on the immune response in human skin have also been extensively studied, and include pro-inflammatory and anti-inflammatory functions (McCully et al., 2012, Nicolaou, 2013). It has been shown previously that epidermal keratinocytes and dermal fibroblasts are both sources of PGE_2. In the context of traffic of immune cells to human skin, we have reported that PGE_2 primes naïve T cells for responses toward the skin-expressed chemokine CCL1 (McCully et al., 2015). These results show that PGE_2 is a factor for induction of the skin-homing chemokine receptor CCR8 on human T cells. It could be postulated, therefore, that PGE_2 may have a similar effect on monocytes, inducing expression of the skin-homing chemokine receptor for CXCL14. Our group has also published that PGE_2 and the active vitamin D metabolite $1,25(OH)_2D_3$ act in concert in the induction of CCR8 expression on naïve T cells (McCully et al., 2015). Interestingly, I observed that $1,25(OH)_2D_3$ is also able to induce migratory responses to CXCL14 in THP-1 cells (data not shown), providing further evidence that peripheral tissue-specific factors may play an important role in induction of expression of the CXCL14 receptor on

monocytes. Therefore, it was with confidence that I decided to use the model of PGE$_2$-treated THP-1 cells for identification of candidates for the CXCL14 receptor.

RNA sequencing provides only a snapshot of your cells of interest, telling you which genes are expressed and to what extent at only one particular moment in time. Gene expression may be switched on or off very rapidly, while mRNA can be silenced or degraded by endogenous cellular components such as microRNA in a matter of minutes. In addition, chemokine receptors translated from mRNA can be stable, remaining on the cell-surface for a number of days without the requirement for new protein being translated (Neel et al., 2005). All this means that it is very difficult to predict exactly when expression of an unknown gene will peak upon stimulation, and how exactly the presence of mRNA relates to protein expression and the functional response. THP-1 cells treated with PGE$_2$ or PGE$_2$ + sodium butyrate were collected at 24 hours post-stimulation. After 24 hours, THP-1 cells display a robust migration toward CXCL14, which was important for the study as I also wished to collect cells which had migrated toward CXCL14 for analysis. While being optimal for induction of the functional response to CXCL14, it is possible that mRNA expression may peak at an earlier time point. However, we have shown that while expression of CCR8 in naïve T cells peaked at 4 days post-stimulation with PGE$_2$ before coming back down, the mRNA level continued to rise up to day 5 (McCully et al., 2015). Once the identity of the CXCL14 receptor has been confirmed, a time course experiment should be performed to see precisely when its expression peaks at the mRNA level in THP-1 cells upon PGE$_2$-treatment, so that this can be correlated with protein expression and functional responses to the chemokine.

It has been shown that PGE$_2$ enhances migratory responses of human T cells and DCs to CCL19 and CCL21 by inducing formation of CCR7 oligomers at the cell surface which couple to distinct signalling pathways (Hauser et al., 2016, Scandella et al., 2004). In this instance, the enhanced response was not accompanied by an increase in CCR7 expression, either at the mRNA or the protein level. In fact, formation of receptor oligomers has been recognised as an early event in the activation of several chemokine receptors (Thelen et al., 2010). However, where PGE$_2$ does stimulate an increase in surface chemokine receptor expression, in the case of CCR8 on naïve T cells, this increase was shown to be accompanied by an increase at the mRNA level (McCully et al., 2015). I can only postulate, therefore, that induction of CXCL14 responsiveness in THP-1 cells is accompanied by an increase in expression of the CXCL14 receptor at both the mRNA and protein level, and that

the appearance of CXCL14 responses following PGE_2-treatment is not due to events unrelated to expression such as receptor oligomerisation. Upon discovery of the CXCL14 receptor, it will be of utmost importance to investigate whether it forms oligomers at the cell surface. If this is found to be the case. It will be interesting to observe if there is a modulation of its activity in response to ligand binding in terms of coupling to intracellular signalling pathways and functional responses.

In the second RNA-seq study, $CD14^{++}CD16^{-}$ classical monocytes, $CD14^{+}CD16^{++}$ non-classical monocytes and $CD19^{+}$ B cells were sorted from three healthy human donors. Candidates were selected on the basis of expression in classical monocytes (cells which respond to CXCL14) and low or absent expression in non-classical monocytes and B cells (cells which do not respond). Expression of cell-specific markers such as immunoglobulins in B cells confirmed the reliability of the data. Of particular interest, however, was the relative expression levels of certain chemokine receptors, which may reveal new insights into the regulation of the CXCL14 receptor. CCR7 and CXCR5 are two chemokine receptors which are expressed on B cells but not monocytes. Although the level of receptor expression on the surface of B cells is comparable between the two (based on my flow cytometry observations), mRNA levels in B cells were wildly different, expression being 1.3 relative units (RPKM) for CXCR5 and 389 relative units for CCR7 (a 300-fold difference). This discrepancy may be explained by different rates of turnover of the two receptors. For the majority of chemokine receptors, ligand binding induces rapid internalisation of the ligand-receptor complex. However, all chemokine receptors likely exhibit a basal level of turnover in the absence of their ligand, receptors being internalised into intracellular compartments for degradation while newly formed receptors are concomitantly trafficked to the cell surface. Little is known about this process of basal turnover, and the rates of replacement of protein may differ for different chemokine receptors. Obviously, making new receptor is dependent on the availability of mRNA for translation into protein. The difference in expression levels of CCR7 and CXCR5 may therefore be explained by CXCR5 having a longer half-life on the cell surface than CCR7, meaning that the rate of turnover is much slower and that there is much less dependence on mRNA for making new CXCR5 protein. CXCL13, the sole ligand for CXCR5, exhibits remarkable similarity to CXCL14 in terms of its potency, concentrations in the high nanomolar and micromolar range being necessary for both to stimulate migration of their respective target cells (Legler et al., 1998). It could therefore follow that the CXCL14 receptor exhibits a similarly low level of expression

as CXCR5, which is enough to maintain expression of the receptor on the surface of $CD14^+$ monocytes due to a slow rate of turnover.

At this point, the candidates identified from RNA sequencing are still under investigation in our lab, and the reasons for including them in the initial screening have been explained. However, it is likely that the list will be expanded to include more candidates. One such receptor which has not yet been investigated is GPR27. An orphan receptor, GPR27 is expressed at a similar level in $CD14^{++}CD16^-$ monocytes as CXCR5 is in B cells (expression level of GPR27 in monocytes is 2.33), while it is lower in $CD14^+CD16^{++}$ non-classical monocytes (0.66) and completely absent in B cells. As non-classical monocytes likely differentiate from classical monocytes, it would not be surprising that non-classical monocytes would retain some low level expression of the CXCL14 receptor, even though they do not respond by migration. In fact, non-classical monocytes do exhibit a minor shift upon labelling with AF-CXCL14 (Figure 3.4), which might be explained by having low level receptor expression which can be detected with the labelled chemokine, but which is insufficient to mediate chemotaxis. Indeed, as I demonstrated with shRNA-mediated knockdown of CCR2, the functional response to CCL2 was completely abrogated despite some receptors still being present on the cell surface (**Figure 4.16**). Furthermore, although no functional information is available on GPR27, it exhibits 97% identity with the mouse ortholog. This is highly relevant as human and mouse CXCL14 exhibit a similar degree of homology.

In addition to cloning of the GPCRs under investigation, it was our intention to use shRNA-mediated knockdown in THP-1 cells as a technique for screening candidates. I attempted to show the validity of using this technique by demonstrating that knockdown of CCR2 resulted in abrogation of the migratory response toward CCL2 (**Figure 4.16**). Although this was achieved with one of three shRNAs directed against CCR2 that were tested, the other two did not give any knockdown whatsoever, for reasons that are not entirely clear. Furthermore, the one that was successful gave incomplete knockdown at both the mRNA and protein level, despite the functional response to CCL2 being completely lost. To be confident in ruling out candidates for the CXCL14 receptor based on shRNA-mediated knockdown, it is of critical importance that the technique is robust and reliable. Therefore, it was decided that I would not pursue the shRNA approach for screening of selected orphan receptors at this time, although we fully intend to revisit it in the future.

In conclusion, my search for the CXCL14 receptor gene has not yet yielded the identity of this elusive chemokine receptor. The transcriptome analyses, however, have convinced me that this approach is sound and will eventually lead us to the CXCL14 receptor. It needs to be emphasised at this stage that the screening of receptor candidates by functional studies with candidate receptor-transfected cell lines is time consuming. Finally, I would like to point out that the discovery of CXCL14-responsive cells in human skin will provide a new opportunity for fine-tuning the current list of candidate receptors (this point, including interrogation of skin immune cells for expression of CXCL14 receptor(s), is discussed in much greater detail in the General Discussion).

Chapter 5   Synergistic Interaction between CXCL14 and Other Chemokines

5.1   Introduction

The individual actions of most chemokines are now well characterised, including their patterns of expression, the receptor(s) that they activate and the cells which they target. What has become increasingly apparent in recent years, however, is that leukocytes must integrate messages provided by several chemokines that are concomitantly produced *in vivo*. In this regard, there are numerous publications describing functional cooperation or synergism in the chemokine system, occurring in both physiological and pathological situations. Chemokine synergy is considered to occur when a low concentration of a chemokine, inactive by itself, becomes active in inducing leukocyte activation and/or migration in the presence of another chemokine. Several mechanisms have been proposed to explain how the phenomenon of chemokine synergy may occur; these are reviewed in (Gouwy et al., 2012) and summarised in **Figure 5.1**.
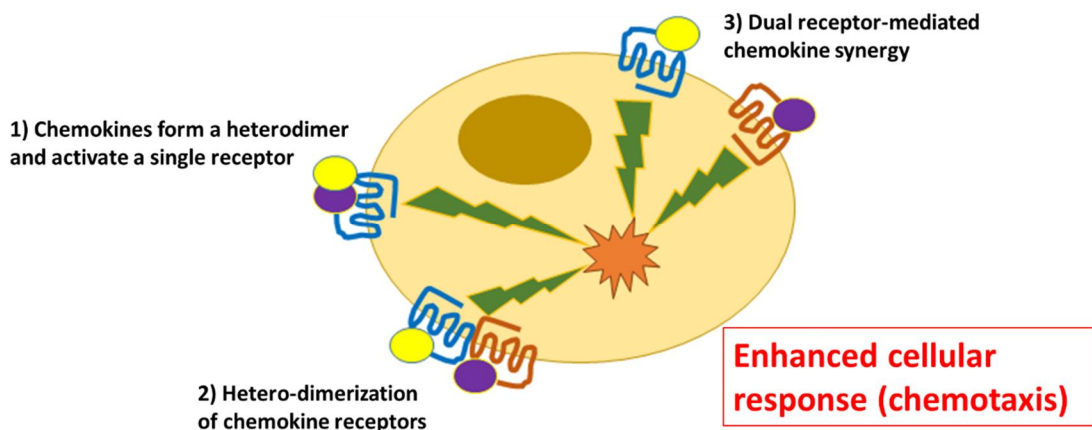
Figure 5.1. Modes of action in chemokine synergy.
Several mechanisms have been proposed to explain the synergy between chemokines leading to enhanced leukocyte responses including chemotaxis, but also including adhesion, intracellular calcium release, MAPK phosphorylation and receptor internalisation. (1) Two chemokines form a heterocomplex, activating a single receptor. (2) Chemokine receptors heterodimerise, and are activated by their respective ligands simultaneously (or sequentially). (3) Two chemokine receptors which have been activated by their respective ligands synergise at the level of downstream signalling. This figure has been adapted from (Gouwy et al., 2012).

Although there is evidence of certain chemokines functioning as monomers (Rajarathnam et al., 1994), it is assumed that many chemokines operate as dimers or even higher order oligomers. It has been shown that chemokine oligomer formation is facilitated *in vivo* by binding to GAGs (Proudfoot et al., 2003). Heterodimerisation of a number of chemokine pairs has been observed at high (micromolar) concentrations, a phenomenon first described for CXCL4 and CXCL8. Here, chemokine synergism was thought to occur due to stabilisation of tertiary motifs, favouring an improved interaction between the chemokines and their cognate receptor, CXCR2 (Nesmelova et al., 2005). This first account involved two chemokines which activate the same receptor. Soon after, however, chemokine synergism mediated by heterodimer formation was described for the CCR7 ligands CCL19 and CCL21, and unrelated, non-CCR7-activating chemokines e.g. CXCL13; the presence of which enabled CCR7 ligands to trigger receptor activation at a much lower concentration (Paoletti et al., 2005). Conversely, CCL19 and CCL21 were shown to enhance CCR2 ligand-induced responses on human monocytes, which do not express CCR7 (Kuscher et al., 2009). This phenomenon has also been described for CCL22, whose ability to stimulate chemotaxis of CCR4^{+} cells was strongly enhanced by the presence of CXCL10, an effect that was independent of binding to CXCR3 or GAGs (Sebastiani et al., 2005). Chemokine heterodimer formation was given *in vivo* relevance when it was demonstrated that CXCL9 and CXCL12 heterocomplexes in the tumour vasculature of primary central nervous system lymphomas were responsible for enhanced recruitment of cytotoxic CD8^{+} T cells and malignant B cells, indicating that synergy between chemokines may influence tumour progression (Venetz et al., 2010). Finally, non-chemokines have been shown to enhance chemokine activity via complex formation, as was demonstrated for the inflammatory molecule high motility group box 1 (HMGB1) and CXCL12 (Schiraldi et al., 2012).

Chemokine synergism has also been attributed to the activation of multiple signalling pathways in cells expressing more than one type of chemokine receptor, induced in response to simultaneous (or possibly sequential) binding of their respective agonists. For instance, it was reported that CXCL8 and CXCL12 significantly enhanced the migration of monocytes, which expressed the corresponding CXC chemokine receptors CXCR2 and CXCR4, toward suboptimal concentrations of the CCR2 ligands CCL2 or CCL7 (Gouwy et al., 2008). In this study, CCL2-mediated MAP kinase phosphorylation and calcium mobilisation was significantly enhanced by

CXCL8 in monocytes, indicating cooperative downstream signalling pathways mediating enhanced chemotaxis. An earlier report detailed enhanced migration of pDC toward CXCL12 in the presence of the CXCR3 ligands CXCL9 and CXCL11. Despite high CXCR3 expression, pDC did not respond efficiently to CXCR3 ligands, indicating that the CXCR3 ligands instead had a sensitising effect that served to decrease the threshold of responsiveness to CXCL12 (Vanbervliet et al., 2003).

Chemokine biology, including synergistic interactions, gets even more complex still. Although there are reports of certain GPCRs functioning *in vitro* as monomers (Ernst et al., 2007, Kuszak et al., 2009), it is assumed that most GPCRs, including chemokine receptors, exist in vivo as dimers and/or higher order oligomers (Thelen et al., 2010). Indeed, ectopically expressed chemokine receptors can form both homodimers and heterodimers, demonstrated using biophysical techniques such as bioluminescence resonance energy transfer (BRET) and fluorescence resonance energy transfer (FRET) that detect protein-protein interactions at the cell surface (Issafras et al., 2002), also reviewed in (Thelen et al., 2010). Although formation of endogenous receptor heterodimers has not conclusively shown, CCR5 and CXCR4 clusters have been detected in primary human macrophages and T cells (Singer et al., 2001). On the Jurkat T cell line, endogenous CXCR4 and CCR5 can co-internalise following stimulation with the cognate ligand of either receptor, thus providing strong evidence for functional heterodimerisation of the two receptors (Contento et al., 2008). Furthermore, the closely related receptors CXCR1 and CXCR2 form homodimers and, when coexpressed, have been shown to heterodimerise (Martinez Munoz et al., 2009, Wilson et al., 2005). The functional relevance of chemokine receptor heterodimerisation remains controversial. For instance, CCR2 and CCR5 have been shown to form both homodimers and heterodimers, however increased and decreased responses following chemokine stimulation have been reported for CCR2-CCR5 heterodimers in comparison to homodimers (El-Asmar et al., 2005, Mellado et al., 2001b). It has been reported that chemokine receptors form heterodimers during synthesis, prior to trafficking to the cell surface and therefore independently of ligand stimulation (El-Asmar et al., 2005, Singer et al., 2001). In contrast, the simultaneous presence of CCL2 and CCL5 has been shown to trigger the formation of CCR2-CCR5 heterodimers on PBMC (Mellado et al., 2001b), although it was later demonstrated that CCR2-CCR5 heterodimers are only capable of binding a single chemokine with high affinity (El-Asmar et al., 2005). Therefore, unlike ligand heterodimerisation, there is as yet no clear evidence that receptor heterodimerisation supports synergistic interaction between chemokines.

CXCL14 is found at many sites around the body, where it is co-expressed with other homeostatic chemokines which govern immune cell traffic during the steady-state, including CXCL12. It may also be expressed alongside inflammatory chemokines, expression of which is induced upon infection or injury at the sites where CXCL14 is present. Recently, it has been demonstrated that CXCL14 modulates the activity of the closely-related chemokine CXCL12, but in an inhibitory manner (Tanegashima et al., 2013a, Tanegashima et al., 2013b). The question of whether or not CXCL14 synergises with other chemokines has not yet been addressed.

5.2 Aims

- To investigate the ability of CXCL14 to synergise with selected homeostatic and inflammatory chemokines in the induction of functional responses (chemotaxis) and activation of intracellular signalling events in human cells

- Upon discovery of a synergistic interaction with other chemokine(s), to investigate the mechanism by which this interaction occurs

5.3 CXCL14 Synergises with other Homeostatic Chemokines

5.3.1 CXCL14 synergises with CXCL12 in the induction of chemotactic responses on CXCR4-expressing cells

PBMC were isolated from peripheral blood of healthy volunteers and tested for chemotactic responses toward CXCL12. The receptor for CXCL12, CXCR4, is expressed on virtually all immune cells. Lymphocytes (T, B and NK cells) displayed normal responses toward CXCL12, as demonstrated by their uniform expression of CXCR4 and robust migratory responses toward CXCL12, consistently displaying maximal responses toward 100 nM of the chemokine. In an unexpected finding, the combination of an inactive concentration (1 nM) of CXCL12 with CXCL14 resulted in strong migratory responses by all three lymphocyte subsets, the magnitude of the response equalling or, in the case of B cells, surpassing that obtained with 100 nM CXCL12 (**Figure 5.2**). As before, T, B and NK cells did not migrate toward up to 1 µM CXCL14 alone. Taking B cells as an example, 12.5 ± 1.5% B cells migrated toward 100 nM CXCL12, compared to 0.78 ± 0.6% toward 1 nM CXCL12 (p=0.0004). The combination of 1 nM CXCL12 with 300 nM CXCL14 stimulated 19.4 ± 3.2% B cells to migrate (p=0.0027 compared to 1 nM CXCL12 alone). Interestingly, 300 nM CXCL14 was by far the most effective CXCL14 concentration at enhancing the activity of 1 nM CXCL12, with neither 100 nM or 1000 nM having much effect. In primary human lymphocytes, therefore, the presence of CXCL14 appeared to decrease by up to 100-fold the threshold of sensitivity to CXCL12 (**Figure 5.2**)
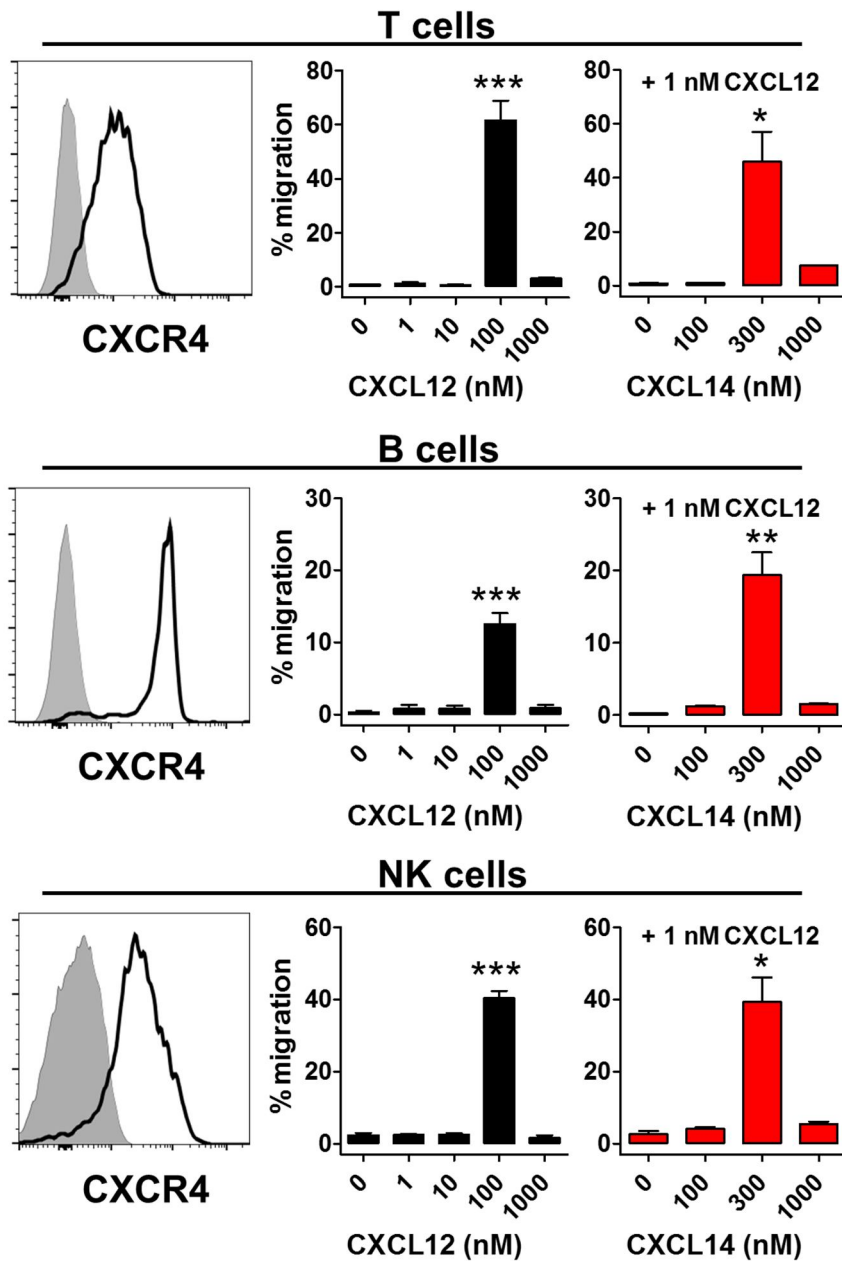
Figure 5.2. CXCL14 synergises with CXCL12 in the induction of chemotactic responses in PBMC.

PBMC freshly isolated from peripheral blood taken from healthy human volunteers were stained for expression of CXCR4 (black histogram; grey filled histogram indicates staining with isotype-matched control antibody). PBMC were assessed for migratory responses toward CXCL12 (black) and 1 nM CXCL12 + CXCL14 (red) by transwell chemotaxis assay. Migrated and input cells were stained and counted by flow cytometry, with gating on CD3, CD19 and CD56 to distinguish T cells (top row), B cells (middle row) and NK cells (bottom row), respectively. Migration is expressed as the percentage of input cells of each cell type recovered from the lower chamber and is mean + s.e.m. of two independent experiments. *P <0.05, **P<0.01 and ***P<0.001 compared to all other groups using a one-way ANOVA.

5.3.2 Synergy between CXCL14 and CXCL12 can be replicated in 300.19 cells stably transfected with CXCR4

300.19 is a mouse pre-B cell-line which has been routinely used by ourselves and others for stable transfection with both mouse and human chemokine receptors, enabling thorough characterisation of their function. 300.19 cells stably transfected with CXCR4 had been generated previously by my group, and I confirmed expression of CXCR4 on the cell surface by flow cytometry (**Figure 5.3a**). CXCR4 transfectants (300.19-CXCR4$^+$) migrated well toward CXCL12 and, like the primary lymphocytes, consistently displayed maximal responses toward 100 nM CXCL12. In contrast, no migration was observed in response to 1 nM CXCL12, or toward 100-1000 nM CXCL14. However, when 1 nM CXCL12 was combined with CXCL14, migration of 300.19-CXCR4$^+$ cells was observed similar to that seen in primary lymphocytes, with 1 nM CXCL12 + 300 nM CXCL14 again proving to be the most effective combination. Migratory responses of untransfected 300.19 cells are shown for comparison, where minimal responses are observed to human CXCL12, likely mediated by endogenous expression of murine CXCR4 by these cells (**Figure 5.3b**).
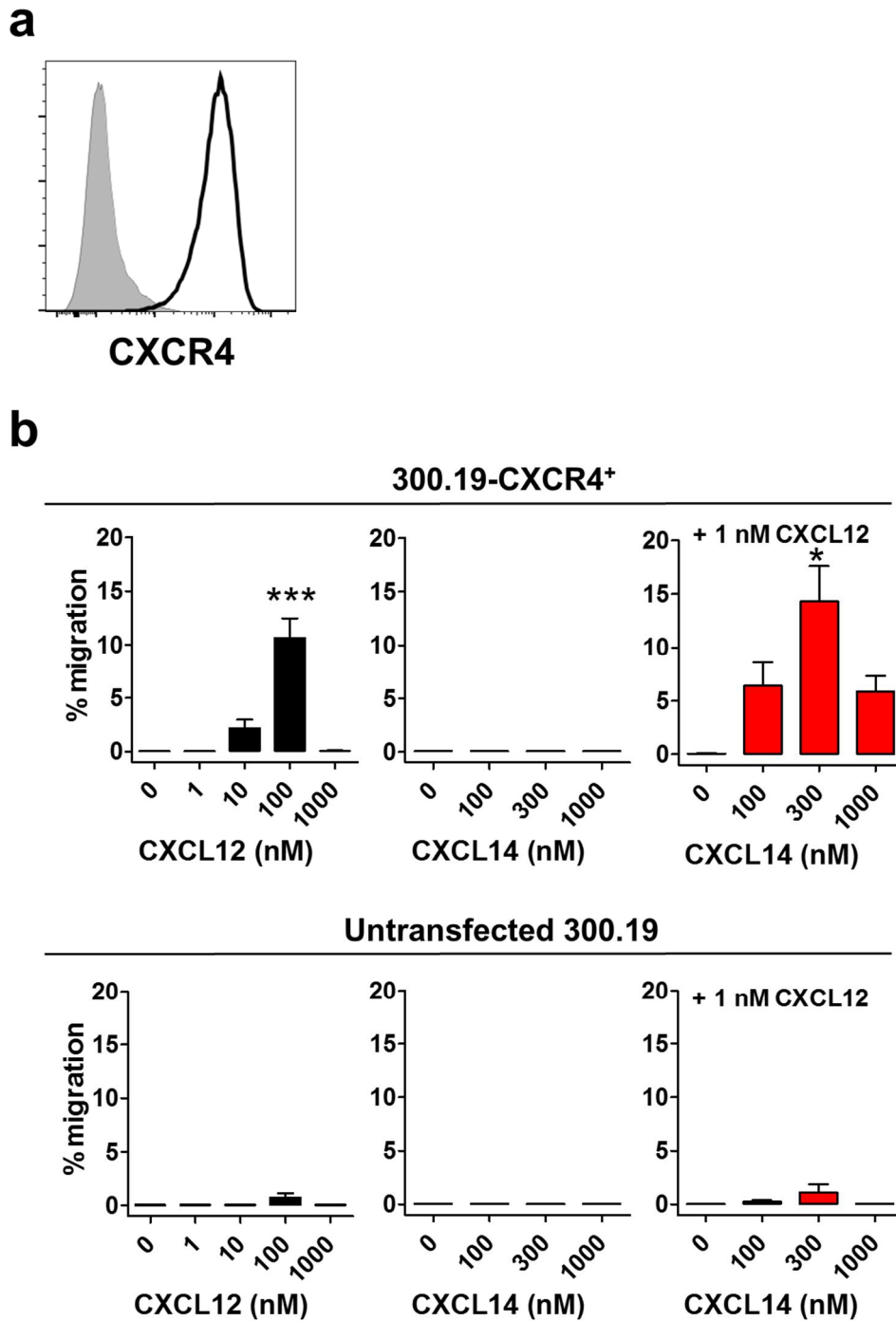
Figure 5.3. CXCL14 synergises with CXCL12 in the induction of chemotaxis in 300.19 cells stably transfected with CXCR4.

(a) CXCR4 expression on 300.19 cells stably transfected with CXCR4 was confirmed by flow cytometry (black histogram). Grey filled histogram shows binding of anti-CXCR4 mAb to untransfected cells. **(b)** Migration of 300.19-CXCR4+ (top) and untransfected 300.19 cells (bottom) toward CXCL12, CXCL14 (both black bars) and 1 nM CXCL12 + CXCL14 (red bars). Migration is expressed as % of input cells and is mean + s.e.m. of 2-8 independent experiments. *P<0.05 and ***P<0.001 compared to 0 nM using a one-way ANOVA.

On both primary lymphocytes and the 300.19-CXCR4$^+$ cell-line, CXCL14 exhibited optimal synergistic activity with CXCL12 when used at a concentration of 300 nM. Therefore, a fixed concentration of 300 nM CXCL14 was combined with a range of CXCL12 concentrations (1-1000 nM), in order to observe the effect that CXCL14 has on the overall response of CXCR4-expressing cells toward CXCL12. All chemokines display an optimal concentration for induction of chemotaxis, with concentrations higher or lower than this inducing only a partial response (the "bell-shaped curve"). In chemotaxis assays using 300.19-CXCR4$^+$ cells, a shift in the CXCL12 response curve to the left was observed upon addition of CXCL14 (**Figure 5.4**). Indeed, although low concentrations of CXCL12 (1 and 10 nM) showed enhanced activity in the presence of CXCL14, the response to 100 nM CXCL12 was reduced by 53% by the addition of CXCL14 (12.3 ± 3.6% of input cells migrated toward 100 nM CXCL12 in the absence of CXCL14, compared to 5.8 ± 0.4% in the presence of 300 nM CXCL14; $P<0.05$). Hence, the threshold of activation of CXCR4-expressing cells by CXCL12 is lowered by the presence of CXCL14.
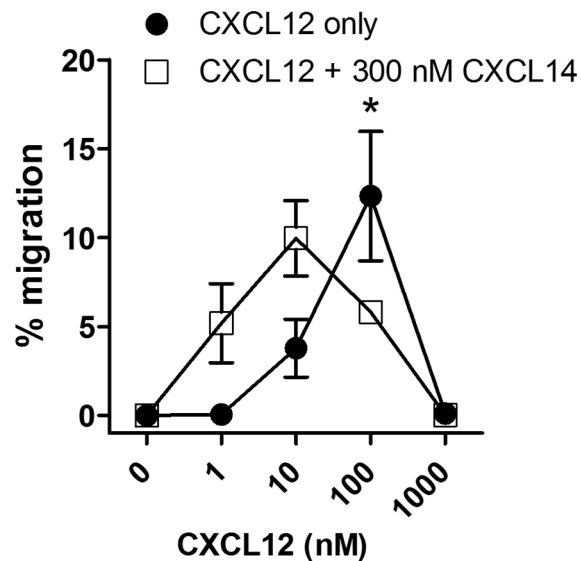
Figure 5.4. CXCL14 lowers the concentration of CXCL12 which is optimal for induction of chemotaxis.

Migration of 300.19-CXCR4$^+$ toward 1-1000 nM CXCL12 (filled circles) or 1-1000 nM CXCL12 in combination with 300 nM CXCL14 (unfilled squares) was assessed by transwell chemotaxis assay. Migration is expressed as % of input cells and is mean ± s.e.m. of three independent experiments. *$P<0.05$, using a two-way ANOVA plus Bonferroni post-test.

5.3.3 CXCL14 synergises with CXCL12 in the triggering of Ca²⁺ mobilisation from intracellular stores

Chemotaxis is not the only response in cells elicited by chemokine receptor activation. Upon binding to their cognate receptor, chemokines induce intracellular signalling cascades involved in cell activation and motility, including release of calcium (Ca^{2+}) ions from intracellular stores and phosphorylation of MAP kinases (Mellado et al., 2001a). Upon addition of agonist, cytoplasmic [Ca^{2+}] rises are very rapid, peaking within seconds before a more gradual return to basal levels. Ca^{2+} release in response to chemokine receptor activation exhibits a different profile to chemotaxis, as unlike in cell migration, the magnitude of Ca^{2+} release reaches a plateau i.e. increasing the amount of chemokine beyond the optimal concentration does not cause the response to diminish. Using 300.19-CXCR4⁺ as responder cells, CXCL12 dilutions ranging from 0.5-100 nM were tested to establish optimal, sub-optimal and inactive concentrations for triggering calcium release. I observed that CXCL12 concentrations equal to or above 30 nM induced maximal rises in intracellular [Ca^{2+}], while concentrations of 3 nM or below failed to elicit a response. As expected from its inability to induce migratory responses in 300.19-CXCR4⁺ cells, CXCL14 (300 nM is shown, but up to 600 nM CXCL14 was tested) did not induce a rise in intracellular [Ca^{2+}]. However, the combination of 3 nM CXCL12 with 300 nM CXCL14 resulted in clear transient [Ca^{2+}] spikes (**Figure 5.5**). The synergy between CXCL12 and CXCL14 is therefore not only limited to chemotaxis but extends to fast acting cellular responses.
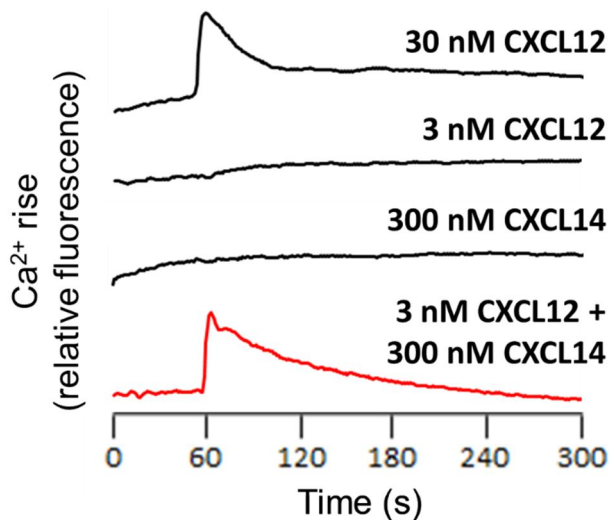
Figure 5.5. CXCL14 synergises with CXCL12 in the induction of rapid cellular responses.

Changes in cytoplasmic free calcium (Ca^{2+}) concentration in 300.19-CXCR4$^+$ cells upon addition of chemokines was monitored by fluorescence microscopy. Cells were loaded with 1 µM Fura-2-AM and stimulated with CXCL12, CXCL14 or the two combined. Chemokine was injected at 50 seconds and recording was stopped at 300 seconds. One representative set of measurements from three independent experiments is shown.

5.3.4 CXCL14 also synergises with the CCR7 ligands CCL19 and CCL21, and the CXCR5 ligand CXCL13

Next, I decided to see if the synergy observed between CXCL14 and CXCL12 extended to other homeostatic chemokines. Naïve and central memory T (T_{CM}) cells, which make up the majority of T cells in peripheral blood, use the chemokine receptor CCR7 to recirculate via secondary lymphoid organs. The remainder are effector memory T cells (T_{EM}) which do not express CCR7 and do not recirculate. As expected, the majority of T cells in peripheral blood expressed CCR7 on their surface (**Figure 5.6a**), although freshly isolated T cells did not display migratory responses toward CCL19 and CCL21 (data not shown). After resting the cells in culture overnight however, robust migration was observed. This can likely be explained by a desensitisation effect caused by constant exposure to CCR7 ligands *in situ*, which is removed upon *ex vivo* culture. Rested T cells displayed robust migratory responses toward CCR7 ligands at concentrations of ≥ 100 nM, while concentrations of below 100 nM were inactive (**Figure 5.6b**). Rested T cells did not acquire responsiveness to CXCL14. In the presence of CXCL14 however, CCL19 and CCL21 were both active

174

at much lower concentrations (1 nM was tested). In similar fashion to CXCL12, the maximal synergistic effect was observed when 300 nM CXCL14 was used in combination with 1 nM CCL19 or CCL21. The majority of peripheral blood B cells also express CCR7, mediating their recirculation via lymphoid organs to facilitate interaction with T cells and the generation of humoral immunity. Similarly, CXCL14 enhanced B cell migratory responses toward low concentrations of CCL19 and CCL21, as shown (**Figure 5.7**).
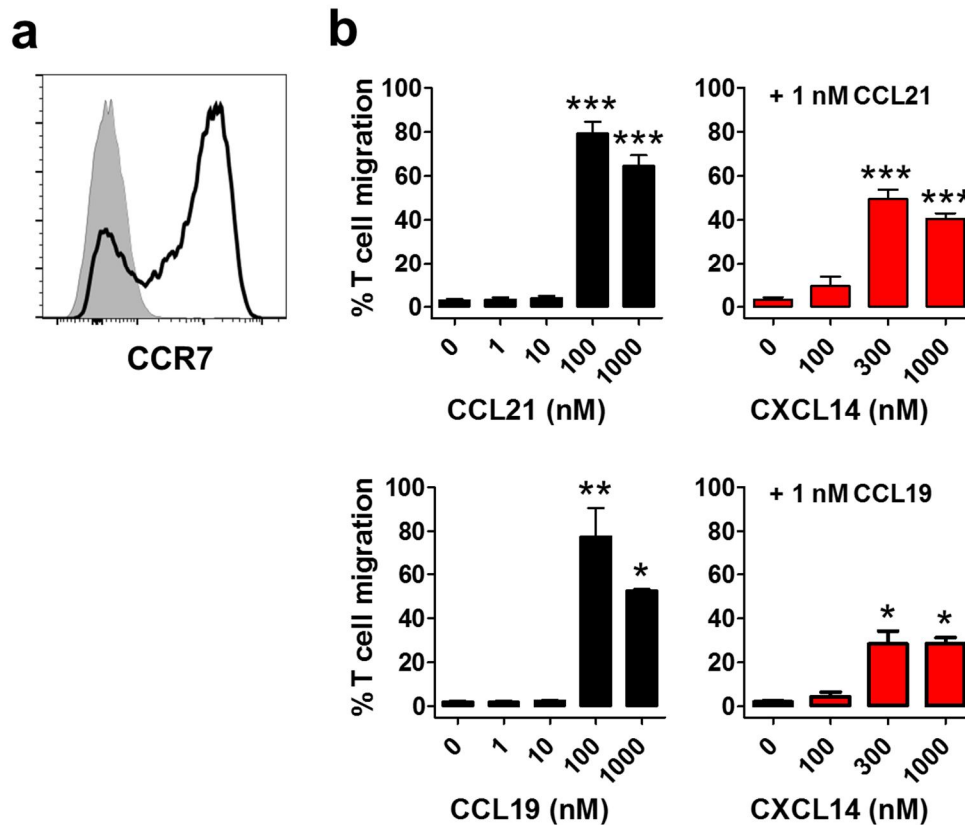
Figure 5.6. CXCL14 also synergises with the CCR7 ligands CCL21 and CCL19 in the induction of chemotactic responses in primary human T cells.

PBMC were isolated from peripheral blood and rested overnight in medium. The following day, staining was performed and migration toward chemokines was assessed by transwell chemotaxis assay. **(a)** Surface expression of CCR7 on T cells (black histogram), detected by flow cytometry. Grey filled histogram indicates staining with isotype-matched control antibody. **(b)** Migration of T cells toward CCL21 (top left), 1 nM CCL21 + CXCL14 (top right), CCL19 (bottom left) or 1 nM CCL19 + CXCL14 (bottom right). Data is mean + s.e.m. of 2-3 independent experiments. *$P<0.05$, **$P<0.01$ and ***$P<0.001$ compared to 0 nM using a one-way ANOVA.
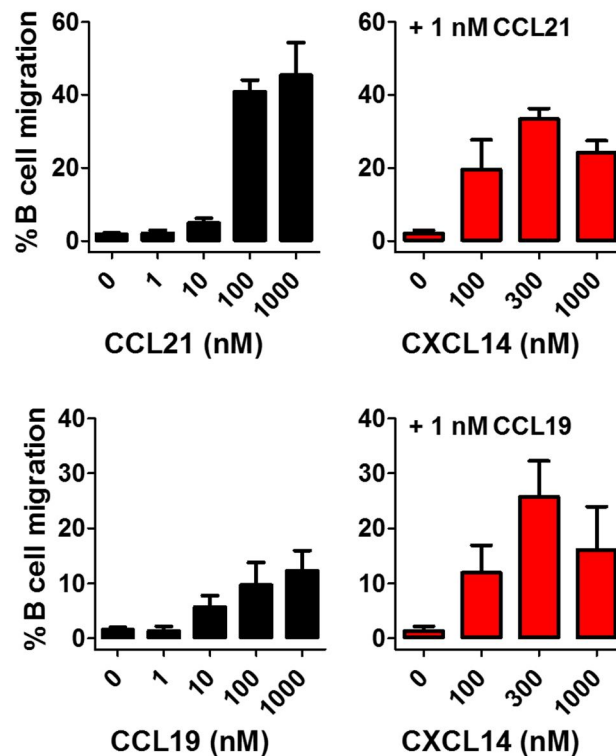
Figure 5.7. CXCL14 synergises with the CCR7 ligands CCL21 and CCL19 in the induction of chemotactic responses in primary human B cells.

PBMC were isolated from peripheral blood and rested overnight in medium. The following day, migration toward chemokines was assessed by transwell chemotaxis assay. Shown is B cell migration toward CCL21 (top left), 1 nM CCL21 + CXCL14 (top right), CCL19 (bottom left) or 1 nM CCL19 + CXCL14 (bottom right). Data is mean + s.e.m. of 2-3 independent experiments.

300.19 transfectants stably expressing CCR7 (300.19-CCR7+) were generated by our group previously, and surface CCR7 expression was confirmed by flow cytometry (**Figure 5.8a**). 300.19-CCR7+ cells showed a greater migratory response toward CCL21 (24.1 ± 3.2% of input cells migrated toward 100 nM CCL21) compared to CCL19 (6.2 ± 1.1% of input cells migrated toward 100 nM CCL19). As was observed with primary cells, both chemokines were inactive on 300.19-CCR7+ cells at concentrations below 100 nM. 300.19-CCR7+ cells did not migrate in response to CXCL14 (not shown). As for the primary cells, in the presence of CXCL14, low concentrations of CCL21 and CCL19 (1 nM) became active, confirming the synergy between the chemokines (**Figure 5.8b**).
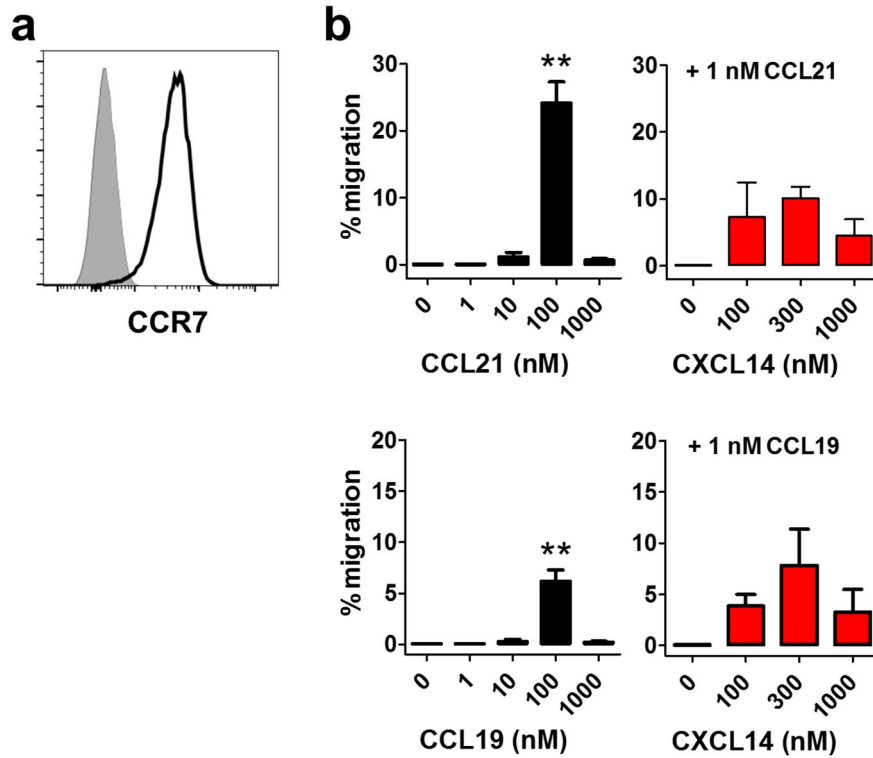
Figure 5.8. CXCL14 synergises with CCL21 and CCL19 in the induction of chemotactic responses in 300.19 cells stably transfected with CCR7.

(a) Surface receptor expression on 300.19 cells stably transfected with CCR7 was confirmed by flow cytometry (black histogram). Grey filled histogram shows binding of anti-CCR7 mAb to untransfected cells. **(b)** Migration of 300.19-CCR7^{+} cells toward CCL21 (top left), 1 nM CCL21 + CXCL14 (top right), CCL19 (bottom left) or 1 nM CCL19 + CXCL14 (bottom right). Data is mean + s.e.m. of 3-5 independent experiments, where **$P<0.01$ compared to 0 nM using a one-way ANOVA.

CXCR5 is also a lymphoid tissue-homing chemokine with expression on B cells, however its expression on T cells is restricted to the minor subset of follicular helper T (T_{FH}) cells, which account for around 5% of total blood T cells. B cells isolated from healthy volunteers displayed uniformly high expression of CXCR5. In agreement with earlier reports (Legler et al., 1998), migration of B cells toward CXCL13 was observed only at 1 μM of the chemokine, with lower concentrations being totally inactive. In the presence of CXCL14 however, 100 nM CXCL13 became active, inducing robust B cell migration (**Figure 5.9a**). This phenomenon was replicated in 300.19 cells stably transfected with CXCR5. Like the B cells, transfectants demonstrated migration toward 1 μM CXCL13 only, with no migration observed at lower concentrations. The magnitude of the response to CXCL13 was very low, with only 3.5 ± 0.5% 300.19-CXCR5$^+$ cells migrating toward 1 μM CXCL13, despite uniformly high surface expression of CXCR5 by transfectants (**Figure 5.9b**). I did not test higher concentrations of CXCL13. Of note, background migration of 300.19-CXCR5$^+$ cells was extremely low, only 0.1% of cells migrating toward buffer alone. In the presence of CXCL14, as low as 10 nM CXCL13 became active in inducing migration, although the effect was more pronounced at 100 nM CXCL13 (**Figure 5.9b**).
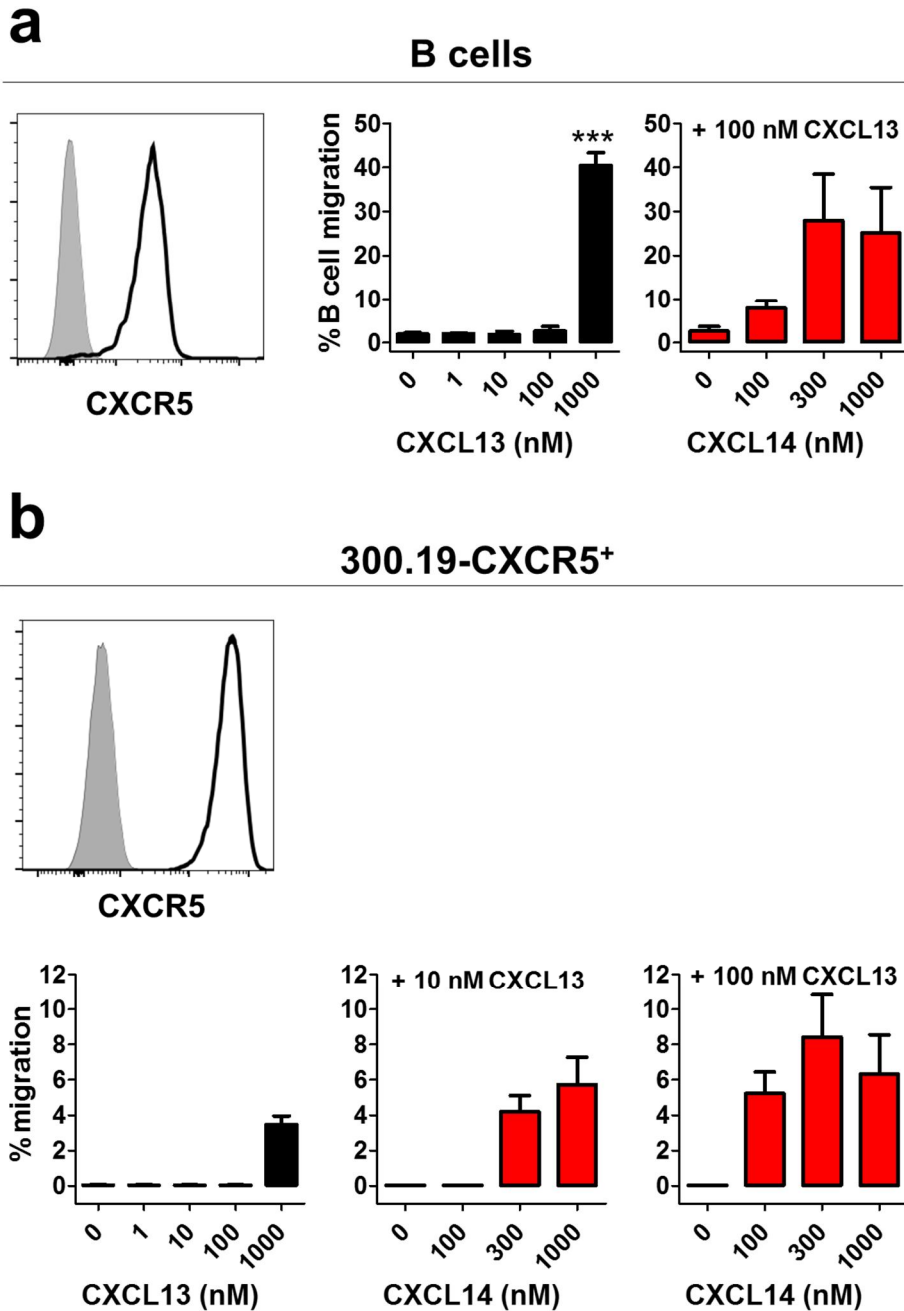
Figure 5.9. CXCL14 synergises with the CXCR5 ligand CXCL13 on primary B cells.
(a) PBMC were isolated from peripheral blood and rested overnight. The following day, staining was performed and migration toward chemokines was assessed by transwell chemotaxis assay. Surface expression of CXCR5 on B cells, detected by flow cytometry (left). B cell migration toward CXCL13 (centre) and 100 nM CXCL13 + CXCL14 (right). Migration is displayed as % of input cells and is mean + s.e.m. of 2-3 independent experiments. ***$P<0.001$ compared to 0 nM, using one-way ANOVA. **(b)** Top - CXCR5 expression on stable 300.19 transfectants was confirmed by flow cytometry. Bottom – migration of 300.19-CXCR5+ cells toward CXCL13 (left), 10 nM CXCL13 + CXCL14 (centre) and 100 nM CXCL13 + CXCL14 (right). Migration is mean + s.e.m. of 2-4 independent experiments.

5.4 CXCL14 Does Not Synergise with the Inflammatory Chemokines CCL2, CCL5 and CXCL10

5.4.1 300.19 Transfectants

CXCL14 has shown synergistic activity with all of the homeostatic chemokines tested, including the CXCR4 ligand CXCL12, the CCR7 ligands CCL21 and CCL19, and the CXCR5 ligand CXCL13. Many inflammatory chemokines are also expressed in peripheral tissues during infection or injury, and while CXCL14 expression is lost in some inflammatory settings, it may be up-regulated in others (Chen et al., 2010). I therefore investigated whether or not CXCL14 was able to synergise with selected inflammatory chemokines. Given, like CXCL14, their recognised roles in the chemoattraction of monocytes, the CCR2 ligand CCL2 (also known as monocyte chemoattractant protein-1; MCP-1) and the CCR5 ligand CCL5 (also known as Regulated on Activation, Normal T cell Expressed and Secreted chemokine; RANTES) were chosen. The CXCR3 ligand CXCL10 (also known as interferon-inducible protein 10; IP-10) was also selected.

Synergy between CXCL14 and inflammatory chemokines was first tested on stable 300.19 transfectants. Expression of CCR2, CCR5 and CXCR3 on the cell surface was confirmed by flow cytometry (**Figure 5.10**). Each of their respective ligands induced robust and reproducible chemotactic responses. In contrast to the homeostatic chemokines, 1 nM inflammatory chemokine was sufficient to induce migration, while peak responses were observed at 10 nM. For all three, therefore, 0.1 nM was selected as an inactive concentration to use in testing for synergistic activity with CXCL14. In contrast to the homeostatic chemokines however, sub-optimal concentrations of CCL2, CCL5 and CXCL10 remained inactive in the presence of 100-1000 nM CXCL14 (**Figure 5.10**).
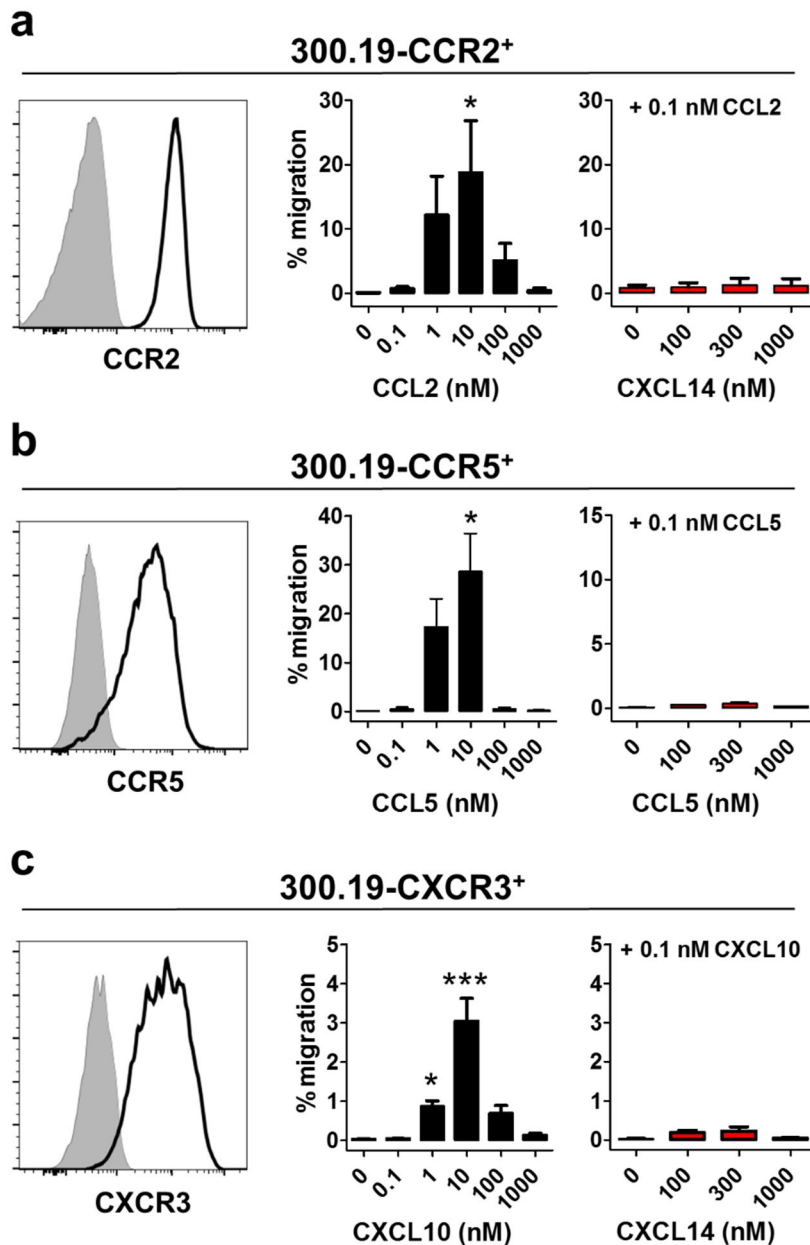
Figure 5.10. CXCL14 does not synergise with the inflammatory chemokines CCL2, CCL5 and CXCL10.

(a) CCR2 expression on stable 300.19 transfectants was confirmed by flow cytometry (left). Migration of 300.19-CCR2+ cells toward CCL2 (0.1 – 1000 nM; centre) or 0.1 nM CCL2 + CXCL14 (right). **(b)** CCR5 expression on stable 300.19 transfectants was confirmed by flow cytometry (left). Migration of 300.19-CCR5+ cells toward CCL5 (0.1 – 1000 nM; centre) or 0.1 nM CCL5 + CXCL14 (right). **(c)** CXCR3 expression on stable 300.19 transfectants was confirmed by flow cytometry (left). Migration of 300.19-CXCR3+ cells toward CXCL10 (0.1 – 1000 nM; centre) or 0.1 nM CXCL10 + CXCL14 (right). In staining plots, grey filled histogram indicates staining of untransfected cells. Migration is expressed as percentage of input and is mean + s.e.m. of 2-6 independent experiments. *$P<0.05$, ***$P<0.001$ compared to 0 nM using Kruskall-Wallis ANOVA.

5.4.2 Primary human T cells

In order to confirm the absence of any synergistic interaction between CXCL14 and the inflammatory chemokines tested, human T cell-lines expressing CCR2, CCR5 and CXCR3 were generated. Resting T cells freshly isolated from peripheral blood have only low level expression of inflammatory chemokine receptors. T cells up-regulate receptor expression upon activation however. T cell lines expressing high levels of CCR2, CCR5 and CXCR3 were established by 3-week expansion of primary human T cells in the presence of IL-2, as described in Materials and Methods and in previous work by our group (Qin et al., 1998, Loetscher et al., 1996). Surface receptor expression, in addition to migratory responses toward CCL2, CCL5 and CXCL10, were confirmed on day 21 of expansion. CD4$^+$ and CD8$^+$ T cells were distinguished in the analysis, however the chemokine receptor expression profiles and migratory responses of each were near identical. For this reason, only CD4$^+$ T cells are shown (**Figure 5.11**). Expanded T cells were uniformly positive for expression of CCR2 and CXCR3, while CCR5 was present on around 50% of CD4$^+$ T cells. Migratory responses toward their corresponding chemokines were similar to that seen in receptor transfectants, with peak responses observed at 10 nM for each. Again, 0.1 nM was taken as a sub-optimal concentration. This was despite the fact that in all three cases, 0.1 nM did induce migration slightly above background. Upon combination of 0.1 nM CCL2, CCL5 or CXCL10 with CXCL14, similarly to the 300.19 transfectants, no synergy was observed.
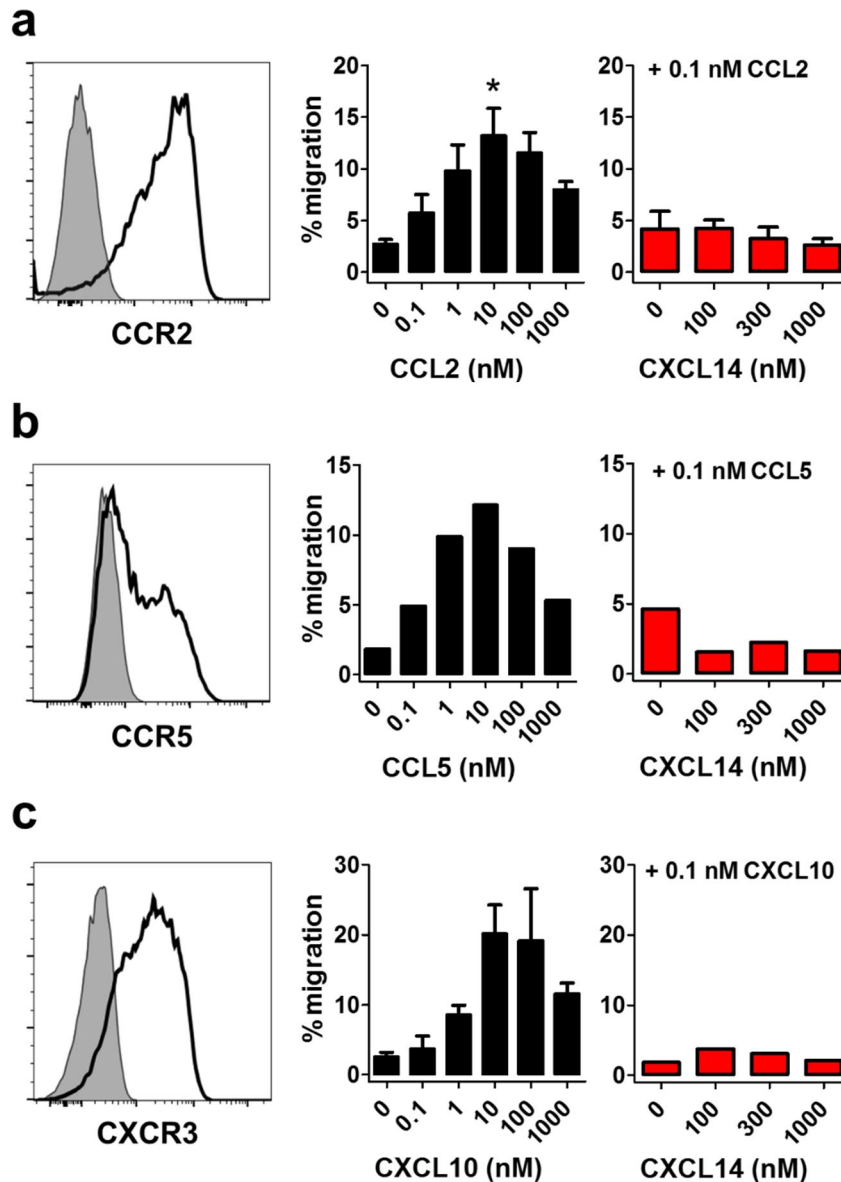
Figure 5.11. CXCL14 does not synergise with inflammatory chemokines on primary human T cells.

Total CD3^{+} T cells were purified from PBMC by negative selction and expanded in the presence of IL-2. On day 21 of expansion, T cells were assessed for chemotactic responses toward CCL2, CCL5 and CXCL10, while expression of the corresponding chemokine receptors (black histograms) was measured by flow cytometry. Grey filled histograms indicate staining with isotype controls. Shown is CD4^{+} T cells. **(a)** Expression of CCR2 (left). Migration toward CCL2 (centre) and 0.1 nM CCL2 + CXCL14 (right). **(b)** Expression of CCR5 (left). Migration toward CCL5 (centre) and 0.1 nM CCL5 + CXCL14 (right). **(c)** Expression of CXCR3 (left). Migration toward CXCL10 (centre) and 0.1 nM CXCL10 + CXCL14 (right). Migration is expressed as percentage of input and is mean + s.e.m. of a single experiment (CCL5) or of two independent experiments (CXCL10 and CCL2). *$P<0.05$ compared to 0 nM using a Kruskall-Wallis ANOVA.

5.5 CXCL14 Synergises with CXCL12 via Interaction with CXCR4

5.5.1 Blockade of CXCR4 abolishes the synergy between CXCL14 and CXCL12 on primary lymphocytes

Binding of AF-CXCL14 to 300.19-CXCR4$^+$ cells could not be demonstrated by flow cytometry (data not shown). This indicates that either these cells lack CXCL14 receptors, or that CXCR4 binds CXCL14 with an affinity below the threshold of detection of this assay. Lack of binding is in agreement with the inability of CXCL14 alone to induce chemotaxis of these cells. Although the identity of the CXCL14 receptor remains unknown, I hypothesised that it likely does not play a role in the observed synergy between CXCL14 and CXCL12. Therefore, to confirm that the synergy between CXCL14 and CXCL12 is mediated by CXCR4, PBMC were treated with the CXCR4 antagonist AMD3100 (Plerixafor) for 30 minutes prior to use in chemotaxis assays. Migratory responses of T, B and NK cells toward 1 nM CXCL12 + 300 nM CXCL14 were completely abolished following treatment with ≥ 1 µM AMD3100 (**Figure 5.12a**). CXCR4 is expressed on most immune cells, including monocytes. Monocyte migratory responses to CXCL14 were unaffected by treatment with up to 10 µM AMD3100, confirming that CXCL14 recruits monocytes via binding to a receptor distinct from CXCR4 (**Figure 5.12b**).
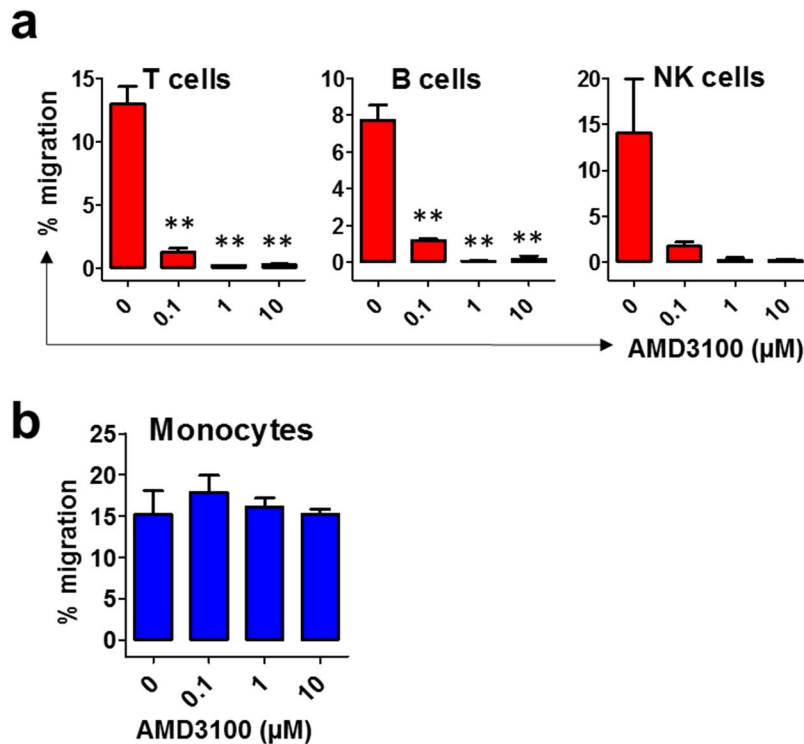
Figure 5.12. CXCR4 blockade completely abolishes the synergistic activity between CXCL14 and CXCL12 on primary human lymphocytes.

PBMC were treated with 0.1-10 µM AMD3100 prior to use in transwell chemotaxis assays. Input and migrated cells were stained as previously described to distinguish cell subsets. **(a)** Migration of T, B and NK cells toward 1 nM CXCL12 + 300 nM CXCL14. **(b)** Migration of monocytes toward 1 µM CXCL14 following pre-treatment of PBMC with AMD3100. Migration is expressed as % of input and is mean + s.e.m. of two independent experiments. ***P*<0.01 compared to no AMD3100 treatment.

5.5.2 CXCL14 primes CXCR4+ cells for responses toward CXCL12

The synergy between CXCL14 and CXCL12 could occur in a temporal (and possibly spatial) sequence, involving interaction of CXCL14 with CXCR4 prior to engagement of CXCL12 with target cells. This hypothesis was tested by addition of CXCL14 to the upper chamber (along with the cells) of transwell assays when testing migration of 300.19-CXCR4^{+} cells toward CXCL12. Addition of 300 nM CXCL14 to the upper chamber led to a shift in the response curve toward 1-1000 nM CXCL12, so that 1 nM CXCL12 became active (**Figure 5.13a**). In fact, the shift was similar (although not identical) to that observed when 300 nM CXCL14 was combined with CXCL12 in the lower chamber (see Figure 5.4). The ability of CXCL14 to "prime" cells for responses

to CXCL12 was also observed in the measurement of rises in intracellular $[Ca^{2+}]$, where prior addition of CXCL14 enabled 300.19-CXCR4$^+$ cells to give a robust response to a low concentration (3 nM) CXCL12 (**Figure 5.13b**). CXCL14 was not washed away prior to addition of CXCL12 however, meaning that simultaneous action of the two chemokines cannot be excluded.
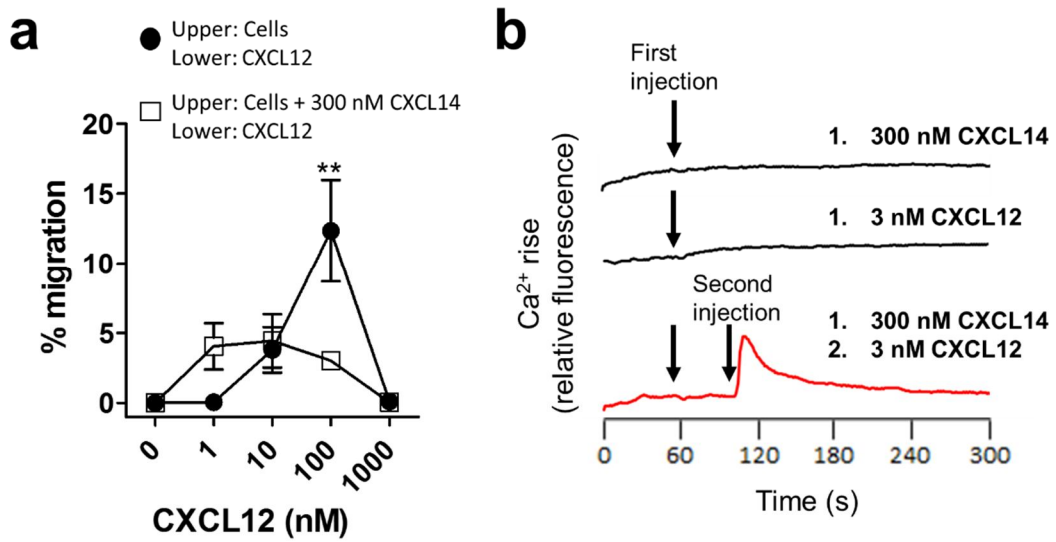
Figure 5.13. CXCL14 primes CXCR4$^+$ cells for responses toward CXCL12.

(a) Migration of 300.19-CXCR4$^+$ cells toward CXCL12 in the absence (filled circles) or presence (unfilled squares) of 300 nM CXCL14 in the upper chamber. Migration is expressed as % of input and is mean ± s.e.m. of three independent experiments. **P<0.01 (two-way ANOVA). **(b)** Changes in cytoplasmic $[Ca^{2+}]$ in 300.19-CXCR4$^+$ cells were monitored by fluorescence microscopy. Cells were loaded with 1 µM Fura-2-AM and stimulated with 300 nM CXCL14, 3 nM CXCL12 or a double injection of 300 nM CXCL14 followed by 3 nM CXCL12 (the first injection was made at 50 seconds, the second at 100 seconds). Recording was stopped at 300 seconds. One representative set of measurements from two independent experiments is shown.

5.5.3 CXCL14 induces internalisation of CXCR4

Receptor internalisation is also a common feature of chemokine receptor activation, endocytosis of receptor-ligand complexes occurring within a few minutes of agonist exposure (Luttrell and Lefkowitz, 2002). 300.19-CXCR4$^+$ cells were incubated with chemokine for 1 hour at 37 °C, surface receptor expression subsequently being assessed by flow cytometry. As expected, an optimal concentration of CXCL12 (100 nM) caused the majority of surface CXCR4 to be internalised, with a ~75% reduction in CXCR4 MFI. Interestingly, 300 nM CXCL14 alone induced approximately 50% decrease in MFI, and is further demonstration of direct binding of CXCL14 to CXCR4. Internalisation was also observed with a low concentration of CXCL12 (1 nM), which like CXCL14 alone, was unable to induce chemotaxis or a rise in intracellular Ca^{2+} (**Figure 5.14**) These data indicate that a threshold of receptor internalisation must be reached before the functional response (chemotaxis, Ca^{2+} release) is elicited, a theory supported by the degree of internalisation observed when CXCL12 and CXCL14 were combined. The combination of 1 nM CXCL12 with 300 nM CXCL14, which synergise with one-another in the induction of functional responses, induced >75% CXCR4 internalisation; identical to that seen with the optimal concentration (100 nM) of CXCL12 alone. In the graph shown in **Figure 5.14b**, MFI of CXCR4 expression was normalised to cells incubated for 1 hour in medium alone (no chemokine).
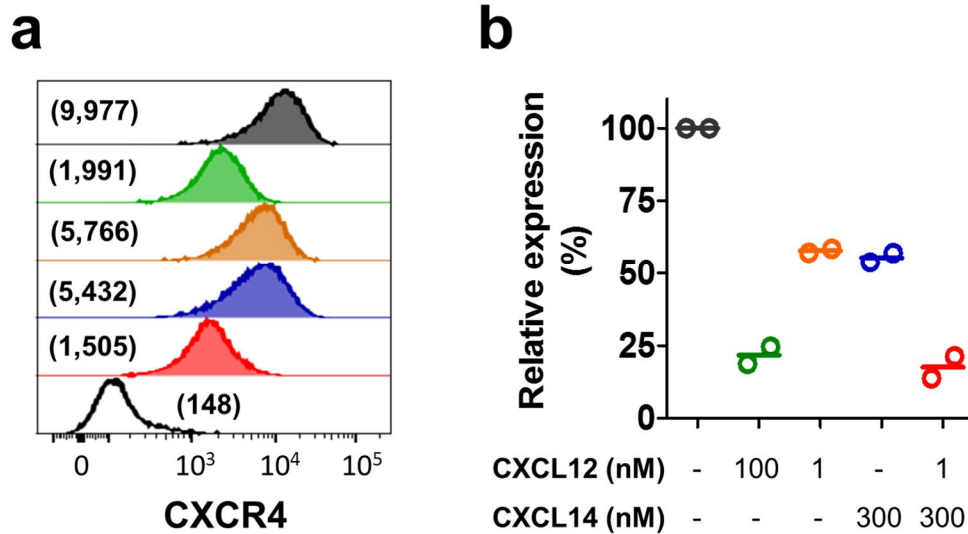
Figure 5.14. CXCL14 induces internalisation of CXCR4.
300.19-CXCR4+ cells were stimulated with medium only (black), 100 nM CXCL12 (green), 1 nM CXCL12 (orange), 300 nM CXCL14 (blue) or 1 nM CXCL12 + 300 nM CXCL14 (red) for 1 hour at 37 °C. CXCR4 surface expression was subsequently detected by flow cytometry. **(a)** Staining plots from a representative experiment are shown, where MFI values (geometric mean) are indicated in brackets. CXCR4 expression by untransfected 300.19 cells (unfilled histogram) is also shown. **(b)** Cumulative data from CXCR4 internalisation experiments, where CXCR4 expression is normalised to medium only (given as 100%). Mean of two independent experiments.

Next, it was decided to test if CXCL14 could mediate internalisation of a receptor where synergy was not observed with its cognate ligand. 300.19-CCR2$^+$ cells were incubated with CCL2 (and/or CXCL14) for one hour at 37 °C, surface receptor expression subsequently being assessed by flow cytometry, as before. 10 nM CCL2, which elicited peak migratory responses, stimulated internalisation of the majority of CCR2 receptors, cells displaying a 74% reduction in MFI. In contrast to CXCR4 internalisation however, a sub-optimal concentration of agonist (0.1 nM CCL2), as well as 300 nM CXCL14, triggered only minimal receptor internalisation (13% and 12% reduction in CCR2 MFI, respectively) (**Figure 5.15**). Furthermore, the combination of 0.1 nM CCL2 with 300 nM CXCL14 triggered only 21% reduction in CCR2 MFI, considerably less than the 75% reduction in CXCR4 expression observed with a sub-optimal concentration of CXCL12 in the presence of CXCL14. These data

suggest that the lack of synergy observed between CXCL14 and CCL2 in the induction of functional responses (chemotaxis) is because, unlike in the case of CXCR4, the threshold of receptor internalisation is not reached.
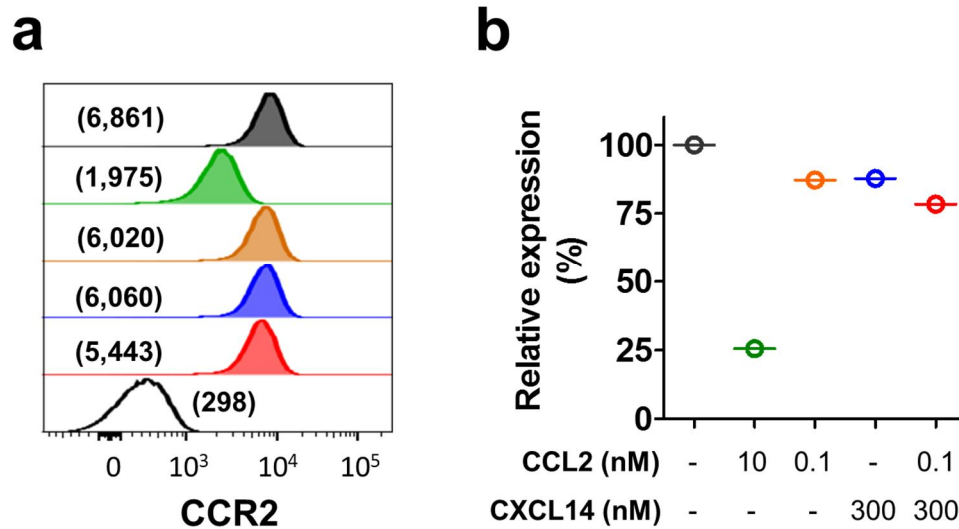
Figure 5.15. CXCL14 does not induce internalisation of CCR2.
(a) 300.19-CCR2+ cells were stimulated with medium only (black), 10 nM CCL2 (green), 0.1 nM CCL2 (orange), 300 nM CXCL14 (blue) or 0.1 nM CCL2 + 300 nM CXCL14 (red) for 1 hour at 37 °C. CCR2 surface expression was subsequently detected by flow cytometry. Staining plots are shown, where MFI values (geometric mean) are indicated in brackets. **(b)** Data from (a) represented graphically, where CCR2 expression is normalised to medium only (given as 100%). Data are from a single experiment.

5.5.4 CXCL14 triggers formation of CXCR4 multimers

Recently, it has been reported by other groups that CXCL14 binds with high-affinity to CXCR4 (Tanegashima et al., 2013a, Tanegashima et al., 2013b). In a subsequent study, and in agreement with our findings, no functional response upon binding of CXCL14 to CXCR4 was observed (Otte et al., 2014). The formation of receptor multimers, where clustering of chemokine receptors occurs in response to agonist stimulation, has been discussed in detail as a possible mechanism behind chemokine synergy (Thelen et al., 2010). Förster (or fluorescence) resonance energy transfer (FRET) describes the transfer of energy between two light-sensitive molecules (chromophores). In its normal application, a donor fluorophore absorbs the energy due to excitation of incident light, and transfers the excitation energy to a nearby acceptor fluorophore. The efficiency of this energy transfer is inversely proportional to the distance between donor and acceptor. The technique of FRET, when applied to optical microscopy, therefore enables the determination of the distance between two molecules. This technique has been applied previously to the study of ligand-receptor interactions in the context of chemokine function, revealing the formation of complex multimeric structures composed of different chemokine receptors (Martinez et al., 2009).

In light of my findings that the synergy between CXCL14 and CXCL12 is mediated by CXCR4, our collaborators at the National Centre for Biotechnology in Madrid carried out a series of FRET studies looking at CXCR4 homodimer formation. Initially, FRET saturation curves were performed using HEK293T cells transiently co-transfected with constant amounts of CXCR4 fused to cyan fluorescent protein (CFP; donor molecules), and increasing amounts of CXCR4 fused to yellow fluorescent protein (YFP; acceptor molecules) (**Figure 5.16a**). This was done to determine the ratio of donor/acceptor that gives optimal FRET efficiency. To analyse the effect of CXCL14 on receptor conformation, new FRET experiments were performed using HEK293T cells transiently cotransfected with a fixed ratio of CXCR4-CFP and CXCR4-YFP. Briefly, 9×10^6 HEK293 cells were plated with 9 μg CXCR4-CFP and 15 μg CXCR4-YFP, with the fluorescence ratio (in arbitrary units; a.u.) being approximately 1. In agreement with the active concentration range for CXCL12 in chemotaxis and Ca^{2+} release assays, 100 nM CXCL12 triggered a significant increase in FRET efficiency (p<0.001 compared to vehicle control), while 1 nM CXCL12 had no effect. As expected based on the chemotaxis data, the combination of 1 nM CXCL12 with 300 nM CXCL14 resulted in a significant increase in FRET efficiency. Most interesting of

all, however, was the observation that stimulation with 300 nM CXCL14 alone resulted in an identical FRET response to that observed with 1 nM CXCL12 + 300 nM CXCL14 (**Figure 5.16b**). This provides further indication of a direct effect of CXCL14 on CXCR4. I hypothesise that CXCL14 induces a change in CXCR4, such as the formation of receptor complexes on the cell surface. While this effect of CXCL14 is not functional by itself, it makes the receptor more amenable to activation by its true agonist by serving to lower the threshold for activation by CXCL12.

FRET studies were also performed to study CCR2 homodimer formation elicited by CXCL14, in the same manner as those performed for CXCR4 above. HEK293 cells were transiently cotransfected with 15 µg CCR2-CFP and 15 µg CCR2-YFP, with the subsequent ratio of fluorescence (a.u.) being approximately 1.5. In contrast to the CXCR4 findings, CXCL14, either alone or in combination with a suboptimal concentration of CCL2, did not trigger an increase in FRET efficiency in HEK293T cells transiently co-transfected with CCR2-CFP and CCR2-YFP. These findings support my hypothesis that CXCL14 interacts selectively with CXCR4 (thereby enhancing the activity of CXCL12), while CXCL14 does not interact with CCR2 (**Figure 5.16**).
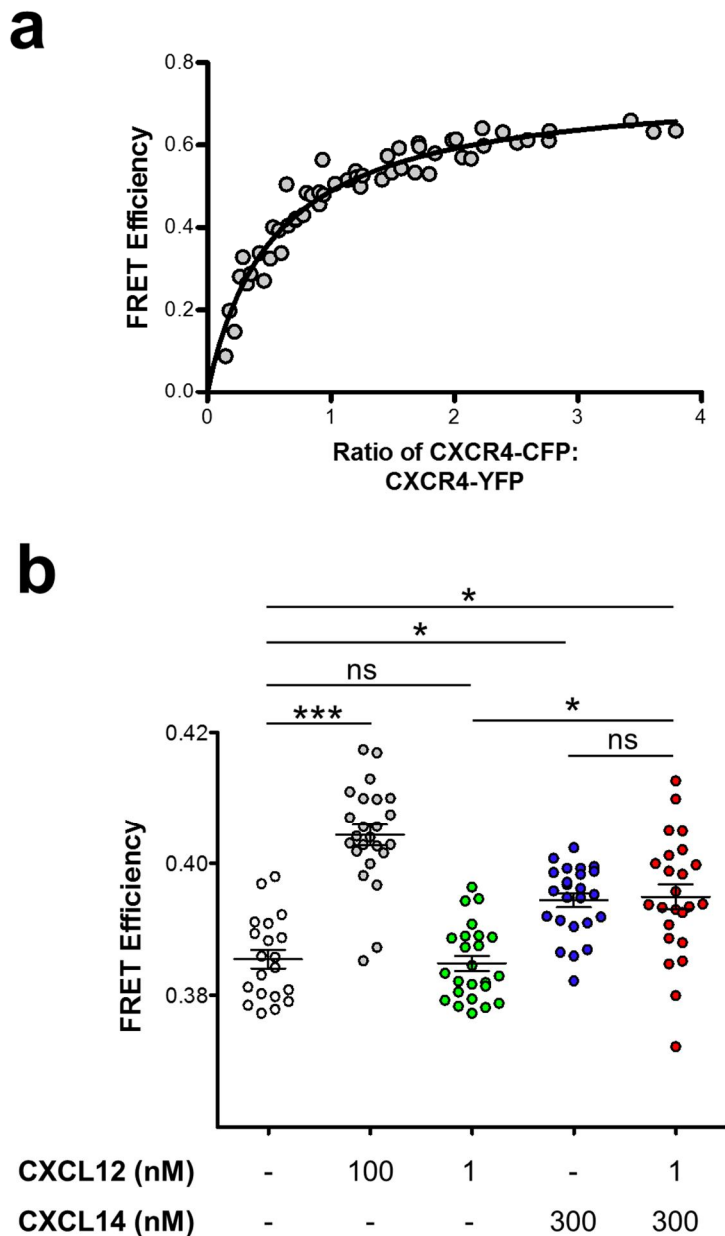
Figure 5.16. CXCL14 induces formation of CXCR4 multimers.

(a) FRET saturation curves were performed using HEK293T cells transiently co-transfected with constant amounts of CXCR4-CFP (FRET donor), and increasing amounts of CXCR4-YFP (FRET acceptor). This enabled identification of the donor/acceptor ratio which gives the maximum FRET efficiency. **(b)** HEK293T cells were cotransfected with CXCR4-CFP and CXCR4-YFP at a unique ratio that ensures maximum FRET efficiency (determined from the FRET saturation curve). The change in FRET efficiency upon stimulation with CXCL12, CXCL14 or the two combined is shown. An increase in FRET efficiency indicates clustering of receptors (formation of multimers). Data shown is mean + s.e.m. of three independent experiments, with several recordings made per experiment. *$P<0.05$ and ***$P<0.001$ using a Kruskall-Wallis ANOVA. ns = not significant.
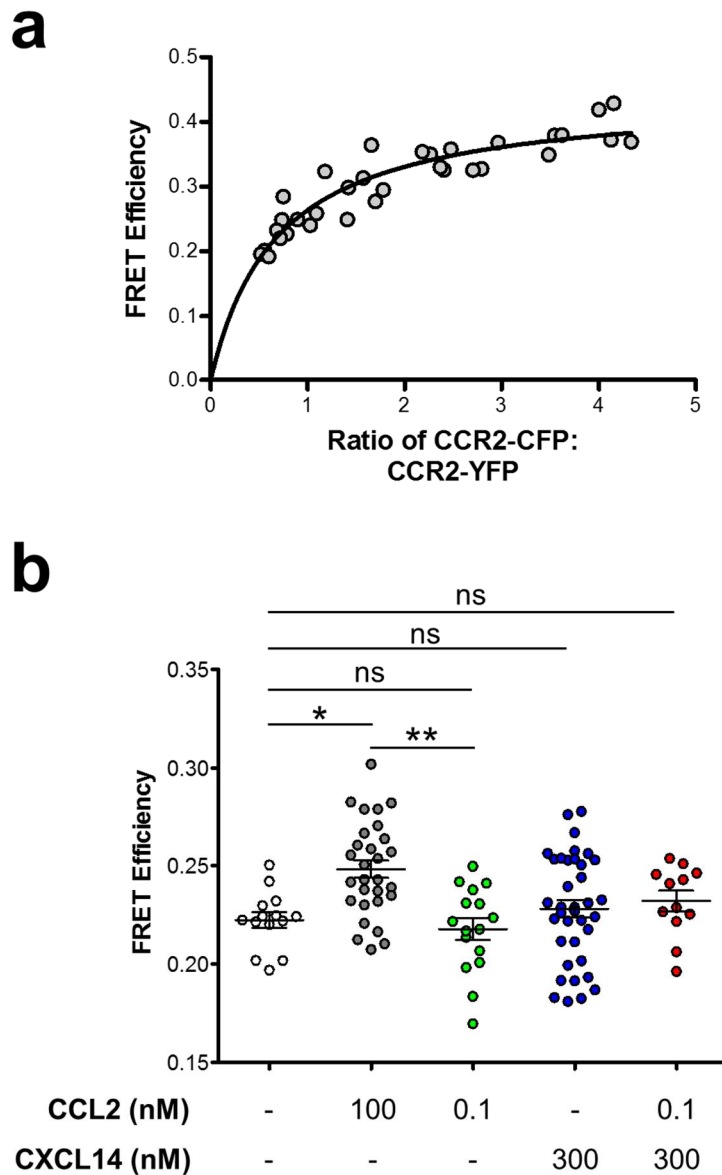
Figure 5.17. CXCL14 does not induce formation of CCR2 multimers.
(a) FRET saturation curves were performed using HEK293T cells transiently co-transfected with constant amounts of CCR2-CFP (FRET donor), and increasing amounts of CCR2-YFP (FRET acceptor). This enabled identification of the donor/acceptor ratio which gives the maximum FRET efficiency. **(b)** HEK293T cells were cotransfected with CCR2-CFP and CCR2-YFP at a unique ratio that ensures maximum FRET efficiency (determined from the FRET saturation curve). The change in FRET efficiency upon stimulation with CCL2, CXCL14 or the two combined is shown. An increase in FRET efficiency indicates clustering of receptors (formation of Multimers). Data shown is mean + s.e.m. of three independent experiments, with several recordings made per experiment. *$P<0.05$ and **$P<0.01$ using a Kruskall-Wallis ANOVA. ns = not significant.

5.5.5 CXCL14 and CXCL12 do not form a heterodimer

Thus far, I have shown that synergy between CXCL14 and CXCL12 is probably mediated by a single receptor, CXCR4. Although I have data to indicate that CXCL14 interacts directly with CXCR4, I cannot rule out the possibility that CXCL14 and CXCL12 form a heterodimer. There are several instances where synergy between chemokines is mediated by the formation of chemokine heterodimer complexes. The ability of chemokine heterodimers to modulate cell migration responses *in vitro* as well as *in vivo* is reviewed in (Gouwy et al., 2012). By comparing $^{15}N^1H$ chemical shift correlation nuclear magnetic resonance spectra of ^{15}N-labelled proteins before and after addition of a second protein, it is possible to detect protein-protein interactions, even between low-affinity binding partners. Furthermore, it is also possible to deduce which residues are involved in the observed interactions (Zuiderweg, 2002). This technique was first applied to the study of chemokine-chemokine interactions by Nesmelova and colleagues, who demonstrated that heterodimers were present in solutions containing a 1:1 mixture of CXCL4 and CXCL8 (Nesmelova et al., 2005). It was later applied to the demonstration that HMGB1 enhances the activity of CXCL12 through formation of a heterodimer (Schiraldi et al., 2012). Our collaborators at the University of Grenoble failed to detect protein-protein interaction between CXCL14 and CXCL12, even at extremely high concentrations (75 µM each) which by far exceeded the concentrations used in functional assays (**Figure 5.18a**). Another technique used to detect protein-protein interaction is surface plasmon resonance (SPR) spectroscopy, which enables the real-time monitoring of binding events of soluble proteins streamed over a sensor chip containing immobilised partner proteins (Khalifa et al., 2001). In support of the NMR data, SPR, again carried by our collaborators in Grenoble, did not reveal significant binding interactions between soluble CXCL14 and immobilised CXCL12, or vice versa (**Figure 5.18b**). When CXCL14 or CXCL12 was injected over a surface containing immobilised heparan sulphate (HS) however, a typical binding response was observed (**Figure 5.18c**). Interaction with GAGs is a common feature of many chemokines (Krohn et al., 2013, Lortat-Jacob, 2009). Furthermore, I have shown in my own experiments that addition of soluble GAG (heparan sulphate or chondroitin sulphate) interferes with the chemoattractant activity of CXCL14 in a dose-dependent manner, indicative of an interaction between CXCL14 and GAG (**Figure 5.19**). Detection of binding between CXCL14 and HS is assurance that the perceived lack of interaction between CXCL14

and CXCL12 is genuine. I can conclude, therefore, that CXCL14 and CXCL12 do not undergo heterocomplex formation.
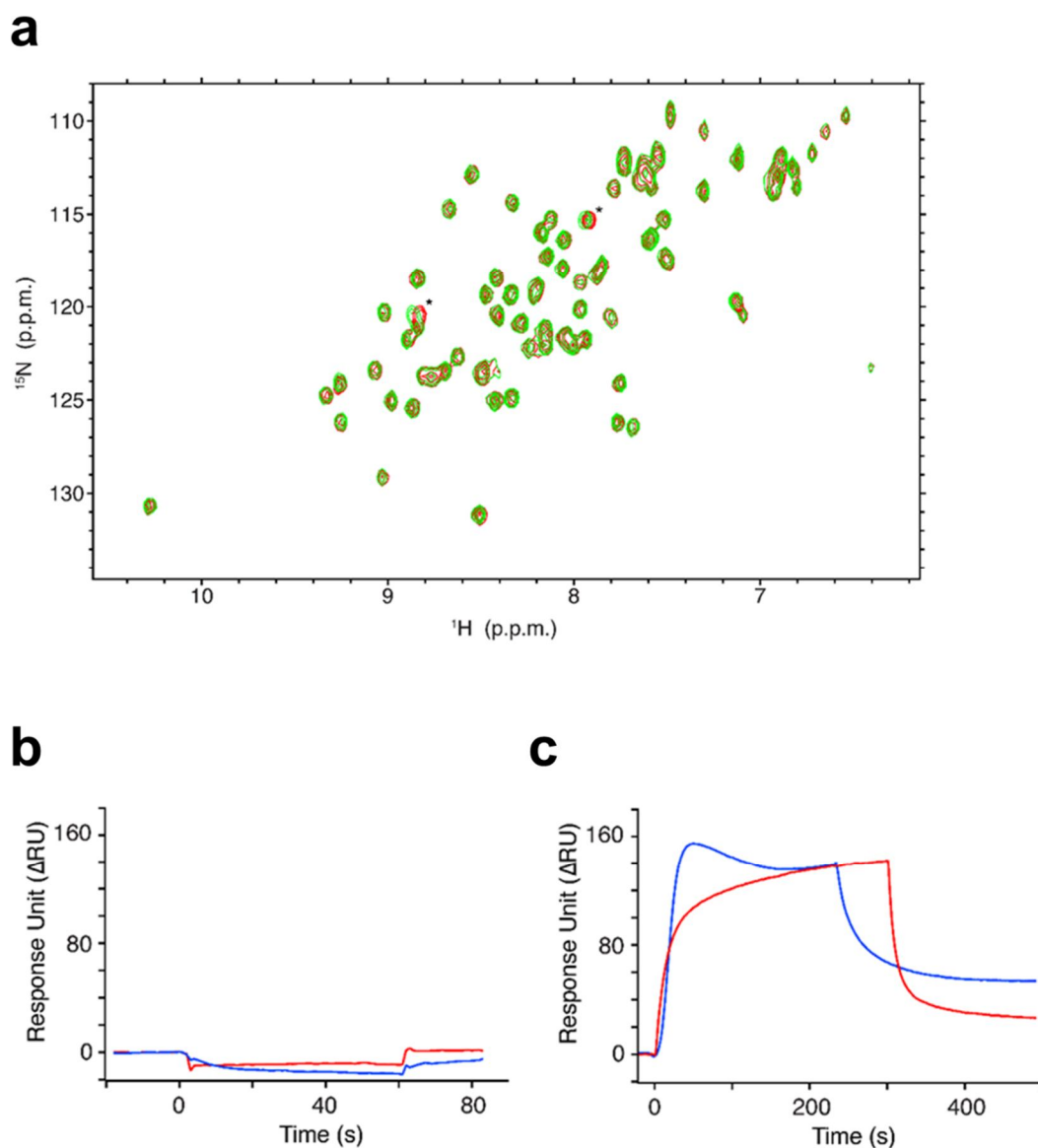
Figure 5.18. CXCL14 does not form a heterocomplex with CXCL12.

(a) ^{15}N-SOFAST-HMQC spectra were recorded at 850 MHz on ^{15}N-labeled CXCL12 at 75 µM alone (red) and in combination with 75 µM CXCL14 (green). Only the two CXCL12 histidine residues have small chemical shift differences, likely due to a slight pH change around imidazole pKa (indicated by asterisks). **(b)** SPR sensograms display the binding in response units (RU) when CXCL12 (50 nM) was injected over a CXCL14 surface (red curve) or when CXCL14 (50 nM) was injected over a CXCL12 surface (blue curve). **(c)** SPR sensograms display the binding response in RU when CXCL14 (blue curve) and CXCL12 (red curve), both at 50 nM, were injected over a heparan sulphate-functionalised surface. (a-c) are representative of two independent experiments, with several recordings made per experiment.
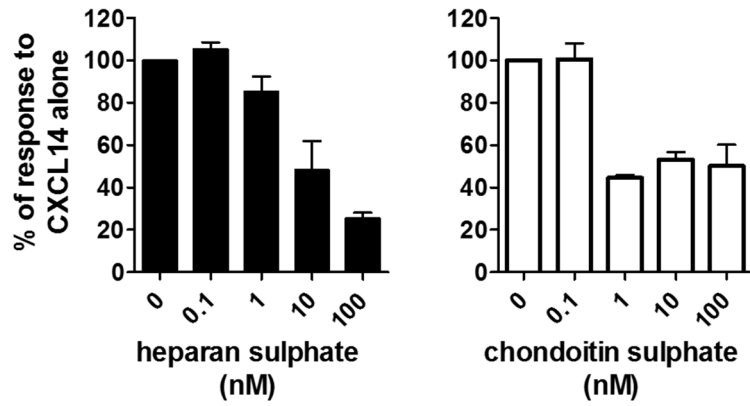
Figure 5.19. The chemoattractant activity of CXCL14 is inhibited by addition of soluble glycosaminoglycan.

Monocytes were purified from PBMC by negative selection and assessed for chemotactic responses toward 1 µM CXCL14 in the presence of 0.1-100 nM heparan sulphate (left) or chondroitin sulphate (right). GAG was added to the lower chamber of the transwell chemotaxis assay, along with the chemokine. Results are normalised to migration toward CXCL14 in the absence of GAG (0 nM; displayed as 100%). Data are mean + s.e.m. of two independent experiments.

5.6 Discussion

Here, I have reported a strong synergistic effect between CXCL14 and CXCL12 in the control of chemotactic migration in $CXCR4^+$ immune cells. CXCL12 is a homeostatic chemokine with expression in peripheral tissues during the steady-state, including at some of the locations where CXCL14 is found including the skin and mucosal surfaces of the intestine (Agace et al., 2000, Pablos et al., 1999). I have also shown that CXCL14 synergises with the lymphoid tissue-homing chemokines CCL19, CCL21 and CXCL13. Homeostatic processes under the control of these chemokines include the CCL19/21-mediated co-localisation of $CCR7^+$ T cells and mature DCs, critical for the initiation of adaptive immune responses (Sallusto et al., 1999), as well as the CXCL13-mediated co-localisation of $CXCR5^+$ B cells and T_{FH} cells during humoral immune responses (Breitfeld et al., 2000, Schaerli et al., 2000). In contrast, CXCL14 does not appear to synergize with inflammatory chemokines in the induction of chemotactic responses, which is consistent with the negative regulation of CXCL14 expression by inflammatory stimuli (Maerki et al., 2009, Schaerli et al., 2005). The inflammatory chemokines CCL2, CCL5 and CXCL10, included in the present study, only represent a fraction of the chemokines that are routinely found to be expressed in inflammatory settings. Therefore, I cannot claim at present that the ability to synergise with CXCL14 is restricted to homeostatic chemokines only.

There have been numerous reports in recent years describing functional synergism in the chemokine system, with several mechanisms being proposed to explain this phenomenon (reviewed in (Gouwy et al., 2012) and shown in **Figure 5.1**). Heterodimerisation of a number of chemokine pairs has been observed at micromolar concentrations in solution, a phenomenon first described using NMR in a pioneering study by Nesmelova et al. Here, formation of heterodimers by CXCL4 and CXCL8 was proposed to stabilise the tertiary motifs of CXCL8 in a conformation which favoured interaction with its cognate receptor, CXCR2 (Nesmelova et al., 2005, Paoletti et al., 2005) Chemokine synergism has also been attributed to the activation of multiple signalling pathways in target cells expressing more than one type of receptor, induced in response to simultaneous (or sequential) binding of their respective chemokines (Gouwy et al., 2012, Gouwy et al., 2008). Chemokine receptors are constantly in motion on cell surfaces, resulting in frequent protein-protein interactions which last for a long enough duration to be detected by FRET analysis (reviewed in (Thelen et al., 2010)). Complex multimeric structures containing different chemokine receptors were induced by synergizing chemokines, while

chemokine receptor multimers mediate enhanced cellular responses by coupling to distinct signalling pathways (Mellado et al., 2001b). Finally, in addition to their cognate receptors, chemokines also interact with GAGs present on extracellular matrices. Immobilisation of chemokines by interaction with GAG is a prerequisite for directional cell migration along chemokine gradients, reviewed in (Lortat-Jacob, 2009). GAGs are also present on the surface of immune cells, where they facilitate the retention of chemokines in close proximity to receptors on the surface of the same cell, assisting receptor activation (Proudfoot et al., 2003). There is evidence that binding to GAG facilitates the formation of chemokine heterodimers with increased biological activity (Proudfoot et al., 2003). However, considering the complexity and diversity of GAGs, in addition to their ability to selectively bind certain chemokines, their contribution to the synergy observed between chemokines has been difficult to ascertain.

The findings we report here with CXCL14 cannot be readily explained by multiple receptors undergoing heterodimerization or cooperative receptor signalling, while our data also do not support heterodimerisation between CXCL14 and CXCL12 as a possible mechanism. Instead we propose a new model of chemokine synergy where the synergistic chemokines interact with a single receptor in a way that does not involve formation of a heterodimer. Instead, both chemokines interact with the same receptor by binding to non-overlapping sites. In this model, CXCL14 binds to alternative sites on CXCR4, resulting in "priming" of cells for subsequent responses to CXCL12. In doing so, CXCL14 lowers the threshold of activation, allowing a normally inactive concentration of CXCL12 to trigger activation of cellular responses. The CXCL14-mediated priming of CXCR4 does not involve the activation of traditional signalling pathways, as a rise in intracellular $[Ca^{2+}]$ was not induced in $CXCR4^+$ cells by CXCL14 alone. Indeed, other prototypical signalling events following chemokine receptor activation including phosphorylation of MAP kinases, have been shown not to be elicited by CXCL14 binding to CXCR4 (Otte et al., 2014). Clarification of whether the observed chemokine synergy is dependent on the simultaneous presence of CXCL14 and CXCL12 is required. Finally, it will be important to investigate whether the proposed receptor priming model for synergy between CXCL14 and CXCL12 also applies to the synergy observed between CXCL14 and the other homeostatic chemokines (CXCL13 and CCL19/CCL21). See **Figure 5.20** for an illustration of the proposed model to explain the chemokine synergy between CXCL14 and CXCL12.
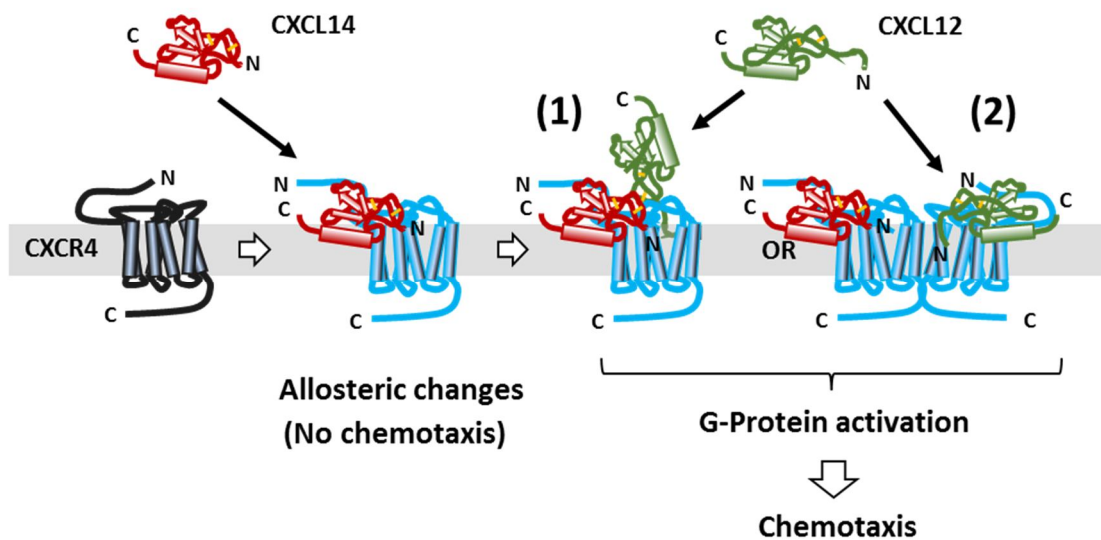
Figure 5.20. A new model of chemokine synergy explains the cooperativity between CXCL12 and CXCL14.

CXCL14 (red) binds to a resting CXCR4 molecule on the cell surface (black). While binding of CXCL14 to CXCR4 does not elicit a functional response, it induces an allosteric change which primes the receptor (blue) for activation by lower concentrations of CXCL12 (green). This priming may take the form of a conformational change in single receptor molecules (1), but more likely induces the formation of receptor homodimers (or higher order oligomers) that are more amenable to activation by CXCL12 (2). My data indicates that scenario (2) is responsible for the synergy observed here. Lack of a physical interaction between CXCL14 and CXCL12, even at high (micromolar) concentrations, indicate that the two chemokines are likely not acting at a single receptor. Furthermore, stimulation of an increase in FRET upon CXCR4 strongly suggests that CXCL14 induces the formation of CXCR4 homodimers. Indeed, SPR has recently confirmed a binding interaction between CXCL14 and CXCR4. Despite this, failure to detect binding of AF-CXCL14 to CXCR4 transfectants by flow cytometry appears to indicate that the interaction is of low stability.

Modulation of CXCL12 activity by CXCL14 has recently been reported by another research group, an effect which they also proposed was dependent on direct binding of CXCL14 to CXCR4 (Tanegashima et al., 2013a, Tanegashima et al., 2013b). Here, however, the authors proposed that CXCL14 inhibited CXCL12-mediated chemotaxis of human haematopoietic progenitor cells and THP-1 cells. Like Tanegashima and colleagues, I observed that upon combination of CXCL14 with a concentration of CXCL12 which is optimal for induction of chemotaxis alone, a reduction in activity is observed ((Tanegashima et al., 2013a) and **Figure 5.4**). However, experiments were not performed in these previous studies to test whether CXCL14 could enhance the

activity of low, normally inactive concentrations of CXCL12, as I have reported. Therefore, rather than contradicting, my findings are an extension of those previously reported.

Synergistic interaction with CXCL14 was shown to be dependent on the presence of the cognate receptors (CXCR4, CXCR5 and CCR7) for the partner chemokines (CXCL12, CXCL13 and CCL19/CCL21) on responding cells. Synergy between CXCL12 and CXCL14 was selected as the model system upon which the mechanism underlying the synergistic interaction was investigated. Blockade of CXCR4 using the specific antagonist AMD3100 completely abrogated the synergistic induction of chemotactic responses in human lymphocytes. T cells, B cells and NK cells (in addition to a CXCR4-transfected mouse pre-B cell line) did not respond to CXCL14 by itself, indicating that the observed synergy did not involve CXCL14 receptor(s). It is worth noting that migratory responses of human monocytes toward CXCL14 were unaffected by CXCR4 blockade with AMD3100, emphasising the fact that the putative CXCL14 receptor is distinct from CXCR4. Interaction between CXCL14 and CXCR4 could not be demonstrated in binding studies using AF-CXCL14. This may be explained by the interaction being of low affinity and not sufficiently stable for the ligand to remain bound throughout the preparation of samples for acquisition on the flow cytometer. To this effect, our collaborators in Madrid (who performed the FRET experiments) are currently attempting to confirm a direct interaction between CXCL14 and CXCR4 by SPR, with CXCR4 immobilised on a sensor chip by a method that has been shown to not interfere with its native conformation or binding activity (Rodriguez-Frade et al., 2016). Preliminary data from these experiments suggest that CXCL14 binds CXCR4 with an approximately 10-fold lower affinity than CXCL12, thus supporting our hypothesis. Further experiments still need to be performed to enable the calculation of reliable affinity constants for binding of CXCL12 and CXCL14 to CXCR4.

Given the enormous complexity of the chemokine superfamily, in terms of the unique spatial and temporal patterns of expression exhibited by each member, it is currently impossible to unequivocally define the physiological relevance of chemokine synergy. There are, however, several reports describing a contribution of synergistic interaction between chemokines to leukocyte recruitment in various *in vivo* rodent models, including mouse models of monocyte recruitment to atherosclerotic lesions (Koenen et al., 2009), and neutrophil recruitment to the peritoneum (Struyf et al., 2005), as well as rat models of leukocyte recruitment to inflamed skin (Stanford and Issekutz, 2003).

Similarly HMGB1, a chromatin-binding protein released by dying cells, was demonstrated to dimerize with CXCL12 and to induce synergistic leukocyte recruitment in several mouse models of tissue necrosis (Schiraldi et al., 2012). Activin A, a member of the TGF-β family, was recently shown to induce migration of immature DCs *in vitro*, as well as in an *ex vivo* model of chemokine-mediated emigration of DCs from mouse ear tissue (Salogni et al., 2009). Activin A by itself had no chemoattractant activity, however it induced in immature DCs (iDC) the coordinate expression of CXCL14 and CXCL12 (but no other chemokine). Importantly, the iDC migration was dependent on CXCR4, as evidenced with blockade using AMD3100 and CXCR4-specific antibodies. The findings of Salogni et al. support of our model of CXCL14-mediated priming of CXCR4$^+$ target cell responses toward CXCL12.

To summarise, exceptional sequence conservation and ubiquitous (and in part overlapping) expression in healthy tissues suggest that CXCL14 and CXCL12 may synergize in the localization of immune surveillance cells (T cells, DCs, macrophages). This process may be most effective in the steady-state or at early stages of antigen exposure, before production of inflammatory mediators and subsequent downregulation of CXCL14 expression. The synergy may pertain not only to immune processes, but also to tissue cell localization (wound repair) and developmental processes (embryogenesis) since both chemokines are also abundantly expressed at discrete locations in the developing mouse embryos (Garcia-Andres and Torres, 2010). As a further interpretation of the novel ability of CXCL14 to synergise with other chemokines, this may also explain, in part, the substantial breeding defect seen in CXCL14-KO mouse colonies (Meuter et al., 2007).

Chapter 6 General Discussion

6.1 Summary

During the course of this project, I have sought to clarify the activity and target cells of one of the least understood members of the chemokine superfamily, CXCL14. In doing so, I have revealed unexpected and novel functions for CXCL14, most notably its ability to influence the activity of other chemokines. In addition, I have revealed new insights into the role of CXCL14 in the maintenance of tissue cells of the MPS. Previous studies into the function of CXCL14 have reported roles in diverse processes such as killing of microorganisms (Dai et al., 2015, Maerki et al., 2009) and tumour progression (Augsten et al., 2009, Ozawa et al., 2006, Shurin et al., 2005, Wente et al., 2008), as well as roles unrelated to immune function including regulation of body weight and glucose metabolism (Hara and Tanegashima, 2012, Tanegashima et al., 2010a). Our research group has an invested interest in the immune surveillance of skin during the steady-state. Constitutively expressed in a number of peripheral tissues including skin, gut, kidney, brain and placenta (Cao et al., 2000, Frederick et al., 2000, Hromas et al., 1999, Kurth et al., 2001, Meuter and Moser, 2008), it has been postulated that CXCL14 has an important role in controlling immune surveillance in these tissues. However, the precise identity of CXCL14 target cells has, up to this point, not been well defined. Often contradictory reports have indicated that among the target cells of CXCL14 are monocytes, B cells, neutrophils, immature DCs, activated blood NK cells and uterine NK cells (Cao et al., 2000, Kurth et al., 2001, Mokhtar et al., 2010, Salogni et al., 2009, Shellenberger et al., 2004, Starnes et al., 2006). With the aid of transwell chemotaxis assays to assess cell migration, as well as a novel reagent in the form of Alexa Fluor 647-conjugated CXCL14 for detecting expression of CXCL14 receptor(s), I have demonstrated that CD14$^+$ monocytes represent the major targets of CXCL14 among peripheral blood mononuclear cells. Further to this, I have shown that certain myeloid populations which are resident in healthy human skin, most notably an apparent novel subset of skin-resident myeloid cells characterised by lack of CD45 expression, are also targets for CXCL14. Critical to definitively identifying the target cells of CXCL14, however, is the discovery of its cognate receptor. While I am unable to report the identity of the CXCL14 receptor at this time, its imminent discovery will facilitate a complete understanding of the role played by CXCL14 in the steady-state control of immune cell function and localisation in peripheral tissues

6.2 Tissue-resident Monocytes (M$_{TR}$)

The health and longevity of peripheral tissues depends on an effective local immune surveillance system, primed to respond to infections, injury and transformed cells rapidly and effectively (Schaerli et al., 2004). The importance of this system is underscored by the recurrent infections and increased susceptibility to cancers observed under conditions of immune suppression, for instance in organ transplant recipients. Undoubtedly, central to the local immune surveillance of virtually all tissues is the mononuclear phagocyte system. Tissue-resident phagocytes including macrophages and DCs form the first line of defence against invading microorganisms, while their antigen-presenting capacity and cytokine production influences the activity of other immune cells (Banchereau and Steinman, 1998, Davies et al., 2013a, Haniffa et al., 2015). The MPS is exceedingly complex however, as demonstrated by the functional diversity of macrophages at different locations which fulfil tissue-specific functions. Examples include clearance of surfactant by alveolar macrophages in the lung, synaptic pruning and immune surveillance in the brain by microglia and regulation of the host-microbe balance by intestinal macrophages (Davies et al., 2013a, Hashimoto et al., 2011). Evidently, the immune surveillance system in healthy peripheral tissues is not dormant; on the contrary, considering the frequency of insults that tissues such as skin and gut have to deal with, it is highly active.

Here, I have described a potential new addition to the MPS in the form of a novel subset of myeloid cells present in healthy human skin, which we hereby cautiously term "tissue-resident monocytes" or "M$_{TR}$". At this point, we know virtually nothing about the origin or function of these cells. M$_{TR}$ were identified by their expression of CXCL14 receptors (as indicated by binding of AF-CXCL14) in addition to displaying robust migratory responses toward CXCL14. They were further defined phenotypically by their co-expression of the myeloid markers CD1a and CD14, in addition to their startling lack of expression of the protein tyrosine phosphatase and pan-leukocyte marker, CD45. It may be postulated that their lack of CD45 expression points to a non-haematopoietic origin of these cells. Recently, microglia isolated from the brains of mice have been identified as CD45^{dim} cells that represent an ontogenetically distinct population in the MPS, derived from macrophage progenitors of the yolk sac rather than bone marrow precursors (Ginhoux et al., 2010, Immig et al., 2015). Lack of CD45 expression may also explain why such a seemingly large cellular compartment in the skin has been overlooked by researchers up to this point. There are numerous examples of studies looking at immune cell subsets in human

skin where the researchers have excluded the CD45$^{dim/neg}$ cells from their analyses (Haniffa et al., 2009, McGovern et al., 2014). It is exciting to speculate that due to their shared ability to respond toward CXCL14, M$_{TR}$ are derived from CD14$^+$ blood monocytes. As of yet, we do not have evidence to support this. Determining the origin of M$_{TR}$ (independent of the haematopoietic system or monocyte-derived?) will be of critical importance to understanding how they integrate with the existing components of the MPS. In this regard, I have recently discovered an equivalent population of CD45^{neg} M$_{TR}$ among cells extracted from the healthy skin of wild-type C57/BL6 mice by enzymatic digestion. In staining of cells for flow cytometry, I have demonstrated that mouse M$_{TR}$ bind AF-CXCL14, in experiments which were performed using the human reagent applied to the detection of CXCL14 receptor(s) on human immune cells. Mouse and human CXCL14 differ by only two amino acid substitutions however, thus I am confident that this reagent can be reliably applied to studying the distribution of CXCL14 receptors on mouse cells. Mouse M$_{TR}$ were also defined phenotypically by expression of the typical murine macrophage cell-surface marker F4/80. As with their human counterparts, mouse M$_{TR}$ were found to be abundant in the skin accounting for as much as 20% of CD45^{neg} cells, thus representing a significant compartment in healthy tissue. Upon initial investigations by our group, the CXCL14-KO mouse did not reveal an immune defect, with special attention paid to the sites where CXCL14 is produced, including the skin (Meuter et al., 2007). However, it is likely that the M$_{TR}$ were overlooked due to their lack of CD45 expression. Therefore, we are in the process of re-establishing a colony of CXCL14-KO mice in our laboratory, with the intention of seeing if the novel cells are present. The absence of M$_{TR}$ would provide the first conclusive evidence for CXCL14 playing an essential role in the maintenance of immune cell populations in the skin during the steady-state, thus having profound implications for mucosal immunity in both mouse and man.

In order for M$_{TR}$ to truly be considered a novel subset of the MPS, further phenotypic and functional characterisation is essential. Studies in human should consider their morphology, functional properties *in vitro* and their relationship to conventional (CD45$^+$) subsets of the MPS. The study of surface marker expression on M$_{TR}$ will include those relevant for the CD45$^+$ cells of the MPS, which include conventional macrophages, dermal CD1a$^+$ and CD14$^+$ DCs, epidermal LCs and peripheral blood monocytes (Haniffa et al., 2009, Ziegler-Heitbrock et al., 2010). Focus should be on particular markers related to migration (chemokine receptors and adhesion molecules), responding to pathogens (TLRs and other pattern-recognition receptors) and antigen presentation (MHC class II and co-stimulatory molecules e.g. CD40 and

CD80/86). Functional analyses, performed initially *in vitro*, should include assays that explore phagocytosis of fluorescent-labelled substrates as well as measurement of responses to pathogens, including the production of cytokines (IL-1β, TNFα, TGFβ etc.), chemokines (CXCL8, CXCL14, CCL1-5, etc.) and anti-microbial agents (defensins, NOS/ROS, etc.). One should also determine if, in similar fashion to LCs of the epidermis and microglia of the brain, M_{TR} are radio-resistant. If they are susceptible to irradiation, it will be fascinating to observe the reconstitution kinetics of M_{TR} in patients following total body irradiation prior to HSCT, in the same way as has been done previously for blood monocytes and dermal macrophages/DCs (Haniffa et al., 2009). Their reconstitution in peripheral tissues in relation to other cell types (blood monocytes in particular) may reveal crucial information regarding the origin of M_{TR}.

The very high sequence conservation between human and mouse CXCL14 suggests that cross-species functional conservation is likely (Wolf and Moser, 2012). Characterisation of M_{TR} in mouse should therefore include the investigations listed above for human M_{TR}, but be extended to their tissue distribution by searching for M_{TR} at other sites where CXCL14 is expressed, including kidney, lung, intestine, placenta and brain (Meuter and Moser, 2008). The use of mouse models will also allow for the function of M_{TR} in inflammatory settings to be assessed. Investigations should focus on their *in situ* phagocytic properties, while it will be important to see if M_{TR} are mobilised (enhanced phagocytic activity and/or turn-over) in response to inflammatory stimuli, as previously done for conventional macrophages (Wang et al., 2006). Due to their possible role in immune surveillance, it may be postulated that recruited monocytes give rise to M_{TR} during the resolution phase of the inflammatory response. This hypothesis may be tested by specific depletion of classical monocytes from wild-type mice using an anti-CCR2 antibody as previously described (Schumak et al., 2015), followed by adoptive transfer of GFP[+] monocytes from CX3CR1creR26-GFP reporter mice (where all monocytes are labelled with GFP). Upon induction of skin inflammation, GFP^{+} tissue cells should be analysed at several time points in inflamed (and non-inflamed) skin. If M_{TR} are found to be present at other sites, these studies may be extended to inflammation models involving other tissues, such as the inflammatory recruitment of monocytes to peritoneum following administration of zymosan or thioglycollate (Davies et al., 2013b). It should therefore be possible to determine whether the M_{TR} pool in mouse tissues is contributed to by circulating precursors such as monocytes, and under what conditions (steady-state or inflammation) this is the case.

Gene expression analysis of human and mouse M_{TR} should also be performed, akin to that described previously for the monocyte subsets (Wong et al., 2011). CD45^{neg}CD1a$^+$AF-CXCL14$^+$ human M_{TR} and CD45^{neg}F4/80$^+$AF-CXCL14$^+$ mouse M_{TR}, sorted by FACS, should be subjected to transcriptome analysis by RNA sequencing. Conventional dermal macrophages, dermal DCs and blood monocytes should also be taken for comparison, with special attention being paid to genes involved in pathways such as phagocytosis, pro-inflammatory cytokine release and antigen presentation. The overall aim of these studies should be to define the characteristics of human and mouse M_{TR}, as well as their phenotypic and functional relatedness with conventional tissue macrophages/DCs and blood monocytes.

6.3 The CXCL14 Receptor

The discovery of M_{TR} provides another source of CXCL14-responsive cells to interrogate for their expression of GPCRs, which should aid our efforts to identify the CXCL14 receptor. Transcriptome analysis of M_{TR} by RNA-seq will provide a new data set of expressed GPCRs in cells which are targets for CXCL14, for comparison to CD14$^+$ monocytes and PGE$_2$-treated THP-1 cells. This will enable refinement of the current list of candidates for the CXCL14 receptor. RNA sequencing of mouse M_{TR} will provide another additional data set to incorporate into our existing analyses, while cross-referencing the expressed GPCR lists from human and mouse should enable refinement of the candidate list even further. Given the pool of CXCL14 target cells in human and mouse now at our disposal, I am confident that it is only a matter of time until the identity of the CXCL14 receptor is revealed.

I chose to go down the route of transcriptome analysis in my efforts to discover the CXCL14 receptor in this project for several reasons. Firstly, since all we could be sure of regarding the properties of the CXCL14 receptor is that it is almost certainly a Gαi-coupled GPCR (due to its sensitivity to pertussis toxin treatment), RNA-seq represented the most unbiased approach to screening CXCL14-responsive cells for expression of GPCRs. Indeed, the GPCR that mediates the physiological effects of neuronostatin, a novel peptide encoded by the somatostatin gene, was found by a similar method (Yosten et al., 2012). Following identification of orphan GPCRs expressed in monocytes and PGE$_2$-treated THP-1 cells, candidates were tested by stable expression in a cell-line, while screening by shRNA-mediated knockdown was also intended but was met with technical difficulties. Unfortunately, the testing of candidates proved unsuccessful and the identity of the CXCL14 receptor remains elusive. For the reasons outlined above, including new cell subsets to screen for

expression of GPCRs, I still consider transcriptome analysis to be the best approach for discovering the CXCL14 receptor. Alternatively, however, a proteomics-based approach could be taken. In this regard, a potential tactic would be to use the fluorochrome-labelled chemokine AF-CXCL14 to pull down the receptor, followed by purification of ligand-receptor complexes and analysis by mass spectrometry. Attempts to isolate the receptor by ligand-binding and subsequent pull-down would likely be more straightforward if one was able to use biotinylated CXCL14 (bio-CXCL14), since following binding of bio-CXCL14 and solubilisation of the cells, receptor-ligand complexes could be pulled down easily using a streptavidin column. We have the bio-CXCL14 reagent in our lab, however it was found to be totally inactive up to 5 µM concentration in transwell chemotaxis assays (data not shown). Proteomics analysis may also be complicated by the fact that we do not know the nature of the interaction between CXCL14 and its receptor. There is evidence that many chemokines form dimers or higher-order multimers when interacting with their receptor (Proudfoot and Uguccioni, 2016). Whether CXCL14 binds to its receptor at a 1:1 ratio or not is yet to be elucidated. Finally, there are question marks over whether or not the interaction between CXCL14 and its receptor is sufficiently stable to enable this approach to work. Detection of AF-CXCL14 binding to monocytes by flow cytometry, in spite of several wash steps in between incubation of cells with the reagent and sample acquisition, indicates that the interaction is fairly stable and not subject to rapid dissociation. Binding is also performed at 4 °C, at which very little receptor internalisation should occur. In theory, therefore, binding of AF-CXCL14 may be stable enough to pull down the receptor for analysis by proteomics-based methodologies. If this were shown to be the case, the use of proteomics in parallel with transcriptome analysis will enhance our efforts to discover the CXCL14 receptor.

6.4 Interaction with CXCR4 and Synergy with Other Chemokines

Although the receptor via which CXCL14 induces migration of monocytic cells remains unknown, I have presented evidence to suggest that CXCL14 interacts with the chemokine receptor CXCR4, albeit in a non-signalling manner. By interacting with CXCR4, CXCL14 considerably modulates the activity of CXCL12. Based on the data obtained from NMR, SPR and FRET experiments, I hypothesise that CXCL14 binds to CXCR4 at a site distinct from where CXCL12 binds, and in doing so induces clustering of CXCR4 receptors on the cell-surface (which may or may not be accompanied by a conformational change to the receptor) which makes CXCR4 more

amenable to activation by low concentrations of CXCL12. Mechanisms of chemokine synergy described previously include 1) a chemokine heterodimer activating a single receptor, 2) two different receptors forming a heterodimer on the cell surface, with each member being activated simultaneously by their respective ligands, and 3) two receptors, separated on the cell surface, that are activated simultaneously and synergise at the level of downstream signalling ((Gouwy et al., 2012, Proudfoot and Uguccioni, 2016) and Figure 5.1). My model of cooperation between CXCL14 and CXCL12 therefore represents a novel mechanism of chemokine synergy, as I do not find evidence elsewhere in the literature of a chemokine enhancing the potency of another chemokine through binding to its receptor in a non-signalling manner. These findings also build on those reported recently by others, who have shown that CXCL14 binds CXCR4 but does not trigger downstream signalling events (Otte et al., 2014, Tanegashima et al., 2013a, Tanegashima et al., 2013b). In revealing the cooperative nature of this interaction, my work provides a potential physiological relevance to these earlier findings. CXCL12, like CXCL14, is ubiquitously expressed in many healthy peripheral tissues including skin and gut (Agace et al., 2000, Pablos et al., 1999). It can therefore be postulated that CXCL14 and CXCL12 synergise *in vivo* in the recruitment of immune cells from blood, during the steady-state. Synergy between chemoattractants in the recruitment of immune cells has been demonstrated *in vivo* previously using the air pouch model, in which sterile air is administered by subcutaneous injection into the back of a mouse. The pouch mimics the synovial cavity thus providing a localised environment, in the absence of any inflammation or infectious agent, in which to study cell trafficking (Sin et al., 1986). Synergistic interaction between CXCL12 and the chemoattractant HMGB1 in the recruitment of lymphocytes was confirmed to occur *in vivo* using the air pouch model (Schiraldi et al., 2012). This model of sterile immune cell traffic to a peripheral site should be applied in order to confirm that the synergistic interaction between CXCL14 and CXCL12 takes place *in vivo*.

The physiological relevance of the observed synergistic interaction between CXCL14 and the lymphoid tissue-homing chemokines CCL19, CCL21 and CXCL13 is somewhat less clear. Secondary lymphoid organs represent one of the few peripheral tissues where CXCL14 expression is low to non-detectable (Meuter and Moser, 2008). Therefore, it seems unlikely that CXCL14 cooperates with the lymphoid tissue-homing chemokines to control the steady-state recruitment of T cells, B cells and mature DCs to these sites. It has been recently proposed that despite its high expression in healthy tissues, CXCL14 may have a more prominent role in

inflammatory processes than initially thought (reviewed in (Lu et al., 2016)). Indeed, although CXCL14 expression is down-regulated in most inflammatory settings, there are examples of where its expression is up-regulated, for instance in the inflammatory lesion in the joint that is characteristic of the autoimmune disease rheumatoid arthritis (RA) (Chen et al., 2010). Such chronic inflammatory disorders are often characterised by the appearance of ectopic or tertiary lymphoid organs in the tissue, responsible for local activation of adaptive immune responses leading to release of pro-inflammatory cytokines, further influx of inflammatory cells and autoantibody production. Lymphoid tissue-associated chemokines including CXCL13, CCL19 and CCL21 (in addition to CXCL12) are all expressed in these ectopic lymphoid structures (Hjelmstrom et al., 2000, Pitzalis et al., 2014), and it may be postulated that CXCL14 synergises with these chemokines to exacerbate the inflammatory cell recruitment. Indeed, CXCL14 expression has been shown to be up-regulated in the joint in a murine model of collagen-induced arthritis, while transgenic mice that over-expressed CXCL14 developed a more severe arthritis than wild type controls (Chen et al., 2010). Paradoxically therefore, CXCL14 may synergise with these other 'homeostatic' chemokines, but rather than doing so in the context of homeostatic cell recruitment, instead enhance the recruitment of immune effector cells to sites of inflammation. The air pouch model (described previously) could potentially be applied to determining whether CXCL14 is able to synergise with the lymphoid tissue-homing chemokines in the context of lymphocyte (and DC) recruitment *in vivo*. If this is shown to be the case, blockade of CXCL14 may represent a potential therapeutic intervention in the treatment of RA, and possibly other chronic inflammatory disorders characterised by the presence of ectopic lymphoid organs.

Skin
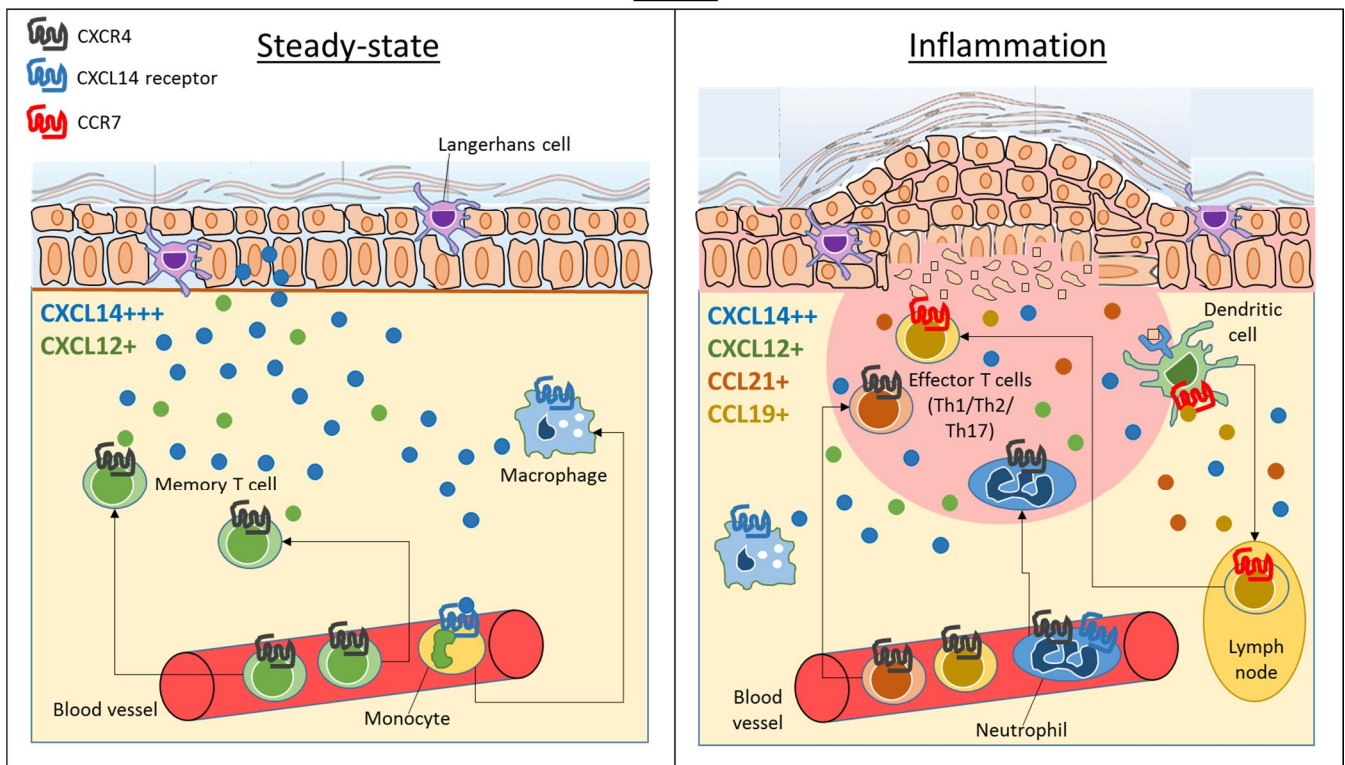
Figure 6.1. The role of CXCL14 in the control of leukocyte recruitment to peripheral sites during the steady-state (left) and inflammation (right).

Here, the skin is used as an example, but this scenario may apply to other anatomical locations and disease situations. During the steady-state, CXCL14 is produced in large quantities by epidermal keratinocytes as well as by discrete cells within the dermis, including resident macrophages. CXCL12 is also produced in the skin, and these two chemokines cooperate to control the basal recruitment of long-lived memory T cells via their expression of CXCR4. In parallel, CXCL14 recruits classical monocytes which extravasate from the blood into the dermis, where they give rise to dermal macrophages and/or DCs. During inflammation of the skin, such as that associated with chronic inflammatory disorders including psoriasis, other chemokines including the CCR7 ligands CCL21 and CCL19 are produced (in addition to a host of inflammatory chemokines and other inflammatory mediators, which are not shown). CCR7^{+} DCs traffic antigen to lymph nodes where they activate naïve T cells. CXCL14 synergises with the CCR7 ligands to recruit effector T cells to the inflammatory site. CXCL14 may also synergise with CXCL12 in the recruitment of other immune effector cells; an example being neutrophils, which likely express both CXCR4 and the CXCL14 receptor. Formation of ectopic lymphoid structures, a characteristic feature of many chronic inflammatory diseases, is driven by chemokines including CCL21, CCL19, CXCL12 and CXCL14.

6.5 Conclusion

In the ever-expanding field of chemokine research, CXCL14 remains as one of the least understood members of this family of structurally- and functionally-related peptides. Since its discovery 17 years ago, our knowledge of the functions of CXCL14 has increased incrementally. Its selectivity for monocytic cells is unique among the chemokine family, while its role in maintaining tissue phagocyte populations in addition to the relevance of its ability to influence the activity of other chemokines, will surely be revealed in the years to come. Indeed, the observation that CXCL14 expression is lost in many cancers and chronic inflammatory diseases highlights its non-redundant role in regulating peripheral immunity. Finally, discovery of the cognate receptor of CXCL14 will facilitate a rapid escalation in the gathering of knowledge regarding its functions in immunity, made possible by the generation of CXCL14– reporter mouse strains.

Chapter 7   References

ABTIN, A., JAIN, R., MITCHELL, A. J., ROEDIGER, B., BRZOSKA, A. J., TIKOO, S., CHENG, Q., NG, L. G., CAVANAGH, L. L., VON ANDRIAN, U. H., HICKEY, M. J., FIRTH, N. & WENINGER, W. 2014. Perivascular macrophages mediate neutrophil recruitment during bacterial skin infection. *Nat Immunol,* 15**,** 45-53.

AGACE, W. W., AMARA, A., ROBERTS, A. I., PABLOS, J. L., THELEN, S., UGUCCIONI, M., LI, X. Y., MARSAL, J., ARENZANA-SEISDEDOS, F., DELAUNAY, T., EBERT, E. C., MOSER, B. & PARKER, C. M. 2000. Constitutive expression of stromal derived factor-1 by mucosal epithelia and its role in HIV transmission and propagation. *Curr Biol,* 10**,** 325-8.

ALTIN, J. G. & SLOAN, E. K. 1997. The role of CD45 and CD45-associated molecules in T cell activation. *Immunol Cell Biol,* 75**,** 430-45.

ANCUTA, P., LIU, K. Y., MISRA, V., WACLECHE, V. S., GOSSELIN, A., ZHOU, X. & GABUZDA, D. 2009. Transcriptional profiling reveals developmental relationship and distinct biological functions of CD16+ and CD16- monocyte subsets. *BMC Genomics,* 10**,** 403.

ANGEL, C. E., GEORGE, E., BROOKS, A. E., OSTROVSKY, L. L., BROWN, T. L. & DUNBAR, P. R. 2006. Cutting edge: CD1a+ antigen-presenting cells in human dermis respond rapidly to CCR7 ligands. *J Immunol,* 176**,** 5730-4.

ARA, T., TOKOYODA, K., SUGIYAMA, T., EGAWA, T., KAWABATA, K. & NAGASAWA, T. 2003. Long-term hematopoietic stem cells require stromal cell-derived factor-1 for colonizing bone marrow during ontogeny. *Immunity,* 19**,** 257-67.

AUFFRAY, C., SIEWEKE, M. H. & GEISSMANN, F. 2009. Blood monocytes: development, heterogeneity, and relationship with dendritic cells. *Annu Rev Immunol,* 27**,** 669-92.

AUGSTEN, M., HAGGLOF, C., OLSSON, E., STOLZ, C., TSAGOZIS, P., LEVCHENKO, T., FREDERICK, M. J., BORG, A., MICKE, P., EGEVAD, L. & OSTMAN, A. 2009. CXCL14 is an autocrine growth factor for fibroblasts and acts as a multi-modal stimulator of prostate tumor growth. *Proc Natl Acad Sci U S A,* 106**,** 3414-9.

BAGGIOLINI, M., WALZ, A. & KUNKEL, S. L. 1989. Neutrophil-activating peptide-1/interleukin 8, a novel cytokine that activates neutrophils. *J Clin Invest,* 84**,** 1045-9.

BANCHEREAU, J. & STEINMAN, R. M. 1998. Dendritic cells and the control of immunity. *Nature,* 392**,** 245-52.

BARROSO, R., MARTINEZ MUNOZ, L., BARRONDO, S., VEGA, B., HOLGADO, B. L., LUCAS, P., BAILLO, A., SALLES, J., RODRIGUEZ-FRADE, J. M. & MELLADO, M. 2012. EBI2 regulates CXCL13-mediated responses by heterodimerization with CXCR5. *FASEB J,* 26**,** 4841-54.

BELGE, K. U., DAYYANI, F., HORELT, A., SIEDLAR, M., FRANKENBERGER, M., FRANKENBERGER, B., ESPEVIK, T. & ZIEGLER-HEITBROCK, L. 2002. The proinflammatory CD14+CD16+DR++ monocytes are a major source of TNF. *J Immunol,* 168**,** 3536-42.

BERGER, E. A., MURPHY, P. M. & FARBER, J. M. 1999. Chemokine receptors as HIV-1 coreceptors: roles in viral entry, tropism, and disease. *Annu Rev Immunol,* 17**,** 657-700.

BIEBER, T. 2007. The pro- and anti-inflammatory properties of human antigen-presenting cells expressing the high affinity receptor for IgE (Fc epsilon RI). *Immunobiology,* 212**,** 499-503.

BIGLEY, V., HANIFFA, M., DOULATOV, S., WANG, X. N., DICKINSON, R., MCGOVERN, N., JARDINE, L., PAGAN, S., DIMMICK, I., CHUA, I., WALLIS, J., LORDAN, J., MORGAN, C., KUMARARATNE, D. S., DOFFINGER, R., VAN DER BURG, M., VAN DONGEN, J., CANT, A., DICK, J. E., HAMBLETON, S. & COLLIN, M. 2011. The human syndrome of dendritic cell, monocyte, B and NK lymphoid deficiency. *J Exp Med,* 208**,** 227-34.

BIRKENBACH, M., JOSEFSEN, K., YALAMANCHILI, R., LENOIR, G. & KIEFF, E. 1993. Epstein-Barr virus-induced genes: first lymphocyte-specific G protein-coupled peptide receptors. *J Virol,* 67**,** 2209-20.

BLUESTONE, J. A., MACKAY, C. R., O'SHEA, J. J. & STOCKINGER, B. 2009. The functional plasticity of T cell subsets. *Nat Rev Immunol,* 9**,** 811-6.

BLUMENSTEIN, M., BOEKSTEGERS, P., FRAUNBERGER, P., ANDREESEN, R., ZIEGLER-HEITBROCK, H. W. & FINGERLE-ROWSON, G. 1997. Cytokine production precedes the expansion of CD14+CD16+ monocytes in human sepsis: a case report of a patient with self-induced septicemia. *Shock,* 8**,** 73-5.

BOLTJES, A. & VAN WIJK, F. 2014. Human dendritic cell functional specialization in steady-state and inflammation. *Front Immunol,* 5**,** 131.

BORING, L., GOSLING, J., CHENSUE, S. W., KUNKEL, S. L., FARESE, R. V., JR., BROXMEYER, H. E. & CHARO, I. F. 1997. Impaired monocyte migration and reduced type 1 (Th1) cytokine responses in C-C chemokine receptor 2 knockout mice. *J Clin Invest,* 100**,** 2552-61.

BORKOWSKI, T. A., LETTERIO, J. J., FARR, A. G. & UDEY, M. C. 1996. A role for endogenous transforming growth factor beta 1 in Langerhans cell biology: the skin of transforming growth factor beta 1 null mice is devoid of epidermal Langerhans cells. *J Exp Med,* 184**,** 2417-22.

BREITFELD, D., OHL, L., KREMMER, E., ELLWART, J., SALLUSTO, F., LIPP, M. & FORSTER, R. 2000. Follicular B helper T cells express CXC chemokine receptor 5, localize to B cell follicles, and support immunoglobulin production. *J Exp Med,* 192**,** 1545-52.

BRUMMELKAMP, T. R., BERNARDS, R. & AGAMI, R. 2002. A system for stable expression of short interfering RNAs in mammalian cells. *Science,* 296**,** 550-3.

BRYCE, P. J., MATHIAS, C. B., HARRISON, K. L., WATANABE, T., GEHA, R. S. & OETTGEN, H. C. 2006. The H1 histamine receptor regulates allergic lung responses. *J Clin Invest,* 116**,** 1624-32.

BURNS, J. M., SUMMERS, B. C., WANG, Y., MELIKIAN, A., BERAHOVICH, R., MIAO, Z., PENFOLD, M. E., SUNSHINE, M. J., LITTMAN, D. R., KUO, C. J., WEI, K., MCMASTER, B. E., WRIGHT, K., HOWARD, M. C. & SCHALL, T. J. 2006. A novel chemokine receptor for SDF-1 and I-TAC involved in cell survival, cell adhesion, and tumor development. *J Exp Med,* 203**,** 2201-13.

CANDIDO, E. P., REEVES, R. & DAVIE, J. R. 1978. Sodium butyrate inhibits histone deacetylation in cultured cells. *Cell,* 14**,** 105-13.

CAO, Q., CHEN, H., DENG, Z., YUE, J., CHEN, Q., CAO, Y., NING, L., LEI, X. & DUAN, E. 2013. Genetic deletion of Cxcl14 in mice alters uterine NK cells. *Biochem Biophys Res Commun,* 435**,** 664-70.

CAO, X., ZHANG, W., WAN, T., HE, L., CHEN, T., YUAN, Z., MA, S., YU, Y. & CHEN, G. 2000. Molecular cloning and characterization of a novel CXC chemokine macrophage inflammatory protein-2 gamma chemoattractant for human neutrophils and dendritic cells. *J Immunol,* 165**,** 2588-95.

CELLA, M., JARROSSAY, D., FACCHETTI, F., ALEBARDI, O., NAKAJIMA, H., LANZAVECCHIA, A. & COLONNA, M. 1999. Plasmacytoid monocytes migrate to inflamed lymph nodes and produce large amounts of type I interferon. *Nat Med,* 5**,** 919-23.

CHEN, L., GUO, L., TIAN, J., HE, H., MARINOVA, E., ZHANG, P., ZHENG, B. & HAN, S. 2010. Overexpression of CXC chemokine ligand 14 exacerbates collagen-induced arthritis. *J Immunol,* 184**,** 4455-9.

CHU, C. C., ALI, N., KARAGIANNIS, P., DI MEGLIO, P., SKOWERA, A., NAPOLITANO, L., BARINAGA, G., GRYS, K., SHARIF-PAGHALEH, E., KARAGIANNIS, S. N., PEAKMAN, M., LOMBARDI, G. & NESTLE, F. O. 2012. Resident CD141 (BDCA3)+ dendritic cells in human skin produce IL-10 and induce regulatory T cells that suppress skin inflammation. *J Exp Med,* 209**,** 935-45.

CLARK-LEWIS, I., DEWALD, B., LOETSCHER, M., MOSER, B. & BAGGIOLINI, M. 1994. Structural requirements for interleukin-8 function identified by design of analogs and CXC chemokine hybrids. *J Biol Chem,* 269**,** 16075-81.

CLARK-LEWIS, I., KIM, K. S., RAJARATHNAM, K., GONG, J. H., DEWALD, B., MOSER, B., BAGGIOLINI, M. & SYKES, B. D. 1995. Structure-activity relationships of chemokines. *J Leukoc Biol,* 57**,** 703-11.

CLARK-LEWIS, I., MOSER, B., WALZ, A., BAGGIOLINI, M., SCOTT, G. J. & AEBERSOLD, R. 1991. Chemical synthesis, purification, and characterization of two inflammatory proteins, neutrophil activating peptide 1 (interleukin-8) and neutrophil activating peptide. *Biochemistry,* 30**,** 3128-35.

CLORE, G. M., APPELLA, E., YAMADA, M., MATSUSHIMA, K. & GRONENBORN, A. M. 1990. Three-dimensional structure of interleukin 8 in solution. *Biochemistry,* 29**,** 1689-96.

COLLIN, M. P., HART, D. N., JACKSON, G. H., COOK, G., CAVET, J., MACKINNON, S., MIDDLETON, P. G. & DICKINSON, A. M. 2006. The fate of human Langerhans cells in hematopoietic stem cell transplantation. *J Exp Med,* 203**,** 27-33.

CONTENTO, R. L., MOLON, B., BOULARAN, C., POZZAN, T., MANES, S., MARULLO, S. & VIOLA, A. 2008. CXCR4-CCR5: a couple modulating T cell functions. *Proc Natl Acad Sci U S A,* 105**,** 10101-6.

COOK, D. N., PROSSER, D. M., FORSTER, R., ZHANG, J., KUKLIN, N. A., ABBONDANZO, S. J., NIU, X. D., CHEN, S. C., MANFRA, D. J., WIEKOWSKI, M. T., SULLIVAN, L. M., SMITH, S. R., GREENBERG, H. B., NARULA, S. K., LIPP, M. & LIRA, S. A. 2000. CCR6 mediates dendritic cell localization, lymphocyte homeostasis, and immune responses in mucosal tissue. *Immunity,* 12**,** 495-503.

CROS, J., CAGNARD, N., WOOLLARD, K., PATEY, N., ZHANG, S. Y., SENECHAL, B., PUEL, A., BISWAS, S. K., MOSHOUS, D., PICARD, C., JAIS, J. P., D'CRUZ, D., CASANOVA, J. L., TROUILLET, C. & GEISSMANN, F. 2010. Human CD14dim monocytes patrol and sense nucleic acids and viruses via TLR7 and TLR8 receptors. *Immunity,* 33**,** 375-86.

CYSTER, J. G. 2005. Chemokines, sphingosine-1-phosphate, and cell migration in secondary lymphoid organs. *Annu Rev Immunol,* 23**,** 127-59.

CZERNIELEWSKI, J. M. & DEMARCHEZ, M. 1987. Further evidence for the self-reproducing capacity of Langerhans cells in human skin. *J Invest Dermatol,* 88**,** 17-20.

DAI, C., BASILICO, P., CREMONA, T. P., COLLINS, P., MOSER, B., BENARAFA, C. & WOLF, M. 2015. CXCL14 displays antimicrobial activity against respiratory tract bacteria and contributes to clearance of Streptococcus pneumoniae pulmonary infection. *J Immunol,* 194**,** 5980-9.

DAI, X. M., RYAN, G. R., HAPEL, A. J., DOMINGUEZ, M. G., RUSSELL, R. G., KAPP, S., SYLVESTRE, V. & STANLEY, E. R. 2002. Targeted disruption of the mouse colony-stimulating factor 1 receptor gene results in osteopetrosis, mononuclear phagocyte deficiency, increased primitive progenitor cell frequencies, and reproductive defects. *Blood,* 99**,** 111-20.

DAVIE, J. R. 2003. Inhibition of histone deacetylase activity by butyrate. *J Nutr,* 133**,** 2485S-2493S.

DAVIES, L. C., JENKINS, S. J., ALLEN, J. E. & TAYLOR, P. R. 2013a. Tissue-resident macrophages. *Nat Immunol,* 14**,** 986-95.

DAVIES, L. C., ROSAS, M., JENKINS, S. J., LIAO, C. T., SCURR, M. J., BROMBACHER, F., FRASER, D. J., ALLEN, J. E., JONES, S. A. & TAYLOR, P. R. 2013b. Distinct bone marrow-derived and tissue-resident macrophage lineages proliferate at key stages during inflammation. *Nat Commun,* 4**,** 1886.

DEVRIES, M. E., KELVIN, A. A., XU, L., RAN, L., ROBINSON, J. & KELVIN, D. J. 2006. Defining the origins and evolution of the chemokine/chemokine receptor system. *J Immunol,* 176**,** 401-15.

DOMINSKA, M. & DYKXHOORN, D. M. 2010. Breaking down the barriers: siRNA delivery and endosome escape. *J Cell Sci,* 123**,** 1183-9.

EL-ASMAR, L., SPRINGAEL, J. Y., BALLET, S., ANDRIEU, E. U., VASSART, G. & PARMENTIER, M. 2005. Evidence for negative binding cooperativity within CCR5-CCR2b heterodimers. *Mol Pharmacol,* 67**,** 460-9.

EPELMAN, S., LAVINE, K. J., BEAUDIN, A. E., SOJKA, D. K., CARRERO, J. A., CALDERON, B., BRIJA, T., GAUTIER, E. L., IVANOV, S., SATPATHY, A. T., SCHILLING, J. D., SCHWENDENER, R., SERGIN, I., RAZANI, B., FORSBERG, E. C., YOKOYAMA, W. M., UNANUE, E. R., COLONNA, M., RANDOLPH, G. J. & MANN, D. L. 2014. Embryonic and adult-derived resident cardiac macrophages are maintained through distinct mechanisms at steady state and during inflammation. *Immunity,* 40**,** 91-104.

ERNST, O. P., GRAMSE, V., KOLBE, M., HOFMANN, K. P. & HECK, M. 2007. Monomeric G protein-coupled receptor rhodopsin in solution activates its G protein transducin at the diffusion limit. *Proc Natl Acad Sci U S A,* 104**,** 10859-64.

ESA, A. H., NOGA, S. J., DONNENBERG, A. D. & HESS, A. D. 1986. Immunological heterogeneity of human monocyte subsets prepared by counterflow centrifugation elutriation. *Immunology,* 59**,** 95-9.

FERNANDEZ, E. J. & LOLIS, E. 2002. Structure, function, and inhibition of chemokines. *Annu Rev Pharmacol Toxicol,* 42**,** 469-99.

FRANCO, C. B., CHEN, C. C., DRUKKER, M., WEISSMAN, I. L. & GALLI, S. J. 2010. Distinguishing mast cell and granulocyte differentiation at the single-cell level. *Cell Stem Cell,* 6**,** 361-8.

FREDERICK, M. J., HENDERSON, Y., XU, X., DEAVERS, M. T., SAHIN, A. A., WU, H., LEWIS, D. E., EL-NAGGAR, A. K. & CLAYMAN, G. L. 2000. In vivo expression of the novel CXC chemokine BRAK in normal and cancerous human tissue. *Am J Pathol,* 156**,** 1937-50.

FREDRIKSSON, R., HOGLUND, P. J., GLORIAM, D. E., LAGERSTROM, M. C. & SCHIOTH, H. B. 2003a. Seven evolutionarily conserved human rhodopsin G protein-coupled receptors lacking close relatives. *FEBS Lett,* 554**,** 381-8.

FREDRIKSSON, R., LAGERSTROM, M. C., LUNDIN, L. G. & SCHIOTH, H. B. 2003b. The G-protein-coupled receptors in the human genome form five main families. Phylogenetic analysis, paralogon groups, and fingerprints. *Mol Pharmacol,* 63**,** 1256-72.

GATTO, D., PAUS, D., BASTEN, A., MACKAY, C. R. & BRINK, R. 2009. Guidance of B cells by the orphan G protein-coupled receptor EBI2 shapes humoral immune responses. *Immunity,* 31**,** 259-69.

GEBHARDT, T., WAKIM, L. M., EIDSMO, L., READING, P. C., HEATH, W. R. & CARBONE, F. R. 2009. Memory T cells in nonlymphoid tissue that provide enhanced local immunity during infection with herpes simplex virus. *Nat Immunol,* 10**,** 524-30.

GEISSMANN, F., AUFFRAY, C., PALFRAMAN, R., WIRRIG, C., CIOCCA, A., CAMPISI, L., NARNI-MANCINELLI, E. & LAUVAU, G. 2008. Blood monocytes: distinct subsets, how they relate to dendritic cells, and their possible roles in the regulation of T-cell responses. *Immunol Cell Biol,* 86**,** 398-408.

GEISSMANN, F., JUNG, S. & LITTMAN, D. R. 2003. Blood monocytes consist of two principal subsets with distinct migratory properties. *Immunity,* 19**,** 71-82.

GEISSMANN, F., MANZ, M. G., JUNG, S., SIEWEKE, M. H., MERAD, M. & LEY, K. 2010. Development of monocytes, macrophages, and dendritic cells. *Science,* 327**,** 656-61.

GEISSMANN, F., PROST, C., MONNET, J. P., DY, M., BROUSSE, N. & HERMINE, O. 1998. Transforming growth factor beta1, in the presence of granulocyte/macrophage colony-stimulating factor and interleukin 4, induces differentiation of human peripheral blood monocytes into dendritic Langerhans cells. *J Exp Med,* 187**,** 961-6.

GINHOUX, F., GRETER, M., LEBOEUF, M., NANDI, S., SEE, P., GOKHAN, S., MEHLER, M. F., CONWAY, S. J., NG, L. G., STANLEY, E. R., SAMOKHVALOV, I. M. & MERAD, M. 2010.

Fate mapping analysis reveals that adult microglia derive from primitive macrophages. *Science,* 330**,** 841-5.

GINHOUX, F., TACKE, F., ANGELI, V., BOGUNOVIC, M., LOUBEAU, M., DAI, X. M., STANLEY, E. R., RANDOLPH, G. J. & MERAD, M. 2006. Langerhans cells arise from monocytes in vivo. *Nat Immunol,* 7**,** 265-73.

GORDON, S. 2008. Elie Metchnikoff: father of natural immunity. *Eur J Immunol,* 38**,** 3257-64.

GOUWY, M., SCHIRALDI, M., STRUYF, S., VAN DAMME, J. & UGUCCIONI, M. 2012. Possible mechanisms involved in chemokine synergy fine tuning the inflammatory response. *Immunol Lett,* 145**,** 10-4.

GOUWY, M., STRUYF, S., NOPPEN, S., SCHUTYSER, E., SPRINGAEL, J. Y., PARMENTIER, M., PROOST, P. & VAN DAMME, J. 2008. Synergy between coproduced CC and CXC chemokines in monocyte chemotaxis through receptor-mediated events. *Mol Pharmacol,* 74**,** 485-95.

GOVAERTS, C., BONDUE, A., SPRINGAEL, J. Y., OLIVELLA, M., DEUPI, X., LE POUL, E., WODAK, S. J., PARMENTIER, M., PARDO, L. & BLANPAIN, C. 2003. Activation of CCR5 by chemokines involves an aromatic cluster between transmembrane helices 2 and 3. *J Biol Chem,* 278**,** 1892-903.

GREGORIO, J., MELLER, S., CONRAD, C., DI NARDO, A., HOMEY, B., LAUERMA, A., ARAI, N., GALLO, R. L., DIGIOVANNI, J. & GILLIET, M. 2010. Plasmacytoid dendritic cells sense skin injury and promote wound healing through type I interferons. *J Exp Med,* 207**,** 2921-30.

GRIFFITH, J. W., SOKOL, C. L. & LUSTER, A. D. 2014. Chemokines and chemokine receptors: positioning cells for host defense and immunity. *Annu Rev Immunol,* 32**,** 659-702.

HAMBLETON, S., SALEM, S., BUSTAMANTE, J., BIGLEY, V., BOISSON-DUPUIS, S., AZEVEDO, J., FORTIN, A., HANIFFA, M., CERON-GUTIERREZ, L., BACON, C. M., MENON, G., TROUILLET, C., MCDONALD, D., CAREY, P., GINHOUX, F., ALSINA, L., ZUMWALT, T. J., KONG, X. F., KUMARARATNE, D., BUTLER, K., HUBEAU, M., FEINBERG, J., AL-MUHSEN, S., CANT, A., ABEL, L., CHAUSSABEL, D., DOFFINGER, R., TALESNIK, E., GRUMACH, A., DUARTE, A., ABARCA, K., MORAES-VASCONCELOS, D., BURK, D., BERGHUIS, A., GEISSMANN, F., COLLIN, M., CASANOVA, J. L. & GROS, P. 2011. IRF8 mutations and human dendritic-cell immunodeficiency. *N Engl J Med,* 365**,** 127-38.

HANDEL, T. M., JOHNSON, Z., CROWN, S. E., LAU, E. K. & PROUDFOOT, A. E. 2005. Regulation of protein function by glycosaminoglycans--as exemplified by chemokines. *Annu Rev Biochem,* 74**,** 385-410.

HANIFFA, M., GINHOUX, F., WANG, X. N., BIGLEY, V., ABEL, M., DIMMICK, I., BULLOCK, S., GRISOTTO, M., BOOTH, T., TAUB, P., HILKENS, C., MERAD, M. & COLLIN, M. 2009. Differential rates of replacement of human dermal dendritic cells and macrophages during hematopoietic stem cell transplantation. *J Exp Med,* 206**,** 371-85.

HANIFFA, M., GUNAWAN, M. & JARDINE, L. 2015. Human skin dendritic cells in health and disease. *J Dermatol Sci,* 77**,** 85-92.

HANIFFA, M., SHIN, A., BIGLEY, V., MCGOVERN, N., TEO, P., SEE, P., WASAN, P. S., WANG, X. N., MALINARICH, F., MALLERET, B., LARBI, A., TAN, P., ZHAO, H., POIDINGER, M., PAGAN, S., COOKSON, S., DICKINSON, R., DIMMICK, I., JARRETT, R. F., RENIA, L., TAM, J., SONG, C., CONNOLLY, J., CHAN, J. K., GEHRING, A., BERTOLETTI, A., COLLIN, M. & GINHOUX, F. 2012. Human tissues contain CD141hi cross-presenting dendritic cells with functional homology to mouse CD103+ nonlymphoid dendritic cells. *Immunity,* 37**,** 60-73.

HANNA, R. N., CEKIC, C., SAG, D., TACKE, R., THOMAS, G. D., NOWYHED, H., HERRLEY, E., RASQUINHA, N., MCARDLE, S., WU, R., PELUSO, E., METZGER, D., ICHINOSE, H., SHAKED, I., CHODACZEK, G., BISWAS, S. K. & HEDRICK, C. C. 2015. Patrolling monocytes control tumor metastasis to the lung. *Science,* 350**,** 985-90.

HANNEDOUCHE, S., ZHANG, J., YI, T., SHEN, W., NGUYEN, D., PEREIRA, J. P., GUERINI, D., BAUMGARTEN, B. U., ROGGO, S., WEN, B., KNOCHENMUSS, R., NOEL, S., GESSIER, F., KELLY, L. M., VANEK, M., LAURENT, S., PREUSS, I., MIAULT, C., CHRISTEN, I., KARUNA, R., LI, W., KOO, D. I., SUPLY, T., SCHMEDT, C., PETERS, E. C., FALCHETTO, R., KATOPODIS, A., SPANKA, C., ROY, M. O., DETHEUX, M., CHEN, Y. A., SCHULTZ, P. G., CHO, C. Y., SEUWEN, K., CYSTER, J. G. & SAILER, A. W. 2011. Oxysterols direct immune cell migration via EBI2. *Nature,* 475**,** 524-7.

HARA, T. & TANEGASHIMA, K. 2012. Pleiotropic functions of the CXC-type chemokine CXCL14 in mammals. *J Biochem,* 151**,** 469-76.

HARTMANN, T. N., LEICK, M., EWERS, S., DIEFENBACHER, A., SCHRAUFSTATTER, I., HONCZARENKO, M. & BURGER, M. 2008. Human B cells express the orphan chemokine receptor CRAM-A/B in a maturation-stage-dependent and CCL5-modulated manner. *Immunology,* 125**,** 252-62.

HASHIMOTO, D., MILLER, J. & MERAD, M. 2011. Dendritic cell and macrophage heterogeneity in vivo. *Immunity,* 35**,** 323-35.

HAUSER, M. A., SCHAEUBLE, K., KINDINGER, I., IMPELLIZZIERI, D., KRUEGER, W. A., HAUCK, C. R., BOYMAN, O. & LEGLER, D. F. 2016. Inflammation-Induced CCR7 Oligomers Form Scaffolds to Integrate Distinct Signaling Pathways for Efficient Cell Migration. *Immunity,* 44**,** 59-72.

HEMMI, H., YOSHINO, M., YAMAZAKI, H., NAITO, M., IYODA, T., OMATSU, Y., SHIMOYAMA, S., LETTERIO, J. J., NAKABAYASHI, T., TAGAYA, H., YAMANE, T., OGAWA, M., NISHIKAWA, S., RYOKE, K., INABA, K., HAYASHI, S. & KUNISADA, T. 2001. Skin antigens in the steady state are trafficked to regional lymph nodes by transforming growth factor-beta1-dependent cells. *Int Immunol,* 13**,** 695-704.

HEVEZI, P., MOYER, B. D., LU, M., GAO, N., WHITE, E., ECHEVERRI, F., KALABAT, D., SOTO, H., LAITA, B., LI, C., YEH, S. A., ZOLLER, M. & ZLOTNIK, A. 2009. Genome-wide analysis of gene expression in primate taste buds reveals links to diverse processes. *PLoS One,* 4**,** e6395.

HJELMSTROM, P., FJELL, J., NAKAGAWA, T., SACCA, R., CUFF, C. A. & RUDDLE, N. H. 2000. Lymphoid tissue homing chemokines are expressed in chronic inflammation. *Am J Pathol,* 156**,** 1133-8.

HOLT, P. G., HAINING, S., NELSON, D. J. & SEDGWICK, J. D. 1994. Origin and steady-state turnover of class II MHC-bearing dendritic cells in the epithelium of the conducting airways. *J Immunol,* 153**,** 256-61.

HORIKAWA, Y., ODA, N., COX, N. J., LI, X., ORHO-MELANDER, M., HARA, M., HINOKIO, Y., LINDNER, T. H., MASHIMA, H., SCHWARZ, P. E., DEL BOSQUE-PLATA, L., HORIKAWA, Y., ODA, Y., YOSHIUCHI, I., COLILLA, S., POLONSKY, K. S., WEI, S., CONCANNON, P., IWASAKI, N., SCHULZE, J., BAIER, L. J., BOGARDUS, C., GROOP, L., BOERWINKLE, E., HANIS, C. L. & BELL, G. I. 2000. Genetic variation in the gene encoding calpain-10 is associated with type 2 diabetes mellitus. *Nat Genet,* 26**,** 163-75.

HROMAS, R., BROXMEYER, H. E., KIM, C., NAKSHATRI, H., CHRISTOPHERSON, K., 2ND, AZAM, M. & HOU, Y. H. 1999. Cloning of BRAK, a novel divergent CXC chemokine preferentially expressed in normal versus malignant cells. *Biochem Biophys Res Commun,* 255**,** 703-6.

IIJIMA, N., LINEHAN, M. M., SAELAND, S. & IWASAKI, A. 2007. Vaginal epithelial dendritic cells renew from bone marrow precursors. *Proc Natl Acad Sci U S A,* 104**,** 19061-6.

IMAI, T., HIESHIMA, K., HASKELL, C., BABA, M., NAGIRA, M., NISHIMURA, M., KAKIZAKI, M., TAKAGI, S., NOMIYAMA, H., SCHALL, T. J. & YOSHIE, O. 1997. Identification and molecular characterization of fractalkine receptor CX3CR1, which mediates both leukocyte migration and adhesion. *Cell,* 91**,** 521-30.

IMMIG, K., GERICKE, M., MENZEL, F., MERZ, F., KRUEGER, M., SCHIEFENHOVEL, F., LOSCHE, A., JAGER, K., HANISCH, U. K., BIBER, K. & BECHMANN, I. 2015. CD11c-positive cells

from brain, spleen, lung, and liver exhibit site-specific immune phenotypes and plastically adapt to new environments. *Glia,* 63**,** 611-25.

INGERSOLL, M. A., SPANBROEK, R., LOTTAZ, C., GAUTIER, E. L., FRANKENBERGER, M., HOFFMANN, R., LANG, R., HANIFFA, M., COLLIN, M., TACKE, F., HABENICHT, A. J., ZIEGLER-HEITBROCK, L. & RANDOLPH, G. J. 2010. Comparison of gene expression profiles between human and mouse monocyte subsets. *Blood,* 115**,** e10-9.

ISSAFRAS, H., ANGERS, S., BULENGER, S., BLANPAIN, C., PARMENTIER, M., LABBE-JULLIE, C., BOUVIER, M. & MARULLO, S. 2002. Constitutive agonist-independent CCR5 oligomerization and antibody-mediated clustering occurring at physiological levels of receptors. *J Biol Chem,* 277**,** 34666-73.

IWATA, M., HIRAKIYAMA, A., ESHIMA, Y., KAGECHIKA, H., KATO, C. & SONG, S. Y. 2004. Retinoic acid imprints gut-homing specificity on T cells. *Immunity,* 21**,** 527-38.

JAKUBZICK, C., GAUTIER, E. L., GIBBINGS, S. L., SOJKA, D. K., SCHLITZER, A., JOHNSON, T. E., IVANOV, S., DUAN, Q., BALA, S., CONDON, T., VAN ROOIJEN, N., GRAINGER, J. R., BELKAID, Y., MA'AYAN, A., RICHES, D. W., YOKOYAMA, W. M., GINHOUX, F., HENSON, P. M. & RANDOLPH, G. J. 2013. Minimal differentiation of classical monocytes as they survey steady-state tissues and transport antigen to lymph nodes. *Immunity,* 39**,** 599-610.

JANEWAY, C. A., JR. 1989. Approaching the asymptote? Evolution and revolution in immunology. *Cold Spring Harb Symp Quant Biol,* 54 Pt 1**,** 1-13.

JIANG, S. & DONG, C. 2013. A complex issue on CD4(+) T-cell subsets. *Immunol Rev,* 252**,** 5-11.

JUTEL, M., WATANABE, T., KLUNKER, S., AKDIS, M., THOMET, O. A., MALOLEPSZY, J., ZAK-NEJMARK, T., KOGA, R., KOBAYASHI, T., BLASER, K. & AKDIS, C. A. 2001. Histamine regulates T-cell and antibody responses by differential expression of H1 and H2 receptors. *Nature,* 413**,** 420-5.

KABASHIMA, K., SAKATA, D., NAGAMACHI, M., MIYACHI, Y., INABA, K. & NARUMIYA, S. 2003. Prostaglandin E2-EP4 signaling initiates skin immune responses by promoting migration and maturation of Langerhans cells. *Nat Med,* 9**,** 744-9.

KANITAKIS, J., PETRUZZO, P. & DUBERNARD, J. M. 2004. Turnover of epidermal Langerhans' cells. *N Engl J Med,* 351**,** 2661-2.

KARRE, K., LJUNGGREN, H. G., PIONTEK, G. & KIESSLING, R. 1986. Selective rejection of H-2-deficient lymphoma variants suggests alternative immune defence strategy. *Nature,* 319**,** 675-8.

KENNEDY, D. W. & ABKOWITZ, J. L. 1998. Mature monocytic cells enter tissues and engraft. *Proc Natl Acad Sci U S A,* 95**,** 14944-9.

KHALIFA, M. B., CHOULIER, L., LORTAT-JACOB, H., ALTSCHUH, D. & VERNET, T. 2001. BIACORE data processing: an evaluation of the global fitting procedure. *Anal Biochem,* 293**,** 194-203.

KIM, W. K., SUN, Y., DO, H., AUTISSIER, P., HALPERN, E. F., PIATAK, M., JR., LIFSON, J. D., BURDO, T. H., MCGRATH, M. S. & WILLIAMS, K. 2010. Monocyte heterogeneity underlying phenotypic changes in monocytes according to SIV disease stage. *J Leukoc Biol,* 87**,** 557-67.

KISSENPFENNIG, A., HENRI, S., DUBOIS, B., LAPLACE-BUILHE, C., PERRIN, P., ROMANI, N., TRIPP, C. H., DOUILLARD, P., LESERMAN, L., KAISERLIAN, D., SAELAND, S., DAVOUST, J. & MALISSEN, B. 2005. Dynamics and function of Langerhans cells in vivo: dermal dendritic cells colonize lymph node areas distinct from slower migrating Langerhans cells. *Immunity,* 22**,** 643-54.

KITAYA, K. & YAMADA, H. 2011. Pathophysiological roles of chemokines in human reproduction: an overview. *Am J Reprod Immunol,* 65**,** 449-59.

KOENEN, R. R., VON HUNDELSHAUSEN, P., NESMELOVA, I. V., ZERNECKE, A., LIEHN, E. A., SARABI, A., KRAMP, B. K., PICCININI, A. M., PALUDAN, S. R., KOWALSKA, M. A.,

KUNGL, A. J., HACKENG, T. M., MAYO, K. H. & WEBER, C. 2009. Disrupting functional interactions between platelet chemokines inhibits atherosclerosis in hyperlipidemic mice. *Nat Med,* 15**,** 97-103.

KOHRGRUBER, N., HALANEK, N., GROGER, M., WINTER, D., RAPPERSBERGER, K., SCHMITT-EGENOLF, M., STINGL, G. & MAURER, D. 1999. Survival, maturation, and function of CD11c- and CD11c+ peripheral blood dendritic cells are differentially regulated by cytokines. *J Immunol,* 163**,** 3250-9.

KROHN, S., GARIN, A., GABAY, C. & PROUDFOOT, A. E. 2013. The Activity of CCL18 is Principally Mediated through Interaction with Glycosaminoglycans. *Front Immunol,* 4**,** 193.

KRUSE, P. H., MATTA, J., UGOLINI, S. & VIVIER, E. 2014. Natural cytotoxicity receptors and their ligands. *Immunol Cell Biol,* 92**,** 221-9.

KUANG, H., CHEN, Q., FAN, X., ZHANG, Y., ZHANG, L., PENG, H., CAO, Y. & DUAN, E. 2009a. CXCL14 inhibits trophoblast outgrowth via a paracrine/autocrine manner during early pregnancy in mice. *J Cell Physiol,* 221**,** 448-57.

KUANG, H., CHEN, Q., ZHANG, Y., ZHANG, L., PENG, H., NING, L., CAO, Y. & DUAN, E. 2009b. The cytokine gene CXCL14 restricts human trophoblast cell invasion by suppressing gelatinase activity. *Endocrinology,* 150**,** 5596-605.

KUMAMOTO, T., SHALHEVET, D., MATSUE, H., MUMMERT, M. E., WARD, B. R., JESTER, J. V. & TAKASHIMA, A. 2003. Hair follicles serve as local reservoirs of skin mast cell precursors. *Blood,* 102**,** 1654-60.

KURTH, I., WILLIMANN, K., SCHAERLI, P., HUNZIKER, T., CLARK-LEWIS, I. & MOSER, B. 2001. Monocyte selectivity and tissue localization suggests a role for breast and kidney-expressed chemokine (BRAK) in macrophage development. *J Exp Med,* 194**,** 855-61.

KUSCHER, K., DANELON, G., PAOLETTI, S., STEFANO, L., SCHIRALDI, M., PETKOVIC, V., LOCATI, M., GERBER, B. O. & UGUCCIONI, M. 2009. Synergy-inducing chemokines enhance CCR2 ligand activities on monocytes. *Eur J Immunol,* 39**,** 1118-28.

KUSZAK, A. J., PITCHIAYA, S., ANAND, J. P., MOSBERG, H. I., WALTER, N. G. & SUNAHARA, R. K. 2009. Purification and functional reconstitution of monomeric mu-opioid receptors: allosteric modulation of agonist binding by Gi2. *J Biol Chem,* 284**,** 26732-41.

LARSEN, C. P., STEINMAN, R. M., WITMER-PACK, M., HANKINS, D. F., MORRIS, P. J. & AUSTYN, J. M. 1990. Migration and maturation of Langerhans cells in skin transplants and explants. *J Exp Med,* 172**,** 1483-93.

LAWRENCE, T. & NATOLI, G. 2011. Transcriptional regulation of macrophage polarization: enabling diversity with identity. *Nat Rev Immunol,* 11**,** 750-61.

LEGLER, D. F., LOETSCHER, M., ROOS, R. S., CLARK-LEWIS, I., BAGGIOLINI, M. & MOSER, B. 1998. B cell-attracting chemokine 1, a human CXC chemokine expressed in lymphoid tissues, selectively attracts B lymphocytes via BLR1/CXCR5. *J Exp Med,* 187**,** 655-60.

LEICK, M., CATUSSE, J., FOLLO, M., NIBBS, R. J., HARTMANN, T. N., VEELKEN, H. & BURGER, M. 2010. CCL19 is a specific ligand of the constitutively recycling atypical human chemokine receptor CRAM-B. *Immunology,* 129**,** 536-46.

LENZ, A., HEINE, M., SCHULER, G. & ROMANI, N. 1993. Human and murine dermis contain dendritic cells. Isolation by means of a novel method and phenotypical and functional characterization. *J Clin Invest,* 92**,** 2587-96.

LIU, C., YANG, X. V., WU, J., KUEI, C., MANI, N. S., ZHANG, L., YU, J., SUTTON, S. W., QIN, N., BANIE, H., KARLSSON, L., SUN, S. & LOVENBERG, T. W. 2011a. Oxysterols direct B-cell migration through EBI2. *Nature,* 475**,** 519-23.

LIU, F. T., GOODARZI, H. & CHEN, H. Y. 2011b. IgE, mast cells, and eosinophils in atopic dermatitis. *Clin Rev Allergy Immunol,* 41**,** 298-310.

LIVAK, K. J. & SCHMITTGEN, T. D. 2001. Analysis of relative gene expression data using real-time quantitative PCR and the 2(-Delta Delta C(T)) Method. *Methods,* 25**,** 402-8.

LOETSCHER, M., GERBER, B., LOETSCHER, P., JONES, S. A., PIALI, L., CLARK-LEWIS, I., BAGGIOLINI, M. & MOSER, B. 1996. Chemokine receptor specific for IP10 and mig: structure, function, and expression in activated T-lymphocytes. *J Exp Med,* 184**,** 963-9.

LORTAT-JACOB, H. 2009. The molecular basis and functional implications of chemokine interactions with heparan sulphate. *Curr Opin Struct Biol,* 19**,** 543-8.

LORTAT-JACOB, H., GROSDIDIER, A. & IMBERTY, A. 2002. Structural diversity of heparan sulfate binding domains in chemokines. *Proc Natl Acad Sci U S A,* 99**,** 1229-34.

LOVE, P. E. & BHANDOOLA, A. 2011. Signal integration and crosstalk during thymocyte migration and emigration. *Nat Rev Immunol,* 11**,** 469-77.

LU, J., CHATTERJEE, M., SCHMID, H., BECK, S. & GAWAZ, M. 2016. CXCL14 as an emerging immune and inflammatory modulator. *J Inflamm (Lond),* 13**,** 1.

LUDWIG, M. G., VANEK, M., GUERINI, D., GASSER, J. A., JONES, C. E., JUNKER, U., HOFSTETTER, H., WOLF, R. M. & SEUWEN, K. 2003. Proton-sensing G-protein-coupled receptors. *Nature,* 425**,** 93-8.

LUTTRELL, L. M. & LEFKOWITZ, R. J. 2002. The role of beta-arrestins in the termination and transduction of G-protein-coupled receptor signals. *J Cell Sci,* 115**,** 455-65.

MAERKI, C., MEUTER, S., LIEBI, M., MUHLEMANN, K., FREDERICK, M. J., YAWALKAR, N., MOSER, B. & WOLF, M. 2009. Potent and broad-spectrum antimicrobial activity of CXCL14 suggests an immediate role in skin infections. *J Immunol,* 182**,** 507-14.

MALOSSE, C. & HENRI, S. 2016. Isolation of Mouse Dendritic Cell Subsets and Macrophages from the Skin. *Methods Mol Biol,* 1423**,** 129-37.

MANTOVANI, A., SICA, A. & LOCATI, M. 2005. Macrophage polarization comes of age. *Immunity,* 23**,** 344-6.

MARAVILLAS-MONTERO, J. L., BURKHARDT, A. M., HEVEZI, P. A., CARNEVALE, C. D., SMIT, M. J. & ZLOTNIK, A. 2015. Cutting edge: GPR35/CXCR8 is the receptor of the mucosal chemokine CXCL17. *J Immunol,* 194**,** 29-33.

MARTINEZ, F. O. & GORDON, S. 2014. The M1 and M2 paradigm of macrophage activation: time for reassessment. *F1000Prime Rep,* 6**,** 13.

MARTINEZ, L. B., WALSH, S. M., JACOBSEN, M. T., SATO, S., WIEDERIN, J., CIBOROWSKI, P. & IKEZU, T. 2009. Calpain and proteasomal regulation of antiretroviral zinc finger protein OTK18 in human macrophages: visualization in live cells by intramolecular FRET. *J Neuroimmune Pharmacol,* 4**,** 116-28.

MARTINEZ MUNOZ, L., LUCAS, P., NAVARRO, G., CHECA, A. I., FRANCO, R., MARTINEZ, A. C., RODRIGUEZ-FRADE, J. M. & MELLADO, M. 2009. Dynamic regulation of CXCR1 and CXCR2 homo- and heterodimers. *J Immunol,* 183**,** 7337-46.

MASOPUST, D. & SCHENKEL, J. M. 2013. The integration of T cell migration, differentiation and function. *Nat Rev Immunol,* 13**,** 309-20.

MATLOUBIAN, M., DAVID, A., ENGEL, S., RYAN, J. E. & CYSTER, J. G. 2000. A transmembrane CXC chemokine is a ligand for HIV-coreceptor Bonzo. *Nat Immunol,* 1**,** 298-304.

MCCULLY, M. L., COLLINS, P. J., HUGHES, T. R., THOMAS, C. P., BILLEN, J., O'DONNELL, V. B. & MOSER, B. 2015. Skin Metabolites Define a New Paradigm in the Localization of Skin Tropic Memory T Cells. *J Immunol,* 195**,** 96-104.

MCCULLY, M. L., LADELL, K., HAKOBYAN, S., MANSEL, R. E., PRICE, D. A. & MOSER, B. 2012. Epidermis instructs skin homing receptor expression in human T cells. *Blood,* 120**,** 4591-8.

MCCULLY, M. L. & MOSER, B. 2011. The human cutaneous chemokine system. *Front Immunol,* 2**,** 33.

MCDERMOTT, D. H., GAO, J. L., LIU, Q., SIWICKI, M., MARTENS, C., JACOBS, P., VELEZ, D., YIM, E., BRYKE, C. R., HSU, N., DAI, Z., MARQUESEN, M. M., STREGEVSKY, E., KWATEMAA, N., THEOBALD, N., LONG PRIEL, D. A., PITTALUGA, S., RAFFELD, M. A., CALVO, K. R., MARIC, I., DESMOND, R., HOLMES, K. L., KUHNS, D. B., BALABANIAN, K., BACHELERIE,

F., PORCELLA, S. F., MALECH, H. L. & MURPHY, P. M. 2015. Chromothriptic cure of WHIM syndrome. *Cell,* 160**,** 686-99.

MCGOVERN, N., SCHLITZER, A., GUNAWAN, M., JARDINE, L., SHIN, A., POYNER, E., GREEN, K., DICKINSON, R., WANG, X. N., LOW, D., BEST, K., COVINS, S., MILNE, P., PAGAN, S., ALJEFRI, K., WINDEBANK, M., MIRANDA-SAAVEDRA, D., LARBI, A., WASAN, P. S., DUAN, K., POIDINGER, M., BIGLEY, V., GINHOUX, F., COLLIN, M. & HANIFFA, M. 2014. Human dermal CD14(+) cells are a transient population of monocyte-derived macrophages. *Immunity,* 41**,** 465-77.

MEISER, A., MUELLER, A., WISE, E. L., MCDONAGH, E. M., PETIT, S. J., SARAN, N., CLARK, P. C., WILLIAMS, T. J. & PEASE, J. E. 2008. The chemokine receptor CXCR3 is degraded following internalization and is replenished at the cell surface by de novo synthesis of receptor. *J Immunol,* 180**,** 6713-24.

MELLADO, M., RODRIGUEZ-FRADE, J. M., MANES, S. & MARTINEZ, A. C. 2001a. Chemokine signaling and functional responses: the role of receptor dimerization and TK pathway activation. *Annu Rev Immunol,* 19**,** 397-421.

MELLADO, M., RODRIGUEZ-FRADE, J. M., VILA-CORO, A. J., FERNANDEZ, S., MARTIN DE ANA, A., JONES, D. R., TORAN, J. L. & MARTINEZ, A. C. 2001b. Chemokine receptor homo- or heterodimerization activates distinct signaling pathways. *EMBO J,* 20**,** 2497-507.

MERAD, M., GINHOUX, F. & COLLIN, M. 2008. Origin, homeostasis and function of Langerhans cells and other langerin-expressing dendritic cells. *Nat Rev Immunol,* 8**,** 935-47.

MERAD, M., MANZ, M. G., KARSUNKY, H., WAGERS, A., PETERS, W., CHARO, I., WEISSMAN, I. L., CYSTER, J. G. & ENGLEMAN, E. G. 2002. Langerhans cells renew in the skin throughout life under steady-state conditions. *Nat Immunol,* 3**,** 1135-41.

MERCIER, F. E., RAGU, C. & SCADDEN, D. T. 2012. The bone marrow at the crossroads of blood and immunity. *Nat Rev Immunol,* 12**,** 49-60.

MEUTER, S. & MOSER, B. 2008. Constitutive expression of CXCL14 in healthy human and murine epithelial tissues. *Cytokine,* 44**,** 248-55.

MEUTER, S., SCHAERLI, P., ROOS, R. S., BRANDAU, O., BOSL, M. R., VON ANDRIAN, U. H. & MOSER, B. 2007. Murine CXCL14 is dispensable for dendritic cell function and localization within peripheral tissues. *Mol Cell Biol,* 27**,** 983-92.

MILLER, L. S. & MODLIN, R. L. 2007. Human keratinocyte Toll-like receptors promote distinct immune responses. *J Invest Dermatol,* 127**,** 262-3.

MOGI, C., TOMURA, H., TOBO, M., WANG, J. Q., DAMIRIN, A., KON, J., KOMACHI, M., HASHIMOTO, K., SATO, K. & OKAJIMA, F. 2005. Sphingosylphosphorylcholine antagonizes proton-sensing ovarian cancer G-protein-coupled receptor 1 (OGR1)-mediated inositol phosphate production and cAMP accumulation. *J Pharmacol Sci,* 99**,** 160-7.

MOKHTAR, N. M., CHENG, C. W., COOK, E., BIELBY, H., SMITH, S. K. & CHARNOCK-JONES, D. S. 2010. Progestin regulates chemokine (C-X-C motif) ligand 14 transcript level in human endometrium. *Mol Hum Reprod,* 16**,** 170-7.

MOMBAERTS, P. 2004. Genes and ligands for odorant, vomeronasal and taste receptors. *Nat Rev Neurosci,* 5**,** 263-78.

MONIUSZKO, M., BODZENTA-LUKASZYK, A., KOWAL, K., LENCZEWSKA, D. & DABROWSKA, M. 2009. Enhanced frequencies of CD14++CD16+, but not CD14+CD16+, peripheral blood monocytes in severe asthmatic patients. *Clin Immunol,* 130**,** 338-46.

MONTECLARO, F. S. & CHARO, I. F. 1996. The amino-terminal extracellular domain of the MCP-1 receptor, but not the RANTES/MIP-1alpha receptor, confers chemokine selectivity. Evidence for a two-step mechanism for MCP-1 receptor activation. *J Biol Chem,* 271**,** 19084-92.

MORETTA, L. & MORETTA, A. 2004. Killer immunoglobulin-like receptors. *Curr Opin Immunol,* 16**,** 626-33.

MORTIER, A., VAN DAMME, J. & PROOST, P. 2008. Regulation of chemokine activity by posttranslational modification. *Pharmacol Ther,* 120**,** 197-217.

MUELLER, S. N., ZAID, A. & CARBONE, F. R. 2014. Tissue-resident T cells: dynamic players in skin immunity. *Front Immunol,* 5**,** 332.

MUROOKA, T. T., WONG, M. M., RAHBAR, R., MAJCHRZAK-KITA, B., PROUDFOOT, A. E. & FISH, E. N. 2006. CCL5-CCR5-mediated apoptosis in T cells: Requirement for glycosaminoglycan binding and CCL5 aggregation. *J Biol Chem,* 281**,** 25184-94.

MURPHY, P. M., BAGGIOLINI, M., CHARO, I. F., HEBERT, C. A., HORUK, R., MATSUSHIMA, K., MILLER, L. H., OPPENHEIM, J. J. & POWER, C. A. 2000. International union of pharmacology. XXII. Nomenclature for chemokine receptors. *Pharmacol Rev,* 52**,** 145-76.

NAKAYAMADA, S., TAKAHASHI, H., KANNO, Y. & O'SHEA, J. J. 2012. Helper T cell diversity and plasticity. *Curr Opin Immunol,* 24**,** 297-302.

NEEL, N. F., SCHUTYSER, E., SAI, J., FAN, G. H. & RICHMOND, A. 2005. Chemokine receptor internalization and intracellular trafficking. *Cytokine Growth Factor Rev,* 16**,** 637-58.

NESMELOVA, I. V., SHAM, Y., DUDEK, A. Z., VAN EIJK, L. I., WU, G., SLUNGAARD, A., MORTARI, F., GRIFFIOEN, A. W. & MAYO, K. H. 2005. Platelet factor 4 and interleukin-8 CXC chemokine heterodimer formation modulates function at the quaternary structural level. *J Biol Chem,* 280**,** 4948-58.

NESTLE, F. O., DI MEGLIO, P., QIN, J. Z. & NICKOLOFF, B. J. 2009. Skin immune sentinels in health and disease. *Nat Rev Immunol,* 9**,** 679-91.

NESTLE, F. O., ZHENG, X. G., THOMPSON, C. B., TURKA, L. A. & NICKOLOFF, B. J. 1993. Characterization of dermal dendritic cells obtained from normal human skin reveals phenotypic and functionally distinctive subsets. *J Immunol,* 151**,** 6535-45.

NIBBS, R. J. & GRAHAM, G. J. 2013. Immune regulation by atypical chemokine receptors. *Nat Rev Immunol,* 13**,** 815-29.

NICOLAOU, A. 2013. Eicosanoids in skin inflammation. *Prostaglandins Leukot Essent Fatty Acids,* 88**,** 131-8.

NOMIYAMA, H. & YOSHIE, O. 2015. Functional roles of evolutionary conserved motifs and residues in vertebrate chemokine receptors. *J Leukoc Biol,* 97**,** 39-47.

NYGAARD, R., FRIMURER, T. M., HOLST, B., ROSENKILDE, M. M. & SCHWARTZ, T. W. 2009. Ligand binding and micro-switches in 7TM receptor structures. *Trends Pharmacol Sci,* 30**,** 249-59.

O'DOWD, B. F., NGUYEN, T., MARCHESE, A., CHENG, R., LYNCH, K. R., HENG, H. H., KOLAKOWSKI, L. F., JR. & GEORGE, S. R. 1998. Discovery of three novel G-protein-coupled receptor genes. *Genomics,* 47**,** 310-3.

O'HAYRE, M., SALANGA, C. L., HANDEL, T. M. & ALLEN, S. J. 2008. Chemokines and cancer: migration, intracellular signalling and intercellular communication in the microenvironment. *Biochem J,* 409**,** 635-49.

OBERLIN, E., AMARA, A., BACHELERIE, F., BESSIA, C., VIRELIZIER, J. L., ARENZANA-SEISDEDOS, F., SCHWARTZ, O., HEARD, J. M., CLARK-LEWIS, I., LEGLER, D. F., LOETSCHER, M., BAGGIOLINI, M. & MOSER, B. 1996. The CXC chemokine SDF-1 is the ligand for LESTR/fusin and prevents infection by T-cell-line-adapted HIV-1. *Nature,* 382**,** 833-5.

OHL, L., MOHAUPT, M., CZELOTH, N., HINTZEN, G., KIAFARD, Z., ZWIRNER, J., BLANKENSTEIN, T., HENNING, G. & FORSTER, R. 2004. CCR7 governs skin dendritic cell migration under inflammatory and steady-state conditions. *Immunity,* 21**,** 279-88.

OO, Y. H., WESTON, C. J., LALOR, P. F., CURBISHLEY, S. M., WITHERS, D. R., REYNOLDS, G. M., SHETTY, S., HARKI, J., SHAW, J. C., EKSTEEN, B., HUBSCHER, S. G., WALKER, L. S. & ADAMS, D. H. 2010. Distinct roles for CCR4 and CXCR3 in the recruitment and positioning of regulatory T cells in the inflamed human liver. *J Immunol,* 184**,** 2886-98.

OTTE, M., KLIEWER, A., SCHUTZ, D., REIMANN, C., SCHULZ, S. & STUMM, R. 2014. CXCL14 is no direct modulator of CXCR4. *FEBS Lett,* 588**,** 4769-75.

OVERINGTON, J. P., AL-LAZIKANI, B. & HOPKINS, A. L. 2006. How many drug targets are there? *Nat Rev Drug Discov,* 5**,** 993-6.

OZAWA, S., KATO, Y., KOMORI, R., MAEHATA, Y., KUBOTA, E. & HATA, R. 2006. BRAK/CXCL14 expression suppresses tumor growth in vivo in human oral carcinoma cells. *Biochem Biophys Res Commun,* 348**,** 406-12.

PABLOS, J. L., AMARA, A., BOULOC, A., SANTIAGO, B., CARUZ, A., GALINDO, M., DELAUNAY, T., VIRELIZIER, J. L. & ARENZANA-SEISDEDOS, F. 1999. Stromal-cell derived factor is expressed by dendritic cells and endothelium in human skin. *Am J Pathol,* 155**,** 1577-86.

PALCZEWSKI, K., KUMASAKA, T., HORI, T., BEHNKE, C. A., MOTOSHIMA, H., FOX, B. A., LE TRONG, I., TELLER, D. C., OKADA, T., STENKAMP, R. E., YAMAMOTO, M. & MIYANO, M. 2000. Crystal structure of rhodopsin: A G protein-coupled receptor. *Science,* 289**,** 739-45.

PANZER, U. & UGUCCIONI, M. 2004. Prostaglandin E2 modulates the functional responsiveness of human monocytes to chemokines. *Eur J Immunol,* 34**,** 3682-9.

PAOLETTI, S., PETKOVIC, V., SEBASTIANI, S., DANELON, M. G., UGUCCIONI, M. & GERBER, B. O. 2005. A rich chemokine environment strongly enhances leukocyte migration and activities. *Blood,* 105**,** 3405-12.

PATEL, J., CHANNON, K. M. & MCNEILL, E. 2013. The downstream regulation of chemokine receptor signalling: implications for atherosclerosis. *Mediators Inflamm,* 2013**,** 459520.

PENNISI, E. 2012. Genomics. ENCODE project writes eulogy for junk DNA. *Science,* 337**,** 1159, 1161.

PERDIGUERO, E. G. & GEISSMANN, F. 2016. The development and maintenance of resident macrophages. *Nat Immunol,* 17**,** 2-8.

PEREIRA, J. P., KELLY, L. M., XU, Y. & CYSTER, J. G. 2009. EBI2 mediates B cell segregation between the outer and centre follicle. *Nature,* 460**,** 1122-6.

PETIT, I., SZYPER-KRAVITZ, M., NAGLER, A., LAHAV, M., PELED, A., HABLER, L., PONOMARYOV, T., TAICHMAN, R. S., ARENZANA-SEISDEDOS, F., FUJII, N., SANDBANK, J., ZIPORI, D. & LAPIDOT, T. 2002. G-CSF induces stem cell mobilization by decreasing bone marrow SDF-1 and up-regulating CXCR4. *Nat Immunol,* 3**,** 687-94.

PETKOVIC, V., MOGHINI, C., PAOLETTI, S., UGUCCIONI, M. & GERBER, B. 2004. I-TAC/CXCL11 is a natural antagonist for CCR5. *J Leukoc Biol,* 76**,** 701-8.

PICCIOLI, D., TAVARINI, S., BORGOGNI, E., STERI, V., NUTI, S., SAMMICHELI, C., BARDELLI, M., MONTAGNA, D., LOCATELLI, F. & WACK, A. 2007. Functional specialization of human circulating CD16 and CD1c myeloid dendritic-cell subsets. *Blood,* 109**,** 5371-9.

PISABARRO, M. T., LEUNG, B., KWONG, M., CORPUZ, R., FRANTZ, G. D., CHIANG, N., VANDLEN, R., DIEHL, L. J., SKELTON, N., KIM, H. S., EATON, D. & SCHMIDT, K. N. 2006. Cutting edge: novel human dendritic cell- and monocyte-attracting chemokine-like protein identified by fold recognition methods. *J Immunol,* 176**,** 2069-73.

PITZALIS, C., JONES, G. W., BOMBARDIERI, M. & JONES, S. A. 2014. Ectopic lymphoid-like structures in infection, cancer and autoimmunity. *Nat Rev Immunol,* 14**,** 447-62.

PROUDFOOT, A. E. 2006. The biological relevance of chemokine-proteoglycan interactions. *Biochem Soc Trans,* 34**,** 422-6.

PROUDFOOT, A. E., HANDEL, T. M., JOHNSON, Z., LAU, E. K., LIWANG, P., CLARK-LEWIS, I., BORLAT, F., WELLS, T. N. & KOSCO-VILBOIS, M. H. 2003. Glycosaminoglycan binding and oligomerization are essential for the in vivo activity of certain chemokines. *Proc Natl Acad Sci U S A,* 100**,** 1885-90.

PROUDFOOT, A. E. & UGUCCIONI, M. 2016. Modulation of Chemokine Responses: Synergy and Cooperativity. *Front Immunol,* 7**,** 183.

QIN, S., ROTTMAN, J. B., MYERS, P., KASSAM, N., WEINBLATT, M., LOETSCHER, M., KOCH, A. E., MOSER, B. & MACKAY, C. R. 1998. The chemokine receptors CXCR3 and CCR5 mark subsets of T cells associated with certain inflammatory reactions. *J Clin Invest,* 101**,** 746-54.

RAJAGOPALAN, L. & RAJARATHNAM, K. 2006. Structural basis of chemokine receptor function--a model for binding affinity and ligand selectivity. *Biosci Rep,* 26**,** 325-39.

RAJARATHNAM, K., SYKES, B. D., KAY, C. M., DEWALD, B., GEISER, T., BAGGIOLINI, M. & CLARK-LEWIS, I. 1994. Neutrophil activation by monomeric interleukin-8. *Science,* 264**,** 90-2.

RANDOLPH, G. J., OCHANDO, J. & PARTIDA-SANCHEZ, S. 2008. Migration of dendritic cell subsets and their precursors. *Annu Rev Immunol,* 26**,** 293-316.

RANDOLPH, G. J., SANCHEZ-SCHMITZ, G., LIEBMAN, R. M. & SCHAKEL, K. 2002. The CD16(+) (FcgammaRIII(+)) subset of human monocytes preferentially becomes migratory dendritic cells in a model tissue setting. *J Exp Med,* 196**,** 517-27.

ROACH, T., SLATER, S., KOVAL, M., WHITE, L., CAHIR MCFARLAND, E. D., OKUMURA, M., THOMAS, M. & BROWN, E. 1997. CD45 regulates Src family member kinase activity associated with macrophage integrin-mediated adhesion. *Curr Biol,* 7**,** 408-17.

ROBINSON, S. P., PATTERSON, S., ENGLISH, N., DAVIES, D., KNIGHT, S. C. & REID, C. D. 1999. Human peripheral blood contains two distinct lineages of dendritic cells. *Eur J Immunol,* 29**,** 2769-78.

RODRIGUEZ-FRADE, J. M., MARTINEZ-MUNOZ, L., VILLARES, R., CASCIO, G., LUCAS, P., GOMARIZ, R. P. & MELLADO, M. 2016. Chemokine Detection Using Receptors Immobilized on an SPR Sensor Surface. *Methods Enzymol,* 570**,** 1-18.

ROSSI, D. & ZLOTNIK, A. 2000. The biology of chemokines and their receptors. *Annu Rev Immunol,* 18**,** 217-42.

SABROE, I., PECK, M. J., VAN KEULEN, B. J., JORRITSMA, A., SIMMONS, G., CLAPHAM, P. R., WILLIAMS, T. J. & PEASE, J. E. 2000. A small molecule antagonist of chemokine receptors CCR1 and CCR3. Potent inhibition of eosinophil function and CCR3-mediated HIV-1 entry. *J Biol Chem,* 275**,** 25985-92.

SADIR, R., IMBERTY, A., BALEUX, F. & LORTAT-JACOB, H. 2004. Heparan sulfate/heparin oligosaccharides protect stromal cell-derived factor-1 (SDF-1)/CXCL12 against proteolysis induced by CD26/dipeptidyl peptidase IV. *J Biol Chem,* 279**,** 43854-60.

SALLUSTO, F. & LANZAVECCHIA, A. 1994. Efficient presentation of soluble antigen by cultured human dendritic cells is maintained by granulocyte/macrophage colony-stimulating factor plus interleukin 4 and downregulated by tumor necrosis factor alpha. *J Exp Med,* 179**,** 1109-18.

SALLUSTO, F., LENIG, D., FORSTER, R., LIPP, M. & LANZAVECCHIA, A. 1999. Two subsets of memory T lymphocytes with distinct homing potentials and effector functions. *Nature,* 401**,** 708-12.

SALOGNI, L., MUSSO, T., BOSISIO, D., MIROLO, M., JALA, V. R., HARIBABU, B., LOCATI, M. & SOZZANI, S. 2009. Activin A induces dendritic cell migration through the polarized release of CXC chemokine ligands 12 and 14. *Blood,* 113**,** 5848-56.

SANCHEZ-TORRES, C., GARCIA-ROMO, G. S., CORNEJO-CORTES, M. A., RIVAS-CARVALHO, A. & SANCHEZ-SCHMITZ, G. 2001. CD16+ and CD16- human blood monocyte subsets differentiate in vitro to dendritic cells with different abilities to stimulate CD4+ T cells. *Int Immunol,* 13**,** 1571-81.

SARRAZIN, S., BONNAFFE, D., LUBINEAU, A. & LORTAT-JACOB, H. 2005. Heparan sulfate mimicry: a synthetic glycoconjugate that recognizes the heparin binding domain of interferon-gamma inhibits the cytokine activity. *J Biol Chem,* 280**,** 37558-64.

SATO, N., AHUJA, S. K., QUINONES, M., KOSTECKI, V., REDDICK, R. L., MELBY, P. C., KUZIEL, W. A. & AHUJA, S. S. 2000. CC chemokine receptor (CCR)2 is required for langerhans cell migration and localization of T helper cell type 1 (Th1)-inducing dendritic cells.

Absence of CCR2 shifts the Leishmania major-resistant phenotype to a susceptible state dominated by Th2 cytokines, b cell outgrowth, and sustained neutrophilic inflammation. *J Exp Med,* 192**,** 205-18.

SCANDELLA, E., MEN, Y., LEGLER, D. F., GILLESSEN, S., PRIKLER, L., LUDEWIG, B. & GROETTRUP, M. 2004. CCL19/CCL21-triggered signal transduction and migration of dendritic cells requires prostaglandin E2. *Blood,* 103**,** 1595-601.

SCHAERLI, P., EBERT, L., WILLIMANN, K., BLASER, A., ROOS, R. S., LOETSCHER, P. & MOSER, B. 2004. A skin-selective homing mechanism for human immune surveillance T cells. *J Exp Med,* 199**,** 1265-75.

SCHAERLI, P., WILLIMANN, K., EBERT, L. M., WALZ, A. & MOSER, B. 2005. Cutaneous CXCL14 targets blood precursors to epidermal niches for Langerhans cell differentiation. *Immunity,* 23**,** 331-42.

SCHAERLI, P., WILLIMANN, K., LANG, A. B., LIPP, M., LOETSCHER, P. & MOSER, B. 2000. CXC chemokine receptor 5 expression defines follicular homing T cells with B cell helper function. *J Exp Med,* 192**,** 1553-62.

SCHIRALDI, M., RAUCCI, A., MUNOZ, L. M., LIVOTI, E., CELONA, B., VENEREAU, E., APUZZO, T., DE MARCHIS, F., PEDOTTI, M., BACHI, A., THELEN, M., VARANI, L., MELLADO, M., PROUDFOOT, A., BIANCHI, M. E. & UGUCCIONI, M. 2012. HMGB1 promotes recruitment of inflammatory cells to damaged tissues by forming a complex with CXCL12 and signaling via CXCR4. *J Exp Med,* 209**,** 551-63.

SCHMITTGEN, T. D., ZAKRAJSEK, B. A., MILLS, A. G., GORN, V., SINGER, M. J. & REED, M. W. 2000. Quantitative reverse transcription-polymerase chain reaction to study mRNA decay: comparison of endpoint and real-time methods. *Anal Biochem,* 285**,** 194-204.

SCHOLTEN, D. J., CANALS, M., MAUSSANG, D., ROUMEN, L., SMIT, M. J., WIJTMANS, M., DE GRAAF, C., VISCHER, H. F. & LEURS, R. 2012. Pharmacological modulation of chemokine receptor function. *Br J Pharmacol,* 165**,** 1617-43.

SCHULZ, C., GOMEZ PERDIGUERO, E., CHORRO, L., SZABO-ROGERS, H., CAGNARD, N., KIERDORF, K., PRINZ, M., WU, B., JACOBSEN, S. E., POLLARD, J. W., FRAMPTON, J., LIU, K. J. & GEISSMANN, F. 2012. A lineage of myeloid cells independent of Myb and hematopoietic stem cells. *Science,* 336**,** 86-90.

SCHUMAK, B., KLOCKE, K., KUEPPER, J. M., BISWAS, A., DJIE-MALETZ, A., LIMMER, A., VAN ROOIJEN, N., MACK, M., HOERAUF, A. & DUNAY, I. R. 2015. Specific depletion of Ly6C(hi) inflammatory monocytes prevents immunopathology in experimental cerebral malaria. *PLoS One,* 10**,** e0124080.

SEBASTIANI, S., DANELON, G., GERBER, B. & UGUCCIONI, M. 2005. CCL22-induced responses are powerfully enhanced by synergy inducing chemokines via CCR4: evidence for the involvement of first beta-strand of chemokine. *Eur J Immunol,* 35**,** 746-56.

SHELLENBERGER, T. D., WANG, M., GUJRATI, M., JAYAKUMAR, A., STRIETER, R. M., BURDICK, M. D., IOANNIDES, C. G., EFFERSON, C. L., EL-NAGGAR, A. K., ROBERTS, D., CLAYMAN, G. L. & FREDERICK, M. J. 2004. BRAK/CXCL14 is a potent inhibitor of angiogenesis and a chemotactic factor for immature dendritic cells. *Cancer Res,* 64**,** 8262-70.

SHURIN, G. V., FERRIS, R. L., TOURKOVA, I. L., PEREZ, L., LOKSHIN, A., BALKIR, L., COLLINS, B., CHATTA, G. S. & SHURIN, M. R. 2005. Loss of new chemokine CXCL14 in tumor tissue is associated with low infiltration by dendritic cells (DC), while restoration of human CXCL14 expression in tumor cells causes attraction of DC both in vitro and in vivo. *J Immunol,* 174**,** 5490-8.

SIEGAL, F. P., KADOWAKI, N., SHODELL, M., FITZGERALD-BOCARSLY, P. A., SHAH, K., HO, S., ANTONENKO, S. & LIU, Y. J. 1999. The nature of the principal type 1 interferon-producing cells in human blood. *Science,* 284**,** 1835-7.

SIN, Y. M., SEDGWICK, A. D., CHEA, E. P. & WILLOUGHBY, D. A. 1986. Mast cells in newly formed lining tissue during acute inflammation: a six day air pouch model in the mouse. *Ann Rheum Dis,* 45**,** 873-7.

SINGER, II, SCOTT, S., KAWKA, D. W., CHIN, J., DAUGHERTY, B. L., DEMARTINO, J. A., DISALVO, J., GOULD, S. L., LINEBERGER, J. E., MALKOWITZ, L., MILLER, M. D., MITNAUL, L., SICILIANO, S. J., STARUCH, M. J., WILLIAMS, H. R., ZWEERINK, H. J. & SPRINGER, M. S. 2001. CCR5, CXCR4, and CD4 are clustered and closely apposed on microvilli of human macrophages and T cells. *J Virol*, 75**,** 3779-90.

SKRZECZYNSKA-MONCZNIK, J., BZOWSKA, M., LOSEKE, S., GRAGE-GRIEBENOW, E., ZEMBALA, M. & PRYJMA, J. 2008. Peripheral blood CD14high CD16+ monocytes are main producers of IL-10. *Scand J Immunol*, 67**,** 152-9.

SLEEMAN, M. A., FRASER, J. K., MURISON, J. G., KELLY, S. L., PRESTIDGE, R. L., PALMER, D. J., WATSON, J. D. & KUMBLE, K. D. 2000. B cell- and monocyte-activating chemokine (BMAC), a novel non-ELR alpha-chemokine. *Int Immunol*, 12**,** 677-89.

STANFORD, M. M. & ISSEKUTZ, T. B. 2003. The relative activity of CXCR3 and CCR5 ligands in T lymphocyte migration: concordant and disparate activities in vitro and in vivo. *J Leukoc Biol*, 74**,** 791-9.

STANLEY, E. R., CIFONE, M., HEARD, P. M. & DEFENDI, V. 1976. Factors regulating macrophage production and growth: identity of colony-stimulating factor and macrophage growth factor. *J Exp Med*, 143**,** 631-47.

STANLEY, E. R., HANSEN, G., WOODCOCK, J. & METCALF, D. 1975. Colony stimulating factor and the regulation of granulopoiesis and macrophage production. *Fed Proc*, 34**,** 2272-8.

STARNES, T., RASILA, K. K., ROBERTSON, M. J., BRAHMI, Z., DAHL, R., CHRISTOPHERSON, K. & HROMAS, R. 2006. The chemokine CXCL14 (BRAK) stimulates activated NK cell migration: implications for the downregulation of CXCL14 in malignancy. *Exp Hematol*, 34**,** 1101-5.

STEINMAN, R. M., LUSTIG, D. S. & COHN, Z. A. 1974. Identification of a novel cell type in peripheral lymphoid organs of mice. 3. Functional properties in vivo. *J Exp Med*, 139**,** 1431-45.

STOCK, A., BOOTH, S. & CERUNDOLO, V. 2011. Prostaglandin E2 suppresses the differentiation of retinoic acid-producing dendritic cells in mice and humans. *J Exp Med*, 208**,** 761-73.

STOITZNER, P., TRIPP, C. H., DOUILLARD, P., SAELAND, S. & ROMANI, N. 2005. Migratory Langerhans cells in mouse lymph nodes in steady state and inflammation. *J Invest Dermatol*, 125**,** 116-25.

STRIETER, R. M., POLVERINI, P. J., KUNKEL, S. L., ARENBERG, D. A., BURDICK, M. D., KASPER, J., DZUIBA, J., VAN DAMME, J., WALZ, A., MARRIOTT, D. & ET AL. 1995. The functional role of the ELR motif in CXC chemokine-mediated angiogenesis. *J Biol Chem*, 270**,** 27348-57.

STRONG, A. E., THIERRY, A. C., COUSIN, P., MOULON, C. & DEMOTZ, S. 2006. Synthetic chemokines directly labeled with a fluorescent dye as tools for studying chemokine and chemokine receptor interactions. *Eur Cytokine Netw*, 17**,** 49-59.

STRUYF, S., GOUWY, M., DILLEN, C., PROOST, P., OPDENAKKER, G. & VAN DAMME, J. 2005. Chemokines synergize in the recruitment of circulating neutrophils into inflamed tissue. *Eur J Immunol*, 35**,** 1583-91.

STRUYF, S., PROOST, P. & VAN DAMME, J. 2003. Regulation of the immune response by the interaction of chemokines and proteases. *Adv Immunol*, 81**,** 1-44.

SUGIMOTO, Y. & NARUMIYA, S. 2007. Prostaglandin E receptors. *J Biol Chem*, 282**,** 11613-7.

TAKAHAMA, Y. 2006. Journey through the thymus: stromal guides for T-cell development and selection. *Nat Rev Immunol*, 6**,** 127-35.

TAMOUTOUNOUR, S., GUILLIAMS, M., MONTANANA SANCHIS, F., LIU, H., TERHORST, D., MALOSSE, C., POLLET, E., ARDOUIN, L., LUCHE, H., SANCHEZ, C., DALOD, M., MALISSEN, B. & HENRI, S. 2013. Origins and functional specialization of macrophages

and of conventional and monocyte-derived dendritic cells in mouse skin. *Immunity,* 39**,** 925-38.

TANEGASHIMA, K., OKAMOTO, S., NAKAYAMA, Y., TAYA, C., SHITARA, H., ISHII, R., YONEKAWA, H., MINOKOSHI, Y. & HARA, T. 2010a. CXCL14 deficiency in mice attenuates obesity and inhibits feeding behavior in a novel environment. *PLoS One,* 5**,** e10321.

TANEGASHIMA, K., SUZUKI, K., NAKAYAMA, Y. & HARA, T. 2010b. Antibody-assisted enhancement of biological activities of CXCL14 in human monocytic leukemia-derived THP-1 cells and high fat diet-induced obese mice. *Exp Cell Res,* 316**,** 1263-70.

TANEGASHIMA, K., SUZUKI, K., NAKAYAMA, Y., TSUJI, K., SHIGENAGA, A., OTAKA, A. & HARA, T. 2013a. CXCL14 is a natural inhibitor of the CXCL12-CXCR4 signaling axis. *FEBS Lett,* 587**,** 1731-5.

TANEGASHIMA, K., TSUJI, K., SUZUKI, K., SHIGENAGA, A., OTAKA, A. & HARA, T. 2013b. Dimeric peptides of the C-terminal region of CXCL14 function as CXCL12 inhibitors. *FEBS Lett,* 587**,** 3770-5.

TANG, A., AMAGAI, M., GRANGER, L. G., STANLEY, J. R. & UDEY, M. C. 1993. Adhesion of epidermal Langerhans cells to keratinocytes mediated by E-cadherin. *Nature,* 361**,** 82-5.

THELEN, M., MUNOZ, L. M., RODRIGUEZ-FRADE, J. M. & MELLADO, M. 2010. Chemokine receptor oligomerization: functional considerations. *Curr Opin Pharmacol,* 10**,** 38-43.

THELEN, M., PEVERI, P., KERNEN, P., VON TSCHARNER, V., WALZ, A. & BAGGIOLINI, M. 1988. Mechanism of neutrophil activation by NAF, a novel monocyte-derived peptide agonist. *FASEB J,* 2**,** 2702-6.

TSOU, C. L., PETERS, W., SI, Y., SLAYMAKER, S., ASLANIAN, A. M., WEISBERG, S. P., MACK, M. & CHARO, I. F. 2007. Critical roles for CCR2 and MCP-3 in monocyte mobilization from bone marrow and recruitment to inflammatory sites. *J Clin Invest,* 117**,** 902-9.

UGUCCIONI, M., MACKAY, C. R., OCHENSBERGER, B., LOETSCHER, P., RHIS, S., LAROSA, G. J., RAO, P., PONATH, P. D., BAGGIOLINI, M. & DAHINDEN, C. A. 1997. High expression of the chemokine receptor CCR3 in human blood basophils. Role in activation by eotaxin, MCP-4, and other chemokines. *J Clin Invest,* 100**,** 1137-43.

VAIGOT, P., CZERNIELEWSKI, J. & PRUNIERAS, M. 1985. Detection of distinct subpopulations of Langerhans cells by flow cytometry and sorting. *Cytometry,* 6**,** 422-7.

VALENT, P. & BETTELHEIM, P. 1992. Cell surface structures on human basophils and mast cells: biochemical and functional characterization. *Adv Immunol,* 52**,** 333-423.

VALLADEAU, J., RAVEL, O., DEZUTTER-DAMBUYANT, C., MOORE, K., KLEIJMEER, M., LIU, Y., DUVERT-FRANCES, V., VINCENT, C., SCHMITT, D., DAVOUST, J., CAUX, C., LEBECQUE, S. & SAELAND, S. 2000. Langerin, a novel C-type lectin specific to Langerhans cells, is an endocytic receptor that induces the formation of Birbeck granules. *Immunity,* 12**,** 71-81.

VALLADEAU, J. & SAELAND, S. 2005. Cutaneous dendritic cells. *Semin Immunol,* 17**,** 273-83.

VAN FURTH, R. & COHN, Z. A. 1968. The origin and kinetics of mononuclear phagocytes. *J Exp Med,* 128**,** 415-35.

VAN FURTH, R., NIBBERING, P. H., VAN DISSEL, J. T. & DIESSELHOFF-DEN DULK, M. M. 1985. The characterization, origin, and kinetics of skin macrophages during inflammation. *J Invest Dermatol,* 85**,** 398-402.

VANBERVLIET, B., BENDRISS-VERMARE, N., MASSACRIER, C., HOMEY, B., DE BOUTEILLER, O., BRIERE, F., TRINCHIERI, G. & CAUX, C. 2003. The inducible CXCR3 ligands control plasmacytoid dendritic cell responsiveness to the constitutive chemokine stromal cell-derived factor 1 (SDF-1)/CXCL12. *J Exp Med,* 198**,** 823-30.

VENETZ, D., PONZONI, M., SCHIRALDI, M., FERRERI, A. J., BERTONI, F., DOGLIONI, C. & UGUCCIONI, M. 2010. Perivascular expression of CXCL9 and CXCL12 in primary

central nervous system lymphoma: T-cell infiltration and positioning of malignant B cells. *Int J Cancer,* 127**,** 2300-12.

VIJAYANAND, P., DURKIN, K., HARTMANN, G., MORJARIA, J., SEUMOIS, G., STAPLES, K. J., HALL, D., BESSANT, C., BARTHOLOMEW, M., HOWARTH, P. H., FRIEDMANN, P. S. & DJUKANOVIC, R. 2010. Chemokine receptor 4 plays a key role in T cell recruitment into the airways of asthmatic patients. *J Immunol,* 184**,** 4568-74.

VISHWANATH, M., NISHIBU, A., SAELAND, S., WARD, B. R., MIZUMOTO, N., PLOEGH, H. L., BOES, M. & TAKASHIMA, A. 2006. Development of intravital intermittent confocal imaging system for studying Langerhans cell turnover. *J Invest Dermatol,* 126**,** 2452-7.

WANG, H., PETERS, T., KESS, D., SINDRILARU, A., ORESHKOVA, T., VAN ROOIJEN, N., STRATIS, A., RENKL, A. C., SUNDERKOTTER, C., WLASCHEK, M., HAASE, I. & SCHARFFETTER-KOCHANEK, K. 2006. Activated macrophages are essential in a murine model for T cell-mediated chronic psoriasiform skin inflammation. *J Clin Invest,* 116**,** 2105-14.

WEINER, L. M., LI, W., HOLMES, M., CATALANO, R. B., DOVNARSKY, M., PADAVIC, K. & ALPAUGH, R. K. 1994. Phase I trial of recombinant macrophage colony-stimulating factor and recombinant gamma-interferon: toxicity, monocytosis, and clinical effects. *Cancer Res,* 54**,** 4084-90.

WENTE, M. N., MAYER, C., GAIDA, M. M., MICHALSKI, C. W., GIESE, T., BERGMANN, F., GIESE, N. A., BUCHLER, M. W. & FRIESS, H. 2008. CXCL14 expression and potential function in pancreatic cancer. *Cancer Lett,* 259**,** 209-17.

WIKTOR-JEDRZEJCZAK, W. & GORDON, S. 1996. Cytokine regulation of the macrophage (M phi) system studied using the colony stimulating factor-1-deficient op/op mouse. *Physiol Rev,* 76**,** 927-47.

WILBANKS, A., ZONDLO, S. C., MURPHY, K., MAK, S., SOLER, D., LANGDON, P., ANDREW, D. P., WU, L. & BRISKIN, M. 2001. Expression cloning of the STRL33/BONZO/TYMSTRligand reveals elements of CC, CXC, and CX3C chemokines. *J Immunol,* 166**,** 5145-54.

WILSON, S., WILKINSON, G. & MILLIGAN, G. 2005. The CXCR1 and CXCR2 receptors form constitutive homo- and heterodimers selectively and with equal apparent affinities. *J Biol Chem,* 280**,** 28663-74.

WITTENBERGER, T., SCHALLER, H. C. & HELLEBRAND, S. 2001. An expressed sequence tag (EST) data mining strategy succeeding in the discovery of new G-protein coupled receptors. *J Mol Biol,* 307**,** 799-813.

WOLF, M. & MOSER, B. 2012. Antimicrobial activities of chemokines: not just a side-effect? *Front Immunol,* 3**,** 213.

WOLLENBERG, A., MOMMAAS, M., OPPEL, T., SCHOTTDORF, E. M., GUNTHER, S. & MODERER, M. 2002. Expression and function of the mannose receptor CD206 on epidermal dendritic cells in inflammatory skin diseases. *J Invest Dermatol,* 118**,** 327-34.

WONG, K. L., TAI, J. J., WONG, W. C., HAN, H., SEM, X., YEAP, W. H., KOURILSKY, P. & WONG, S. C. 2011. Gene expression profiling reveals the defining features of the classical, intermediate, and nonclassical human monocyte subsets. *Blood,* 118**,** e16-31.

XU, L., KITADE, H., NI, Y. & OTA, T. 2015. Roles of Chemokines and Chemokine Receptors in Obesity-Associated Insulin Resistance and Nonalcoholic Fatty Liver Disease. *Biomolecules,* 5**,** 1563-79.

XU, Y. & CASEY, G. 1996. Identification of human OGR1, a novel G protein-coupled receptor that maps to chromosome 14. *Genomics,* 35**,** 397-402.

XU, Y., ZHU, K., HONG, G., WU, W., BAUDHUIN, L. M., XIAO, Y. & DAMRON, D. S. 2000. Sphingosylphosphorylcholine is a ligand for ovarian cancer G-protein-coupled receptor 1. *Nat Cell Biol,* 2**,** 261-7.

YASAKA, T., MANTICH, N. M., BOXER, L. A. & BAEHNER, R. L. 1981. Functions of human monocyte and lymphocyte subsets obtained by countercurrent centrifugal elutriation: differing functional capacities of human monocyte subsets. *J Immunol,* 127**,** 1515-8.

YING, S., MENG, Q., ZEIBECOGLOU, K., ROBINSON, D. S., MACFARLANE, A., HUMBERT, M. & KAY, A. B. 1999. Eosinophil chemotactic chemokines (eotaxin, eotaxin-2, RANTES, monocyte chemoattractant protein-3 (MCP-3), and MCP-4), and C-C chemokine receptor 3 expression in bronchial biopsies from atopic and nonatopic (Intrinsic) asthmatics. *J Immunol,* 163**,** 6321-9.

YONA, S., KIM, K. W., WOLF, Y., MILDNER, A., VAROL, D., BREKER, M., STRAUSS-AYALI, D., VIUKOV, S., GUILLIAMS, M., MISHARIN, A., HUME, D. A., PERLMAN, H., MALISSEN, B., ZELZER, E. & JUNG, S. 2013. Fate mapping reveals origins and dynamics of monocytes and tissue macrophages under homeostasis. *Immunity,* 38**,** 79-91.

YOSTEN, G. L., REDLINGER, L. J. & SAMSON, W. K. 2012. Evidence for an interaction of neuronostatin with the orphan G protein-coupled receptor, GPR107. *Am J Physiol Regul Integr Comp Physiol,* 303, R941-9.

YU, J. Y., DERUITER, S. L. & TURNER, D. L. 2002. RNA interference by expression of short-interfering RNAs and hairpin RNAs in mammalian cells. *Proc Natl Acad Sci U S A,* 99**,** 6047-52.

ZABA, L. C., FUENTES-DUCULAN, J., STEINMAN, R. M., KRUEGER, J. G. & LOWES, M. A. 2007. Normal human dermis contains distinct populations of CD11c+BDCA-1+ dendritic cells and CD163+FXIIIA+ macrophages. *J Clin Invest,* 117**,** 2517-25.

ZABEL, B. A., NAKAE, S., ZUNIGA, L., KIM, J. Y., OHYAMA, T., ALT, C., PAN, J., SUTO, H., SOLER, D., ALLEN, S. J., HANDEL, T. M., SONG, C. H., GALLI, S. J. & BUTCHER, E. C. 2008. Mast cell-expressed orphan receptor CCRL2 binds chemerin and is required for optimal induction of IgE-mediated passive cutaneous anaphylaxis. *J Exp Med,* 205, 2207-20.

ZHOU, L. J. & TEDDER, T. F. 1996. CD14+ blood monocytes can differentiate into functionally mature CD83+ dendritic cells. *Proc Natl Acad Sci U S A,* 93**,** 2588-92.

ZHU, J. W., BRDICKA, T., KATSUMOTO, T. R., LIN, J. & WEISS, A. 2008. Structurally distinct phosphatases CD45 and CD148 both regulate B cell and macrophage immunoreceptor signaling. *Immunity,* 28**,** 183-96.

ZIEGLER-HEITBROCK, H. W. 1996. Heterogeneity of human blood monocytes: the CD14+ CD16+ subpopulation. *Immunol Today,* 17**,** 424-8.

ZIEGLER-HEITBROCK, H. W. 2000. Definition of human blood monocytes. *J Leukoc Biol,* 67**,** 603-6.

ZIEGLER-HEITBROCK, L., ANCUTA, P., CROWE, S., DALOD, M., GRAU, V., HART, D. N., LEENEN, P. J., LIU, Y. J., MACPHERSON, G., RANDOLPH, G. J., SCHERBERICH, J., SCHMITZ, J., SHORTMAN, K., SOZZANI, S., STROBL, H., ZEMBALA, M., AUSTYN, J. M. & LUTZ, M. B. 2010. Nomenclature of monocytes and dendritic cells in blood. *Blood,* 116**,** e74-80.

ZLOTNIK, A. 2006. Chemokines and cancer. *Int J Cancer,* 119**,** 2026-9.

ZLOTNIK, A., YOSHIE, O. & NOMIYAMA, H. 2006. The chemokine and chemokine receptor superfamilies and their molecular evolution. *Genome Biol,* 7**,** 243.

ZUIDERWEG, E. R. 2002. Mapping protein-protein interactions in solution by NMR spectroscopy. *Biochemistry,* 41**,** 1-7.